ZooKeys 1134: 1–22 (2022)
doi: 10.3897/zookeys.1134.89587
https://zookeys.pensoft.net

RESEARCH ARTICLE

A peer-reviewed open-access journal
ZooKeys
Launched to accelerate biodiversity research

Penile shape discriminates two cryptic species of *Akodon* Meyen, 1833 (Mammalia, Rodentia, Cricetidae) from eastern Brazil

Leonardo Campana[1], Letícia Rosário Cruz[1,2], Roberta Paresque[2,3], Valéria Fagundes[1,2]

1 *Departamento de Ciências Biológicas, Centro de Ciências Humanas e Naturais, Universidade Federal do Espírito Santo, 29.075-910, Vitória, Espírito Santo, Brazil* **2** *Programa de Pós-graduação em Ciências Biológicas, Universidade Federal do Espírito Santo, 29.075-910, Vitória, Espírito Santo, Brazil* **3** *Centro Universitário do Norte do Espírito Santo, Universidade Federal do Espírito Santo, 29.932-540, São Mateus, Espírito Santo, Brazil*

Corresponding author: Valéria Fagundes (valeria.fagundes@ufes.br)

Academic editor: Raquel López-Antoñanzas | Received 28 June 2022 | Accepted 2 November 2022 | Published 5 December 2022

https://zoobank.org/330D8CDC-3D16-41D8-9B7B-9AE74546C535

Citation: Campana L, Cruz LR, Paresque R, Fagundes V (2022) Penile shape discriminates two cryptic species of *Akodon* Meyen, 1833 (Mammalia, Rodentia, Cricetidae) from eastern Brazil. ZooKeys 1134: 1–22. https://doi.org/10.3897/zookeys.1134.89587

Abstract

Glans penis morphology has been used as a powerful tool in mammal taxonomy to differentiate cryptic species. Neotropical rodent species *Akodon cursor* and *A. montensis* are cryptic, and interspecific hybrids are like their parental species. We investigated non-metric and metric phallic characters aiming to differentiate *A. cursor* from *A. montensis*. We also evaluated the parental species' influence of the phallic characters on hybrids. We analysed 96 male adults—56 *A. cursor*, 27 *A. montensis*, and 13 hybrids, subgrouping species by locality and hybrids by parental species (paternal vs maternal). We verified that *A. cursor* and *A. montensis* are distinguishable by penile-shape morphology: *A. cursor* has an elongated penile form with a flare in the distal portion and *A. montensis* has a barrel-shaped form. Also, dark spots in ventral view, if present in *A. montensis*, distinguish *A. montensis* from *A. cursor*. Although the non-metric characters differentiate the species, they do not distinguish the subgroups of *A. cursor*, *A. montensis*, and hybrids. The metric phallic characters indicated a significant difference between species and hybrids. These characters also differentiate the population groups of *A. cursor*. However, *A. montensis* subgroups and hybrids subgroups did not present a significant difference. This study shows the importance of penis morphology in the taxonomy of the cryptic rodent species *A. cursor* and *A. montensis*, representing a powerful tool to discriminate male specimens in mammal collections without karyotyping or sequencing, even though the specimens occurred in sympatric areas. Since most taxidermy protocols do not preserve the penis in mammal preparations, liquid preservation of some specimens or the removal of the penis before taxidermy

for liquid preservation could be beneficial. We also recommend the organisation in museum collections of a penis bank for the *A. cursor* species group (or even all rodent species) to avoid losing this important information for species identification.

Keywords
Glans penis, hybrids, interspecific variation, population variation

Introduction

Akodon Meyen, 1833 (Mammalia, Rodentia, Cricetidae) is the most diverse genus of the tribe Akodontini, with 42 species, one of the most speciose in the subfamily Sigmodontinae, and is widely distributed throughout South America (Pardiñas et al. 2015; Brandão et al. 2021, 2022). Among *Akodon* species, *A. cursor* (Winge, 1887) and *A. montensis* Thomas, 1913 are cryptic and sister species, being members of the *Akodon cursor* species group. *Akodon cursor* is endemic to eastern Brazil, distributed from the north in the states of Paraíba, Pernambuco, Alagoas and Bahia, throughout Minas Gerais, Espírito Santo, Rio de Janeiro and São Paulo, up to south in the state of Paraná. *Akodon montensis*, in turn, occurs in Paraguay, northern Argentina, and in Brazil in states of Rio Grande do Sul, Santa Catarina, Paraná, Mato Grosso do Sul, São Paulo, Rio de Janeiro, and Minas Gerais, in the southeastern. These two species were found in sympatry in the states of Minas Gerais, Rio de Janeiro, São Paulo, and northern Paraná (Fagundes et al. 1998; Fagundes and Nogueira 2007; Valdez and D'Elía 2013; Pardiñas et al. 2015).

Despite being undistinguished by morphology, the karyotype information has been a diagnostic feature to identify these two species, as each species has very distinctive karyotypes based on the diploid number, the fundamental number (or number of autosome arms), and the polymorphisms of some autosome pairs. *Akodon cursor* has three diploid numbers (2n = 14, 15, and 16) and nine different fundamental numbers (FN = 18–26), which are due to a combination of pericentric inversions and centric fusions in five autosomal pairs (Sbalqueiro and Nascimento 1996; Fagundes et al. 1997; Fagundes et al. 1998). On the other hand, *A. montensis* presents a basic karyotype with 2n = 24 and FN = 42, with variation of diploid number due to the monosomy of X (2n = 23) or the presence of 1–3 supernumerary chromosomes (2n = 25–27) (Soares et al. 2018). Furthermore, each species has a very particular karyotype, with different pairs of autosomes involved in polymorphic rearrangements, making their identification by karyotype effective. Interspecific hybrids have already been reported, as wild-caught animals in forests of São Paulo or from offspring of crosses in captivity. They are easily distinguished from parentals by having cells with 2n = 19 or 20, due to fusions of the gametes of *A. montensis* (n = 12) with *A. cursor* (n = 7 or n = 8) (Fagundes et al. 1998).

Despite being easily characterised by karyotype, the search for strong characters to morphologically distinguish these two species has challenged researchers for

decades. So far, these species differ from each other by the relative size of the upper molars, which are larger than 4.4 mm in *A. cursor* but smaller in *A. montensis* (Geise et al. 2005; Gonçalves et al. 2007); the absence of the gallbladder in *A. montensis* and its presence in *A. cursor* (Geise et al. 2004); the cranial size and shape (Astúa et al. 2015), and the microstructure of the hair (Silveira et al. 2013). The need of dissecting animals to verify the presence of a gallbladder and using a magnification to analyse other characters are some of the difficulties encountered in identifying these two species by morphology.

In the last decade, several authors have shown the effectiveness of external penile features to differentiate mammals' species that are very close morphologically (e.g., Rocha-Barbosa et al. 2013; Cserkész et al. 2016, 2019; Comelis et al. 2018; Fasel et al. 2020). In the past, phallic apparatus morphology was of importance in the systematics of mammals, giving information on the interrelationship of species (Hooper 1958; Lidicker 1968; Balbontin et al. 1996). Thus, new perspectives for taxonomy pointed that penile features may be remarkable for rodents and may provide important characteristics to help distinguish cryptic species (Adebayo et al. 2011).

Therefore, this study aims to provide an additional tool to distinguish *A. cursor* and *A. montensis*. Looking for intra- and interspecific variations, we evaluated non-metric and metric penile characteristics of *A. cursor*, *A. montensis*, and their hybrids using an unprecedented sample including wild- and captive-born individuals. We also evaluated if parental species (paternal or maternal) influenced the composition of phallic forms in hybrids.

Methods

Sampling

For penis analyses, we used 96 male adults (Table 1, Fig. 1A, Suppl. material 1), including 14 wild-born (11 *A. cursor* and 3 *A. montensis*) and 82 captive-born (56 *A. cursor*, 27 *A. montensis*, and 13 hybrids). See Table 1 for subgroup acronyms. For captive-born grouping, we analysed individuals aged at least 3 months old. The species identification and their hybrids were based on karyotype features: diploid number (2n), the number of autosomal arms or fundamental number (FN), and the morphology of autosomes. Metaphases were obtained from bone marrow after *in vivo* injection of colchicine, following Fagundes et al. (1998). All wild-born individuals were deposited in the Mammalian Collection at Universidade Federal do Espírito Santo (UFES-MAM), Vitória, Brazil. The captive-born individuals were kept in the Mammalian Collection of the Laboratory of Animal Genetics in UFES. For euthanization, we used xylazine (Sedanew) and ketamine (Quetamina), following the recommendation of the Animal Ethics Committee from UFES (CEUA-UFES), under process 037/2015.

Table 1. Sampling of *Akodon* species and their hybrids, considering wild- and captive-born individuals, their origins, and hybrids, with the origin of parental species in experimental crossings.

Species	Subgroup acronyms	Wild-type individuals		Captive-born individuals		Total
		Origin	Number of individuals	Origin of parentals*	Number of individuals	
A. cursor	ACU^{BA}	Una, BA	1	Una, BA × Una, BA	23	24
	ACU^{ES}	Domingos Martins, ES	1	Domingos Martins, ES × Domingos Martins, ES	10	11
	ACU^{PE}	Camaragibe, PE	9	Camaragibe, PE × Camaragibe, PE	12	21
A. montensis	AMO^{SP}	Ilha Comprida, SP	3	Ilha Comprida, SP × Ilha Comprida, SP	13	16
	$AMO^{SP\times MG}$**	-	-	Ilha Comprida, SP × Luminárias, MG	11	11
Hybrids**	$HYB^{AMO\times ACU}$	-	-	Ilha Comprida, SP × Domingos Martins, ES	6	6
	$HYB^{ACU\times AMO}$	-	-	Una, BA × Ilha Comprida, SP	7	7
Total			14		82	96

BA = Bahia; SP = São Paulo; ES = Espírito Santo and MG = Minas Gerais states in Brazil. *For subgroups of captive-borns, the origin of paternal × maternal parentals, respectively. **The subscript represents the paternal × maternal parental species, respectively.

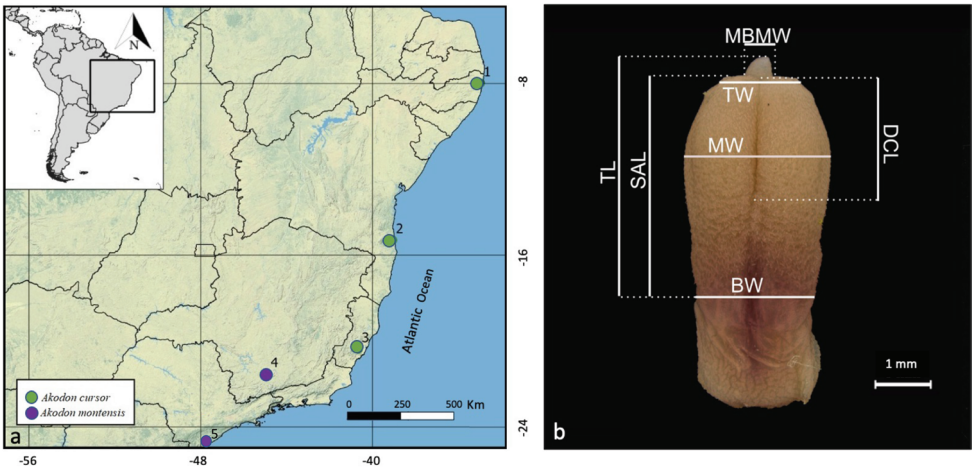

Figure 1. A sampling sites of wild-born specimens in Brazil: (1) Camaragibe, Pernambuco state (–8.02, –34.99); (2) Una, Bahia state (–15.30, –39.07); (3) Domingos Martins, Espírito Santo state (–20.37, –40.67); (4) Luminárias, Minas Gerais state (–21.57, –44.79), and (5) Ilha Comprida, São Paulo state (–24.73, –47.55) **B** glans penis of *A. cursor* in dorsal view. Abbreviation of measurements indicated in the image: spined area length (SAL), total length (TL), base width (BW), tip width (TW), middle width (MW), dorsal cleft length (DCL), and medial bacular mound width (MBMW).

Penile preparations and measurements

The penises were extracted using scissors, fixed in a 10% formalin solution for 24 h, and stored in 70% ethanol. Before analysis, they were air dried at room temperature and then photographed in ventral and dorsal views using an extended-focus imaging

system (GT-Vision, Leica Microsystems). We used digital photographs with a scale bar to determine the linear measurements of each specimen.

Firstly, six non-metric characters of the penile morphology were described to identify the character states. We focused on the following characters: spine morphology, dorsal cleft, dorsal cleft depth, ventral cleft, glans shape, and presence/absence of at least one dark spot on the ventral side of the glans (Table 2).

Then, using the TPSDig2 v. 2.31 (Rohlf 2009), we took seven linear measurements of the ventral and dorsal sides of the glans penises (Fig. 1B), as follows: total length (TL; the distance from the beginning of the dorsal base of the spined area to the distalmost point on the glans); spined area length (SAL; distance from the beginning of the dorsal base of the spined area to the distalmost point on the spined area); base width (BW; diameter of the glans at the beginning of the base of the spined area); meddle width (MW; greatest diameter of the glans penis, usually at the middle part of the spined area); tip width (TW; diameter of the distal end of the spined area); dorsal cleft width (DCL; distance from the distalmost point to the proximal-most point of the dorsal cleft); and medial bacular mound width (MBMW; diameter of the base of the medial bacular mound). To guarantee the reliability of the measuring methods, the measurements were taken five times by the same researcher.

We used scanning electron microscopy (SEM) in a subsample (one specimen of each morphology) to describe glans spines. SEM was performed at the Laboratory of Cellular Ultrastructure Carlos Alberto Redins at UFES (LUCCAR-UFES) using a JEOL JSM 6610 LV scanning electron microscope. Penises were dehydrated in three baths of 70%, 90%, and 100% ethanol for 30 min at each step, followed by two final baths in 100% ethanol. Samples were then dried by using a Autosamdri-815 automatic critical point dryer (Tousimis) and coated with gold using a desk V sample preparation system (Denton Vacuum).

Table 2. Non-Metric characters of the spines and glans penis with their respective character-states.

	Non-metric character	Character states
Spines (S)	Robust: base spine larger than 70 μm	0
	Intermediate: base spine with size >50 μm and <70 μm	1
	Narrow: base spine smaller than 50 μm	2
Dorsal cleft (DC)	Smaller: than half the length of the Spined Area	0
	Same size: as half the length of the Spined Area	1
	Larger: than half the length of the Spined Area	2
Dorsal cleft depth (DCD)	Shallow	0
	Intermediate between shallow and deep	1
	Deep	2
Ventral cleft (VC)	Absent	0
	Shallow	1
	Deep	2
Glans shape (GS)	Cylindric: long, cylinder shape with a flare distally	0
	Barrel-shaped: short, barrel shape without a flare distally	1
Dark spots on ventral view (DS)	Absent	0
	Present, with one or more spots	1

Statistical analyses

The six non-metric characters were analysed using PAST3 (Hammer et al. 2001). The similarity degree was assessed by classical clustering with 1000 replications (bootstrap) using Bray-Curtis distances to generate the current phenograms.

The seven metric characters were analysed using SPSS software statistics v. 26.0 (IBM 2019), and differences were considered significant when $p < 0.05$. To confirm the repeatability of the five repeated measurements for each character, we performed an ANOVA test. Then, all subsequent analyses were performed using the means of repeated measures for each specimen. The variables were also tested for normality with the Shapiro-Wilk and Kolmogorov-Smirnov test, and homoscedasticity with Levene's test.

Once descriptive statistics were obtained for all groups and subgroups, we used an independent sample *t*-test to compare wild- and captive-born individuals of the same species (Pernambuco for *A. cursor* and from São Paulo for *A. montensis*), with our aim to find differences among each group.

To compare *A. cursor* (hereafter ACU), *A. montensis* (AMO), and hybrids (HYB), we arranged one general group of individuals per locality (Table 1). Hybrids were compared with their parental species. The mean values of statistical significance were estimated using a *t*-test for independent samples to compare only two groups.

For the comparative analyses of three groups, we performed a one-way ANOVA to evaluate which variables have significant differences among groups. Following the ANOVA, multiple comparison tests (Tukey's HSD) established which group differed from one another.

We also performed a linear discriminant analysis for the metric characters on PAST3 to access the pattern of the morphological traits that differentiate the groups.

Data resources

The data underpinning the analysis reported in this paper are deposited in the Global Biodiversity Information Facility (GBIF) and are available at https://doi.org/10.15468/24hz7g.

Results

Glans penis morphology

The medial bacular mound projects beyond the glans tip of the penis, and the glans surface is extensively covered by spines, which are thicker at the penile base and sharper at the tip (Fig. 2). Spines vary in size gradually along the glans, being larger at the base and narrower at the tip. All spines face toward the penile base and have three morphologies: (1) robust, with a base larger than 70.0 μm; (2) narrow, with the base less than

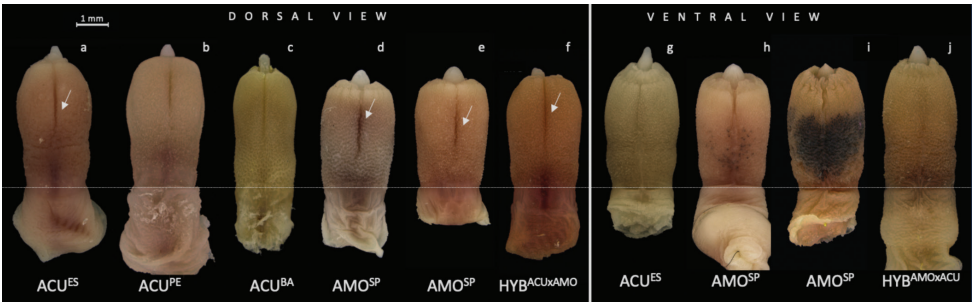

Figure 2. Representatives of the glans penis in dorsal and ventral views of *A. cursor* from Espírito Santo (ACU^{ES}), Pernambuco (ACU^{PE}), and Bahia (ACU^{BA}) states; *A. montensis* from São Paulo state (AMO^{SP}); hybrids from *A. cursor* paternal and *A. montensis* maternal parental ($HYB^{ACU\times AMO}$) and hybrids from *A. montensis* paternal and *A. cursor* maternal parental ($HYB^{AMO\times ACU}$). The horizontal line delimits the beginning of the glans spined area **A** elongated shape, dorsal cleft as long as half of the length of the spined area, with a deep dorsal cleft **B** elongated shape, dorsal cleft smaller than half of the length of the spined area, with intermediate dorsal cleft depth **C** elongated shape, dorsal cleft as long as half the length of the spined area, with a shallow dorsal cleft **D** barrel-shaped, dorsal cleft longer than half of the length of the spined area, with a deep dorsal cleft (at arrow) **E** barrel-shaped, dorsal cleft longer than half of the length of the spined area, with a deep dorsal cleft (at arrow) **F** barrel-shaped, dorsal cleft longer than half of the length of the spined area, with deep dorsal cleft (at arrow) **G** elongated shape with an absent ventral cleft **H** barrel-shaped, with a deep ventral cleft and presence of small dark spots **I** barrel-shaped, with deep ventral cleft and presence of a large dark spot **J** elongated shape, with ventral cleft absent. Arrow points to the deep dorsal cleft. Scale bar: 1 mm.

50.0 μm; and (3) intermediate, with the base between 50.0 μm and 70.0 μm (Fig. 3, Table 2). We detected two shapes of the glans penis: (1) elongated, with the distal part flared and larger in diameter than the proximal part; and (2) barrel-like in shape, with the central area more enlarged than the base and the tip. We also observed two clefts in the glans: a dorsal cleft which varied in length and depth among individuals, and a ventral cleft, which is always smaller than the dorsal cleft.

Comparison wild- and captive-born individuals

Firstly, we tested whether wild- and captive-born individuals show significant differences in their metric characters. The captive-born ACU^{PE} individuals (n = 12) showed no significant differences in metric characters compared to the wild-born ones (n = 9), likewise, the captive-born AMO^{SP} individuals (n = 13) showed no significant differences when compared to the wild-born ones (n = 3) (Suppl. material 2). Based on these analyses, we grouped captive- and wild-born individuals and set a total sample size of 19 ACU^{PE} and 16 AMO^{SP} individuals. The ACU^{BA} and ACU^{ES} populations consisted of only one wild-born specimen each, and a comparative analysis between wild- and captive-born individuals was not performed. Finally, for estimating interspecific and intraspecific variations, we used the total sample for each population, as indicated in Table 1.

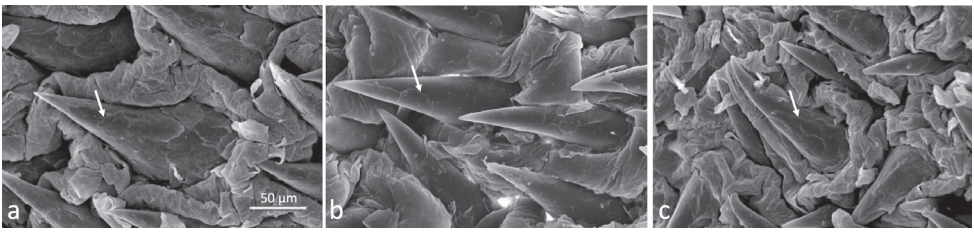

Figure 3. Electron microscopy (450×) of the spines on the dorsal side of the glans penis showing the three morphologies (at arrows) **A** robust **B** intermediate **C** narrow.

Intraspecific variation in *Akodon cursor*

Based on our analysis of non-metric characters, all individuals of the ACU species presented a glans with an elongated morphology (Fig. 4, Suppl. material 3). All three spine morphologies (Fig. 3) were found among ACU^{BA}, ACU^{ES}, and ACU^{PE} subgroups, although the "robust" form was the most frequent for the ACU^{BA} (65.2%) and ACU^{ES} (55.0%) subgroups, while the "intermediate" form was more frequent for ACU^{PE} (45.4%).

Two morphologies of the dorsal cleft ("larger" and "same size" than half of the spined area) were observed on all ACU populations, while the dorsal cleft "smaller" than half of the spined area occurred only in ACU^{ES} population. The dorsal cleft "larger" than half of the spined area was the character with highest frequency among the three subgroups: ACU^{BA} (73.9%), ACU^{PE} (90.9%), and ACU^{ES} (47.3%).

The dorsal cleft presented three morphologies in ACU populations, with the "intermediate" morphology most frequent in ACU^{BA} (60.8%) and ACU^{PE} (45.4%), while for ACU^{ES} the three morphologies showed non-significant differences.

All ACU populations showed the ventral cleft "absent" and "shallow" morphologies, with "absent" the most frequent: ACU^{BA} with 72.2%, ACU^{PE} with 50.0%, and ACU^{ES} with 62.5%. A "deep" ventral cleft was observed exclusively in ACU^{ES}. Comparing the ACU subgroups, the discriminant function 1 explained 58.55% of the total variance. Overall, subgroups discriminant success was 76.79% (Fig. 5B). ACU^{ES} showed higher means for all variables (Table 3).

Table 3. Mean and *SD* of glans penis spined area length (SAL); total length (TL); base width (BW); tip width (TW); meddle width (MW); dorsal cleft length (DCL); medial bacular mound width (MBMW) of *A. cursor*, *A. montensis* and subgroups, and hybrids.

Group	N	SAL	TL	BW	TW	MW	DCL	MBMW
A. cursor	56	5.01 (±0.35)	5.76 (±0.38)	2.67 (±0.26)	1.89 (±0.28)	3.07 (±0.33)	2.63 (±0.32)	0.65 (±0.11)
A. montensis	27	4.73 (±0.35)	5.27 (±0.27)	2.78 (±0.22)	2.02 (±0.38)	3.17 (±0.30)	2.86 (±0.47)	0.70 (±0.15)
Hybrids	13	4.84 (±0.23)	5.58 (±0.23)	2.93 (±0.23)	1.95 (±0.24)	3.23 (±0.21)	3.01 (±0.25)	0.66 (±0.11)
ACU^{BA}	24	5.03 (±0.29)	5.78 (±0.38)	2.68 (±0.22)	1.82 (±0.26)	2.98 (±0.27)	2.64 (±0.26)	0.61 (±0.10)
ACU^{ES}	11	5.29 (±0.29)	6.06 (±0.43)	2.84 (±0.13)	2.00 (±0.24)	3.40 (±0.19)	2.88 (±0.21)	0.76 (±0.05)
ACU^{PE}	21	4.85 (±0.36)	5.58 (±0.25)	2.56 (±0.24)	1.91 (±0.32)	3.01 (±0.35)	2.45 (±0.35)	0.63 (±0.10)
AMO^{SP}	16	4.82 (±0.34)	5.28 (±0.27)	2.08 (±0.21)	1.98 (±0.35)	3.16 (±0.30)	2.73 (±0.50)	0.61 (±0.14)
AMO$^{SP\text{-}MG}$	11	4.58 (±0.33)	5.26 (±0.27)	2.74 (±0.24)	2.08 (±0.44)	3.19 (±0.30)	3.04 (±0.38)	0.71 (±0.15)
HYB$^{ACU\times AMO}$	7	4.87 (±0.28)	5.47 (±0.24)	2.89 (±0.23)	1.84 (±0.21)	3.16 (±0.23)	2.99 (±0.22)	0.64 (±0.05)
HYB$^{AMO\times ACU}$	6	4.79 (±0.17)	5.70 (±0.15)	2.97 (±0.26)	2.09 (±0.21)	3.32 (±0.17)	3.04 (±0.30)	0.78 (±0.12)

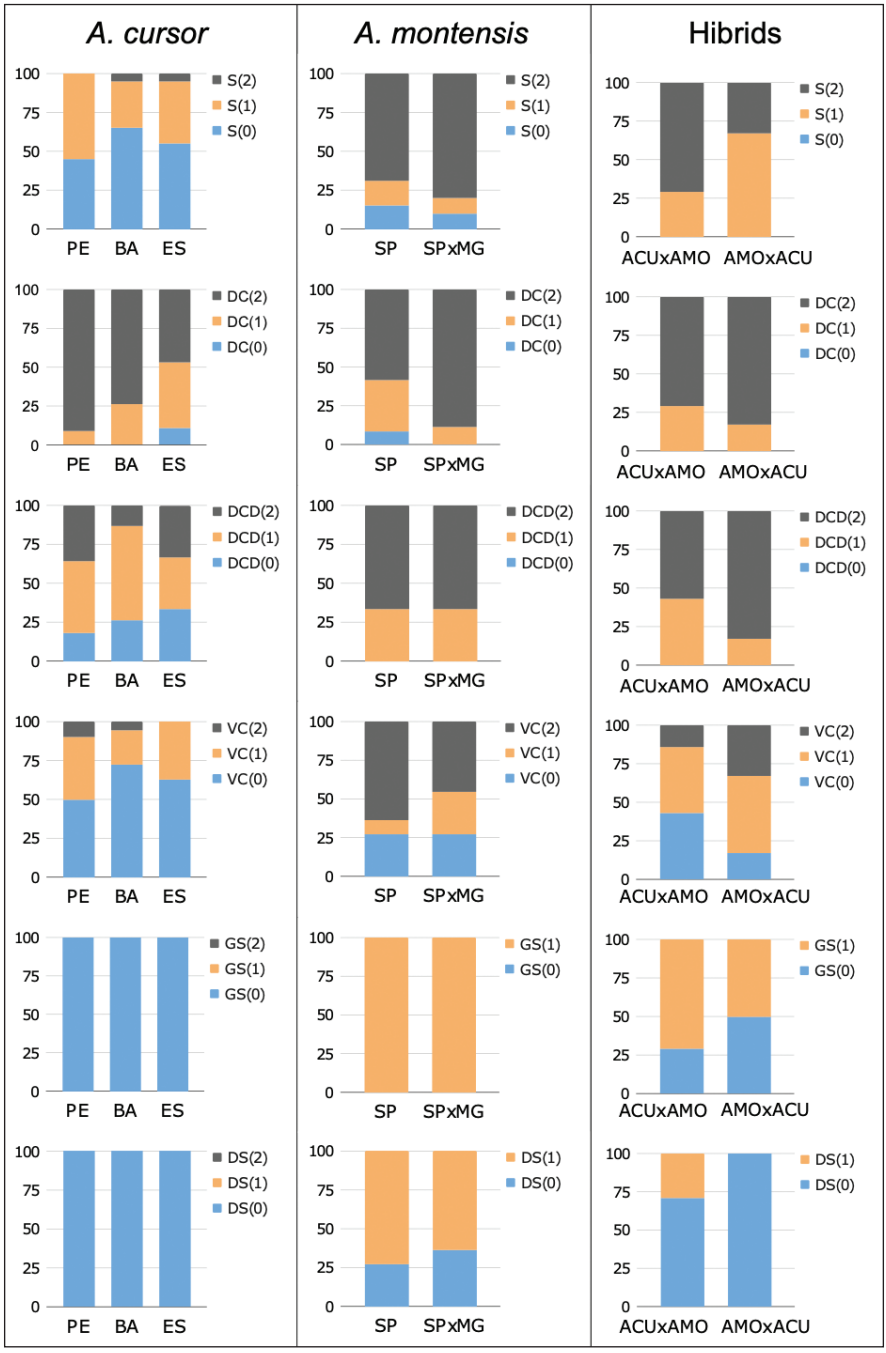

Figure 4. Frequency of the non-metric characters in the subgroups *A. cursor* from Pernambuco (PE), Bahia (BA), and Espírito Santo (ES) states; *A. montensis* from São Paulo (SP) and captive-borns from crossings between individuals from São Paulo and Minas Gerais states (SP×MG); and hybrids with paternal *A. cursor* and maternal *A. montensis* parentals (ACU×AMO), and with paternal *A. montensis* and maternal *A. cursor* parentals (AMO×ACU). Character abbreviation: S = spines; DC = dorsal cleft; DCD = dorsal cleft depth; VC = ventral cleft; GS = glans shape; DS = dark spots.

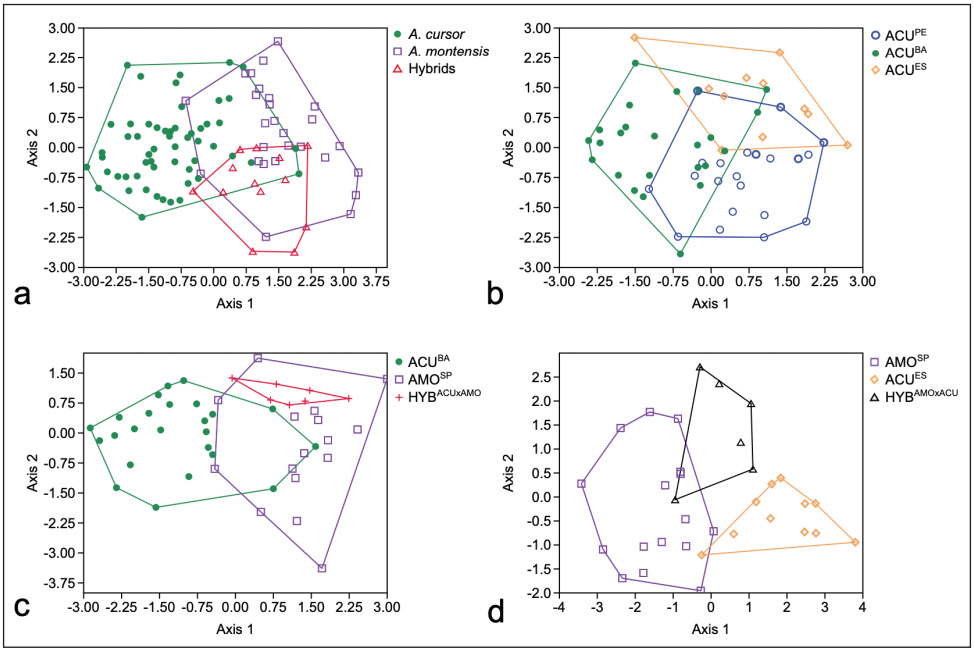

Figure 5. Linear discriminant analyses of **a** *A. cursor* (green dot), *A. montensis* (purple square), and hybrids (red triangle) **b** locality groups of *A. cursor*: ACU^{PE} (blue circle), ACU^{BA} (green dot), and ACU^{ES} (orange diamond) **c** hybrid subgroup $HYB^{ACU\times AMO}$ (red cross) and their parental subgroups ACU^{BA} (green dot) and AMO^{SP} (purple square) **d** hybrid subgroup $HYB^{AMO\times ACU}$ (black triangle) and their parental subgroups AMO^{SP} (purple square) and ACU^{ES} (orange diamond).

Six out of seven metric characters showed significant differences in the one-way ANOVA test among the three subgroups of *A. cursor*: length of the spined area (SAL, $F_2 = 6.884$; $P = 0.002$), total length (TL, $F_2 = 7.182$; $P = 0.002$), width of the base (BW, $F_2 = 4.907$; $P = 0.011$), width of the glans middle part (MW, $F_2 = 8.812$; $P < 0.001$), length of the dorsal cleft (DCL, $F_2 = 8.030$; $P = 0.001$), and width of the medial bacular mound (MBMW, $F_2 = 10.197$; $P < 0.001$). Pairwise Tukey's tests showed that ACU^{ES} showed a significant difference when compared with ACU^{PE} for all the ANOVA significant characters. Compared to ACU^{BA}, ACU^{ES} showed a significant difference just for the characters middle width (MW, $P = 0.001$) and medial bacular mound width (MBMW, $P = 0.000$). On the other hand, ACU^{BA} did not present a significant difference when compared to ACU^{PE}.

In short, *A. cursor* is mainly characterised by an elongated glans penis morphology, and no dark spots on the glans ventral side. The non-metric characters do not distinguish the subgroups in *A. cursor*. On the other hand, the metric characters were able to distinguish subgroup ACU^{PE} from ACU^{ES}, while only two characters differentiated ACU^{ES} from ACU^{BA}.

Intraspecific variation in *Akodon montensis*

The two *A. montensis* subgroups were not distinguished by non-metric characters (Fig. 4, Suppl. material 3). All individuals showed glans with a barrel-shape form and the three spine morphologies, although the narrow morphology was the most frequent. The SP population presented the three dorsal cleft (DC) morphologies, and the DC larger than half of the spined area was the most frequent morphology in both subgroups. Black spots on the ventral side of the glans were exclusive to *A. montensis*; they were present in 64% and 73% of the individuals of the $AMO^{SP \times MG}$ and AMO^{SP} subgroups, respectively. When present, spots were either small and numerous (Fig. 2H) or single, large, and covering the three-quarters of the ventral side of the glans (Fig. 2I). Based on the metric characters, no significant differences were found between these subgroups using the independent samples *t*-test. In short, *A. montensis* can be characterised by a barrel-shaped glans penis and, if present, by dark spots in the ventral side.

Comparing interspecific variation between *Akodon cursor* and *A. montensis*

Akodon cursor and *A. montensis* were distinguished by the matrix of the six non-metric characters (Fig. 5A). Comparing the metric characters of each species, the discriminant analysis classified 79.2% of the two groups correctly, and the functions 1 explained 88.7% of the variance. In *A. cursor* the mean of the total length of the spined area was higher than in *A. montensis*. In *A. montensis* the means of the base width and dorsal cleft length were higher than in *A. cursor* (Table 3).

The *t*-test showed that *A. cursor* and *A. montensis* differed significantly by four characters: total length of the glans penis (TL, $t_{81} = 5.917$; $P < 0.001$), base width of the glans (BW, $t_{81} = -2.006$; $P = 0.048$), length of the spined area (SAL, $t_{81} = 3.498$; $P = 0.001$), and length of the dorsal cleft (DCL, $t_{69} = -2.404$; $P = 0.019$). While *A. cursor* (elongated glans penis) presented higher means for TL and SAL, *A. montensis* (barrel-shaped glans penis) presented higher BW and DCL.

In short, seven non-metric characters differentiated *A. cursor* and *A. montensis* by classical clustering (Fig. 6). On the other hand, hybrids were not differentiated by non-metric characters. Of the metric characters, total length of the glans penis, base width of the glans, length of the spined area, and length of the dorsal cleft also differentiated *A. cursor* and *A. montensis*.

Hybrids × parental variations

Although the matrix of the six non-metric characters found parental groups of *A. cursor* and *A. montensis* as separate, the hybrids were not separately clustered and showed no clear correspondence to either the paternal or maternal species group (Fig. 5A, C, D).

On the other hand, hybrids showed distinct frequencies of non-metric characters, depending on the species of the paternal and maternal parental species. With regards to the

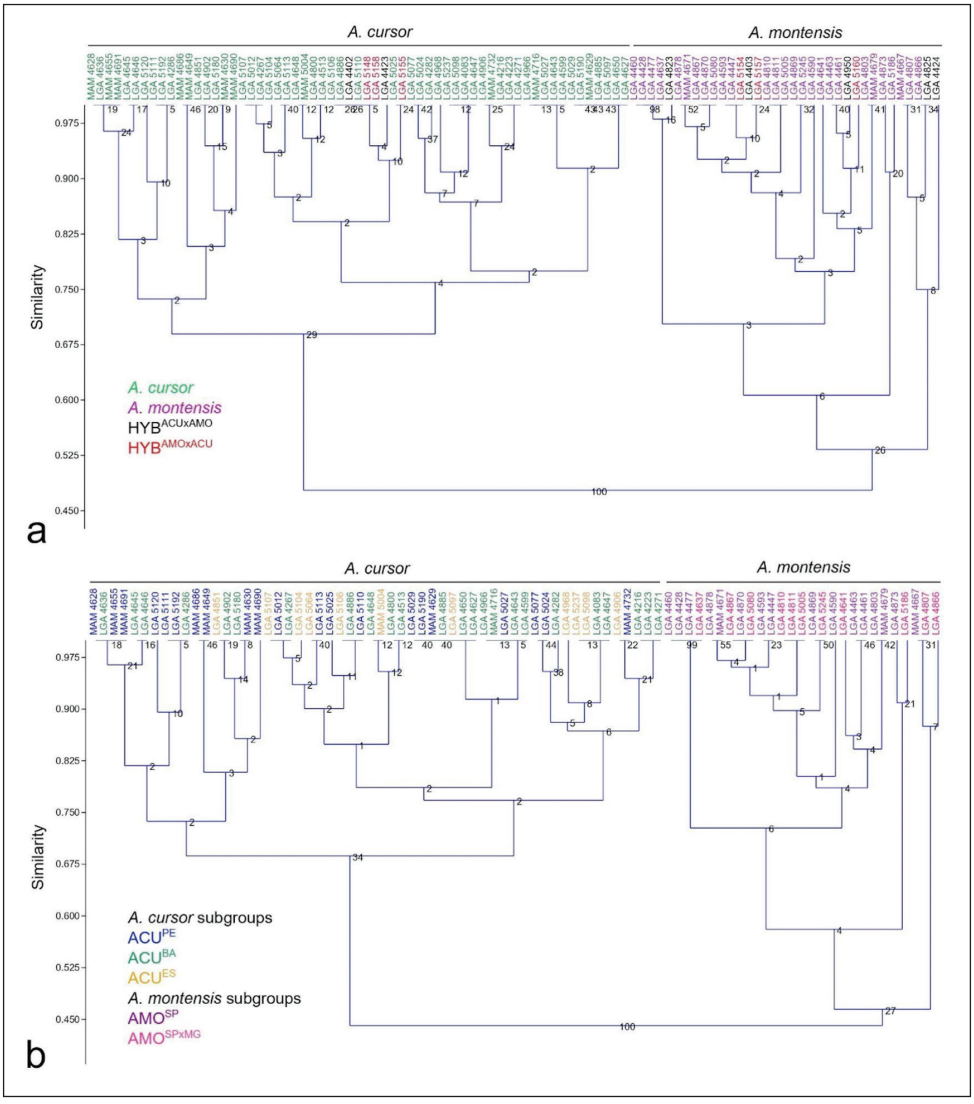

Figure 6. Classical clustering phenogram showing distinction of species group *A. cursor* and *A. montensis*. Bootstrap with 1000 replications **A** hybrids are arbitrarily distributed over groups, despite the origin of paternal and maternal parentals: *A. cursor* (green), *A. montensis* (purple), and $HYB^{ACU\times AMO}$ (black) and $HYB^{AMO\times ACU}$ (red) **B** *A. cursor* and *A. montensis* subgroup representatives are also arbitrarily distributed over group species. Locality groups of *A. cursor*: ACU^{PE} (blue), ACU^{BA} (green), and ACU^{ES} (orange): *A. montensis* subgroups: AMO^{SP} (purple) and $AMO^{SP\times MG}$ (pink).

glans shape (GS), in the $HYB^{ACU\times AMO}$ subgroup (n = 7), in which ACU^{BA} is the paternal and AMO^{SP} is the maternal parental, 71% of the individuals had a barrel-shaped glans, like AMO species. In the $HYB^{AMO\times ACU}$ subgroup (n = 6), in which AMO^{SP} is the paternal and ACU^{ES} is the maternal parental species, we verified an even frequency of the two GS

morphologies (Fig. 4, Suppl. material 3). The narrow spines were more frequent (71.0%) in the $HYB^{ACU\times AMO}$ subgroup, like the maternal AMO species; however, the $HYB^{AMO\times ACU}$ subgroup showed a higher frequency of intermediate spines (67.0%), and a lack of the robust spines, distinct from the maternal ACU^{ES}. No subgroup had the DC smaller than half of the spined area. However, both subgroups showed a higher frequency of a larger dorsal cleft: $HYB^{ACU\times AMO}$ at 71.0%, and $HYB^{AMO\times ACU}$ at 83.0%. The shallow dorsal cleft was not present in either subgroup, but the deep dorsal cleft showed a higher frequency for $HYB^{ACU\times AMO}$ at 57.0% and $HYB^{AMO\times ACU}$ at 83.0%. The three ventral cleft morphologies were present on the two subgroups. For $HYB^{ACU\times AMO}$, the absent ventral cleft and the shallow ventral cleft showed the same frequency at 43.0%. Whereas $HYB^{AMO\times ACU}$ showed a higher frequency for the intermediate ventral cleft at 50.0%. Finally, only the $HYB^{ACU\times AMO}$ subgroup had dark spots on the ventral surface of the glans, at frequency of 69.0%.

Regarding metric characters, while the means of the spined area length and total length in *A. cursor* were higher than in *A. montensis*, the hybrids showed intermediate values. The mean values of the base width and the dorsal cleft length in hybrids were higher than in both parental species (Table 3). The one-way ANOVA test, followed by the pairwise Tukey's test, comparing the hybrids and the parental species groups showed that the former presents a significant difference for three characters: the base width of the glans with a significant difference between *A. cursor* and hybrids (BW, $P = 0.003$), the length of the dorsal cleft between *A. cursor* and hybrids (DCL, $P = 0.003$), and the total length between *A. montensis* and hybrids (TL, $P = 0.025$). The independent samples *t*-test of the two hybrids subgroups showed significant differences only for the width of medial bacular mound (MBMW, $t_{11} = -2.701$; $P = 0.016$). The subgroup $HYB^{AMO\times ACU}$, which has *A. montensis* as the paternal parental species, showed the mean width of the medial bacular mound was higher than in $HYB^{ACU\times AMO}$, which has *A. cursor* as the paternal species (Table 3).

In comparing the subgroup $HYB^{ACU\times AMO}$ with its paternal ACU^{BA} and maternal AMO^{SP} subgroups, the discriminant function 1 explained 87.74% of the variance (Fig. 5C), with 80.85% of the specimens correctly classified. The only variable that showed significant difference in the one-way ANOVA was the total length (TL, $F_2 = 11.756$; $P < 0.001$).

Comparing the subgroup $HYB^{AMO\times ACU}$ with its paternal AMO^{SP} and maternal group ACU^{ES} subgroups, the discriminant function 1 explained 82.27% of the variance (Fig. 5d), with 87.88% of the individuals correctly classified. One-way ANOVA showed significant differences for three of the seven metric characters: length of the spined area (SAL, $F_2 = 8.982$; $P = 0.001$), total length (TL, $F_2 = 19.381$; $P < 0.001$), and the width of the medial bacular mound (MBMW, $F_2 = 7.422$; $P = 0.002$). Pairwise Tukey's tests showed that for the length of the spined area, the only significant difference is between $HYB^{AMO\times ACU}$ and ACU^{ES} (SAL, $P = 0.008$). Hybrids showed a mean less than the ACU^{ES} mean for the length of the spined area. For the other two characters, total length (TL, $P = 0.028$) and width of the medial bacular mound (MBMW, $P = 0.012$), a significant difference was observed between $HYB^{AMO\times ACU}$ and AMO^{SP}. In this case, hybrids showed mean values greater than *A. montensis* for total length and medial bacular mound.

Discussion

In the *Akodon cursor* group, *A. cursor* and *A. montensis* show exceptional morphological similarity, despite karyological and molecular divergences, and the difficulties with field identification may hamper ecological and conservation research. Museum specimens without known diploid numbers or molecular data may be randomly clustered and generate inaccurate information on occurrence and geographic distributions of these species.

A previous study has described the phallic morphology of the akodont group, focusing on internal characters and in the morphology of the baculum (Hooper and Musser 1964), and pointed to a combination of characters that distinguished *A. montensis* from some other akodonts, including *A. cursor*. In their study, Hooper and Musser (1964) included only two individuals, which were then classified as *A. arviculoides cursor* (from Rio de Janeiro, Brazil) and *A. a. montensis* (from Misiones, Argentina). However, a more recent study by Pardiñas et al. (2015) considered the geographic distribution of the supposed species, and the sample from Argentina was thought to be representative of *A. montensis*, but that from Rio de Janeiro could represent either *A. cursor* or *A. montensis*. Pardiñas et al. (2015) mentioned internal differences for the Brazilian individual against the Argentine one: baculum slightly larger, lateral bacular mounds larger, and spinous dorsally, and the urethral flap longer. However, they wrote nothing about the glans shape.

To the best of our knowledge, this is the first study focusing on penile morphology as a diagnostic character for distinguishing between *A. cursor* and *A. montensis*. Herein, we were able to discriminate the cryptic species based solely on morphological characters of the glans penis: elongated with a distal flare in *A. cursor* and barrel-shaped in *A. montensis*. Furthermore, dark spots on ventral view, when present, were exclusive to *A. montensis*. From these findings, we propose a dichotomous diagnosis to differentiate these two cryptic species based on their glans penis morphology.

Considering that the present study included 2–4-month-old individuals only, we assume that the dark spots on the glans are not correlated to the old age of the individuals. However, this character could still be associated with populational variation because our São Paulo sample is formed by individuals and descendants from Ilha Comprida (São Paulo), and our analyses did not include individuals from southern Brazil or Argentina. Chromatic anomalies like piebaldism, leucism, albinism, and melanism has been described for very few rodent species in Brazil (Silva et al. 2020), and anomalous colours on some body parts may occur due to an excess or deficit of the production of melanin (Abreu et al. 2013). Therefore, dark spots on the glans penis are entirely new for this taxon.

In this work, we verified that all specimens had the glans penis completely covered by spines with a thick base and a sharpened tip. Although we have observed three spine morphologies among *A. cursor* and *A. montensis*, at frequencies specific to each species, *A. cursor* showed a higher frequency of robust spines while *A. montensis* had higher frequency of narrow spines. However, the spine morphology was insufficient to differentiate the two species.

According to Rocha-Barbosa et al. (2013), complex penises and ornamentations, like spines, can have several functions, such as inducing ovulation through vaginal

stimulation. This stimulation is caused by the friction of the penile spines on the vaginal wall. Solitary rodent species with seasonal breeding and a promiscuous mating system generally present induced ovulation, and the males are generally more often have penile ornamentation (Parag 2006).

Promiscuous mating is typical for both *A. cursor* and *A. montensis*, and this equates to having complex penises and the presence of spines (Gentile et al. 1997; Rosalino et al. 2013). The sperm competition in promiscuous mating systems may also be influenced by spines on the glans, which have the function of removing sperm present on vagina from previous mattings (Parag et al. 2006). Spines can also be genital locks during the copulation by holding the walls of the vagina (Altuna and Lessa 1985). Therefore, describing and characterising these structures in glans penis in cryptic and sympatric species may help improve our knowledge about the still poorly studied reproductive system of genus *Akodon*, enabling researchers to initiate innovative studies on sperm competition and postcopulatory selective pressures driving the evolution of sperm morphology.

Four metric characters showed a significant difference between *A. cursor* and *A. montensis* (spined area length, total length, base width, and dorsal cleft length), and in general, the metrics were greater in *A. cursor* than in *A. montensis*. These results are in accordance with craniodental metric characters in which *A. cursor* is larger than *A. montensis* (Geise et al. 2005; Astúa et al. 2015). On the other hand, two other metrics not associated with size of the penis (base width and dorsal cleft length) were smaller in *A. cursor* than in *A. montensis*.

The *A. cursor* subgroups organised by locality were not separated in distinct clusters using non-metric characters. Qualitatively, *A. cursor* subgroups showed the same frequency of characters. However, all the metric characters showed differences between groups with the mean values of the Espírito Santo group (in the south) being significantly different than those of the Pernambuco and Bahia groups (in the north). The differentiation among Espírito Santo and Bahia/Pernambuco was also observed in cytochrome-b molecular data (Colombi et al. 2010; Maestri et al. 2016), which found a genetic differences between samples from south of the Jequitinhonha River and those of north of the river (including Bahia and Pernambuco). Even though the three groups are genetically distinct, individuals from Bahia to Pernambuco are morphologically similar. The variation in the penile metrics in distinct geographic groups can be explained by the already known variation in geographic groups of mammals. Even though we analysed three populations of *A. cursor*, we assume additional specimens using this approach would show new patterns to understand the overall population variability of this species.

One of the most outstanding results of this study is the data on *A. cursor* and *A. montensis* hybrids, in which qualitative characters are insufficient to differentiate hybrids from the parental species. The hybrids did not display an intermediate state for the glans shape, but instead displayed either one morphology or the other, like the parental species. It is noteworthy that most of the seven hybrid descendants had a barrel-shaped glans morphology (likewise *A. montensis*) when the maternal species was *A. montensis*. However, the other way around, when *A. cursor* was the maternal species, this predominance was not observed, and the glans shape varied equally between

elongated and barrel-shaped. One could say that our findings should be cautiously considered, because of the small sample size of hybrids. We agree.

For the quantitative characters, the glans of the hybrid subgroup morphologies was not clearly associated with one of the parental species and the hybrids seem to have a distinct identity from their parental species, probably due to the combination of the expression of these characters independently. This pattern is observed in characters of the skull of subterranean tuco-tucos, whose combination of parental features generates a distinct configuration (Kubiak et al. 2020). Characters that display intermediate metrics compared to parentals seem to follow a complex multigenic determinism due to additive genetic variation in hybrids (Renaud et al. 2012). On the other hand, we can observe some examples of hybrids that follow one of the parental species. Hybrids between *Mus musculus domesticus* and *M. musculus* showed a skull-shape gradient more like one parent than the other one (Auffray et al. 1996). Bat hybrids *Myotis myotis* and *M. oxygnathus* showed mixed results in skull traits, with the skull size closer to one parental species but the tooth row construction closer to the other species (Bachanek and Postawa 2010).

Our study showed the importance of penis morphology in the taxonomy of the rodent cryptic species *A. cursor* and *A. montensis*. Our results represent a powerful tool that allows us to identify male specimens in fieldwork, without karyotyping or sequencing, especially in sympatric areas. On the other hand, the absence of an intermediate or a unique shape for hybrids could result in an imprecise identification for this group in sympatric areas. Therefore, we strongly recommend the concatenate analysis of the morphology of the dorsal spines with the glans penises. Only individuals of *A. cursor* presented the combination of elongated glans and robust spines, a profile that can help differentiate this species from *A. montensis* and their hybrids when in sympatry.

Our work contributes by bringing new strategies to facilitate specimen identification in the field with the naked eye or with the help of a magnifying glass. However, considering that the observation of the penile glans in animals that are awake can be very stressful, analyses of the penile glans should minimally be performed in anaesthetised individuals. For identification of specimens in museum collections, on the other hand, we strongly recommend that the penile is important and must be preserved. Since most taxidermy protocols do not include the penis in mammal preparations, in our interpretation, we consider as essential that some individuals be preserved whole in ethanol or, if not possible, at least the penis be removed and preserved. We recommend that there be a penis bank in collections.

Acknowledgements

This work was funded by the Foundation for Research and Innovation of the state of Espírito Santo - Fapes (grant #80600417/17 to VF) and the National Council for Scientific and Technological Development - CNPq (undergraduate bursary to LC and LRC and research bursary to VF). We thank the Laboratory of Cellular Ultrastructure Carlos Alberto Redins at UFES (LUCCAR-UFES) for assistance with Scanning Electron Microscopy. We are indebted to all fields and the crossbreeding lab teams that,

without them, this study would not be possible. We also thank Dr Wesley D. Colombo for assistance with photographing using the extended focus imaging system. In this study the collecting and processing specimens as well as access to the genetic heritage was duly registered with SisGen - Sistema Nacional de Gestão do Patrimônio Genético e dos Conhecimentos Tradicionais Associados, as required by Brazilian law. The authors have declared that no competing interests exist. We are also indebted to the editors and anonymous reviewers for revisions which have improved the manuscript.

References

Abreu MSL, Machado R, Barbieri F, Freitas NS, Oliveira LR (2013) Anomalous colour in Neotropical mammals: a review with new records for *Didelphis* sp. (Didelphidae: Didelphimorphia) and *Arctocephalus australis* (Otariidae: Carnivora). Brazilian Journal of Biology 73(1): 185–194. https://doi.org/10.1590/S1519-69842013000100020

Adebayo AO, Akinloye AK, Olurode SA, Anis EO, Oke BO (2011) The structure of the penis with the associated baculum in the male greater cane rat (*Thryonomys swinderianus*). Folia Morphologica 70(3): 197–203.

Altuna CA, Lessa EP (1985) Penial morphology in Uruguayan species of *Ctenomys* (Rodentia: Octodontidae). Journal of Mammalogy 66(3): 483–488. https://doi.org/10.2307/1380923

Astúa D, Bandeira I, Geise L (2015) Cranial morphometric analyses of the cryptic rodent species *Akodon cursor* and *Akodon montensis* (Rodentia, Sigmodontinae). Oecologia Australis 19(1): 143–157. https://doi.org/10.4257/oeco.2015.1901.09

Auffray JC, Alibert P, Latieule C, Dod B (1996) Relative warp analysis of skull shape across the hybrid zone of the house mouse (*Mus musculus*) in Denmark. Journal of Zoology 240(3): 441–455. https://doi.org/10.1111/j.1469-7998.1996.tb05297.x

Bachanek J, Postawa T (2010) Morphological evidence for hybridization in the sister species *Myotis myotis* and *Myotis oxygnathus* (Chiroptera: Vespertilionidae) in the Carpathian Basin. Acta Chiroptogica 12(2): 439–448. https://doi.org/10.3161/150811010X538007

Balbontin J, Reig S, Moreno S (1996) Evolutionary relationships of *Ctenomys* (Rodentia: Octodontidae) from Argentina, based on penis morphology. Acta Theriologica 41: 237–253. https://doi.org/10.4098/AT.arch.96-25

Brandão MV, Percequillo AR, D'Elía G, Paresque R, Carmignotto AP (2021) A new species of *Akodon* Meyen, 1833 (Rodentia: Cricetidae: Sigmodontinae) endemic from the Brazilian Cerrado. Journal of Mammalogy 102(1): 101–122. https://doi.org/10.1093/jmammal/gyaa126

Brandão MV, Carmignotto AP, Percequillo AR, Christoff AU, Mendes-Oliveira AC, Geise L (2022) A new species of *Akodon* Meyen, 1833 (Rodentia: Cricetidae) from dry forests of the Amazonia-Cerrado transition. Zootaxa 5205(5): 401–435. https://doi.org/10.11646/zootaxa.5205.5.1

Colombi VH, Lopes SR, Fagundes V (2010) Testing the Rio Doce as a riverine barrier in shaping the Atlantic Rainforest population divergence in the rodent *Akodon cursor*. Genetics and Molecular Biology 33(4): 785–789. https://doi.org/10.1590/S1415-47572010000400029

Comelis MT, Bueno LM, Góes RM, Taboga SR, Morielle-Versute E (2018) Morphological and histological characters of penile organisation in eleven species of molossid bats. Zoology (Jena, Germany) 127: 70–83. https://doi.org/10.1016/j.zool.2018.01.006

Cserkész T, Rusin M, Sramkó G (2016) An integrative systematic revision of the European southern birch mice (Rodentia: Sminthidae, *Sicista subtilis* group). Mammal Review 46(2): 114–130. https://doi.org/10.1111/mam.12058

Cserkész T, Fülöp A, Almerekova S, Kondor T, Laczkó L, Sramkó G (2019) Phylogenetic and morphological analysis of birch mice (Genus *Sicista*, Family Sminthidae, Rodentia) in the Kazak Cradle with description of a new species. Journal of Mammalian Evolution 26(1): 147–163. https://doi.org/10.1007/s10914-017-9409-6

Fagundes V, Nogueira CDA (2007) The use of PCR-RFLP as an identification tool for three closely related species of rodents of the genus *Akodon* (Sigmodontinae, Akodontini). Genetics and Molecular Biology 30(3): 698–701. https://doi.org/10.1590/S1415-47572007000400031

Fagundes V, Vianna-Morgante AM, Yonenaga-Yassuda Y (1997) Telomeric sequences localization and G-banding patterns in the identification of a polymorphic chromosomal rearrangement in the rodent *Akodon cursor* (2n = 14, 15 and 16). Chromosome Research 5(4): 228–232. https://doi.org/10.1023/A:1018463401887

Fagundes V, Christoff AU, Yonenaga-Yassuda Y (1998) Extraordinary chromosomal polymorphism with 28 different karyotypes in the neotropical species *Akodon cursor* (Muridae, Sigmodontinae), one of the smallest diploid numbers in rodents (2n = 16, 15 and 14). Hereditas 129(3): 263–274. https://doi.org/10.1111/j.1601-5223.1998.00263.x

Fasel NJ, Mamba ML, Monadjem A (2020) Penis morphology facilitates identification of cryptic African bat species. Journal of Mammalogy 101(5): 1392–1399. https://doi.org/10.1093/jmammal/gyaa073

Geise L, Weksler M, Bonvicino CR (2004) Presence or absence of gallbladder in some Akodontini rodents (Muridae, Sigmodontinae). Mammalian Biology 69(3): 210–214. https://doi.org/10.1078/1616-5047-00136

Geise L, Moraes DA, Silva HS (2005) Morphometric differentiation and distributional notes of three species of *Akodon* (Muridae, Sigmodontinae, Akodontini) in the Atlantic coastal area of Brazil. Arquivos do Museu Nacional 63(1): 63–74.

Gentile R, D'Andrea PS, Cerqueira R (1997) Home ranges of *Philander frenata* and *Akodon cursor* in a Brazilian restinga (coastal shrubland). Mastozoología Neotropical 4: 105–112.

Gonçalves PR, Myers P, Vilela JF, Oliveira JA (2007) Systematics of species of the genus *Akodon* (Rodentia: Sigmodontinae) in southeastern Brazil and implications for the biogeography of the Campos de Altitude. Miscellaneous Publications, Museum of Zoology. University of Michigan 197: 1–24.

Hammer Ø, Harper DA, Ryan PD (2001) PAST: Paleontological statistics software package for education and data analysis. Palaeontologia Electronica 4(1): 9.

Hooper ET (1958) The male phallus in mice of the genus *Peromyscus*. Miscellaneous Publications, Museum of Zoology, University of Michigan 105: 1–40.

Hooper ET, Musser GG (1964) The glans penis in Neotropical cricetines (Family Muridae) with comments on classification of muroid rodents. Miscellaneous Publications, Museum of Zoology, University of Michigan 123: 1–57.

IBM (2019) IBM SPSS statistics. Ver. 26.0. IBM Corporation, Armonk, NY.

Kubiak BB, Kretschmer R, Leipnitz LT, Maestri R, de Almeida TS, Borges LR, de Freitas TRO (2020) Hybridization between subterranean tuco-tucos (Rodentia, Ctenomyidae) with contrasting phylogenetic positions. Scientific Reports 10(1): 1–13. https://doi.org/10.1038/s41598-020-58433-5

Lidicker Jr WZ (1968) A phylogeny of New Guinea rodent genera based on phallic morphology. Journal of Mammalogy 49(4): 609–643. https://doi.org/10.2307/1378724

Maestri R, Fornel R, Gonçalves GL, Geise L, de Freitas TRO, Carnaval AC (2016) Predictors of intraspecific morphological variability in a tropical hotspot: Comparing the influence of random and non random factors. Journal of Biogeography 43(11): 2160–2172. https://doi.org/10.1111/jbi.12815

Parag A, Bennett NC, Faulkes CG, Bateman PW (2006) Penile morphology of African mole rats (Bathyergidae): Structural modification in relation to mode of ovulation and degree of sociality. Journal of Zoology 270(2): 323–329. https://doi.org/10.1111/j.1469-7998.2006.00141.x

Pardiñas UF, Teta P, Alvarado-Serrano D, Geise L, Jayat JP, Ortiz PE, Gonçalves PR, D'Elía G (2015) Genus *Akodon* Meyen. In: Patton JL, Pardiñas UF, D'Elía G (Eds) Mammals of South America, Volume 2: Rodents. University of Chicago Press, Chicago, 144–204.

Renaud S, Alibert P, Auffray JC (2012) Modularity as a source of new morphological variation in the mandible of hybrid mice. BMC Evolutionary Biology 12(1): 141. https://doi.org/10.1186/1471-2148-12-141

Rocha-Barbosa O, Bernardo JL, Loguercio MFC, Freitas TRO, Santos-Mallet JR, Bidau CJ (2013) Penial morphology in three species of Brazilian Tuco-tucos, *Ctenomys torquatus*, *C. minutus*, and *C. flamarioni* (Rodentia: Ctenomyidae). Brazilian Journal of Biology 73(1): 201–209. https://doi.org/10.1590/S1519-69842013000100022

Rohlf FJ (2009) TPSDig. Ver. 2.14. State University of New York, Stony Brook, NY.

Rosalino LM, Martin PS, Gheler-Costa C, Lopes PC, Verdade LM (2013) Allometric relations of Neotropical small rodents (Sigmodontinae) in anthropogenic environments. Zoological Science 30(7): 585–590. https://doi.org/10.2108/zsj.30.585

Sbalqueiro IJ, Nascimento AP (1996) Occurrence of *Akodon cursor* (Rodentia, Cricetidae) with 14, 15 and 16 chromosome cytotypes in the same geographic area in southern Brazil. Revista Brasileira de Genetica 19(4): 565–569. https://doi.org/10.1590/S0100-84551996000400005

Silva FA, Lessa G, Bertuol F, Freitas TRO, Quintela FM (2020) Chromatic anomalies in Akodontini (Cricetidae: Sigmodontinae). Brazilian Journal of Biology 80(2): 479–481. https://doi.org/10.1590/1519-6984.214680

Silveira F, Sbalqueiro IJ, Monteiro-Filho ELDA (2013) Identification of the Brazilian species of *Akodon* (Rodentia: Cricetidae: Sigmodontinae) through the microstructure of the hair. Biota Neotropica 13(1): 339–345. https://doi.org/10.1590/S1676-06032013000100033

Soares AA, Castro JP, Balieiro P, Dornelles S, Degrandi TM, Sbalqueiro IJ, Hass I (2018) B Chromosome diversity and repetitive sequence distribution in an isolated population of *Akodon montensis* (Rodentia, Sigmodontinae). Cytogenetic and Genome Research 154(2): 79–85. https://doi.org/10.1159/000487471

Valdez L, D'Elía G (2013) Differentiation in the Atlantic Forest: Phylogeography of *Akodon montensis* (Rodentia, Sigmodontinae) and the Carnaval–Moritz model of Pleistocene refugia. Journal of Mammalogy 94(4): 911–922. https://doi.org/10.1644/12-MAMM-A-227.1

Supplementary material 1

Gazetteer of collecting localities and specimens examined

Authors: Leonardo Campana, Letícia Rosário Cruz, Roberta Paresque, Valéria Fagundes

Data type: occurrences, morphological (excel file)

Explanation note: Species ID, voucher number, diploid number, the origin of specimens (if wild caught or captive born), the crossing origin, if captive-born (generation, parentals, diploid number and locality of parentals), locality with latitude and longitude, the grouping according to the present study. For each specimen, the values of qualitative characters (S = Spines; DC = Dorsal Cleft; DCD = Dorsal Cleft Depth; VC = Ventral Cleft; GS = Glans Shape and DS = Dark Spots), and the mean of quantitative characters, in millimetres (SAL = Spined Area Length; TL = Total Length; BW = Base Width; TW = Tip Width; MW = Middle width; DCL = Dorsal Cleft Length; MBMW = Medial Bacular Mound Width Wild.

Link: https://doi.org/10.3897/zookeys.1134.89587.suppl1

Supplementary material 2

Frequency of characters

Authors: Leonardo Campana, Letícia Rosário Cruz, Roberta Paresque, Valéria Fagundes

Data type: table (word document)

Explanation note: Frequency of the presence of the characters states in *A. cursor*, *A. montensis* and hybrids.

Link: https://doi.org/10.3897/zookeys.1134.89587.suppl2

Supplementary material 3

Comparing data from *A. cursor* individuals from Pernambuco (ACU^{PE}) and *A. montensis* from São Paulo (AMO^{SP})

Authors: Leonardo Campana, Letícia Rosário Cruz, Roberta Paresque, Valéria Fagundes

Data type: table (word document)

Explanation note: Independent samples t-test between wild-type group and captive-born group. The upper table compared *A. cursor* individuals from Pernambuco (ACU^{PE}) and the lower table compared *A. montensis* individuals from São Paulo (AMO^{SP}).

Link: https://doi.org/10.3897/zookeys.1134.89587.suppl3

Supplementary material 4

Photographs of glans penis of both species and hybrids

Authors: Leonardo Campana, Letícia Rosário Cruz, Roberta Paresque, Valéria Fagundes

Data type: Morphological images (PDF file)

Explanation note: Photographs of glans penis using the extended focus imaging system GT-Vision (Leica microsystems). PE = Pernambuco; ES = Espírito Santo; BA = Bahia; SP = São Paulo and MG = Minas Gerais. *Akodon cursor*, cylindric shape. 1. Dorsal and 2. Ventral views, LGA 5064, ES. 3. Dorsal and 4. Ventral views, LGA 5052, PE. 5. Dorsal and 6. Ventral views, LGA 4645, BA. 7. Dorsal view, LGA 4987, PE. 8. Dorsal view, LGA 4968, ES. 9. Dorsal view, LGA 5113, PE. 10. Dorsal view, LGA 5111, PE. 11. Dorsal view, LGA 5106, ES. 12. Dorsal view, LGA 5107, ES. 13. Dorsal view, LGA 4083, BA. 14. Dorsal view, LGA 4216, BA. 15. Dorsal view, LGA 4282, BA. 16. Dorsal view, LGA 4471, ES. 17. Dorsal view, LGA 5110, PE. *Akodon montensis*, barrel shape. 18. Dorsal and 19. Lateral views, LGA 5245, SP. 20. Dorsal view, LGA 4878, SP. 21. Dorsal view, LGA 4870, SP. 20. Dorsal view, LGA 4869, SP. 23. Dorsal view, LGA 4867, SP. 20. Dorsal view, LGA 4878, SP. 24. Dorsal view, LGA 5186, SP×MG. 25. Dorsal view, LGA 4866, SP×MG. Ventral view. *A. montensis* and presence of dark spots. 26. LGA 5245, SP. 27. LGA 4810, SP. 28. LGA 4867, SP. 29. LGA 4803, SP. 30. LGA 4869, SP. 31. 4870, SP. Ventral view. *A. cursor* and lack of dark spots. 32. LGA 5120, PE. 33. LGA 5025, PE. 34. LGA 4645, BA. 35. LGA 5064, ES. Hybrids, dorsal, lateral and ventral views, respectively. 36–38. LGA 4403, hybrid ACU×AMO. 39–41. LGA 5154, hybrid AMO×ACU. Hybrids, dorsal and ventral views, respectively. 42–43. LGA 5155, hybrid AMO×ACU.

Link: https://doi.org/10.3897/zookeys.1134.89587.suppl4

ZooKeys 1134: 23–37 (2022)
doi: 10.3897/zookeys.1134.94198
https://zookeys.pensoft.net

RESEARCH ARTICLE

A peer-reviewed open-access journal
ZooKeys
Launched to accelerate biodiversity research

A new eyeless species of *Nereis* (Annelida, Nereididae) from deep-sea sediments of the northern South China Sea

Jun-Hui Lin[1], Ya-Qin Huang[1], Qian-Yong Liang[2], Xue-Bao He[1]

1 *Third Institute of Oceanography, Ministry of Natural Resources, 178 Daxue Road, Xiamen 361005, China*
2 *MLR Key Laboratory of Marine Mineral Resources, Guangzhou Marine Geological Survey, China Geological Survey, Guangzhou 510070, China*

Corresponding author: Xue-Bao He (hexuebao@tio.org.cn)

Academic editor: Christopher Glasby | Received 29 August 2022 | Accepted 2 November 2022 | Published 5 December 2022

https://zoobank.org/080F785C-D7E0-4514-96DA-908B2E06A934

Citation: Lin J-H, Huang Y-Q, Liang Q-Y, He X-B (2022) A new eyeless species of *Nereis* (Annelida, Nereididae) from deep-sea sediments of the northern South China Sea. ZooKeys 1134: 23–37. https://doi.org/10.3897/zookeys.1134.94198

Abstract

A variety of nereidid species have been reported from the South China Sea, although little is known about the deep-sea species in this area. Recently, two specimens belonging to a novel nereidid polychaete were collected from a sedimentary habitat during an environmental survey to a deep-sea basin where cold seeps occur. This new species, *Nereis tricirrata* **sp. nov.**, is described herein, based on morphological and molecular analyses. The most noteworthy feature is the absence of eyes on the prostomium; it can be distinguished from other eyeless *Nereis* species by the arrangement of conical paragnaths on the pharynx, the nature of homogomph falcigers and the shape of notopodial lobes in posterior chaetigers. The reconstructed phylogenetic tree, using concatenated sequences of mtCOI, 16S, and 18S rRNA, showed that all *Nereis* species included in this study form a monophyletic clade with full support. The mtCOI-based interspecific comparisons revealed a high genetic divergence (23.1%–37.3% K2P) from four-eyed *Nereis* species with the available sequences. This is the first record of an eyeless *Nereis* species in the South China Sea.

Keywords

Nereidiformia, phylogeny, polychaete, systematics, taxonomy

Introduction

Members of the annelid family Nereididae are commonly seen in marine and brackish benthic communities. The family is among the most diverse taxa groups, with 709 nominal species in 43 genera (Read and Fauchald 2021) distributed from the intertidal to the abyss (Wilson 2000). Nereidids are well represented in the deep sea at depths greater than 2000 m (Paterson et al. 2009). To date, a large number of deep-sea nereidid species have been recorded in previous surveys conducted in areas off New England to Bermuda (Hartman and Fauchald 1971), off western Mexico, east Pacific (Fauchald 1972), off the Japanese Pacific (Imajima 2009), and in the vicinity of eastern Pacific vents (Blake 1985; Blake and Hilbig 1990). Interestingly, some of these species lack eyes on the prostomium or have a sunken depression in place where the eyes usually occur (Blake 1985). These eyeless species have been assigned to a variety of nereidid genera, such as *Ceratocephale* (Hutchings and Reid 1990; Böggemann 2009), *Micronereides* (Day 1963), *Neanthes* (Kirkegaard 1995; Shimabukuro et al. 2017), *Nereis* (Fauchald 1972; Blake 1985; Blake and Hilbig 1990; Imajima 2009), *Nicon* (Fauchald 1972), *Rullierinereis* (Böggemann 2009; Imajima 2009), *Tambalagamia* (Shen and Wu 1993), and *Typhlonereis* (Bakken 2003), with *Nereis* species being the richest in species number. *Nereis* Linnaeus, 1758, is the type genus of the family Nereididae with more than 300 described species around the world, characterized by the presence of conical paragnaths in both pharyngeal rings and homogomph falcigers in the posterior notopodia (Sun and Yang 2004).

The South China Sea (SCS) is the largest marginal sea in the western Pacific, a biogeographic region which harbors diverse marine fauna (Salazar-Vallejo et al. 2014). Quite a few polychaete species in the family Nereididae have been reported from this area (Gallardo 1968; Sun and Yang 2004). Recently, Glasby et al. (2016) compiled a list of annelid species (excluding clitellates and siboglinids) from separate taxonomic publications and prepared a catalogue of polychaete fauna recorded in the South China Sea. In this species list, 1257 species in 73 families were reported from this area, with Nereididae being the most well-studied and diverse annelid family consisting of 134 species. These nereidid species are mostly recorded from shallow water, whereas little is known about the deep-sea species in this area owing to the difficulty in collecting specimens.

During an environmental survey to a deep-sea basin of the northern South China Sea in 2019, where cold seeps occur, two interesting nereidid specimens without prostomial eyes were collected from a sedimentary habitat. In this study, they are described and illustrated as a new species, *Nereis tricirrata* sp. nov., based on morphological and molecular analyses. This is the first record of an eyeless *Nereis* species in the South China Sea.

Materials and methods

Field sampling

In June 2019, sediment samples were collected at two sites in a deep-sea basin of the northern South China Sea (Fig. 1) using a box sampler onboard the R/V ‘Haiyangdizhi

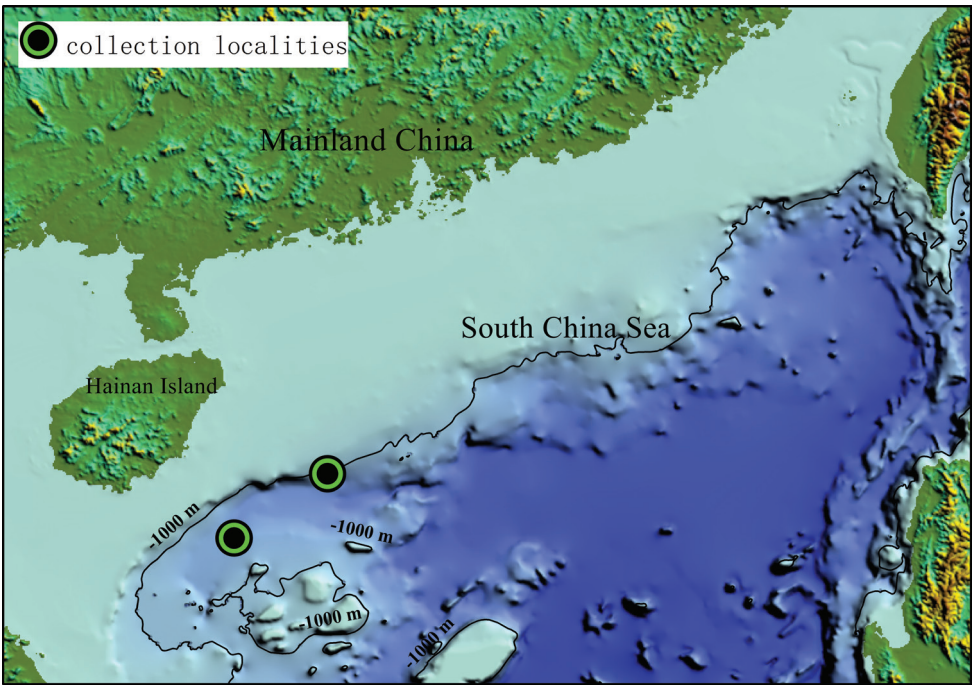

Figure 1. Map showing the two collection localities in the South China Sea.

10'. Subsequently, the sediment samples were washed through a 0.25 mm sieve with chilled, filtered seawater (4 °C) on board. The fauna retained by the sieve were fixed in either 95% ethanol or 8% diluted formalin. One of these specimens was complete, but broken into two fragments. For the complete specimen, chaetigers of the posterior fragment were dissected in the field and then preserved in 95% ethanol. The anterior fragment and the remaining posterior fragment were preserved in 8% diluted formalin in seawater.

Morphological observations

In the laboratory, the specimens were examined using a Leica MZ9.5 optical stereoscope and a Leica DM6B compound microscope. Several parapodia from anterior, middle, and posterior parts of the holotype were dissected and mounted on slides for observation. Light photographs were taken under a Leica M205A stereoscope, equipped with a DFC 550 digital camera. The shape of the chaetae was observed and photographed under a Leica compound microscope (DM6B). Plates were prepared using the software Adobe Photoshop CS5. The terminology of parapodial structures used in this study follows Bakken and Wilson (2005) and Villalobos-Guerrero and Bakken (2018). The type material examined in this study was deposited at the Third Institute of Oceanography, Ministry of Natural Resources, Xiamen, China (**TIO, MNR**).

Molecular analysis

The total genomic DNA was extracted from the ethanol-preserved tissue sample of the holotype using a Transgen Micro Genomic DNA EE 181 Kit (Transgen, Beijing, China), following the manufacturer's protocol. Polymerase chain reactions (PCRs) were conducted to amplify partial sequences of mitochondrial (mtCOI, 16S) and nuclear (18S, H3) genes using primer sets as shown in Table 1. The PCR mixtures contained 10 μl of TakaRa 10× Ex Taq buffer, 8 μl of dNTP mixture (2.5 mM), 2 μl of each primer (10 μM), 0.5 μl of TakaRa Ex Taq (5 U/μl), and 4 μl of DNA template and deionized water was added to make up a final volume of 100 μl. The thermal cycling conditions were as follows: 95 °C/240s – (95 °C/45s – 42 °C/60s – 72 °C/80s) *35 cycles – 72 °C/420s for mtCOI and 16S; 95 °C/240s – (95 °C/45s – 45 °C/60s – 72 °C/80s) *35 cycles – 72 °C/420s for 18S1, 18S2, 18S3, H3. The resulting PCR products were checked using 1% agarose gel electrophoresis and the successful PCR products were purified using a Transgen Quick Gel Extraction EG 101 Kit (Transgen, Beijing, China), following the manufacturer's protocol. Sequencing of the purified DNA samples was performed on an ABI 3730XL DNA Analyzer (Applied Biosystems) at Biosune Company (Xiamen, China). Obtained sequences (18S1, 18S2 and 18S3) were manually assembled into a consensus sequence using the software DNAMAN 8 (Lynnon Biosoft, Quebec, Canada), then checked for potential contamination using BLAST. Eventually, about 649 bp of COI, 437 bp of 16S, 1330 bp of 18S, and 308 bp of H3 were successfully amplified in this study.

For phylogenetic analyses, the sequences of related genera of Nereididae were downloaded from GenBank, as well as species from Hesionidae (sister to Nereididae as verified by Dahlgren et al. 2000) as outgroups (more detail see Appendix 1). Sequences for each gene were aligned, respectively, using MUSCLE (Edgar 2004) implemented in MEGA X (Kumar et al. 2018) for COI and MAFFT (Katoh et al. 2002) for 16S and 18S with default setting. The unaligned sequences and highly divergent regions were removed using Gblocks 0.91b (Castresana 2000). SequenceMatrix v. 1.7.8 (Vaidya et al. 2011) was used to achieve a concatenated sequence of the three genes. Phylogenetic analyses were performed using the maximum likelihood (ML) and Bayesian inference (BI) methods.

Table 1. List of primer sets used for PCRs and sequencing in this study.

Gene	Primer name	Sequence (5' to 3')	Reference
COI	LCO 1490	GGTCAACAAATCATAAAGATATTGG	Folmer et al. (1994)
	HCO 2198	TAAACTTCAGGGTGACCAAAAAATCA	Folmer et al. (1994)
16S	16SarL	CGCCTGTTTAACAAAAACAT	Palumbi (1996)
	16SbrH	CCGGTCTGAACTCAGATCACGT	Palumbi (1996)
H3	aF	ATGGCTCGTACCAAGCAGAC	Colgan et al. (1998)
	aR	ATATCCTTRGGCATRATRGTGAC	Colgan et al. (1998)
18S1	F	GCTGTATGTACTGTGAAACTGCG	Song et al. (2018)
	R	GGAATTACCGCGGCTGCTGGCACC	Song et al. (2018)
18S2	F	GTTCGATTCCGGAGAGGGAGCCT	Song et al. (2018)
	R	GTTTCGGCCTTGCGACTATACTT	Song et al. (2018)
18S3	F	ACTGCGAAAGCATTTGCCAAGAGT	Song et al. (2018)
	R	CACCTACGGAAACCTTGTTACGAC	Song et al. (2018)

The ML analysis on the concatenated sequence was conducted in raxmlGUI 1.5 beta (Silvestro and Michalak 2012) using the GTR+G+I model and 1000 thorough bootstrap pseudoreplicates. The BI analysis was performed using MrBayes v. 3.2.6 (Ronquist et al. 2012), with four Markov chains run for 10 million generations, sampled every 1000 generations. The first 25% of these were discarded as burn-in. The tree was edited using FigTree v. 1.4 (Rambaut 2012) and Adobe Photoshop CS5. Interspecific comparisons were made with aligned COI sequences of *Nereis* species available in GenBank, using the Kimura's two-parameter (K2P) model (Kimura 1980) implemented in MEGA X.

Results

Systematics

Order Phyllodocida Dales, 1962
Family Nereididae de Blainville, 1818

Genus *Nereis* Linnaeus, 1758

Type species. *Nereis pelagica* Linnaeus, 1758.

Generic diagnosis (after Bakken and Wilson 2005; Bakken et al. 2018). Prostomium with entire anterior margin, one pair of antennae, one pair of biarticulated palps with conical palpostyles. Peristomium apodous, greater than length of chaetiger 1, with four pairs of tentacular cirri. Eyes present or absent. Conical paragnaths present on both maxillary and oral ring of pharynx. Notopodial dorsal ligule similar in size in anterior and posterior chaetigers or markedly reduced on posterior chaetigers. Notopodial prechaetal lobe present or absent, smaller than notopodial dorsal ligule on anterior chaetigers, usually reduced or absent posteriorly. Dorsal cirrus basally attached to notopodial dorsal ligule throughout all chaetigers, lacking basal cirrophore. Notoaciculae absent from chaetigers 1 and 2. Notochaetae: homogomph spinigers, homogomph falcigers present. Neurochaetae, dorsal fascicle: homogomph spinigers present, heterogomph falcigers on anterior chaetigers present or absent, on posterior chaetigers present. Neurochaetae, ventral fascicle: heterogomph spinigers present or absent, heterogomph falcigers present or absent.

***Nereis tricirrata* sp. nov.**
https://zoobank.org/67AD5443-63CA-4E5E-9710-B81A4CF60349
Figs 2A–H, 3A–L, 4A–F

Material examined. *Holotype*: TIO-BTS-Poly-137, complete, northern South China Sea, (17°33'N, 111°9'E), 1766 m depth, coll. Jun-Hui Lin, 16 June 2019. ***Paratype*:** TIO-BTS-Poly-138, incomplete, northern South China Sea, (18°26'N, 112°26'E), 1157 m depth, coll. Jun-Hui Lin, 21 June 2019.

Sequences. OP292645, COI gene, 649 bp; OP292646, 16S gene, 437 bp; OP292647, 18S gene, 1330 bp; OP292648, histone H3, 308 bp; extracted from ethanol-preserved tissue of the holotype.

Diagnosis. The new species is characterized by: (1) absence of eyes on the prostomium; (2) possession of three anal cirri instead of two on the pygidium; (3) few paragnaths on both rings of the pharynx; (4) notopodial and neuropodial ligules acutely conical; and (5) homogomph falcigers in posterior notopodia with several coarse teeth.

Description. Holotype complete but broken into two fragments. Body tapering posteriorly. Anterior fragment 35.27 mm long for 44 chaetigers, remaining posterior fragment 7.28 mm long for 15 chaetigers (including regenerated segments), maximum width 2.1 mm (excluding parapodia) at chaetiger 7. Paratype incomplete, broken into three fragments with 45 chaetigers, 12 chaetigers and 7 chaetigers, respectively. Body in formalin light brown. Preserved specimens without pigmentation (Fig. 2A).

Prostomium pentagonal and slightly longer than wide, with one pair of digitiform frontal antennae (Fig. 2B). One pair of biarticulated palps arising antero-laterally, palpophores cylindrical, palpostyles globular. Eyes absent (Fig. 2B).

Peristomium apodous, 1.5 times as long as chaetiger 1. Four pairs of tentacular cirri slender, distally tapered (Fig. 2B); postero-dorsal pair the longest, extending to chaetiger 3.

Pharynx dissected, with dark brown jaws, distally curved, each with 15 blunt teeth on cutting edge. Small conical paragnaths sparse on both rings, arranged as follows: Area I = 0; II = 4 cones in a row; III = 0; IV = 2; V = 0; VI = 1; VII-VII = 2.

First two chaetigers uniramous, remaining ones biramous. Uniramous chaetigers with acutely conical dorsal ligules, subequal in length and of similar shape to ventral ligule (Fig. 2D). Dorsal cirri slightly longer than dorsal ligules.

Notopodia of biramous chaetigers with dorsal and ventral ligules, without notopodial prechaetal lobes. Notopodial dorsal ligules acutely conical (Fig. 2E–H), gradually becoming reduced towards posterior end (Fig. 2F–H). Dorsal cirri slender and attached to base of dorsal ligule throughout, subequal in length to notopodial dorsal ligules in anterior parapodia (Fig. 2D), and markedly longer than dorsal ligules in middle and posterior parapodia (Fig. 2G, H). Notopodial ventral ligules acutely conical, subequal in length to dorsal ligules in anterior parapodia (Fig. 2E), and 1.5–2 times length of dorsal ligules in posterior parapodia (Fig. 2G, H).

Neuropodia of biramous chaetigers with neuroacicular ligules subtriangular, postchaetal lobes rounded (Fig. 2E–H). Neuropodial ventral ligules acutely conical (Fig. 2E), longer than neuroacicular ones, decreasing in size to posterior end (Fig. 2E–H). Ventral cirri attached to ventral edge of parapodia, conical in anterior parapodia, becoming slender and cirriform from middle parapodia (Fig. 2F–H). Ventral cirri shorter than neuropodial ventral ligules in most chaetigers, but longer in chaetigers near pygidium (Fig. 2H).

In anterior parapodia, notochaetae with four homogomph spinigers (Fig. 3A, D); neurochaetae homogomph spinigers and heterogomph falcigers in dorsal fascicles (Fig. 3B, C, E, F), heterogomph spinigers and falcigers in ventral fascicles (Fig. 3B, E). In mid-body, notochaetae with two homogomph spinigers and one homogomph falciger (Fig. 3G); neurochaetae as in anterior parapodia (Fig. 3H, I). In posterior parapodia,

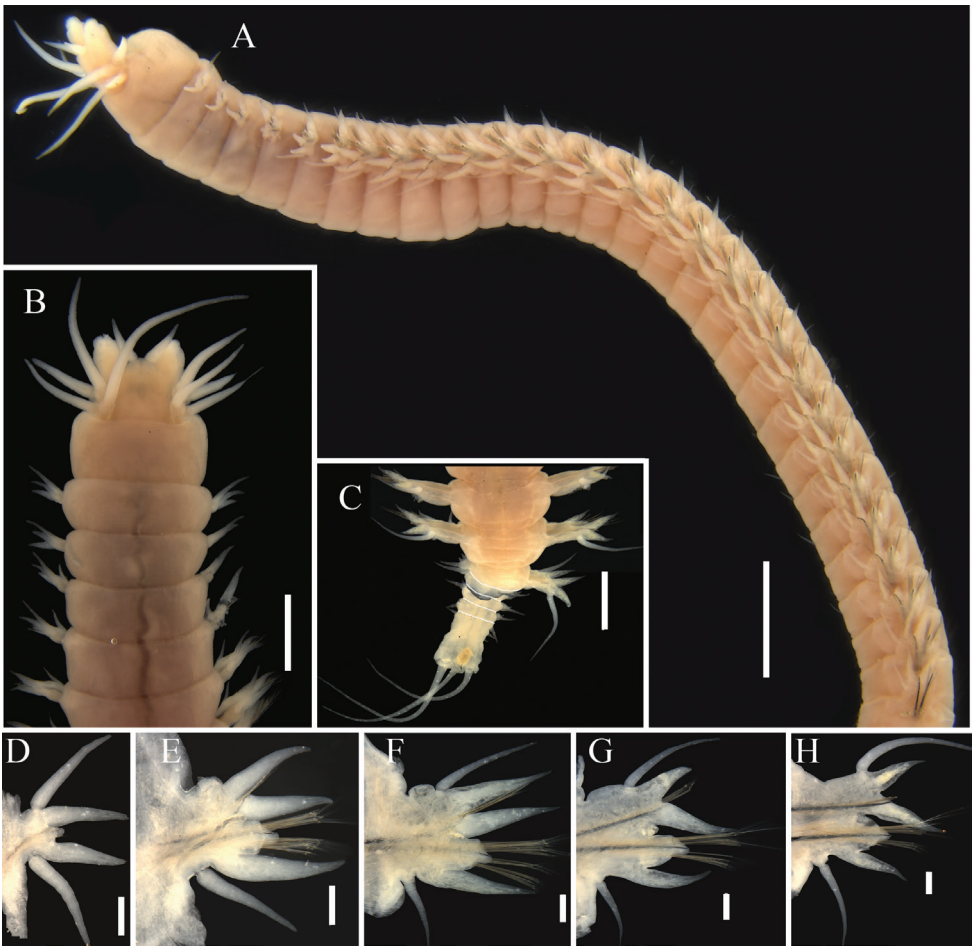

Figure 2. *Nereis tricirrata* sp. nov., holotype (TIO-BTS-Poly-137) **A** anterior fragment, lateral view **B** anterior end, dorsal view **C** posterior end, dorsal view, intersegmental grooves of regenerated segments have been outlined with white lines **D–H** right parapodia (chaetigers 1, 5, 20, 40, posterior end), posterior view. Scale bars: 1 mm (**A–C**); 0.5 mm (**D–H**).

notochaetae with two homogomph falcigers (Fig. 3J); neurochaetae as in anterior parapodia (Fig. 3K, L). Neurochaetae decreasing gradually in number towards posterior end.

All spinigers with long blades finely serrated (Fig. 4A–C); blade of notopodial spinigers shorter, but thicker than neuropodial ones. Notopodial falcigers commencing between chaetigers 20–30 (chaetiger 24 in paratype), with straight, finely serrated, blunt-tipped blade in mid-body (Fig. 4D), but with coarse teeth on relatively short blade in posterior parapodia (Fig. 4F). Neuropodial falcigers with relatively long, serrated, and blunt-tipped blade (Fig. 4E).

Posterior end with six or seven regenerated chaetigers (Fig. 2C), which are disproportionately smaller than normal chaetigers. Pygidium with three anal cirri, all filiform, one on mid-dorsal and one on each of the ventro-lateral sides (Fig. 2C).

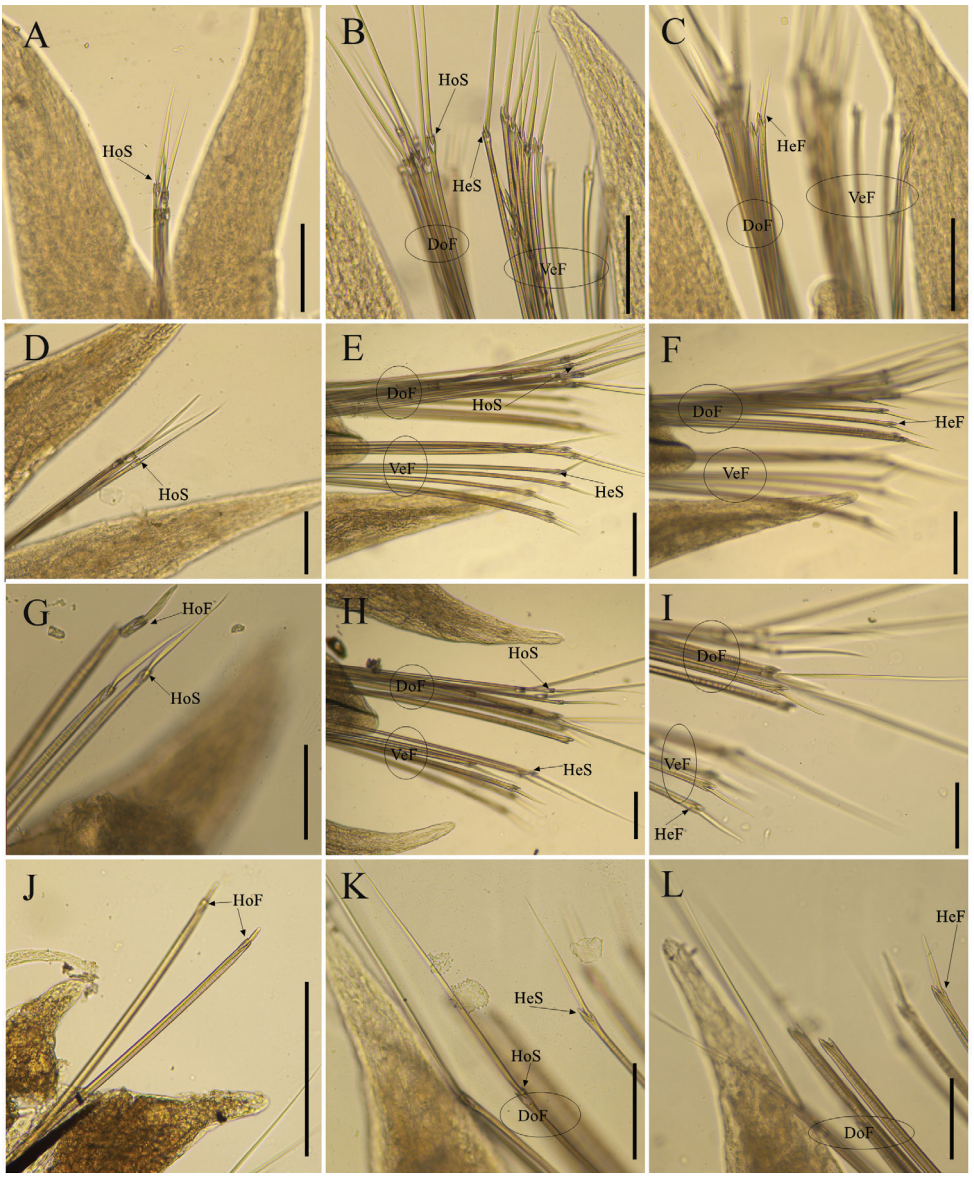

Figure 3. *Nereis tricirrata* sp. nov., holotype and paratype **A** chaetiger 5, notochaetae **B, C** chaetiger 5, neurochaetae **D** chaetiger 20, notochaetae **E, F** chaetiger 20, neurochaetae **G** chaetiger 40, notochaetae **H, I** chaetiger 40, neurochaetae **J** posterior end, notochaetae (from paratype, as blades of notochaetae missing in the posterior fragment of holotype) **K, L** posterior end, neurochaetae. Abbreviations: HoS, homogomph spiniger; HoF, homogomph falciger; HeS, heterogomph spiniger; HeF, heterogomph falciger; DoF, dorsal fascicle; VeF, ventral fascicle. Scale bars: 100 μm (**A–L**).

Etymology. The specific epithet *tricirrata* is composed by the Latin prefix *tri-*, meaning three, and the Latin noun *cirrus*, and refers to the three anal cirri present on the pygidium, one on the mid-dorsal and one on each of the ventro-lateral sides.

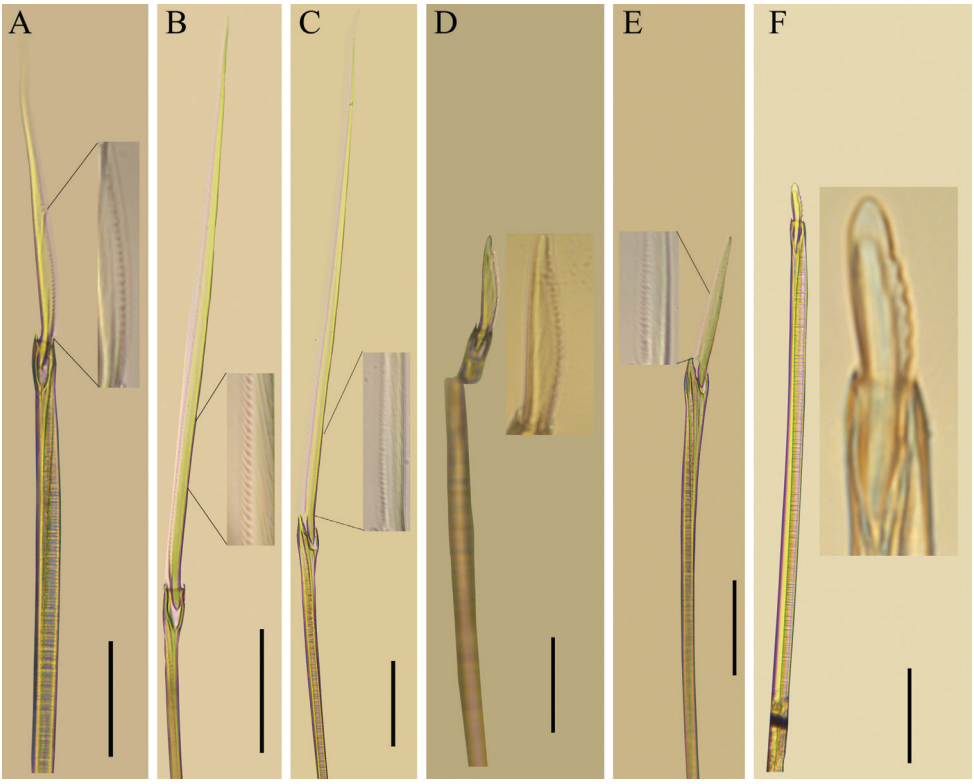

Figure 4. A–E *Nereis tricirrata* sp. nov. holotype (TIO-BTS-Poly-137) and **F** paratype (TIO-BTS-Poly-138) **A** notochaetae, homogomph spiniger, chaetiger 40 **B** neurochaetae, homogomph spiniger, dorsal fascicle, chaetiger 5 **C** neurochaetae, heterogomph spiniger, ventral fascicle, chaetiger 40 **D** notochaetae, homogomph falciger, chaetiger 40 **E** neurochaetae, heterogomph falciger, dorsal fascicle, chaetiger 20 **F** notochaetae, homogomph falciger, posterior parapodia. Scale bars: 50 μm (**A–F**).

Distribution. Currently only known from the deep-sea sedimentary habitat in the northern South China Sea.

Habitat. Deep-sea soft sediments characterized by foraminiferal ooze at depths between 1100 m and 1800 m.

Phylogenetic analysis. There are no identical sequence matches on GenBank for COI and 16S. The low 18S gene divergence (0–1.9% K2P) between *Nereis tricirrata* sp. nov. and other *Nereis* species revealed their close genetic relationship, including an eyeless species, *Nereis sanderi* Blake, 1985 (AM159579). The reconstructed phylogenetic tree (Fig. 5), using the maximum likelihood and Bayesian inference analyses, indicates that all *Nereis* species form a monophyletic clade with 100% nodal support and confirms the placement of *Nereis tricirrata* sp. nov. within the genus *Nereis*. Currently, limited sequences of eyeless *Nereis* species are available, which hinders a better understanding of the relationship among eyeless *Nereis* species. When comparing the new species to other described *Nereis* species with COI genes available in GenBank, the mtCOI-based genetic divergence (K2P) ranged from 23.1% to 37.3% (Table 2), which was comparable to that of previous studies on other nereidid

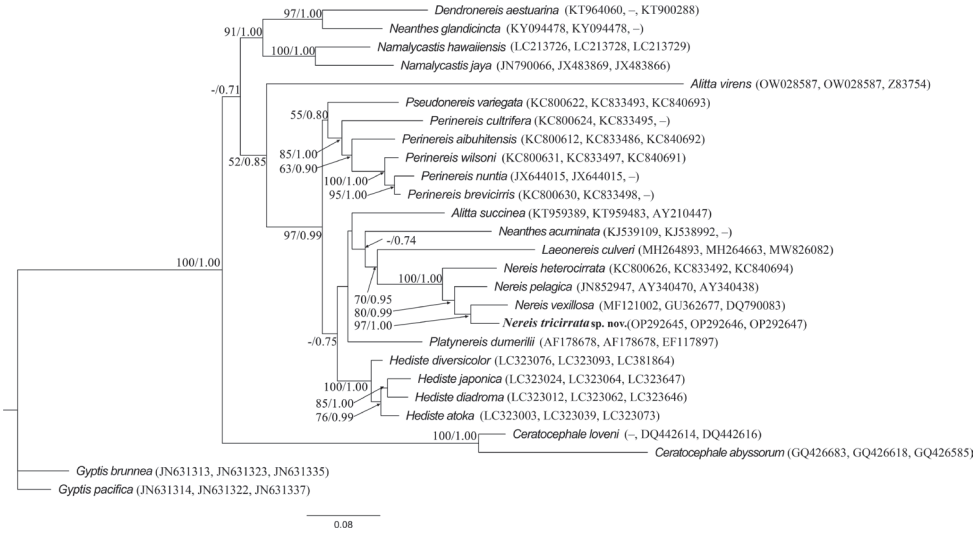

Figure 5. The maximum likelihood (ML) tree inferred from the concatenated sequences of three genes (mtCOI, 16S and 18S rRNA) with GenBank accession numbers. Bootstrap values and posterior probabilities values at nodes were calculated from the ML and Bayesian inference (BI) analyses, respectively. Only bootstrap values ≥ 50 and posterior probabilities ≥ 0.7 are shown. GenBank accession numbers in parenthesis are present in the order of COI, 16S, and 18S; missing markers are denoted by a dash (–).

genera, such as *Alitta* species (Villalobos-Guerrero and Carrera-Parra 2015), *Neanthes* species (Shimabukuro et al. 2017), and cryptic species of *Nereis denhamensis* (Glasby et al. 2013).

Remarks. *Nereis tricirrata* sp. nov. is distinguished from most *Nereis* species around the world by the absence of eyes on the prostomium. With the new species in this study, seven other described *Nereis* species from the deep Pacific also lack prostomial eyes. Six of these species belong to a distinct group with greatly prolonged notopodia in the posterior parapodia, including *N. profundi* Kirkegaard, 1956, *N. anoculis* Hartman, 1960, *N. anoculopsis* Fauchald, 1972, *N. sandersi* Blake, 1985, *N. piscesae* Blake & Hilbig, 1990, and *N. abyssa* Imajima, 1990. Comparison of the two eyeless species bearing normal notopodia throughout the body showed that *Nereis tricirrata* sp. nov. differs from *Nereis izukai* Okuda, 1939 (Imajima 1996) from the Japanese Pacific in the arrangement of paragnaths on the pharynx and the nature of notopodial falcigers in the posterior parapodia. *Nereis izukai* possesses far denser paragnaths on the pharynx (Area I = 11; II = 52–56; III = ~ 70; IV = 50–60; V = 0; VI = 6–12; VII-VIII = ~ 62), and its notopodial falcigers lack coarse teeth on the cutting edge in the posterior parapodia. A not-formally-named *Nereis* species without prostomial eyes, labelled as *Nereis* sp. B, was recorded from off eastern Taiwan Island at depths of 2233–2551 m (Hsueh 2020). It was unclear whether *Nereis* sp. B possessed prolonged notopodia in the posterior parapodia as it was incomplete and lacked the posterior end. Despite this, *Nereis* sp. B is distinct from *Nereis tricirrata* sp. nov. in that the former possesses more paragnaths than the latter (Area I = 2; II = 21; III = 37; IV = 11–30; V = 0; VI = 5–7; VII-VIII = 74). Finally, it should be noted that the new species bears three slender anal cirri on the pygidium instead of two as usually occurs in nereidid species.

Table 2. The mtCOI-based genetic divergence (K2P) between described *Nereis* species with the available sequences.

	Taxa	Locality	1	2	3	4	5	6	7	8	9	10	11
1	*N. multignatha* MT712473	China											
2	*N. pelagica* HQ023592	Canada	0.286										
3	*N. vexillosa* HM473512	Canada	0.285	0.259									
4	*N. zonata* HQ024404	Canada	0.262	0.238	0.284								
5	*N. denhamensis* JX294511	Australia	0.313	0.336	0.302	0.335							
6	*N. falsa* KR916890	Portugal	0.344	0.282	0.330	0.339	0.360						
7	*N. heterocirrata* MN256589	China	0.291	0.263	0.304	0.317	0.309	0.343					
8	*N. eakini* MN138408	USA	0.238	0.242	0.250	0.272	0.343	0.338	0.314				
9	*N. riisei* JF293304	Colombia	0.304	0.294	0.312	0.262	0.351	0.313	0.291	0.324			
10	*N. heronensis* JX392066	Australia	0.287	0.248	0.311	0.306	0.332	0.364	0.302	0.319	0.336		
11	*N. lizardensis* JX392060	Australia	0.290	0.307	0.296	0.306	0.277	0.320	0.291	0.287	0.303	0.327	
12	***N. tricirrata* sp. nov. OP292645**	SCS	0.288	0.231	0.254	0.275	0.337	0.359	0.308	0.267	0.373	0.344	0.314

Acknowledgements

We are grateful to the captain and crew of the R/V 'Haiyangdizhi 10' for help in collecting the deep-sea samples during the cruise organized by the Guangzhou Marine Geological Survey (Guangzhou, China). We thank Drs Chris Glasby and Torkild Bakken for their valuable comments that improved the manuscript. This study was supported by the National Natural Science Foundation of China (42006127), the Marine Geological Survey Program of China Geological Survey (DD20221706), and the Scientific Research Foundation of Third Institute of Oceanography, MNR (2016043).

References

Abe H, Tanaka M, Ueno Y (2017) First report of the non-native freshwater nereidid polychaete *Namalycastis hawaiiensis* (Johnson, 1903) from a private goldfish aquarium in eastern Japan. Bioinvasions Records 6(3): 217–223. https://doi.org/10.3391/bir.2017.6.3.06

Bakken T (2003) Redescription and resurrection of *Typhlonereis gracilis* Hansen, 1879 (Polychaeta, Nereididae). Sarsia 88(5): 346–352. https://doi.org/10.1080/00364820310002894

Bakken T, Wilson RS (2005) Phylogeny of nereidids (Polychaeta, Nereididae) with paragnaths. Zoologica Scripta 34(5): 507–547. https://doi.org/10.1111/j.1463-6409.2005.00200.x

Bakken T, Glasby CJ, Santos CSG, Wilson RS (2018) Nereididae Blainville, 1818. In: Westheide W, Purschke G, Böggemann M (Eds) Handbook of Zoology Online. A Natural History of the Phyla of the Animal Kingdom. Annelida, Polychaetes. De Gruyter, Ösnabruck, 1–43.

Blake JA (1985) Polychaeta from the Vicinity of Deep-Sea Geothermal Vents in the Eastern Pacific. I. Euphrosinidae, Phyllodocidae, Hesionidae, Nereididae, Glyceridae, Dorvilleidae, Orbiniidae and Maldanidae. Bulletin of the Biological Society of Washington 6: 67–101.

Blake JA, Hilbig B (1990) Polychaeta from the vicinity of deep-sea hydrothermal vents in the eastern Pacific. 2. New species and records from the Juan de Fuca and Explorer Ridge systems. Pacific Science 44: 219–253.

Boore JL, Brown WM (2000) Mitochondrial genomes of *Galathealinum*, *Helobdella*, and *Platynereis*: sequence and gene arrangement comparisons indicate that Pogonophora is not a phylum and Annelida and Arthropoda are not sister taxa. Molecular Biology and Evolution 17(1): 87–106. https://doi.org/10.1093/oxfordjournals.molbev.a026241

Böggemann M (2009) Polychaetes (Annelida) of the abyssal SE Atlantic. Organisms, Diversity & Evolution 9: 251–428.

Castresana J (2000) Selection of conserved blocks from multiple alignments for their use in phylogenetic analysis. Molecular Biology and Evolution 17(4): 540–552. https://doi.org/10.1093/oxfordjournals.molbev.a026334

Colgan DJ, McLauchlan A, Wilson GDF, Livingston SP, Edgecombe GD, Macaranas J, Cassis G, Gray MR (1998) Histone H3 and U2 snRNA DNA sequences and arthropod molecular evolution. Australian Journal of Zoology 46(5): 419–437. https://doi.org/10.1071/ZO98048

Dahlgren TG, Lundberg J, Pleijel F, Sundberg P (2000) Morphological and molecular evidence of the phylogeny of Nereidiform polychaetes (Annelida). Journal of Zoological Systematics and Evolutionary Research 38(4): 249–253. https://doi.org/10.1046/j.1439-0469.2000.384150.x

Day JH (1963) The polychaete fauna of South Africa. Part 8: New species and records from grab samples and dredgings. Bulletin of the British Museum (Natural History). Zoology 10(7): 381–445. https://doi.org/10.5962/bhl.part.20530

Edgar RC (2004) MUSCLE: Multiple sequence alignment with high accuracy and high throughput. Nucleic Acids Research 32(5): 1792–1797. https://doi.org/10.1093/nar/gkh340

Fauchald K (1972) Benthic polychaetous annelids from deep water off western Mexico and adjacent areas in the eastern Pacific Ocean. Allan Hancock Monographs in Marine Biology 7: l–575.

Folmer O, Black M, Hoeh W, Lutz R, Vrijenhoek R (1994) DNA primers for amplification of mitochondrial cytochrome c oxidase subunit I from diverse metazoan invertebrates. Molecular Marine Biology and Biotechnology 3(5): 294–299.

Gallardo VA (1968) (erroneously dated 1967) Polychaeta from the Bay of Nha Trang, South Vietnam. In: Naga Report 4 Part 3: Scientific results of marine investigations of the South China Sea and the Gulf of Thailand 1959–1961. University of California Press, La Jolla, USA, 35–279.

Glasby CJ, Wei NV, Gibb KS (2013) Cryptic species of Nereididae (Annelida: Polychaeta) on Australian coral reefs. Invertebrate Systematics 27(3): 245–264. https://doi.org/10.1071/IS12031

Glasby CJ, Lee Y-L, Hsueh P-W (2016) Marine Annelida (excluding clitellates and siboglinids) from the South China Sea. The Raffles Bulletin of Zoology (Supplement 34): 178–234.

Hartman O, Fauchald K (1971) Deep-water benthic polychaetous annelids off New England to Bermuda and other North Atlantic Areas. Part II. Allan Hancock Monographs in Marine Biology 6: 1–327.

Hsueh P-W (2020) New species of *Nereis* (Annelida, Polychaeta, Nereididae) from Taiwanese waters. Zootaxa 4652(3): 544–556. https://doi.org/10.11646/zootaxa.4652.3.10

Hui JHL, Kortchagina N, Arendt D, Balavoine G, Ferrier DEK (2007) Duplication of the ribosomal gene cluster in the marine polychaete *Platynereis dumerilii* correlates with ITS polymorphism. Journal of the Marine Biological Association of the United Kingdom 87(2): 443–449. https://doi.org/10.1017/S002531540705566X

Hutchings P, Reid A (1990) The Nereididae (Polychaeta) from Australia – Gymnonereidinae sensu Fitzhugh, 1987: *Australonereis*, *Ceratocephale*, *Dendronereides*, *Gymnonereis*, *Nicon*, *Olganereis* and *Websterinereis*. Records of the Australian Museum 42(1): 69–100. https://doi.org/10.3853/j.0067-1975.42.1990.107

Imajima M (1996) Annelida Polychaeta. Biological Research, Tokyo, Japan, 530 pp. [in Japanese]

Imajima M (2009) Deep-sea Benthic polychaetes off Pacific Coast of the northern Honshu, Japan. In: Fujita T (Ed.) National Museum of Nature and Science Monographs 2009: Deep-sea fauna and pollutants off Pacific Coast of northern Japan. National Museum of Nature and Science, Tokyo, Japan, 39–192.

Katoh K, Misawa K, Kuma K, Miyata T (2002) MAFFT: A novel method for rapid multiple sequence alignment based on fast Fourier transform. Nucleic Acids Research 30(14): 3059–3066. https://doi.org/10.1093/nar/gkf436

Kim CB, Moon SY, Gelder SR, Kim W (1996) Phylogenetic relationships of annelids, molluscs, and arthropods evidenced from molecules and morphology. Journal of Molecular Evolution 43: 207–215. https://doi.org/10.1007/BF02338828

Kimura M (1980) A simple method for estimating evolutionary rates of base substitutions through comparative studies of nucleotide sequences. Journal of Molecular Evolution 16(2): 111–120. https://doi.org/10.1007/BF01731581

Kirkegaard JB (1995) Bathyal and abyssal polychaetes (errant species). Galathea Report 17: 7–56.

Kumar S, Stecher G, Li M, Knyaz C, Tamura K (2018) MEGA X: Molecular evolutionary genetics analysis across computing platforms. Molecular Biology and Evolution 35(6): 1547–1549. https://doi.org/10.1093/molbev/msy096

Lin G-M, Audira G, Hsiao C-D (2017) The complete mitogenome of nereid worm, *Neanthes glandicincta* (Annelida: Nereididae). Mitochondrial DNA B Resource 2(2): 471–472. https://doi.org/10.1080/23802359.2017.1361346

Magesh M, Kvist S, Glasby CJ (2012) Description and phylogeny of *Namalycastis jaya* sp. n. (Polychaeta, Nereididae, Namanereidinae) from the southwest coast of India. Zookeys 238: 31–43. https://doi.org/10.3897/zookeys.238.4014

Norlinder E, Nygren A, Wiklund H, Pleijel F (2012) Phylogeny of scale-worms (Aphroditiformia, Annelida), assessed from 18SrRNA, 28SrRNA, 16SrRNA, mitochondrial cytochrome c oxidase subunit I (COI), and morphology. Molecular Phylogenetics and Evolution 65(2): 490–500. https://doi.org/10.1016/j.ympev.2012.07.002

Palumbi SR (1996) Nucleic acids II: The polymerase chain reaction. In: Hillis DM, Moritz C, Mable BK (Eds) Molecular Systematics. Sinauer Associates, Sunderland, MA, 205–247.

Passamaneck Y, Halanych KM (2006) Lophotrochozoan phylogeny assessed with LSU and SSU data: Evidence of lophophorate polyphyly. Molecular Phylogenetics and Evolution 40(1): 20–28. https://doi.org/10.1016/j.ympev.2006.02.001

Paterson GLJ, Glover AG, Froján CRS, Whitaker A, Budaeva N, Chimonides J, Doner S (2009) A census of abyssal polychaetes. Deep-sea Research Part II 56(19–20): 1739–1746. https://doi.org/10.1016/j.dsr2.2009.05.018

Pleijel F, Rouse GW, Sundkvist T, Nygren A (2012) A partial revision of *Gyptis* (Gyptini, Ophiodrominae, Hesionidae, Aciculata, Annelida), with descriptions of a new tribe, a new genus and five new species. Zoological Journal of the Linnean Society 165: 471–494. https://doi.org/10.1111/j.1096-3642.2012.00819.x

Rambaut A (2012) FigTree v1.4. Molecular evolution, phylogenetics and epidemiology. University of Edinburgh, Institute of Evolutionary Biology, Edinburgh.

Read G, Fauchald K [Ed.] (2021) World Polychaeta Database. Nereididae Blainville, 1818. http://www.marinespecies.org/polychaeta/aphia.php?p=taxdetails&id=22496 [accessed 15 July 2022]

Reish DJ, Anderson FE, Horn KM, Hardege J (2014) Molecular Phylogenetics of the *Neanthes acuminata* (Annelida: Nereididae) Complex. Memoirs of Museum Victoria 71: 271–278. https://doi.org/10.24199/j.mmv.2014.71.20

Ronquist F, Teslenko M, van der Mark P, Ayres DL, Darling A, Höhna S, Larget B, Liang L, Suchard MA, Huelsenbeck JP (2012) MrBayes 3.2: Efficient Bayesian phylogenetic inference and model choice across a large model space. Systematic Biology 61(3): 539–542. https://doi.org/10.1093/sysbio/sys029

Ruta C, Nygren A, Rousset V, Sundberg P, Tillier A, Wiklund H, Pleijel F (2007) Phylogeny of Hesionidae (Aciculata, Polychaeta), assessed from morphology, 18S rDNA, 28S rDNA, 16S rDNA and COI. Zoologica Scripta 36: 99–107. https://doi.org/10.1111/j.1463-6409.2006.00255.x

Salazar-Vallejo SI, Carrera-Parra LF, Muir AI, de León-González JA, Piotrowski C, Sato M (2014) Polychaete species (Annelida) described from the Philippine and China Seas. Magnolia Press, Auckland, New Zealand, 68 pp.

Shen S, Wu B (1993) A new species of *Tambalagamia* (Polychaeta) from Nansha Islands in South China Sea. Oceanologia et Limnologia Sinica 24(6): 641–644. [in Chinese with English summary]

Shimabukuro M, Santos CSG, Alfaro-Lucas JM, Fujiwara Y, Sumida PYG (2017) A new eyeless species of *Neanthes* (Annelida: Nereididae) associated with a whale-fall community from the deep Southwest Atlantic Ocean. Deep-Sea Research Part II 146: 27–34. https://doi.org/10.1016/j.dsr2.2017.10.013

Silvestro D, Michalak I (2012) RaxmlGUI: A graphical front-end for RAxML. Organisms, Diversity & Evolution 12(4): 335–337. https://doi.org/10.1007/s13127-011-0056-0

Song X, Gravili C, Ruthensteiner B, Lyu M, Wang J (2018) Incongruent cladistics reveal a new hydrozoan genus (Cnidaria: Sertularellidae) endemic to the eastern and western coasts of the North Pacific Ocean. Invertebrate Systematics 32(5): 1083–1101. https://doi.org/10.1071/IS17070

Sun R, Yang D (2004) Annelida. Polychaeta II. Nereidida (Nereimorpha). Nereididae, Syllidae, Hesionidae, Pilargidae, Nephtyidae. Science Press, Beijing, China, 520 pp. [in Chinese]

Tosuji H, Bastrop R, Götting M, Park T, Hong J-S, Sato M (2019) Worldwide molecular phylogeny of common estuarine polychaetes of the genus *Hediste* (Annelida: Nereididae), with special reference to interspecific common haplotypes found in southern Japan. Marine Biodiversity 49: 1385–1402. https://doi.org/10.1007/s12526-018-0917-2

Vaidya G, Lohman DJ, Meier R (2011) SequenceMatrix: Concatenation software for the fast assembly of multigene datasets with character set and codon information. Cladistics 27(2): 171–180. https://doi.org/10.1111/j.1096-0031.2010.00329.x

Villalobos-Guerrero TF, Bakken T (2018) Revision of the *Alitta virens* species complex (Annelida: Nereididae) from the North Pacific Ocean. Zootaxa 4483(2): 201–257. https://doi.org/10.11646/zootaxa.4483.2.1

Villalobos-Guerrero TF, Carrera-Parra LF (2015) Redescription of *Alitta succinea* (Leuckart, 1847) and reinstatement of *A. acutifolia* (Ehlers, 1901) n. comb. based upon morphological and molecular data (Polychaeta: Nereididae). Zootaxa 3919(1): 157–178. https://doi.org/10.11646/zootaxa.3919.1.7

Wilson RS (2000) Family Nereididae. In: Beesley PL, Ross GJB, Glasby CJ (Eds) Polychaetes and Allies: The Southern Synthesis. CSIRO Publishing, Melbourne, Australia, 138–141.

Won EJ, Rhee JS, Shin KH, Lee JS (2013) Complete mitochondrial genome of the marine polychaete, *Perinereis nuntia* (Polychaeta, Nereididae). Mitochondrial DNA 24(4): 342–343. https://doi.org/10.3109/19401736.2012.760082

Appendix 1

Table A1. DNA sequences with GenBank accession numbers used for the phylogenetic analysis; new sequences in bold.

Species	Localities	Voucher/isolate	CO1	16S	18S	References
Alitta succinea	USA	USNM: lZ: 1286800	KT959389	KT959483	AY210447*	18S from Passamaneck and Halanych 2006
Alitta virens	UK (COI, 16S); France (18S)	–	OW028587	OW028587	Z83754*	18S from Kim et al. 1996
Ceratocephale abyssorum	Abyssal SE Atlantic	–	GQ426683	GQ426618	GQ426585	Böggemann 2009
Ceratocephale loveni	Sweden	SMNH 83517	–	DQ442614	DQ442616	Ruta et al. 2007
Dendronereis aestuarina	India	–	KT964060	–	KT900288	Direct submission
Hediste atoka	Japan	–	LC323003	LC323039	LC323073	Tosuji et al. 2019
Hediste diadroma	Japan	–	LC323012	LC323062	LC323646	Tosuji et al. 2019
Hediste diversicolor	Japan	–	LC323076	LC323093	LC381864	Tosuji et al. 2019
Hediste japonica	Japan	–	LC323024	LC323064	LC323647	Tosuji et al. 2019
Laeonereis culveri	Brazil	–	MH264893	MH264663	MW826082	Direct submission
Namalycastis hawaiiensis	Narashino, Japan	isolate 35–1	LC213726	LC213728	LC213729	Abe et al. 2017
Namalycastis jaya	Kerala, India	AQJ3	JN790066	JX483869	JX483866	Magesh et al. 2012
Neanthes acuminata	California, USA	isolate RLF3	KJ539109	KJ538992	–	Reish et al. 2014
Neanthes glandicincta	Xiamen, China	497	KY094478	KY094478	–	Lin et al. 2017
Nereis heterocirrata	China	–	KC800626	KC833492	KC840694	Direct submission
Nereis pelagica	Sweden	SMNH118992; SMNH 75831	JN852947	AY340470	AY340438	Norlinder et al. 2012
***Nereis tricirrata* sp. nov.**	deep SCS	TIO–BTS–Poly–137	**OP292645**	**OP292646**	**OP292647**	This study
Nereis vexillosa	Alaska (COI); China (16S); Germany (18S)	–	MF121002	GU362677	DQ790083	Direct submission
Perinereis aibuhitensis	China	–	KC800612	KC833486	KC840692	Direct submission
Perinereis brevicirris	China	–	KC800630	KC833498	–	Direct submission
Perinereis cultrifera	China	–	KC800624	KC833495	–	Direct submission
Perinereis nuntia	Korea	–	JX644015	JX644015	–	Won et al. 2013
Perinereis wilsoni	China	–	KC800631	KC833497	KC840691	Direct submission
Platynereis dumerilii	USA (COI & 16S); UK (18S)	–	AF178678	AF178678	EF117897	COI & 16S from Boore and Brown 2000; 18S Hui et al. 2007
Pseudonereis variegata	China	–	KC800622	KC833493	KC840693	Direct submission
Gyptis pacifica	Japan	SIO–BIC A2516, A2517	JN631314	JN631322	JN631337	Pleijel et al. 2012
Gyptis brunnea	California, USA	FP collection	JN631313	JN631323	JN631335	Pleijel et al. 2012

ZooKeys 1134: 39–52 (2022)
doi: 10.3897/zookeys.1134.95637
https://zookeys.pensoft.net

CATALOGUE

A peer-reviewed open-access journal
ZooKeys
Launched to accelerate biodiversity research

Annotated catalogue of Orthoptera (Orthoptera, Insecta) of Latvia

Rūta Starka[1], Uģis Piterāns[2], Voldemārs Spuņģis[1]

1 *Department of Zoology and Animal Ecology, University of Latvia, Riga, Latvia* **2** *Zoology Department, Latvian National Museum of Natural History, Riga, Latvia*

Corresponding author: Rūta Starka (ruta.starka@lu.lv)

Academic editor: Zhu-Qing He | Received 25 September 2022 | Accepted 28 October 2022 | Published 5 December 2022

https://zoobank.org/281B1BFE-1F9F-4584-B765-D205692AD714

Citation: Starka R, Piterāns U, Spuņģis V (2022) Annotated catalogue of Orthoptera (Orthoptera, Insecta) of Latvia. ZooKeys 1134: 39–52. https://doi.org/10.3897/zookeys.1134.95637

Abstract

We present a revised list of Latvian species of Orthoptera and provide notes on their occurrence and present knowledge. New information on orthopteran observations from online databases, local unpublished studies, entomological collections, and our direct observations is combined, and a dataset of more than 1500 recent observations is provided. All historical synonyms used in the reviewed information sources are presented. As a result, an annotated list of 52 Orthoptera species is compiled, from which five newly reported species in Latvia are presented here for the first time together with distribution maps. In conclusion, the presence of 43 species of Orthoptera is confirmed in Latvia.

Keywords

Baltics, citizen science, diversity, faunal checklist, historic review

Introduction

The first mentions of orthopteroids in the territory of Latvia date back to 18th century (Fischer 1778), shortly after the work of C. Linnaeus (Linnæus 1758). At that time, they were treated as a part of Hemiptera, and the first existing list of species contains only nine orthopteroid species (Fischer 1778). Later Orthoptera was treated as a separate taxonomic group which included at that time earwigs (Dermaptera) and cockroaches (Blattodea) (Kawall 1864). At this point, 23 species were already listed in Courland's (western Latvia) fauna. The first thorough review of Latvian Orthoptera fauna

was published in 1943 by the renowned Latvian entomologist Kārlis Princis. At that time Dictyoptera (cockroaches, termites, and mantises) was a suborder of Orthoptera (Princis 1943), until 1979, when the Dictyoptera were removed and treated as a separate order (Miskelly and Paiero 2019). Therefore, while K. Princis (1943) mentioned 54 orthopteran species in Latvia, nowadays it corresponds to only 43 species. After K. Princis left Latvia in 1944 to continue his research on cockroaches (Blattaria) in Sweden (Gurney et al. 1979), fundamental faunal research of Orthoptera in Latvia stopped.

With the growing popularity of citizen science (hereafter referred to as "CS") platforms and successful nominations of some Orthoptera species as "Insect of the Year" by The Entomological Society of Latvia (*Psophus stridulus* in 2001, *Acheta domesticus* in 2002, *Gryllotalpa gryllotalpa* in 2007, and *Oedipoda caerulescens* in 2013), the interest of Orthoptera and other insects has grown and resulted in accumulated, unpublished observational data on CS platforms. In Latvia, the foremost popular and most commonly used CS platform is "Dabasdati.lv" (Latvijas Dabas Fonds and Latvijas Ornitoloģijas biedrība 2021). This database was developed in 2008 by the Latvian Fund for Nature and the Latvian Ornithological Society with the aim to develop a volunteer-based online database where records of any species can be uploaded and pinned to coordinates. After the upload of the observation, the species record is revised by a group of experts, similar as done by "iNaturalist" (California Academy of Sciences 2021). Examples where such CS platforms have proven to give crucial information on distribution and occurrence of species are numerous (Chandler et al. 2017; Moulin 2020). Therefore, it is important to summarize and publish the data obtained on local CS platforms, to ensure knowledge transfer internationally.

Until now, there are a few lists of Latvian Orthoptera, each including up to 45 species. However, none of these lists are annotated, nor do they critically review the historic data, and they are not taxonomically up-to-date. Now, at a time of great declines of biodiversity, it is important to summarize and update information on Latvian Orthoptera to set a new baseline after almost 80 years since the last thorough review. Therefore, the aim of this study is to create a revised, annotated list of Orthoptera species in Latvia and to discuss their distribution and occurrence. To do so, we update the scientific nomenclature to the latest taxonomic changes, review all historical records of each species, gather recent unpublished data, and compile the latest occurrences and habitat preferences in Latvia of each species.

Material and methods

Territory and habitats

Latvia is in the center of the Baltic region, situated between Lithuania in the south and Estonia in the north, and occupies a total area of 64573 km^2, from which 62210 km^2 are land areas (Kūle 2021). The climate in Latvia is significantly influenced by the proximity of the Atlantic Ocean and the long coastline with the Baltic Sea, that

determine the domination of cyclonic activity. The mean annual air temperature varies between 5.2–7.4 °C (mean diurnal temperatures 18.8–16.8 °C in July and –1.6 to –5.8 °C in February), and the mean annual precipitation is 683 mm (Briede 2021). Latvia is in the boreonemoral biome, and, therefore, the final phase of natural succession in most terrestrial habitats, if not managed or disturbed, is forest (Priede 2017).

Grassland, dune, heathland, and mire habitats are important for orthopteran diversity in Latvia (Spuņģis 2007, 2013; Rozenfelde et al. 2017; Rozenfelde 2018; Rūsiņa 2020). The majority of grasslands in Latvia are cultivated, and only ~0.7% of the country's territory is occupied by natural or seminatural grasslands (Rūsiņa 2020) which can be categorized in 10 EU-protected habitat types (Rūsiņa 2013). EU-protected coastal and inland dune habitats make up ~1% of the territory (Rove 2013a), from which secondary dunes (grey and brown dunes) are particularly valuable to orthopteran diversity (Spuņģis 2007). European dry heaths hold a great conservation value and are even rarer than dunes in Latvia (Rove 2013b; Rozenfelde 2018). Mire habitats occupy roughly 5% of the country's territory, and, due to specific environmental conditions, is inhabited by specialized, often rare species (Auniņa 2013). There are 333 Natura 2000 sites in Latvia, of which terrestrial sites make up 12% of the land area (Dabas aizsardzības pārvalde 2021).

Data resources

The species list was created by adding up all the available information from historical records (Fischer 1778; Kawall 1864; Princis 1931, 1932, 1933, 1934a, 1934b, 1935, 1936, 1939, 1943; Spuris 1957, 1998; Ozols 1963), species lists (Heller et al. 1998; Spuņģis and Kalniņš 2002; Matisons 2004; Willemse and Heller 2013), reports of new species (Gailis et al. 2003; Sokolovskis and Suveizda 2012), the entomological collection of the Latvian National Museum of Natural History (LMNH), and previously unpublished data of the observations of new species in Latvia (Latvijas Dabas Fonds and Latvijas Ornitoloģijas biedrība 2021).

Taxonomical hierarchy was obtained from the "Orthoptera Species File" online database (Cigliano et al. 2022). Synonyms from the reviewed literature are provided. If the presence of the species in Latvia is doubtful, but possible, the symbol "(?)" was used in front of the species name. Similarly, if the species presence is insufficiently proven the symbol "(–)" was used.

Notes on occurrence in Latvia were combined from original data of the online databases "Dabasdati.lv" (Latvijas Dabas Fonds and Latvijas Ornitoloģijas biedrība 2021), "iNaturalist" (California Academy of Sciences 2021) and local ecological studies (Matisons 2005; Spuņģis 2007, 2013; Rozenfelde et al. 2017; Rozenfelde 2018). In this article, a species observation from CS record was used only if a photo of the species was provided together with the coordinates, or if the observation was made by a biologist with experience in insect identification. The occurrence and distribution information from "Dabasdati.lv" was interpreted with caution, as these data are not obtained by systematic research, and the number of observations is higher near large

cities where more people live. Because some data may be transferred from one platform to another, a manual cross-reference was carried out to avoid doubling up of data. For "iNaturalist" data, the "Verifiable Observations" filter was used. For many species of Acrididae, data in CS platforms are scarce or lacking due to complicated or impossible species determination from photos. Therefore, some notes on distribution and habitats are added from our own observations. For species that are newly reported from the Latvian Orthoptera fauna, distribution and range maps were created in ArcMap (ArcGIS Desktop v. 10.6), using ETRS89 LAEA Europe coordinate system. A 10 × 10 km grid was intersected with the observation data (Suppl. material 1) to create distribution maps. Then, similarly to the Reporting Guidelines for Article 17 of the EU Habitats Directive methodology (DG Environment 2017), a 40 km buffer was created around each observation point to create range maps.

Results

When combining all the available information on the Latvian orthopteran fauna, a list of 52 species belonging to 34 genera and six families was obtained. From the analyzed species, five are newly reported from Latvia (Fig. 1A–E, Table 1). Overall 43 species are with more-or-less certain occurrence (Table 1), but the presence of nine species is doubtful and not proven; therefore, these nine species should be excluded from the list of Orthoptera in Latvia. A more detailed analysis of all 52 species, the history of their inclusion in the Orthoptera fauna in Latvia, and historically used synonyms, as well as known information on occurrence, conservation status, and habitat preference is available in Suppl. material 2.

Discussion

Local faunal inventories are as important as ecological studies from a biogeographical viewpoint. Compiling all historical information shows how the fauna is changing with climate and how the knowledge of taxonomy and diversity has improved with time. According to the last IUCN Red List assessment of Orthoptera, 1082 species are native to or naturalised in Europe (Hochkirch et al. 2016a). Of these, 43 species (Table 1) are present in Latvia. While the proportion (4%) is not significant, we must consider that some of these species are on the border of their area of distribution. Our findings in this study clearly show that even if the local Orthoptera fauna is not rich in comparison to other insect orders, or compared with that of other European countries, there are some distribution and conservation issues to be dealt with.

Taxonomic changes in genera and species can be easily tracked using regularly updated databases such as Orthoptera Species File (Cigliano et al. 2022). Some unique synonyms were briefly used by Princis in the past for three species: *Metrioptera grisea* for the present-day *Platycleis grisea* (Princis 1931), *Stauroderus* (*Chorthippus*) *longicornis*

Table 1. Check-list of Orthoptera species in Latvia. Newly reported species are indicated with an asterisk (*).

Suborder	Family	Subfamily	Species
Caelifera	Acrididae MacLeay, 1821	Gomphocerinae Fieber, 1853	*Chorthippus* (*Chorthippus*) *albomarginatus* (De Geer, 1773)
			Chorthippus (*Chorthippus*) *dorsatus* (Zetterstedt, 1821)
			Chorthippus (*Glyptobothrus*) *apricarius* (Linnaeus, 1758)
			Chorthippus (*Glyptobothrus*) *biguttulus* (Linnaeus, 1758)
			Chorthippus (*Glyptobothrus*) *brunneus* (Thunberg, 1815)
			Chorthippus (*Glyptobothrus*) *pullus* (Philippi, 1830)
			Chorthippus (*Glyptobothrus*) *vagans* (Eversmann, 1848)*
			Chrysochraon dispar (Germar, 1834)
			Euthystira brachyptera (Ocskay, 1826)
			Myrmeleotettix maculatus (Thunberg, 1815)
			Omocestus (*Omocestus*) *haemorrhoidalis* (Charpentier, 1825)
			Omocestus (*Omocestus*) *viridulus* (Linnaeus, 1758)
			Pseudochorthippus montanus (Charpentier, 1825)
			Pseudochorthippus parallelus (Zetterstedt, 1821)
			Stauroderus scalaris (Fischer von Waldheim, 1846)
			Stenobothrus lineatus (Panzer, 1796)
			Stenobothrus stigmaticus (Rambur, 1838)
		Melanoplinae Scudder, 1897	*Podisma pedestris* (Linnaeus, 1758)
		Oedipodinae Walker, 1871	*Locusta migratoria* (Linnaeus, 1758)
			Oedipoda caerulescens (Linnaeus, 1758)
			Psophus stridulus (Linnaeus, 1758)
			Sphingonotus (*Sphingonotus*) *caerulans* (Linnaeus, 1767)
			Stethophyma grossum (Linnaeus, 1758)
	Tetrigidae Rambur, 1838	Tetriginae Rambur, 1838	*Tetrix bipunctata* (Linnaeus, 1758)
			Tetrix subulata (Linnaeus, 1758)
			Tetrix tenuicornis (Sahlberg, 1891)*
			Tetrix undulata (Sowerby, 1806)
Ensifera	Gryllidae Laicharting, 1781	Gryllinae Laicharting, 1781	*Acheta domesticus* (Linnaeus, 1758)
	Gryllotalpidae Leach, 1815	Gryllotalpinae Leach, 1815	*Gryllotalpa gryllotalpa* (Linnaeus, 1758)
	Rhaphidophoridae Walker, 1869	Aemodogryllinae Jacobson, 1905	*Tachycines* (*Tachycines*) *asynamorus* Adelung, 1902
	Tettigoniidae Krauss, 1902	Conocephalinae Kirby & Spence, 1826	*Conocephalus* (*Anisoptera*) *dorsalis* (Latreille, 1804)
			Conocephalus (*Anisoptera*) *fuscus* (Fabricius, 1793)*
		Meconematinae Burmeister, 1838	*Meconema thalassinum* (De Geer, 1773)*
		Phaneropterinae Burmeister, 1838	*Barbitistes constrictus* Brunner von Wattenwyl, 1878
			Leptophyes punctatissima (Bosc, 1792)*
			Phaneroptera (*Phaneroptera*) *falcata* (Poda, 1761)
		Tettigoniinae Krauss, 1902	*Bicolorana bicolor* (Philippi, 1830)
			Decticus verrucivorus (Linnaeus, 1758)
			Metrioptera brachyptera (Linnaeus, 1761)
			Pholidoptera griseoaptera (De Geer 1773)
			Roeseliana roeselii (Hagenbach, 1822)
			Tettigonia cantans (Fuessly, 1775)
			Tettigonia viridissima (Linnaeus, 1758)

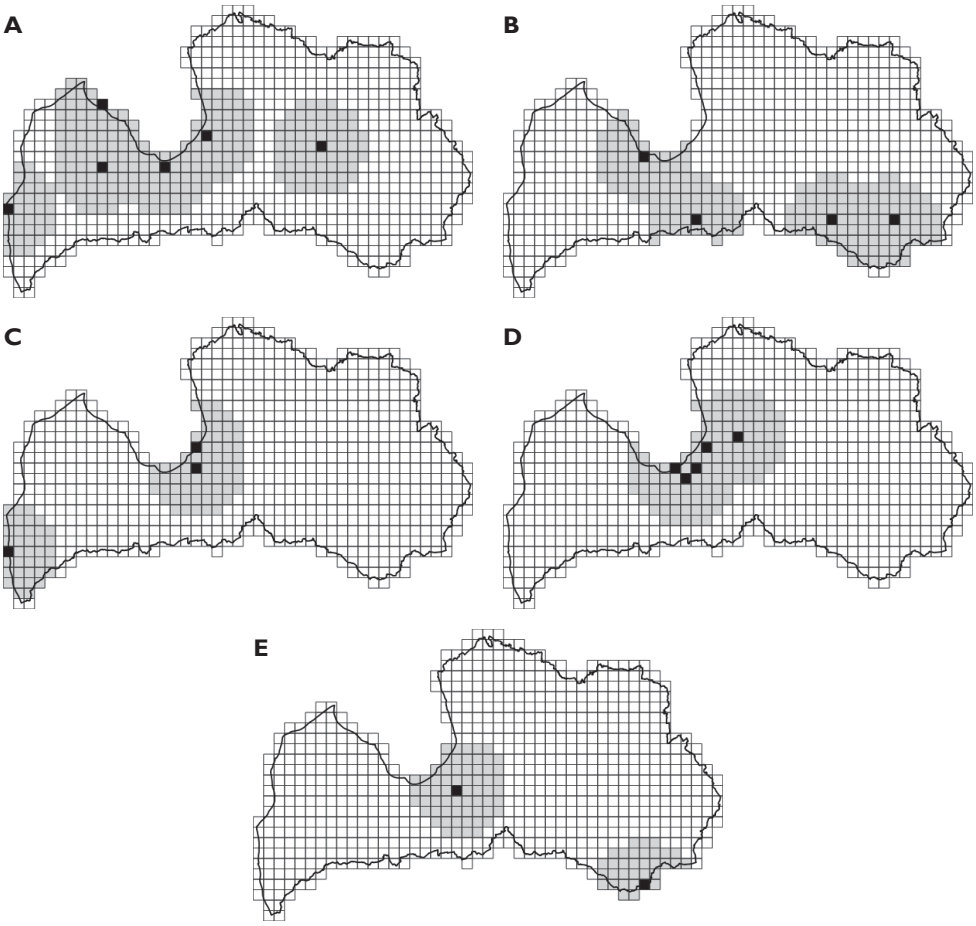

Figure 1. Distribution of five new species to Latvia. Observations are shown on 10 × 10 km grid cells. Black cells indicate distribution derived from observations. Gray cells indicate possible range (40 km buffer from each observation point) **A** *Chorthippus vagans* **B** *Conocephalus fuscus* **C** *Leptophyes punctatissima* **D** *Meconema thalassinum* **E** *Bicolorana bicolor*.

for *Pseudochorthippus montanus* (Princis 1934b), and *Stauroderus parallelus* (Princis 1934b) and *Stauroderus* (*Chorthippus*) *parallelus* (Princis 1935) for *Pseudochorthippus parallelus*. It is important to summarize all possible synonyms to avoid confusion and misinterpretation when analysing historic data in the future.

Some of the species have problematic population status. For example, *Bryodemella tuberculata* is not only locally extinct in Latvia (Spuris 1998; Zuna-Kratky et al. 2016), but also extremely rare and vulnerable in all of Europe (Zuna-Kratky et al. 2016). The main known area of distribution of this species is south-western Russia, with subpopulations in the Baltics and Germany (Cigliano et al. 2022). Clearly there are vast geographical gaps between these populations, and this contributes to the difficulties of conservation. In the IUCN Red List, *B. tuberculata* is listed as Vulnerable in Europe,

and due to a large-scale habitat deterioration, the population trend is decreasing (Zuna-Kratky et al. 2016). The species was recently rediscovered in Lithuania at one historical and one new locality (Budrys et al. 2008; Ūsaitis 2019), which might suggest that with proper habitat management and research effort, the *B. tuberculata* population could be re-established in Latvia. However, with the changes in the Cabinet of Ministers regulations (Ministru kabinets 2004a), the species has already been removed from the protected species list in Latvia, together with two other species of the subfamily Oedipodinae: *Sphingonotus caerulans* and *Psophus stridulus*. *Sphingonotus caerulans*, a species that has somewhat similar habitat requirements as other Oedipodinae, is extremely rarely found in Latvia, and, since 2004, it is no longer a protected species (Ministru kabinets 2004a). Very little is known about the distribution, occurrence, and sustainability of the population of this species. We suggest that *S. caerulans* might be at risk of local extinction. *Gryllus campestris* is another locally extinct species. In general, *G. campestris* is rare in central Europe, and while it is supposed to have stable population dynamics in north-eastern Europe, natural populations have been poorly investigated (Panagiotopoulou et al. 2016). This is also true for Latvia. In the list of European Orthoptera, the only countries or regions where *G. campestris* is considered absent is Finland, Estonia, Latvia, and northern Russia (Heller et al. 1998).

The examples above highlight the necessity of conservation actions. First of all, distributional studies are needed—to this day, no species of Orthoptera are monitored by any monitoring programme. From the available occurrence data, a number of species (e.g., *Myrmeleotettix maculatus*, *Tetrix bipunctata*, *Pholidoptera griseoaptera*, *Conocephalus dorsalis*, and species of the subfamily Oedipodinae) show a coastal distribution pattern (Suppl. material 2). This can be explained by their habitat requirements, which mostly include some rare habitat types like dry heathlands, grey dunes, and calcareous fens along the Baltic Sea coast. In Latvia, three laws are instrumental to the protection of the species inhabiting the Baltic Sea and Riga Gulf coastlines: the Protection Zone Law (Saeima 1997), the Law on the Conservation of Species and Biotopes (Saeima 2000), and the Law on Specially Protected Nature Territories (Augstākā Padome 1993). However, with a monitoring programme, more information could be obtained on the distribution on these species and the efficiency of these laws. Secondly, conservation status needs to be assigned to more orthopteran species to justify conservation efforts. Today, only two species—*Podisma pedestris* and *Oedipoda caerulescens*—are protected in Latvia (Ministru kabinets 2004b). Finally, conservation actions, such as habitat management and restoration, need to take place targeting these species.

The necessity of monitoring also applies to more common and new to Latvia species. For example, the geographical range borders of *Tetrix tenuicornis* are Spain in the south and Finland in the north (Hochkirch et al. 2016d), and the species is listed in the neighbouring Lithuanian Orthoptera checklist (Budrys and Pakalniškis 2007). Therefore, while there are few reliable records of this species in Latvia, it is expected to be found more commonly. Similarly, *Platycleis albopunctata* is also listed in Lithuanian fauna, but seems to be restricted to the south of the country and the Baltic Sea coastline (Budrys and Pakalniškis 2007; California Academy of Sciences 2021). The

population trend of this species is overall increasing, and it is expanding its range to the north (Hochkirch et al. 2016c). A newly reported species for Latvia, *Leptophyes punctatissima*, is a widespread species throughout western Europe, England, and southern Scandinavia (Cigliano et al. 2022), but the occurrence in the Baltics or Finland in unclear. This species has reduced wings in both sexes, but it has been presumed that relocation of individuals occurs via human transport (Hochkirch et al. 2016b). *Conocephalus fuscus* is also known to recently expand its distribution area to the north (Beckmann et al. 2015), while *Meconema thalassinum* is already on its northern border of distribution (Hochkirch et al. 2016e). Climate modelling research conducted in Russia predicted that *Calliptamus italicus* will expand its range to the north (Popova et al. 2016). This species is present in Belarus (California Academy of Sciences 2021; Prischepchik and Storozhenko 2019) but not in Lithuania (Budrys and Pakalniškis 2007; California Academy of Sciences 2021). Today, *C. italicus* is remains distributed in southern Europe and is unlikely to be found in Latvia, except cases of accidental immigration of some individuals. Therefore, we can expect that with time the above-mentioned species, with the exception of *C. italicus*, could become more common or more commonly observed in Latvia.

With a warming climate, the dispersal of species to the north (Poniatowski and Fartmann 2011) will change the local fauna over time, and the arrival and disappearance of species is expected. An example of this is the first arrival of *Phaneroptera falcata* in Daugavpils in 2011 (Sokolovskis and Suveizda 2012) and its observation a year later approximately 230 km north-west from where it was first observed (unpublished data 2013, Ādaži military polygon). Today, *P. falcata* is a common species. Recently three additional species have been recorded in Lithuania (Ferenca et al. 2017; Budrys et al. 2019). While one of them, *Euthystira brachyptera*, is already fairly common in Latvia, the other two species are yet to be found. In 2019, *Aiolopus thalassinus* was first recorded in Nida (only about 100 km south of the Latvian border), and the authors note that this could be yet another example of climate-change driven geographic range expansion to the north (Budrys et al. 2019). *Myrmecophilus acervorum* was found only about 70 km south of the Latvian border, in dead wood colonised by ants (Ferenca et al. 2017). Interestingly, Princis (1931) also mentioned this species as potentially present in Latvia. Kawall (1864) at his time also named 10 additional species that he thought could potentially be present in Latvia, and only one of those species—*Bohemanella frigida*, referred to as *Pezotettix frigida* by Kawall—has not been recorded to this date.

CS platforms, while being extremely useful, are not a substitute to monitoring, as the data obtained from them can be problematic. First of all, more observations are expected from areas with dense human population (higher possibility of observation due to higher research effort). Secondly, in many occasions there is a difficulty in determining species due to a lack of photographs showing the characteristic traits well. Third, some orthopteran species (e.g., *Meconema thalassinum* and *Barbitistes constrictus*) live a hidden lifestyle and are less expected to be observed without particular searching. Some species are "not interesting" to a non-professional observer, due to their unremarkable

appearance (e.g., *Chorthippus* spp.), while some are targeted by observers due to conservation status, interesting biology, or appearance (e.g., Oedipodidae species). This results in some species being underrepresented and others overrepresented. Even so, CS platforms are valuable tools to the scientific community, as they help to build knowledge.

Overall, we can expect additions to the local fauna in the coming years. As there is no monitoring programme for Orthoptera in Latvia, the distribution and population trends in Latvia are little known. However, such information on diversity is crucial to conservation biology.

Conclusions

There are 43 species of Orthoptera in Latvia. Many of these species need more detailed information on occurrence, distribution and ecology, which could be achieved by a dedicated monitoring programme. A re-evaluation of the conservation status for multiple species is needed, especially those in the Oedipodinae subfamily.

Acknowledgements

We thank our colleague Kristaps Vilks from the University of Latvia, Faculty of Biology, Department of Zoology and Animal Ecology for the help with the collection and translation of Fischer's and Kawall's works. We would also like to thank Mārtiņš Kalniņš from Latvian State Forests for sharing the known localities of the rare species *Sphingonotus caerulans*, *Podisma pedestris*, and *Meconema thalassinum*, as well as the collection of some of the historical literature; Dmitry Telnov for consultations on taxonomy; and Gunita Deksne for useful comments on the earlier versions of the manuscript. We are grateful to all the people who contributed to the knowledge of species distribution by uploading their observations to the Dabasdati.lv and iNaturalist platforms. Finally, we thank the reviewers for useful comments on the manuscript. This research was funded by European Social Fund project "Strengthening of the Capacity of Doctoral Studies at the University of Latvia within the Framework of the New Doctoral Model", identification no. 8.2.2.0/20/I/006.

References

Augstākā Padome (1993) Likums "Par īpaši aizsargājamām dabas teritorijām". Latvijas Vēstnesis, 5, 25.03.1993. https://likumi.lv/ta/id/59994-par-ipasi-aizsargajamam-dabas-teritorijam [Accessed on: 2022-10-28]

Auniņa L (2013) Mire habitats. In: Auniņš A (Ed.) European Union Protected Habitats in Latvia. Interpretation Manual. 2nd revised edn. Latvian Fund of Nature, Ministry of Environmental Protection and Regional Development, Rīga, 320 pp.

Beckmann B, Purse B, Roy D, Roy H, Sutton P, Thomas C (2015) Two species with an unusual combination of traits dominate responses of British grasshoppers and crickets to environmental change. PLoS ONE 10(6): e0130488. https://doi.org/10.1371/journal.pone.0130488

Briede A (2021) Klimats Latvijā. Nacionālā enciklopēdija. https://enciklopedija.lv/skirklis/26052-klimats-Latvijā [Accessed on: 2021-10-26]

Budrys E, Pakalniškis S (2007) The Orthoptera (Insecta) of Lithuania. Acta Zoologica Lituanica 17(2): 105–115. https://doi.org/10.1080/13921657.2007.10512821

Budrys E, Bačianskas V, Budrienė A, Dapkus D, Švitra G, Ūsaitis T (2008) Distribution of four species of Oedipodinae grasshoppers in Lithuania (Orthoptera: Acrididae). New and Rare for Lithuania Insect Species 20: 14–19.

Budrys E, Martinaitis K, Valinčienė K, Ferenca R (2019) First records of *Aiolopus thalassinus* (Fabricius, 1781) and *Euthystira brachyptera* (Ocskay, 1826) (Orthoptera: Acrididae) in Lithuania. Bulletin of the Lithuanian Entomological Society 3(31): 8–10.

California Academy of Sciences (2021) iNaturalist. https://www.inaturalist.org/ [Accessed on: 2021-09-02]

Chandler M, See L, Copas K, Bonde AZ, López BC, Danielsen F, Legind JK, Masinde S, Miller-Rushing A, Newman G, Rosemartin A, Turak E (2017) Contribution of citizen science towards international biodiversity monitoring. Biological Conservation 213: 280–294. https://doi.org/10.1016/j.biocon.2016.09.004

Cigliano M, Braun H, Eades D, Otte D (2022) Orthoptera Species File. Version 5.0/5.0. http://Orthoptera.SpeciesFile.org [Accessed on: 2022-25-10]

Dabas aizsardzības pārvalde (2021) Natura 2000 Sites in Latvia. Nature Conservation Agency Republic of Latvia. https://www.daba.gov.lv/en/natura-2000-sites-latvia [Accessed on: 2021-10-27]

Environment DG (2017) Reporting under Article 17 of the Habitats Directive: Explanatory notes and guidelines for the period 2013–2018. European Environment Agency (EEA), European Topic Centre on Biological Diversity (ETC/BD), Brussels, 188 pp.

Ferenca R, Tamutis V, Martinaitis K (2017) *Myrmecophilus acervorum* (Panzer, 1799) (Orthoptera: Myrmecophilidae)—a new species for Lithuanian Fauna. Bulletin of the Lithuanian Entomological Society 1(29): 8–10.

Fischer J (1778) Versuch einer Naturgeschichte von Livland. J.G.I. Breitkopf, Leipzig, 826 pp.

Gailis J, Kalniņš M, Telnov D (2003) New records on synanthropic Blattoptera and Orthoptera in Latvia. Latvijas Entomologs 40: 34–36.

Gurney A, Lindroth C, Danielsson R (1979) Scandinavian entomologists 5 - Karlis Princis. Insect Systematics & Evolution 10(1): 1–8. https://doi.org/10.1163/187631279X00349

Heller K, Korsunovskaya O, Ragge D, Vedenina V, Willemse F, Zhantiev R, Frantsevich L (1998) Check-list of European Orthoptera. Articulata 7: 1–61.

Hochkirch A, Nieto A, García Criado M, Cálix M, Braud Y, Buzzetti FM, Chobanov D, Odé B, Presa Asensio JJ, Willemse L, Zuna-Kratky T, Barranco Vega P, Bushell M, Clemente ME, Correas JR, Dusoulier F, Ferreira S, Fontana P, García MD, Heller KG, Iorgu IŞ, Ivković S, Kati V, Kleukers R, Krištín A, Lemonnier-Darcemont M, Lemos P, Massa B, Monnerat C, Papapavlou KP, Prunier F, Pushkar T, Roesti C, Rutschmann F, Şirin

D, Skejo J, Szövényi G, Tzirkalli E, Vedenina V, Barat Domenech J, Barros F, Cordero Tapia PJ, Defaut B, Fartmann T, Gomboc S, Gutiérrez-Rodríguez J, Holuša J, Illich I, Karjalainen S, Kočárek P, Korsunovskaya O, Liana A, López H, Morin D, Olmo-Vidal JM, Puskás G, Savitsky V, Stalling T, Tumbrinck J (2016a) European Red List of Grasshoppers, Crickets and Bush-crickets. Publications Office of the European Union, Luxembourg, 86 pp.

Hochkirch A, Willemse LP, Rutschmann F, Chobanov DP, Kleukers R, Kristin A, Presa JJ, Szovenyi G (2016b) *Leptophyes punctatissima*. The IUCN Red List of Threatened Species 2016: e.T44709622A74526293. https://doi.org/10.2305/IUCN.UK2016-3.RLTS.T44709622A74526293.en [Accessed on: 2021-10-06]

Hochkirch A, Willemse LP, Szovenyi G, Rutschmann F, Presa JJ, Kristin A, Kleukers R, Chobanov DP (2016c) *Platycleis albopunctata*. The IUCN Red List of Threatened Species 2016: e.T68451982A74622396. https://www.iucnredlist.org/species/68451982/74622396 [Accessed on: 2021-10-06]

Hochkirch A, Willemse LP, Szovenyi G, Rutschmann F, Presa JJ, Kristin A, Kleukers R, Chobanov DP (2016d) *Tetrix tenuicornis*. The IUCN Red List of Threatened Species 2016: e.T68469416A74530618. https://www.iucnredlist.org/species/68469416/74530618 [Accessed on: 2021-10-06]

Hochkirch A, Willemse LP, Szovenyi G, Rutschmann F, Presa JJ, Kristin A, Kleukers R, Chobanov DP (2016e) *Meconema thalassinum*. The IUCN Red List of Threatened Species 2016: e.T68427417A74540428. https://doi.org/10.2305/IUCN.UK.2016-3.RLTS.T68427417A74540428.en [Accessed on: 2021-10-06]

Kawall J (1864) Die Orthopteren und Neuropteren Kurlands. Korrespondenz-Blatt Des Naturforscher-Vereins Zu Riga 14(11): 155–168.

Kūle L (2021) Latvijas teritorija. Nacionālā enciklopēdija. https://enciklopedija.lv/skirklis/25886-Latvijas-teritorija [Accessed on: 2021-10-26]

Latvijas Dabas Fonds Latvijas Ornitoloģijas biedrība (2021) Dabasdati.lv. https://dabasdati.lv/lv [Accessed on: 2021-11-01]

Linnæus C (1758) Systema naturæ per regna tria naturæ, secundum classes, ordines, genera, species, cum characteribus, differentiis, synonymis, locis. 10th revised edn., Volume 1. Holmiæ, Impensis Direct, Laurentii Salvii, 824 pp. https://doi.org/10.5962/bhl.title.542

Matisons R (2004) Taisnspārņi - Orthoptera (Saltatoria) Latvijā. http://raksti.daba.lv/referaati/2004/RMatisons/ [Accessed on: 2020-10-15]

Matisons R (2005) Taisnspārņu (Orthoptera) sugu sabiedrību salīdzinājums pļavu biotopos Ķemeru nacionālajā parkā. University of Latvia, Rīga, 35 pp.

Ministru kabinets (2004a) Grozījumi Ministru kabineta 2000. gada 14. novembra noteikumos Nr.396 "Noteikumi par īpaši aizsargājamo sugu un ierobežoti izmantojamo īpaši aizsargājamo sugu sarakstu". Latvijas Vēstnesis 20: 1–24.

Ministru kabinets (2004b) Noteikumi par īpaši aizsargājamo sugu un ierobežoti izmantojamo īpaši aizsargājamo sugu sarakstu. Latvijas Vēstnesis 413/417: 1–24.

Miskelly J, Paiero S (2019) Mantodea, Blattodea, Orthoptera, Dermaptera, and Phasmida of Canada. ZooKeys 819: 255–269. https://doi.org/10.3897/zookeys.819.27241

Moulin N (2020) When Citizen Science highlights alien invasive species in France: The case of Indochina mantis, *Hierodula patellifera* (Insecta, Mantodea, Mantidae). Biodiversity Data Journal 8: e46989. https://doi.org/10.3897/BDJ.8.e46989

Ozols E (1963) Lauksaimniecības Entomoloģija. Latvijas Valsts izdevniecība, Rīga, 510 pp.

Panagiotopoulou H, Baca M, Baca K, Sienkiewicz P, Slipinski P, Zmihorski M (2016) Genetic identification of a non-native species introgression into wild population of the field cricket *Gryllus campestris* (Orthoptera: Gryllidae) in Central Europe. European Journal of Entomology 113: 446–455. https://doi.org/10.14411/eje.2016.058

Poniatowski D, Fartmann T (2011) Weather-driven changes in population density determine wing dimorphism in a bush-cricket species. Agriculture, Ecosystems & Environment 145(1): 5–9. https://doi.org/10.1016/j.agee.2010.10.006

Popova EN, Semenov SM, Popov IO (2016) Assessment of possible expansion of the climatic range of Italian locust (*Calliptamus italicus* L.) in Russia in the 21st century at simulated climate changes. Russian Meteorology and Hydrology 41(3): 213–217. https://doi.org/10.3103/S1068373916030079

Priede A (2017) Ievads. In: Ikauniece S (Ed.) Aizsargājamo biotopu saglabāšanas vadlīnijas Latvijā. Meži. Volume 6. Dabas aizsardzības pārvalde, Sigulda, 167 pp.

Princis K (1931) Taisnspārņi. Daba 1: 18–35. https://doi.org/10.1515/9783111692623-004

Princis K (1932) Beitrag zur Geradfluglerfauna Lettlands. Folia Zoologica et Hydrobiologica 4(1): 31–38.

Princis K (1933) Einige für Lettland neue Orthopteren-Arten un Varietäten. Folia Zoologica et Hydrobiologica 5(1): 52–56.

Princis K (1934a) Die Gimmerthal'sche Orthopterensammlung in der naturwissenschaftlichen Abteilung des Dommuseums zu Riga. Folia Zoologica et Hydrobiologica 7(1): 149–151.

Princis K (1934b) Einige für Lettland neue Orthopteren. Sonderabdruch aus dem 28. Jahrgange der "Internationalen Etomologischen Zeitschrift". Guben 28(4/5): 36–49.

Princis K (1935) Zur Biologie von *Stauroderus pullus* Phl. (Orth. Loc.). Sonderabdruch aus dem 29. Jahrgange der "Internationalen Etomologischen Zeitschrift". Guben 29(15/16): 178–186.

Princis K (1936) Ergänzungen und Berichtigungen zur Orthopterenfauna Lettlands (I). Folia Zoologica et Hydrobiologica 9(1): 90–92.

Princis K (1939) Ergänzungen und Berichtigungen zur Orthopterenfauna Lettlands (II). Folia Zoologica et Hydrobiologica 9(2): 361–363.

Princis K (1943) Übersicht und über die Orthopteren-Dermapteren fauna Lettlands. Volume 1 (Nr. 2). Latvju grāmata, Rīga, 96 pp.

Prischepchik OV, Storozhenko SY (2019) To the knowledge of Othoptera of the Stolin district of Brest oblast, Republic of Belarus. Far Eastern Entomologist = Dal'nevostochnyi Entomolog 393: 24–28. https://doi.org/10.25221/fee.393.4

Rove I (2013a) Coastal sand dunes and inland dunes. In: Auniņš A (Ed.) European Union Protected Habitats in Latvia. Interpretation Manual. 2nd revised edn. Latvian Fund of Nature, Ministry of Environmental Protection and Regional Development, Rīga, 320 pp.

Rove I (2013b) European dry heaths. In: Auniņš A (Ed.) European Union Protected Habitats in Latvia. Interpretation Manual. 2nd revised edn. Latvian Fund of Nature, Ministry of Environmental Protection and Regional Development, Rīga, 320 pp.

Rozenfelde R (2018) Virsāju kontrolētās dedzināšanas ietekme uz taisnspārņu (Orthoptera) daudzveidību aizsargājamo ainavu apvidū "Ādaži". In: Priede A (Ed.) Aktuāli biotopu un sugu dzīvotņu apsaimniekošanas piemēri Latvijā. Dabas aizsardzības pārvalde, Sigulda, 101–115 pp. https://www.daba.gov.lv/lv/media/8687/download [Accessed on: 2020-10-15]

Rozenfelde R, Reimane L, Spuņģis V (2017) Grasshopper and ground beetle fauna of calcareous grasslands in Abava River valley. In: Rūsiņa S (Ed.) Outstanding Semi-natural Grassland Sites in Latvia: Biodiversity, Management, Restoration. University of Latvia, Rīga, 77–93 pp.

Rūsiņa S (2013) Grassland habitats. In: Auniņš A (Ed.) European Union Protected Habitats in Latvia. Interpretation Manual. 2nd revised edn. Latvian Fund of Nature, Ministry of Environmental Protection and Regional Development, Rīga, 320 pp.

Rūsiņa S (2020) Zālāju ekosistēmas Latvijā. Nacionālā enciklopēija. https://enciklopedija.lv/skirklis/7209-zālāju-ekosistēmas-Latvijā [Accessed on: 2021-10-26]

Saeima (1997) "Aizsargjoslu likums". Latvijas Vēstnesis, 56/57, 25.02.1997. https://likumi.lv/ta/id/42348-aizsargjoslu-likums [Accessed on: 2022-10-28]

Saeima (2000) "Sugu un biotopu aizsardazības likums". Latvijas Vēstnesis, 121/122, 05.04.2000. https://likumi.lv/ta/id/3941-sugu-un-biotopu-aizsardzibas-likums [Accessed on: 2022-10-28]

Sokolovskis K, Suveizda J (2012) First record of *Phaneroptera falcata* (Poda, 1761) (Orthoptera, Phaneropteridae) in Latvia. Latvijas Entomologs 51: 155–157.

Spuņģis V (2007) Fauna and ecology of grasshoppers (Orthoptera) in the coastal dune habitats in Ziemupe Nature Reserve, Latvia. Latvijas Entomologs 44: 58–68.

Spuņģis V (2013) Grasshoppers and locusts in the calcareous fens in Latvia. 71st Scientific Conference of University of Latvia, Biology section, Zoology and Animal Ecology subsection, Riga, 01.02.2013. Conference abstract.

Spuņģis V, Kalniņš M (2002) Taisnspārņi – Orthoptera. Entomological society of Latvia. http://leb.daba.lv/Orthoptera.htm [Accessed on: 2022-10-14]

Spuris Z (1957) Saltatoria – Taisnspārņi. In: Pētersone A (Ed.) Latvijas PSR dzīvnieku noteicējs. Latvijas Valsts izdevniecība, Rīga, 871 pp.

Spuris Z (1998) Rare and threatened species of plants and animals. Invertebrates. In: Andrušaitis G (Ed.) Red Data Book of Latvia. Volume 4. Institute of Biology, University of Latvia, Rīga, 388 pp.

Ūsaitis T (2019) New data on the distribution of *Bryodemella tuberculata* (Fabricius, 1775) (Orthoptera: Acrididae) in Lithuania. Bulletin of the Lithuanian Entomological Society 3(31): 11–12.

Willemse F, Heller K (2013) Orthoptera. Fauna Europea. https://fauna-eu.org [Accessed on: 2021-9-02]

Zuna-Kratky T, Fontana P, Roesti C, Braud Y, Hochkirch A, Monnerat C, Rutschmann F, Presa JJ (2016) *Bryodemella tuberculata*. The IUCN Red List of Threatened Species 2016: e.T16084462A70292211. https://www.iucnredlist.org/species/16084462/70292211 [Accessed on: 2021-6-10]

Supplementary material 1

Orthoptera occurrence data

Authors: Rūta Starka, Uģis Piterāns, Voldemārs Spuņģis

Data type: occurrences

Explanation note: The data table contains over 1500 observations (dating from 2003 to 2021) of 42 Orthoptera species in Latvia. The columns contain the following information: A – species scientific name, B – observation date, C – data source, D and E – x and y coordinates in LKS-92 coordinate system, F and G – international coordinates (latitude, longitude).

Link: https://doi.org/10.3897/zookeys.1134.95637.suppl1

Supplementary material 2

Observational notes on Orthoptera species in Latvia

Authors: Rūta Starka, Uģis Piterāns, Voldemārs Spuņģis

Data type: text

Explanation note: Information from historic resources, ecology research, species lists and observation data bases is combined to give a brief analysis of the known history, habitat preferences and occurrence of Orthoptera species in Latvia is presented. All historically used synonyms for every species is provided.

Link: https://doi.org/10.3897/zookeys.1134.95637.suppl2

ZooKeys 1134: 52–73 (2022)
doi: 10.3897/zookeys.1134.89267
https://zookeys.pensoft.net

RESEARCH ARTICLE

A peer-reviewed open-access journal
ZooKeys
Launched to accelerate biodiversity research

A new species of *Andricus* Hartig, 1840 (Hymenoptera, Cynipidae) from China, with references to DNA taxonomy and *Wolbachia* infection

Yin Pang[1*], Cheng-Yuan Su[1*], Jun-Qiao Zhu[1], Xiao-Hui Yang[2], Jia-Lian Zhong[1], Dao-Hong Zhu[1], Zhiwei Liu[3]

1 *Laboratory of Insect Behavior and Evolutionary Ecology, College of Life Science and Technology, Central South University of Forestry and Technology, Changsha, Hunan, 410004, China* **2** *School of Life Sciences, Hunan Normal University, Changsha, Hunan, 410081, China* **3** *Biological Sciences Department, Eastern Illinois University, Charleston, Illinois 61920, USA*

Corresponding authors: Dao-Hong Zhu (daohongzhu@yeah.net), Zhiwei Liu (zliu@eiu.edu)

Academic editor: Andreas Köhler | Received 19 June 2022 | Accepted 13 November 2022 | Published 7 December 2022

https://zoobank.org/B0A9A45F-CDA6-4E37-8DD3-A9D31C84C698

Citation: Pang Y, Su C-Y, Zhu J-Q, Yang X-H, Zhong J-L, Zhu D-H, Liu Z (2022) A new species of *Andricus* Hartig, 1840 (Hymenoptera, Cynipidae) from China, with references to DNA taxonomy and *Wolbachia* infection. ZooKeys 1134: 52–73. https://doi.org/10.3897/zookeys.1134.89267

Abstract

In the present paper, a new species of cynipid gall wasp, *Andricus elodeoides* Liu & Pang, is described from several provinces in southern China. The new species is closely related to the recently redescribed *A. mairei* (Kieffer, 1906). In addition to differences in adult and gall morphology, the new species is also readily separated by COI sequences, with a 6.2–8.9% genetic distance between populations of the new species and those of *A. mairei*. A contrasting difference in sex ratios was also observed between the two species, with *A. elodeoides* extremely female-biased (95.5–97.8% female) while *A. mairei* male-biased to more balanced (5.4–43.5% female). PCR screening for *Wolbachia* infection further revealed contrasting infection rates between populations of *A. elodeoides* and *A. mairei*: the *Wolbachia* infection rate was 0% in *A. elodeoides* and 100% in *A. mairei*. Cytoplasmic incompatibility induced by *Wolbachia* is proposed as a potential mechanism of speciation of the sympatric *A. elodeoides* and *A. mairei*.

Keywords

Andricus elodeoides, gall wasp, phylogeny, *Quercus serrata*, taxonomy

* These authors contributed equally to the study.

Introduction

The genus *Andricus* Hartig, 1840 (Hymenoptera, Cynipoidea, Cynipidae, Cynipini) is the largest genus of the oak-gall wasp tribe Cynipini, currently comprising approximately 400 known species (Melika 2006) and making up 40% of the known species diversity of the tribe (Wachi et al. 2011). The genus is predominantly Holarctic, with the highest recorded species diversity from the Nearctic and Western Palearctic (Wang et al. 2013). However, a number of new species of the genus have also been described in the last decade or so from Mesoamerica in the Neotropical realm (Melika et al. 2009a, b; Pujade-Villar et al. 2016) and the Oriental realm (Tang et al. 2009, 2012; Wang et al. 2013; Pujade-Villar et al. 2014; Ide et al. 2018). In Eastern Asia, which stretches from the Palearctic to the Oriental, 19 *Andricus* species are known (Ide et al. 2018; Penzes et al. 2018; Pujade-Villar et al. 2020).

The unusually high diversity of *Andricus* species among all the genera of the tribe Cynipini may be an artifact, as the genus is not well defined and often has been treated as a "trash can" genus in Cynipini (Melika 2006). In their taxonomic review of the world genera of cynipine wasps, Melika and Abrahamson (2002) treated several previously recognized genera as junior synonyms of the genus because of the lack of reliable diagnostic characteristics, rather than because of the existence of defining synapomorphies (Melika and Abrahamson 2002). One of the synonymized genera, *Druon* Kinsey, 1937 has since been re-established as a valid genus (Cuesta-Porta et al. 2022). Although multiple phylogenetic studies involving Cynipini have invariably shown *Andricus* to be paraphyletic or polyphyletic (Stone and Cook 1998; Cook et al. 2002; Rokas et al. 2003; Stone and Schönrogge 2003; Liljeblad et al. 2008; Ronquist et al. 2015), the current concept of the genus is still largely based on that of Melika and Abrahamson (2002).

One of the genera synonymized with *Andricus* Hartig, 1840 by Melika and Abrahamson (2002) is *Parandricus* Kieffer, 1906, which is known from China and includes a single species, *P. mairei* Kieffer, 1906. A detailed redescription of the species was done based on specimens collected from Zhejiang Province of China because the original type of *P. mairei* Kieffer, 1906 was lost and the original description was inadequate by today's standards (Pujade-Villar et al. 2020). In the last few years, we have reared a large series of specimens that apparently belong to multiple, known or unknown, species of *Andricus*, including *A. mairei* (Kieffer, 1906) (Yang et al. 2012). In the present paper, we describe a new species from that series of *Andricus* specimens and provide a detailed comparison between it and the apparently closely related *A. mairei* (Kieffer 1906). We also sequenced the mitochondrial COI gene for both species for DNA barcoding as well as the nuclear 28S D2 region to place the new species within the current phylogenetic framework of all *Andricus* species that had both COI and 28S sequences available.

Materials and methods

Specimen collection

The galls of gall wasps were collected from 12 locations in six provinces in southern China in late spring to early summer from 2012 to 2019 (Table 1). The collected galls were cage-reared at room temperature in the laboratory of the College of Life Science and Technology, Central South University of Forestry and Technology (CSUFT) and checked daily for emergence. Adult wasps were directly preserved in 100% ethanol within 2 days after emergence and stored in freezer at −80 °C until being retrieved for morphological and molecular studies.

Morphological observations

Specimens for conventional morphological examination were air dried at room temperature before mounting. Specimens mounted to pinned triangle-card paper were studied under a stereomicroscope (SZX7, Olympus, Japan) and automatically stacked photographs were taken with Leica M205C microscope system (Leica, Germany) equipped with Leica DMC6200 digital camera connected to a computer. Additional specimens were dissected out and transferred to diluted ammonia (5%) and kept overnight to remove debris that might interfere with observation. Cleansed parts were then rinsed in distilled water and dehydrated gradually through 25%, 50%, 75%, and 100% ethanol solutions, and finally stored in 100% ethanol. Dehydrated specimen parts were air-dried before being mounted onto aluminum stub (Ted Pella, Redding, CA, USA) with copper conductive tape (3M). Gold-coated specimens were examined with JEOL JSM-6380Lv SEM (JEOL, Japan) at CSUFT with 15 KV voltage, and selected frames were saved as digitized high-resolution TIFF images.

We follow Ronquist and Nordlander (1989) and Ronquist (1995) for structural terminology, Melika (2006) for measurement definitions, and Harris (1979) for surface sculpture descriptions. Abbreviations: F1 and F2 = the first and second flagellomeres, respectively; POL (post-ocellar distance) = the distance between the inner margins of the posterior ocelli; OOL (ocellar-ocular distance) = the distance from the outer margin of a posterior ocellus to the inner margin of the compound eye; LOL (lateral-frontal ocelli distance) = the distance between anterior and lateral ocelli. Type specimens are deposited in Insect Collection, Central South University of Forestry and Technology (CSUFT), Changsha, Hunan.

DNA extraction and sequencing

Three individuals from each population of two gall wasp species were used for DNA extraction. The insects were washed in sterile water before DNA extraction to avoid

Table 1. Collection information, female ratio and *Wolbachia* infection in *A. elodeoides* sp. nov. and *A. mairei*.

Location(code)	Coordinates	Date of gall collection	Date of adult emergence	Insect species	Female: male	*Wolbachia* infect frequency (%)
Xinyang, Henan (XY)	32°02'N, 113°53'E	May, 2012	May, 2012	*A. mairei*	8: 46 (14.8%*)	100 (20)†
				A. elodeoides	64: 2 (97.0%)	0 (20)
Jinzhai, Anhui (JZ)	31°38'N, 115°58'E	May, 2014	May, 2014	*A. mairei*	64: 318 (16.8%)	100 (20)
				A. elodeoides	224: 5 (97.8%)	0 (40)
		May, 2015	May, 2015	*A. mairei*	12: 63 (16.0%)	100 (20)
				A. elodeoides	78: 2 (97.5%)	0 (20)
		May, 2016	May, 2016	*A. mairei*	19: 213 (8.2%)	100 (20)
				A. elodeoides	86: 3 (96.6%)	0 (20)
		May, 2017	May, 2017	*A. mairei*	9: 43 (17.3%)	100 (20)
				A. elodeoides	123: 4 (96.9%)	0 (20)
		May, 2018	May, 2018	*A. mairei*	29: 512 (5.4%)	–
				A. elodeoides	128: 6 (95.5%)	–
		May, 2019	May, 2019	*A. mairei*	46: 612 (7.0%)	–
				A. elodeoides	224: 8 (96.6%)	–
Shucheng, Anhui (SHC)	31°21'N, 116°04'E	May, 2016	May, 2016	*A. mairei*	34: 104 (24.6%)	100 (20)
				A. elodeoides	426: 13 (97.0%)	0 (40)
		May, 2017	May, 2017	*A. mairei*	6: 46 (11.5%)	100 (20)
				A. elodeoides	91: 2 (97.8%)	0 (20)
		May, 2018	May, 2018	*A. mairei*	16: 65 (19.8%)	100 (20)
				A. elodeoides	73: 3 (96.1%)	0 (20)
		May, 2019	May, 2019	*A. mairei*	9: 56 (13.8%)	100 (20)
				A. elodeoides	129: 6 (95.6%)	0 (20)
Taihu, Anhui (TH)	30°34'N, 116°04'E	May, 2016	May, 2016	*A. mairei*	12: 32 (27.3%)	100 (20)
				A. elodeoides	94: 3 (96.9%)	0 (40)
Wuhan, Hubei (WH)	30°31'N, 114°31'E	May, 2014	May, 2014	*A. mairei*	8: 12 (40.0%)	100 (20)
				A. elodeoides	166: 6 (96.5%)	0 (40)
Changsha, Hunan CS)	28°25'N, 113°07'E	May, 2016	May, 2016	*A. mairei*	102: 136 (42.9%)	100 (20)
		May, 2017	May, 2017	*A. mairei*	258: 349 (42.9%)	–
		May, 2018	May, 2018	*A. mairei*	121: 157 (43.5%)	–
Suichang, Zhejiang (SUC)	28°37'N, 119°19'E	April, 2018	May, 2018	*A. elodeoides*	79: 2 (97.5%)	0 (30)
				A. mairei	124: 987 (11.2%)	100 (20)
Qingyuan, Zhejiang (QY)	27°44'N, 119°15'E	April, 2018	May, 2018	*A. elodeoides*	76: 3 (96.2%)	0 (20)
				A. mairei	23: 245 (8.6%)	100 (20)
Zhenghe, Fujian (ZH)	27°23'N, 118°2'E	April, 2018	May, 2018	*A. mairei*	66: 568 (10.4%)	100 (20)
Zhouning, Fujian (ZN)	27°13'N, 119°20'E	April, 2018	May, 2018	*A. mairei*	13: 86 (13.1%)	100 (20)
Guiding, Guizhou (GD)	26°37'N, 107°14'E	May, 2017	Jun, 2017	*A. mairei*	6: 24 (20.0%)	100 (20)
Shaoguan, Guangdong (SG)	24°59'N, 113°01'E	April, 2017	May, 2017	*A. mairei*	34: 256 (11.7%)	100 (20)

* Percentage of females; † The number in parentheses refers to the number of insect individuals screened.

surface contamination. Total DNA was extracted from each individual using SDS/proteinase K digestion and a phenol-chloroform extraction. Extracted DNA pellets were air dried, resuspended in 50 µl sterile water, and then stored at 4 °C before being processed for PCR and sequencing.

For phylogenetic analysis, we chose a specific region of the mitochondrial cytochrome c oxidase subunit I gene (COI) and the nuclear large ribosomal subunit gene (28S), which were amplified with the primes HCO-2198 (5'-TAAACTTCAGGGTGACCAAAAAATCA-3') and LCO-1490 (5'-GGTCAACAAATCATAAAGATATTGG-3') (Folmer et al. 1994), and D2F (5'-CGTGTTGCTTGATAGTGCAGC-3') and D2R

Table 2. Sequences of mitochondrial COI and nuclear 28S genes used in the phylogenetic analysis.

Gall wasp	COI	28S D2	Reference
Andricus caputmedusae	DQ012619	EF030040	Liljeblad (2002)
Andricus curvator	DQ012621	AF395155	Liljeblad (2002)
Andricus coriarius	DQ012620	DQ012579	Liljeblad (2002)
Andricus crystallinus	MT179597	MT183614	Pujade-Villar et al. (2020)
Andricus hakonensis	MT179612	MT183628	Pujade-Villar et al. (2020)
Andricus kollari	AF395176	AF395156	Rokas et al. (2002)
Andricus pictus	DQ012625	DQ012583	Liljeblad (2002)
Andricus quercusstrobilana	DQ012617	DQ012576	Liljeblad (2002)
Andricus rochai	MT179600	MT183671	Pujade-Villar et al. (2020)
Andricus xishuanghannaus	MT179618	MT183634	Pujade-Villar et al. (2020)
Andricus mairei (ILV92)	MT179620		Pujade-Villar et al. (2020)
(ILV90)	MT179616		
(ILV87)	MT179614		
(ILV86)	MT179613		
(ILV32)	MT179604		
(ILV31)	MT179603		
(ILV30)	MT179602		
(ILV91)	MT179617		
Andricus mairei	ON803612–ON803624	ON911591–ON911603	Present study
Andricus elodeoides	ON803625–ON803631	ON911604–ON911610	Present study
Melikaiella bicolor	MT179619	MT183623	Pujade-Villar et al. (2020)
Dryocosmus liui	MG754067	MN633412	Pang et al. (2018); Pang et al. (2020)

(5' TCAAGACGGGTCCTGAAAGT 3') (Dowton and Austin 2001), respectively. This gene fragment was chosen because of its suitability for recovering inter- and intrageneric phylogenies within the Hymenoptera in general and Cynipidae in particular (Rokas et al. 2002) as well as sequence availability for a reasonable number of congeneric species from public depositories. The PCR mixture was composed of 1 μl of PrimeSTAR HS DNA Polymerase (Takara Biomedical Technology Co., Dalian, China), 10 μl of buffer, 4 μl of dNTPs, 1 μl of each primer, and 2 μl of DNA with water added to achieve a total volume of 50 μl. The amplification was conducted using a C1000 Touch thermal cycler (Bio-Rad, Hercules, CA, United States). The cycling conditions were 98 °C for 3 min, 35 cycles of 98 °C for 10 s, 50–57 °C for 30 s, and 72 °C for 1 min. Amplified PCR products were sequenced in both directions using an ABI 3730XLDNA sequencer (Applied Biosystems, Foster City, CA, USA) with M13F/R at Wuhan Icongene Co., Ltd. The sequences have been deposited in GenBank under the following accession numbers: COI ON803612 to ON803631 and 28S ON911591 to ON911610 (Table 2).

Phylogenetic analysis

The COI and 28S gene sequences of 11 species of *Andricus* (including eight populations of *A. mairei*) and *Dryocosmus liui* and *Melikaiella bicolor* (as outgroups) were retrieved from GenBank (https://www.ncbi.nlm.nih.gov/genbank/) (Table 2). The final dataset consists of 14 species including the new species and outgroup. Multiple sequence alignment was performed using ClustalW (Thompson et al. 1994) implemented in MEGA 11.0 (Kumar et al. 2016) using default parameters. ClustalW

aligned sequences were then visually edited in MEGA 11.0 and trimmed, resulting a final aligned length of 1154 bp nucleotides for COI and 1053 bp nucleotides for 28S.

The final dataset was subjected to MEGA 11.0 for evaluation of best fit nucleotide substitution model (Nei and Kumar 2000) using the maximum likelihood (ML) method with default settings except that we used "very strong" branch swap filter. Phylogenetic analysis was conducted using MrBayes 3.2.6 x64 for Windows (Ronquist et al. 2012) (Bayesian inference method, BI), assuming a generalized Time-reversible (GTR) model with gamma distributed rate variation across sites (+G) based on best fit nucleotide substitution model evaluation performed earlier. For Bayesian analysis, two independent runs were performed with the default priors and MCMC parameters except the following: nst = 6, rates = gamma, MCMC runs comprised 10 million generations sampled at every 1,000 generations with 30% burn-in time. Convergence was achieved as being diagnosed by the average standard deviation of split frequencies between the two independent runs (<0.01) and PSRF values (1 with < 1% deviation). The final tree from both analyses was rooted with *D. liui* and *M. bicolor* based on published phylogeny of Cynipidae (Ronquist et al. 2015).

To compare directly with a recent study on *A. mairei* and related species based solely on COI (Pujade-Villar et al. 2020), we also performed a phylogenetic analysis based on COI only to include the sequences of *A. mairei* from various populations published in that study.

Finally, the pair-wise genetic distance in the COI sequences from all populations of *A. elodeoides* and *A. mairei*, and other two *Andricus* species were calculated, using the MEGA 11.0 (Kumar et al. 2016).

Wolbachia screening

Wolbachia infections were screened by PCR with the *Wolbachia*-specific primers wsp-81F and wsp-691R that amplify a 575–625 bp fragment of the *wsp* gene encoding *Wolbachia* surface protein (Zhou et al. 1998). To verify the presence of *Wolbachia* infection in *A. elodeoides*, *gatB*, *coax*, *ftsZ*, and *hcpA* genes were amplified for various populations using the respective primers reported by Baldo et al. (2006). Amplification methods and conditions were as previously described (Hou et al. 2020).

Results

Taxonomy

Andricus elodeoides **Liu & Pang, sp. nov.**
https://zoobank.org/8FD547C-C534-4F23-8FE8-1E60987D8959
Figs 1–13

Type materials. ***Holotype*** ♀; ***Paratypes*****:** 10♀, 8♂♂. China, Hunan Province, Changsha City (113°07'N, 28°25'E), 2011-V-11–20, leg. Xiao-Hui Yang, deposited in Insect Collection, Central South University of Forestry and Technology (CSUFT), Changsha, Hunan.

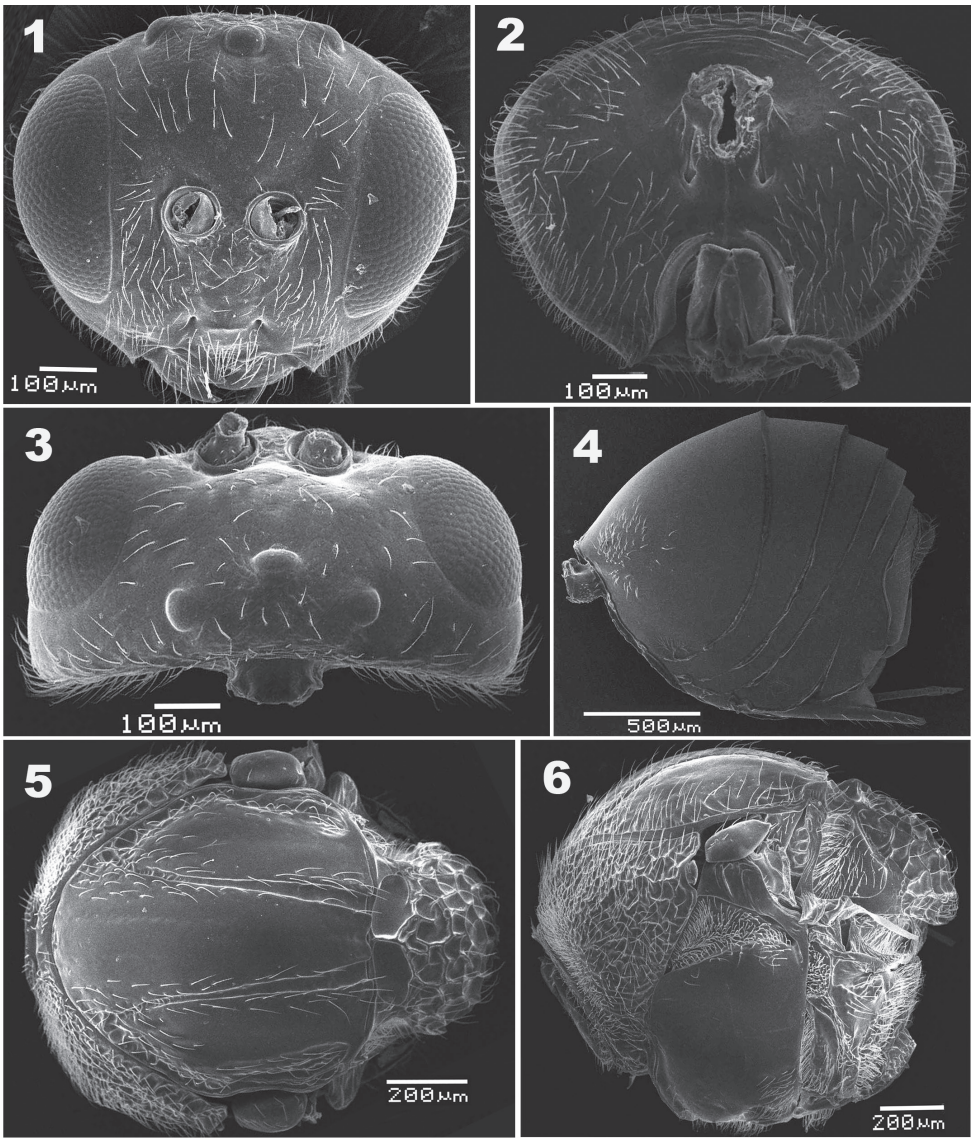

Figures 1–6. *Andricus elodeoides* sp. nov., female **1** head in anterior view **2** head in posterior view **3** head in dorsal view **4** metasoma in lateral view **5** mesosoma in dorsal view **6** mesosoma in lateral view.

Etymology. The species epithet derived from *Elodea*, the genus name of the aquatic plants well known as waterweeds, referring to the superficial resemblance of the cluster of galls of the species to these plants.

Additional materials examined. Same data as holotype, 3♂, 3♀ (Cheng-Yuan Su leg.). Jinzhai (31°38'N, 115°58'E), Anhui province. 3♂, 3♀ (Cheng-Yuan Su leg.). Wuhan (30°31'N, 114°31'E), Hubei province. 3♂, 3♀ (Cheng-Yuan Su leg.). Suichang (28°37'N, 119°19'E), Zhejiang province. 1♂, 1♀ (Cheng-Yuan Su leg.).

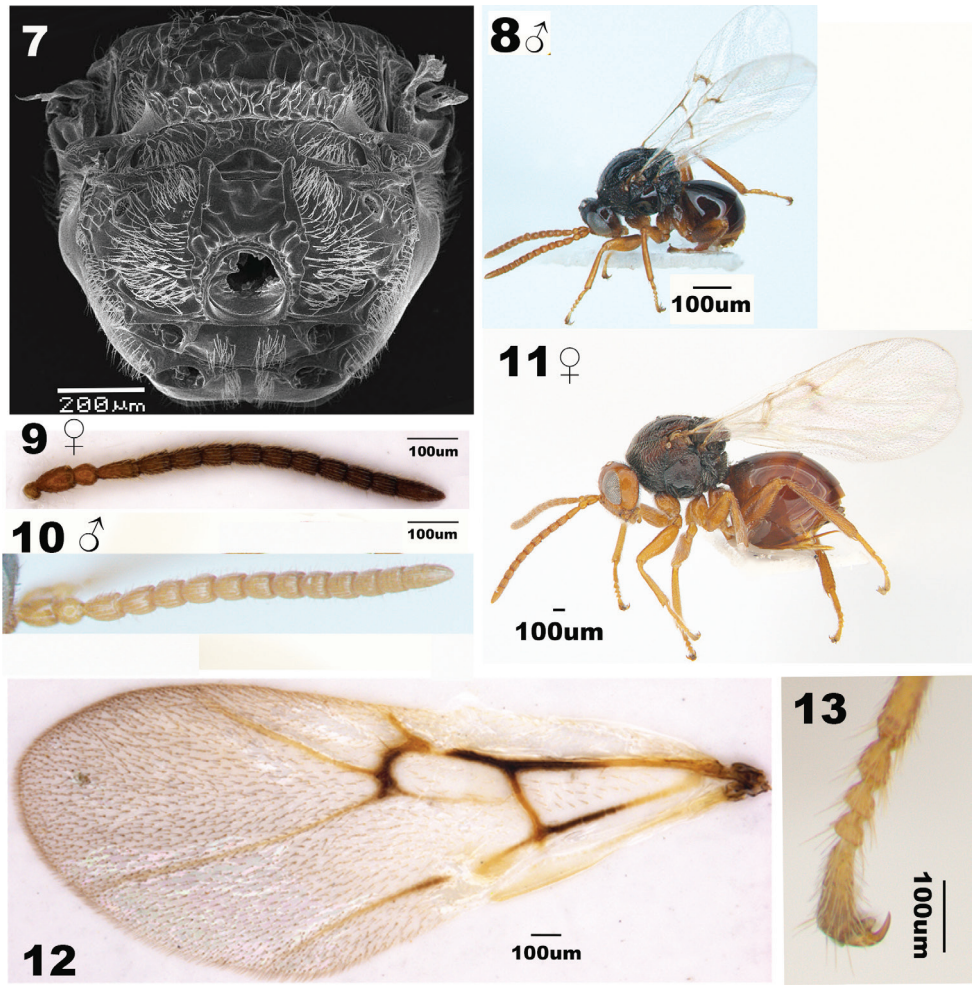

Figures 7–13. *Andricus elodeoides* sp. nov. **7** propodeum of female in dorsal view **8** general habitus of male **9** female antenna **10** male antenna **11** general habitus of female **12** female forewing **13** the claw of hind leg of female.

Xinyang (32°02'N, 113°53'E), Henan province,. 3♂, 3♀ (Cheng-Yuan Su leg.). Taihu (30°34'N, 116°04'E), Anhui province. 3♂, 3♀ (Cheng-Yuan Su leg.), Qingyuan (27°44'N, 119°15'E), Zhejiang province. 3♂, 3♀ (Cheng-Yuan Su leg.), Zhenghe (27°23'N, 118°52'E), Fujian province. 3♂, 3♀ (Cheng-Yuan Su leg.), Zhouning (27°13'N, 119°20'E), Fujian province. 3♂, 3♀ (Cheng-Yuan Su leg.), Guiding (26°37'N, 107°14'E), Guizhou province. 3♂, 3♀ (Cheng-Yuan Su leg.), Shaoguan (24°59'N, 113°01'E), Guangdong province.

Diagnosis. The new species is similar to *A. mairei* (Kieffer 1906), but differs from the latter in having: 1) vertex and frons glabrate with long setae evenly-spaced on vertex and scatted on frons in the new species (Fig. 3), whereas vertex coriaceous and

vertex and frons with sparse short setae in *A. mairei* (Pujade-Villar et al. 2020: fig. 1b, d); 2) male antenna F1 strongly curved medially in the new species (Fig. 10), but straight in *A. mairei* (Pujade-Villar et al. 2020: fig. 2b); 3) mesopleuron glabrous in the new species (Fig. 6), whereas with weak longitudinal striation medially in *A. mairei* (Pujade-Villar et al. 2020: fig. 3c, d, but compare with fig. 3e); 4) mature galls of *A. elodeoides* are straight and cylindrical, fully covered with dense resinous white hairs (Fig. 14), whereas the galls of *A. mairei* are curved or strongly tapering in distal half, mostly shining smooth with an apical cluster of white hairs (Fig. 15).

Description. Female: body length 2.6–2.8 mm (N = 5).

***Coloration*.** Head area of compound eyes and frons black and gena yellow. Antenna uniformly dark brown to black, except for scape, pedicel and F1 brownish yellow. Mandible, maxillar and labial palpi dark brown. Legs uniformly brownish yellow. Mesosoma black; metasoma mostly reddish brown and posteriorly black. Hypopygial spine reddish brown.

Forewing with distinct veins R+Sc, R1+Sc, R1, Rs, Rs+M (somewhat faint basally), M, 2r, M+Cu1, Cu1, Cu1b and Cu1a; areolet distinct and small; marginal cell about 2.6–3.0 times as long as wide; all visible veins yellow except for the distal half of R+Sc, R1+Sc, 2r, and M. The distal half of M+Cu1 black (Fig. 12).

Head coriaceous, 1.2 times as wide as high in anterior view, nearly oval, broader than mesosoma in front view and 2.2 times as broad as long in dorsal view. Gena not broadened behind eyes in dorsal view. Height of eye about 3.4 times the length of malar space. Frons glabrate with evenly spaced long setae, with ocellar triangle indistinctly rugose; lower face and malar space glabrate and distinctly setose. Clypeus distinct and impressed; epistomal sulcus distinct; anterior tentorial pits small, but distinct; clypeo-pleurostomal line distinct. Transfacial distance slightly bigger than height of eye; distance between inner margin of eye and outer rim of antennal torulus slightly wider than distance between antennal toruli, but as wide as diameter of torulus (Fig. 1). Posterior ocelli widely separated from each other, ratios of POL/OOL, POL/LOL, and LOL/OOL 2.1, 2.7 and 0.9, respectively. In dorsal view, posterior margin of anterior ocellus nearly aligned with anterior margin of posterior ocelli (Fig. 3). Vertex glabrate, covered with scattered long setae. Gena coriarious, posteriorly with sparce long setae; postgena mostly glabrate with dense setae in outer edge. Occiput very finely imbricate and setose except medially; posterior tentorial pits distinct. Gular sulci absent; area around occipital foramen glabrous (Fig. 2).

Antenna filiform with 11 flagellomeres, slightly tapering toward apex; pedicel subspherical; relative lengths of scape, pedicel and F1-F11: 10:6:11:9:9:8:8:8:7:7:6:6:13; placoid sensillae distinctly visible on F2–F11 (Fig. 9).

Mesosoma longer than high in lateral view. Pronotum median length two ninth of length of outer lateral margin. Anterior plate of pronotum areolate to rugose and densely setose laterally (Fig. 6); Mesoscutum nearly as long as width measured at anterior tip of tegulae, with some small foveae and setae along outer edge. Notauli distinct and glabrous, lined with setae along sides, and slightly broadened posteriorly.

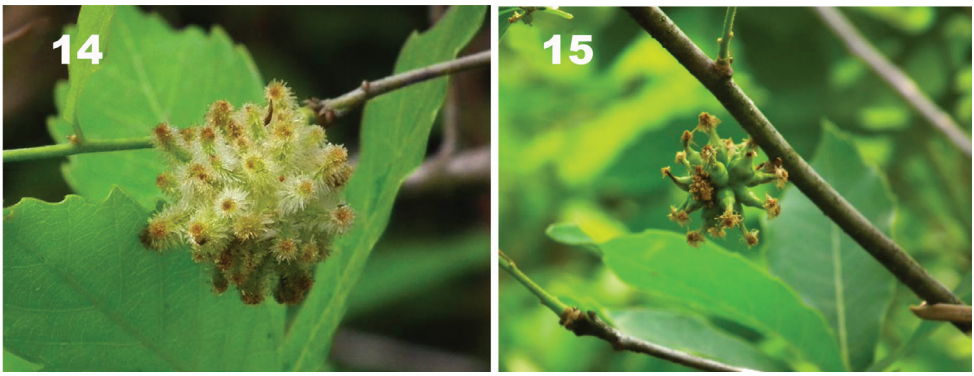

Figures 14, 15. Galls on *Quercus serrata* **14** *Andricus elodeoides* sp. nov. **15** *Andricus mairei*.

Mesoscutellum broader than long, areolate-rugose and sparsely setose. Scutellar foveae deeply impressed and glabrous, separated by a median carina. Mesopleural triangle glabrate and densely setose. Metapleural sulcus reaching mesopleuron in upper 2/3 of its height; metapleuron glabrate with sparse setae (Fig. 6). Median dorsellum area rugose with dense setae. Propodeum with long and dense setae; lateral propodeal carinae distinct and parallel; median propodeal area confused-rugulose, lateral propodeal area with dense long and appressed setae (Fig. 7). Nucha short, width as long in height and lateral view, and longitudinally costate with posterior punctate-areolate ring (Fig. 6).

Metasoma 1.2 times as long as high in lateral view; abdominal tergite II 1.5 times as high as long in lateral view, laterally with anterior patch of short setae; tergite VII dorsally and VIII with long setae. Prominent part of hypopygium slender, distally not pointed; and ventrally with a row of short setae (Fig. 4).

Male: Similar to female, but different as below. Antenna with 12 flagellomeres, length of scape 1.25 times as long as wide; pedicel almost same as long as broad. F1 strongly curved medially. Lengths of scape, pedicel and F1–F12: 10:10:7:8:8:7:7:7:7:7:7:14. Upper face black, lower face yellow (Figs 8, 10).

Gall. Galls are monolocular and form clusters of 50–60 galls on twigs of host plant. Galls are covered with very dense resinous white hairs, which become brown at the terminal of the galls as galls mature. Individual galls straight and cylindrical (Fig. 14), but not curved or strongly tapering in distal half as in *A. mairei* (Fig. 15).

Biology. All specimens emerged from galls collected from *Quercus serrata*. The adults of the new species appeared in early to mid-May (which overlaps with the emergence period of *A. mairei*). Populations were extremely female-biased at 95.5–97.8% (while that of *A. mairei* were 5.4–43.5%) (Table 1).

Distribution. The new species is currently known from China in several provinces in the middle to lower reaches of the Yangtze River, including Henan (Xinyang), Anhui (Jinzhai, Shucheng, and Taihu), Hubei (Wuhan), Hunan (Changsha and Shaoyang), and Zhejiang (Suichang and Qingyuan).

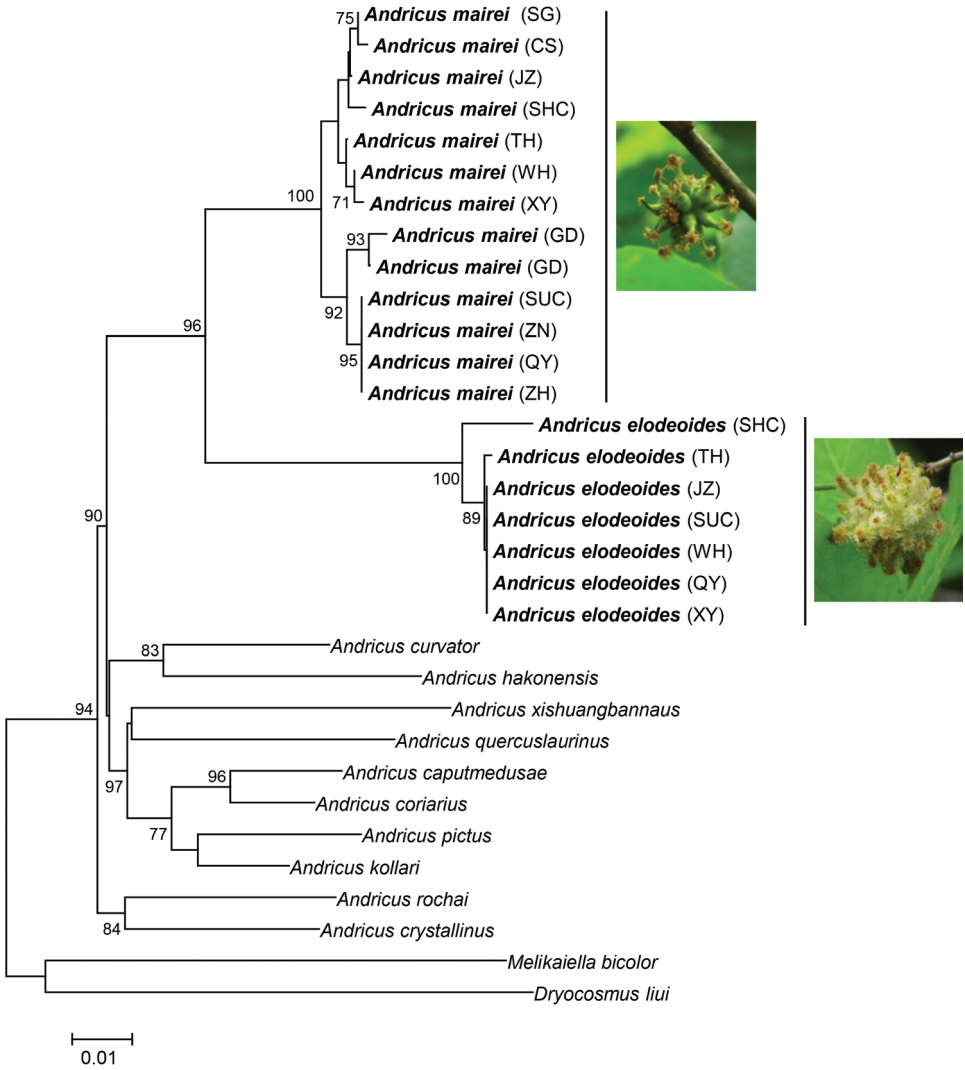

Figure 16. Bayesian phylogenetic tree of *A. elodeoides* sp. nov. and other *Andricus* species based on COI and 28S sequences. Bold font refers to the sequence obtained in this study, and others are downloaded from NCBI. The photograph on the right refers to the gall of adult emergence. The letters in parentheses indicate the sampled populations shown in Table 1. The length of the branches is drawn to scale of genetic distance and the number over branches is posterior probability. *Melikaiella bicolor* and *Dryocosmus liui* were used as the outgroup.

Molecular phylogeny

The Bayesian and maximum-likelihood phylogenetic trees of various populations of *A. elodeoides*, *A. mairei*, and other *Andricus* species based on the COI and 28S genes had identical topology while showing minor differences in support level for some nodes. According to the Bayesian trees presented here (Fig. 16), the sampled populations of

A. elodeoides and *A. mairei* form their own monophyletic clades, and the two species are sister to each other. The genetic distance between the two species is similar to other *Andricus* species pairs, while the distance between this clade and the other including *Andricus* species is rather distinct (Fig. 16).

In the COI tree, all populations of *A. mairei* from Pujade-Villar et al. (2020) formed a single clade with our sampled populations of the species, except for "*A. mairei* ILV91" (MT179617) from Pujade-Villar et al. (2020), which fell into the *A. elodeoides* clade (Fig. 17).

Pair-wise comparison of the COI gene segment used in this study showed interspecific genetic distances ranged from 6.2 to 11.7% among *Andricus* species. In *A. elodeoides* and *A. mairei*, the interspecific genetic distance ranged from 6.2 to 8.9%. The level of intraspecific genetic variation in *A. mairei* was higher than that in *A. elodeoides*. The intraspecific genetic distances were 0–1.8% in *A. elodeoides* and 0–2.6% in *A. mairei*, while the distance between "*A. mairei* ILV91" and *A. elodeoides*, "*A. mairei* ILV91" and *A. mairei* were 0.2–1.8%, and 6.5–8.2%, respectively (Table 3).

Wolbachia infection

Using PCR screening for *Wolbachia* infection with *wsp* gene-specific primers, in all sampled populations of *A. elodeoides* and *A. mairei*, we found that all individuals from 12 populations of *A. mairei* ($N = 360$) were infected with *Wolbachia*, whereas no *Wolbachia* infection was found in the seven studied populations of *A. elodeoides* ($N = 350$), including samples collected from Jinzhai and Shucheng populations through four consecutive years (Table 1). The negative results of *Wolbachia* infection in *A. elodeoides* adults were further verified by PCR using specific primers for the multilocus sequence type genes (*ftsZ*, *coxA*, *hcpA*, and *gatB*).

Discussion

Andricus elodeoides sp. nov. is considered a distinct from *A. mairei* (Kieffer) based on differences in adult and gall morphology, and phylogenetic reconstruction based on COI sequence data (Fig. 17), as well as combined dataset of 28S and COI genes (Fig. 16) and pair-wise genetic distance of the COI gene marker (Table 3). However, intraspecific variation of adult morphology exists in *A. elodeoides* as well as in *A. mairei* (Pujade-Villar et al. 2020). For example, the median propodeal area is rugose in specimens from Hunan (Changsha and Yueyang), but smooth in specimens from Guizhou (Guiding) and Fujian. The lateral propodeal carinae are parallel to each other in *A. elodeoides*, as we observed, which appear to be highly variable in *A. mairei* from being "subparallel to divergent anteriorly and bent outwards in the middle" (Pujade-Villar et al. 2020). Such variations in the morphology of both species, while needing to be further evaluated using large series of specimens from broad regional populations, certainly make it difficult to separate the two species based on adult morphology alone. In such situations, gall morphology and DNA barcoding based on COI sequence is necessary.

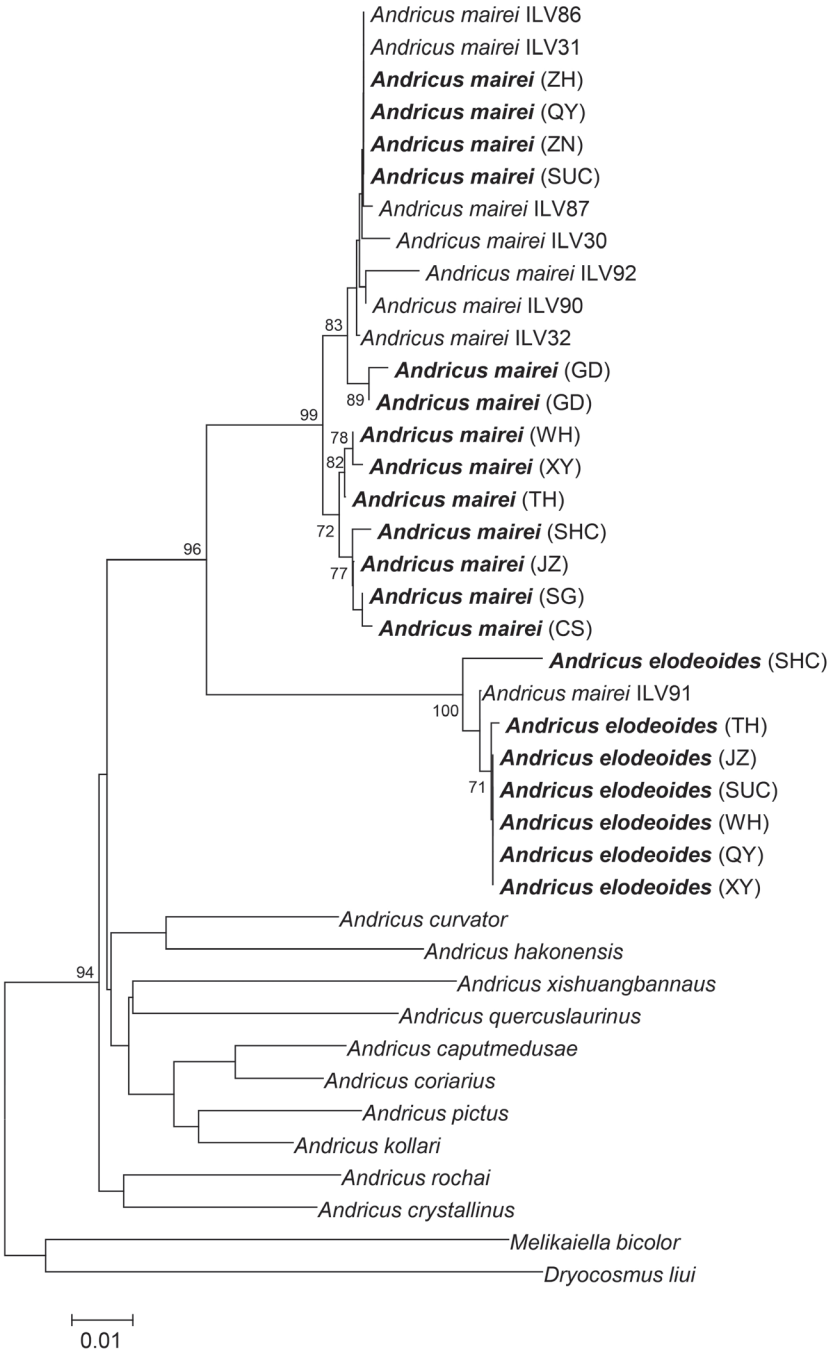

Figure 17. Bayesian phylogenetic tree for *A. elodeoides* sp. nov. and *A. mairei* of different geographic populations using COI sequences. Bold font refers to the sequence obtained in this study, and the others are from Pujade-Villar et al. (2020). The letters in parentheses indicate the sampled populations shown in Table 1. The length of the branches is drawn to scale and show the genetic distances, and the number over branches is posterior probability.

Table 3. Pair-wise COI sequence distances in various geographic populations of *A. elodeoides* sp. nov. and *A. mairei*.

Species	1	2	3	4	5	6	7	8	9	10	11	12	13	14	15	16	17	18	19	20	21	22	23	24	25	26	27	28	29
1 *A. curvator*		0.010	0.011	0.011	0.011	0.011	0.011	0.011	0.011	0.011	0.011	0.011	0.011	0.011	0.011	0.014	0.011	0.011	0.011	0.011	0.011	0.011	0.012	0.012	0.011	0.011	0.011	0.011	0.011
2 *A. hakonensis*	0.070		0.013	0.013	0.012	0.013	0.012	0.012	0.012	0.013	0.012	0.012	0.012	0.013	0.012	0.015	0.012	0.012	0.012	0.012	0.012	0.012	0.014	0.014	0.013	0.013	0.013	0.013	0.013
3 *A.mairei* (SG*)	0.080	0.096																					0.010	0.010	0.010	0.010	0.010	0.010	0.010
4 *A.mairei* (CS)	0.082	0.096	0.002																				0.010	0.011	0.010	0.010	0.010	0.010	0.010
5 *A.mairei* (WH)	0.078	0.096	0.006	0.008																			0.010	0.010	0.010	0.010	0.010	0.010	0.010
6 *A.mairei* (TH)	0.080	0.098	0.005	0.006	0.002																		0.010	0.010	0.010	0.010	0.010	0.010	0.010
7 *A.mairei* (SUC)	0.082	0.092	0.014	0.015	0.011	0.009																	0.011	0.011	0.010	0.010	0.010	0.010	0.010
8 *A.mairei* (XY)	0.080	0.094	0.008	0.009	0.002	0.003	0.012																0.010	0.011	0.010	0.010	0.010	0.010	0.010
9 *A.mairei* (ZN)	0.082	0.092	0.014	0.015	0.011	0.009	0.000	0.012															0.011	0.011	0.010	0.010	0.010	0.010	0.010
10 *A.mairei* (JZ)	0.082	0.098	0.002	0.003	0.005	0.003	0.012	0.006	0.012														0.010	0.010	0.010	0.010	0.010	0.010	0.010
11 *A.mairei* (SHC)	0.082	0.094	0.005	0.006	0.008	0.006	0.015	0.009	0.015	0.003													0.010	0.010	0.010	0.010	0.010	0.010	0.010
12 *A.mairei* (QY)	0.082	0.092	0.014	0.015	0.011	0.009	0.000	0.012	0.000	0.012	0.015					*A. mairei*							0.011	0.011	0.010	0.010	0.010	0.010	0.010
13 *A.mairei* (GD1)	0.083	0.092	0.017	0.018	0.017	0.015	0.009	0.018	0.009	0.015	0.018	0.009											0.011	0.011	0.010	0.010	0.010	0.010	0.010
14 *A.mairei* (GD2)	0.083	0.096	0.014	0.015	0.014	0.012	0.006	0.015	0.006	0.012	0.015	0.006	0.003										0.011	0.011	0.010	0.010	0.010	0.010	0.010
15 *A.mairei* (ZH)	0.082	0.092	0.014	0.015	0.011	0.009	0.000	0.012	0.000	0.012	0.015	0.000	0.009	0.006									0.011	0.011	0.010	0.010	0.010	0.010	0.010
16 *A.mairei* ILV92†	0.091	0.099	0.022	0.024	0.024	0.024	0.011	0.026	0.011	0.020	0.022	0.011	0.020	0.015	0.011								0.013	0.013	0.012	0.012	0.013	0.012	0.012
17 *A. mairei* ILV90†	0.082	0.092	0.012	0.014	0.012	0.011	0.002	0.014	0.002	0.011	0.014	0.002	0.011	0.008	0.002	0.009							0.011	0.011	0.010	0.010	0.010	0.010	0.010
18 *A. mairei* ILV87	0.082	0.094	0.015	0.017	0.012	0.011	0.002	0.014	0.002	0.014	0.017	0.002	0.011	0.008	0.002	0.011	0.003						0.011	0.011	0.010	0.010	0.010	0.010	0.010
19 *A. mairei* ILV86†	0.081	0.092	0.014	0.015	0.011	0.009	0.000	0.012	0.000	0.012	0.015	0.000	0.009	0.006	0.000	0.011	0.002	0.002					0.011	0.011	0.010	0.010	0.010	0.010	
20 *A. mairei* ILV32†	0.081	0.092	0.012	0.014	0.012	0.011	0.002	0.014	0.002	0.011	0.014	0.002	0.008	0.005	0.002	0.009	0.003	0.003	0.002				0.011	0.011	0.010	0.010	0.010	0.010	
21 *A. mairei* ILV31†	0.081	0.092	0.014	0.015	0.011	0.009	0.000	0.012	0.000	0.012	0.015	0.000	0.009	0.006	0.000	0.011	0.002	0.002	0.000	0.002			0.011	0.011	0.010	0.010	0.010	0.010	0.0
22 *A. maire* ILV30†	0.087	0.096	0.016	0.018	0.014	0.013	0.005	0.016	0.005	0.014	0.018	0.005	0.013	0.010	0.005	0.016	0.005	0.006	0.005	0.006	0.005		0.011	0.011	0.010	0.010	0.010	0.010	0.0
23 *A. elodeoides* (SHC)	0.097	0.117	0.076	0.078	0.078	0.080	0.083	0.080	0.083	0.078	0.078	0.083	0.085	0.085	0.083	0.089	0.082	0.086	0.084	0.084	0.084	0.084							
24 *A. mairei* ILV91†	0.090	0.103	0.066	0.068	0.066	0.066	0.070	0.068	0.070	0.068	0.068	0.070	0.072	0.072	0.070	0.082	0.072	0.070	0.070	0.070	0.070	0.071	0.018						
25 *A. elodeoides* (JZ)	0.087	0.105	0.070	0.071	0.068	0.070	0.073	0.070	0.073	0.071	0.071	0.073	0.075	0.075	0.073	0.079	0.076	0.076	0.074	0.074	0.074	0.075	0.017	0.002			*A. elodeoides*		
26 *A. elodeoides* (SUC)	0.087	0.105	0.070	0.071	0.068	0.070	0.073	0.070	0.073	0.071	0.071	0.073	0.075	0.075	0.073	0.079	0.076	0.076	0.074	0.074	0.074	0.075	0.017	0.002	0.000				
27 *A. elodeoides* (TH)	0.088	0.107	0.071	0.073	0.070	0.071	0.075	0.071	0.075	0.073	0.073	0.075	0.076	0.076	0.075	0.082	0.077	0.077	0.076	0.076	0.076	0.077	0.015	0.004	0.002	0.002			
28 *A. elodeoides* (WH)	0.087	0.105	0.070	0.071	0.068	0.070	0.073	0.070	0.073	0.071	0.071	0.073	0.075	0.075	0.073	0.079	0.076	0.076	0.074	0.074	0.074	0.075	0.017	0.002	0.000	0.000	0.002		
29 *A. elodeoides* (XL)	0.087	0.105	0.070	0.071	0.068	0.070	0.073	0.070	0.073	0.071	0.071	0.073	0.075	0.075	0.073	0.079	0.076	0.076	0.074	0.074	0.074	0.075	0.017	0.002	0.000	0.000	0.002	0.000	
30 *A. elodeoides* (XY)	0.087	0.105	0.070	0.071	0.068	0.070	0.073	0.070	0.073	0.071	0.071	0.073	0.075	0.075	0.073	0.079	0.076	0.076	0.074	0.074	0.074	0.075	0.017	0.002	0.000	0.000	0.002	0.000	0.000

*Indicates the population codes shown in Table 1 in this study, while † mean from Pujade-Villar et al. (2020).

Pujade-Villar et al. (2020) suspected that one of specimens included in their study as *A. mairei* (ILV91) was probably a new species based on the COI genetic distance. Our COI tree including this sequence (Fig. 17) and our pairwise genetic distance analysis (Table 3) supported their hypothesis. In addition, galls in one photograph in that paper (Pujade-Villar et al. 2020: fig. 7b) very likely belonged to *A. elodeoides*, although it is not clear to us whether these galls were the same as those which *A. mairei*-ILV91 was reared from.

Our phylogenetic analyses of gene sequence data support *A. elodeoides* and *A. mairei* as sister species (Figs 16, 17). The two species are sympatric in distribution and share the same host plant species, make galls on the same host plant structure (the stalk of male catkins), and overlap in time of gall formation and the emergence of adults. In addition, the galls of the two species share striking structural similarities despite distinct morphological differences (Figs 14, 15). Given these facts, it is intriguing what speciation mechanisms might have been involved given the lack of barriers in biogeography, host plant use, and phenology between the two species. It is possible that *Wolbachia*-induced cytoplasmic incompatibility was one of the potential causes for speciation between *A. mairei*, which is infected with *Wolbachia*, and its uninfected sister species *A. elodeoides*. Nonetheless, we did not conduct interspecific mating experiments after curing of *Wolbachia* due to the difficulties in artificial breeding of gall wasps.

Wolbachia (Anaplasmataceae) are maternally inherited endosymbiotic bacteria that infect arthropods and nematodes and has been shown to be associated with multiple effects on the reproduction of their hosts, such as cytoplasmic incompatibility (CI), induced parthenogenesis, feminization of genetic males, and male killing (Werren et al. 2008). Several studies have revealed *Wolbachia* infection in diverse cynipid species, involving tribe Aylacini, Diplolepidini, Cynipini, and Synergini (Plantard et al. 1998; Abe and Miura 2002; Zhu et al. 2007; Yang et al. 2013; Hou et al. 2020). In this study, we found that all examined individuals of *A. mairei* were infected with *Wolbachia*, whereas individuals of *A. elodeoides* collected from seven sites were all *Wolbachia*-free. Reproductive isolation between different populations or incipient species can evolve in both sympatry and allopatry (Turelli and Bierzychudek 2001). In arthropods, sympatry isolation may result from infection by *Wolbachia* reproductive manipulators (Engelstädter and Hurst 2009; Weinert et al. 2015). Cytoplasmic incompatibility, the most common form of reproductive manipulation induced by *Wolbachia* to its hosts, is characterized by partial or complete embryonic lethality in crosses between infected males and uninfected females or between hosts carrying incompatible symbiont strains. Thus, *Wolbachia*-induced CI may create substantial barriers to genetic exchange between individuals with different infection status and act as an agent of speciation (Werren 1998; Wade 2001; Turelli 2010). Bordenstein et al. (2001) reported a preeminent case of symbiont-assisted isolation because of *Wolbachia*-induced CI in the parasitoid wasp genus *Nasonia* (Hymenoptera, Chalcidoidea). This study demonstrated that *Wolbachia*-induced reproductive isolation via CI preceded the evolution of other mating barriers in *Nasonia* species and was the first major step in the process of speciation.

A contrasting difference in sex ratio was observed between *A. elodeoides* and *A. mairei*. Populations of of *A. elodeoides* were extremely female-biased, with female rates being 95.5–97.8%, while populations of *A. mairei* were more male biased to nearly balanced, with female rates being 5.4–43.5%. For two *A. mairei* populations in Jinzhai and Shucheng, which were investigated for six and four consecutive years, the female rates were 17.3% and 24.6%, or lower, respectively. This is consistent with observations made by other studies. Weld (1952) reported that there was only one female among the six adults of *A. mairei* collected from Hankou. Yang et al. (2012) collected specimens from multiple locations, including Yueyang, Changsha and Shaoyang, in Hunan Province, with a female ratio of less than 20%. The contrasting sex ratio biases of *A. elodeoides* and *A. mairei* are an interesting phenomenon that might be associated with *Wolbachia* infection. Genetic mutation or recombination may result in differences in susceptibility to *Wolbachia* infection in gall wasps and somehow effectively interrupted the genetic exchange between genotypes by mechanisms mentioned above. Consequently, a sympatric speciation event could take place relatively quickly due to founder effect (Joly 2011). This may explain our observation that the COI genetic distance between *A. elodeoides* and *A. mairei* is comparable to the average distance among known *Andricus* species from Eastern Asian while the two species are very similar in morphology, phenology, and gall morphology (Table 3). Nonetheless, the exact mechanism involved could only be understood by further investigations.

Acknowledgements

This study was supported by the National Key Research and Development Program of China (no. 2018YFE0127100).

References

Abe Y, Miura K (2002) Doses *Wolbachia* induce unisexuality in oak gall wasps? (Hymenoptera: Cynipidae). Annals of the Entomological Society of America 95(5): 583–586. https://doi.org/10.1603/0013-8746(2002)095[0583:DWIUIO]2.0.CO;2

Baldo L, Dunning Hotopp JC, Bordenstein SR, Biber S, Jollie K, Hayashi C, Tettelin H, Maiden M, Werren JH (2006) A multilocus sequence typing system for the endosymbiont *Wolbachia*. Molecular Biology and Evolution 23(2): 437–449. https://doi.org/10.1093/molbev/msj049

Bordenstein S, O'Hara FP, Werren JH (2001) *Wolbachia*-induced incompatibility precedes other hybrid incompatibilities in *Nasonia*. Nature 409(6821): 707–710. https://doi.org/10.1038/35055543

Cook TD, Campbell DT, Shadish W (2002) Experimental and quasi-experimental designs for generalized causal inference. Houghton Mifflin, Boston, 1–81. https://doi.org/10.1198/jasa.2005.s22

Cuesta-Porta V, Melika G, Nichols JA, Stone G, Pujade-Villar J (2022) Reestablishment of the Nearctic oak cynipid gall wasp genus *Druon* Kinsey, 1937 (Hymenoptera: Cynipidae: Cynipini), with description of five new species. Zootaxa 5132: 001–092. https://doi.org/10.11646/zootaxa.5132.1.1

Dowton M, Austin AD (2001) Simultaneous analysis of 16S, 28S, COI and morphology in the Hymenoptera: Apocrita - evolutionary transitions among parasitic wasps. Biological Journal of the Linnean Society 74: 87–111. https://doi.org/10.1111/j.1095-8312.2001.tb01379.x

Engelstädter J, Hurst GDD (2009) The ecology and evolution of microbes that manipulate host reproduction. Annual Review of Ecology, Evolution, and Systematics 40(1): 127–149. https://doi.org/10.1146/annurev.ecolsys.110308.120206

Folmer O, Black M, Hoeh W, Lutz R, Vrijenhoek R (1994) DNA primers for amplification of mitochondrial cytochrome c oxidase subunit I from diverse metazoan invertebrates. Molecular Marine Biology and Biotechnology 3: 294–299.

Harris R (1979) A glossary of surface sculpturing. State of California, Department of Food and Agriculture. Occasional Papers in Entomology 28: 1–31.

Hou HQ, Zhao GZ, Su CY, Zhu DH (2020) *Wolbachia* prevalence patterns: Horizontal transmission, recombination, and multiple infections in chestnut gall wasp-parasitoid communities. Entomologia Experimentalis et Applicata 168(10): 752–765. https://doi.org/10.1111/eea.12962

Ide T, Abe Y, Su CY, Zhu DH (2018) Three species of *Andricus* Hartig (Hymenoptera: Cynipidae) inducing similar galls in East Asia, with description of a new species and the asexual generation of *A. pseudocurvator*, and redescription of *A. moriokae*. Proceedings of the Entomological Society of Washington 120(4): 807–824. https://doi.org/10.4289/0013-8797.120.4.807

Joly E (2011) The existence of species rests on a metastable equilibrium between inbreeding and outbreeding. An essay on the close relationship between speciation, inbreeding and recessive mutations. Biology Direct 6(1): 62. https://doi.org/10.1186/1745-6150-6-62

Kieffer JJ (1906) Description d'un genre nouveau et deux especes nouvelles. Marcellia 5: 101–110.

Kumar S, Stecher G, Tamura K (2016) MEGA7: Molecular Evolutionary Genetics Analysis version 7.0 for bigger datasets. Molecular Biology and Evolution 33(7): 1870–1874. https://doi.org/10.1093/molbev/msw054

Liljeblad J (2002) Phylogeny and evolution of gall wasps. PhD thesis, Stockholm University.

Liljeblad J, Ronquist F, Nieves-Aldrey J-L, Fontal-Cazalla F, Ros-Farré P, Gaitros D, Pujade-Villar J (2008) A fully web-illustrated morphological phylogenetic study of relationships among oak gall wasps and their closest relatives (Hymenoptera: Cynipidae). Zootaxa 1796(1): 1–73. https://doi.org/10.11646/zootaxa.1796.1.1

Melika G (2006) Gall wasps of Ukraine. Cynipidae. Vestnik Zoologii (Supplement 21): 1–644.

Melika G, Abrahamson WG (2002) Review of the world genera of oak cynipid wasps (Hymenoptera: Cynipidae: Cynipini). In: Melika G, Thuróczy C (Eds) Parasitic Wasps: Evolution, Systematics, Biodiversity and Biological Control. Agroinform, Budapest, 150–190.

Melika G, Pérez-Hidalgo N, Hanson P, Pujade-Villar J (2009a) New species of oak gallwasp from Costa Rica (Hymenoptera: Cynipidae: Cynipini). Dugesiana 16: 35–39.

Melika G, Cibrián-Tovar D, Cibrián-Llanderal VD, Tormos J, Pujade-Villar J (2009b) New species of oak gallwasp from Mexico (Hymenoptera: Cynipidae: Cynipini) - a serious pest of *Quercus laurina* (Fagaceae). Dugesiana 16: 67–73.

Nei M, Kumar S (2000) Molecular Evolution and Phylogenetics. Oxford University Press, New York, 348 pp.

Pang Y, Su CY, Zhu DH (2018) Discovery of a new species of *Dryocosmus* Giraud, 1859 (Hymenoptera: Cynipidae: Cynipini) on *Castanopsis tibetana* from China. Zootaxa 4403(1): 99–110. https://doi.org/10.11646/zootaxa.4403.1.5

Pang Y, Liu Z, Su CY, Zhu DH (2020) A new species of *Periclistus* Foerster, 1869 from China and review of the tribe Diastrophini (Hymenoptera, Cynipoidea, Cynipidae). ZooKeys 964: 109–126. https://doi.org/10.3897/zookeys.964.47441

Penzes Z, Tang CT, Stone GN, Nicholls JA, Schwéger S, Bozso M, Melika G (2018) Current status of the oak gallwasp (Hymenoptera: Cynipidae: Cynipini) fauna of the Eastern Palaearctic and Oriental Regions. Zootaxa 4433(2): 245–289. https://doi.org/10.11646/zootaxa.4433.2.2

Plantard O, Rasplus JY, Mondor G, Le Clainche I, Solignac M (1998) *Wolbachia* induced thelytoky in the rose gallwasp *Diplolepis spinosissimae* (Giraud) (Hymenoptera: Cynipidae), and its consequences on the genetic structure of its host. Proceedings of the Royal Society of London: Series B, Biological Sciences 265(1401): 1075–1080. https://doi.org/10.1098/rspb.1998.0401

Pujade-Villar J, Wang YP, Guo R, Chen XX (2014) New species of gallwasps inducing in *Quercus fabri* and its inquiline (Hymenoptera: Cynipidae) in China. https://doi.org/10.11865/zs20140308

Pujade-Villar J, Serrano-Muñoz M, García-Martiñón RD, Villecas Guzmán GA, Armando Equihua-Martínez A, Estrada-Venegas EG, Ferrer- Suay M (2016) A new species of gall wasp from Mexico: *Andricus sphaericus* Pujade-Villar n. sp. (Hymenoptera: Cynipidae: Cynipini). Dugesiana 23: 15–20.

Pujade-Villar J, Wang YP, Guo R, Victor C, Miquel A, Melika G (2020) Current status of *Andricus mairei* (Kieffer), with synonymization of two species from China (Hymenoptera: Cynipidae). Zootaxa 4808(3): 507–525. https://doi.org/10.11646/zootaxa.4808.3.6

Rokas A, Nylander JAA, Ronquist F, Stone GN (2002) A maximum likelihood analysis of eight phylogenetic markers in gallwasps (Hymenoptera: Cynipidae); implications for insect phylogenetic studies. Molecular Phylogenetics and Evolution 22(2): 206–219. https://doi.org/10.1006/mpev.2001.1032

Rokas A, Melika G, Abe Y, Nieves-Aldrey J-L, Cook JM, Stone GN (2003) Lifecycle closure, lineage sorting, and hybridization revealed in a phylogenetic analysis of European oak gallwasps (Hymenoptera: Cynipidae: Cynipini) using mitochondrial sequence data. Molecular Phylogenetics and Evolution 26(1): 36–45. https://doi.org/10.1016/S1055-7903(02)00329-9

Ronquist F (1995) Phylogeny and early evolution of the Cynipoidea (Hymenoptera). Systematic Entomology 20(4): 309–335. https://doi.org/10.1111/j.1365-3113.1995.tb00099.x

Ronquist F, Nordlander G (1989) Skeletal morphology of an archaic cynipoid, *Ibalia rufipes* (Hymenoptera: Ibaliidae). Entomologica Scandinavica (Supplement 33): 1–60.

Ronquist F, Teslenko M, Yander-Mark P, Ayres DL, Darling A, Höhna S, Larget B, Liu L, Suchard MA, Huelsenbeck JP (2012) MrBayes 3.2: Efficient Bayesian phylogenetic inference and model choice across a large model space. Systematic Biology 61(3): 539–542. https://doi.org/10.1093/sysbio/sys029

Ronquist F, Nieves-Aldrey J-L, Buffington ML, Liu Z, Liljeblad J, Nylander JAA (2015) Phylogeny, evolution and classification of gall wasps: The plot thickens. PLoS ONE 10(5): e0123301. https://doi.org/10.1371/journal.pone.0123301

Stone GN, Cook JM (1998) The structure of cynipid oak galls: Patterns in the evolution of an extended phenotype. Proceedings of the Royal Society B: Biological Sciences 265(1400): 979–988. https://doi.org/10.1098/rspb.1998.0387

Stone GN, Schönrogge K (2003) The adaptive significance of insect gall morphology. Trends in Ecology & Evolution 18(10): 512–522. https://doi.org/10.1016/S0169-5347(03)00247-7

Tang CT, Melika G, Yang MM, Nicholls J, Csöka GY, Stone GN (2009) First record of an *Andricus* oak gallwasp from the Oriental Region: a new species from Taiwan (Hymenoptera: Cynipidae: Cynipini). Zootaxa 2175(1): 57–65. https://doi.org/10.11646/zootaxa.2175.1.6

Tang CT, Sinclair F, Yang MM, Melika G (2012) A new *Andricus* Hartig oak gallwasp species from China (Hymenoptera: Cynipidae: Cynipini). Journal of Asia-Pacific Entomology 15(4): 601–605. https://doi.org/10.1016/j.aspen.2012.07.005

Thompson JD, Higgins DG, Gibson TJ (1994) CLUSTAL W: Improving the sensitivity of progressive multiple sequence alignment through sequence weighting, position-specific gap penalties and weight matrix choice. Nucleic Acids Research 22(22): 4673–4680. https://doi.org/10.1093/nar/22.22.4673

Turelli M (2010) Cytoplasmic incompatibility in populations with overlapping generations. Evolution 64(1): 232–241. https://doi.org/10.1111/j.1558-5646.2009.00822.x

Turelli M, Bierzychudek SP (2001) Stable two-allele polymorphisms maintained by fluctuating fitnesses and seed banks: Protecting the blues in *Linanthus parryae*. Evolution: International Journal of Organic Evolution 55(7): 1283–1298. https://doi.org/10.1111/j.0014-3820.2001.tb00651.x

Wachi N, Ide T, Abe Y (2011) Taxonomic status of two species of *Andricus* (Hymenoptera: Cynipidae) described by Shinji (1940, 1941) as gall inducers on *Cyclobalanopsis*. Annals of the Entomological Society of America 104(4): 620–626. https://doi.org/10.1603/AN11033

Wade MJ (2001) Infectious speciation. Nature 409(6821): 675–677. https://doi.org/10.1038/35055648

Wang YP, Guo R, Chen XX (2013) A new species of *Andricus* oak gallwasp from China (Hymenoptera: Cynipidae: Cynipini). Biologia 68(5): 974–978. https://doi.org/10.2478/s11756-013-0242-y [Section Zoology]

Weinert LA, Araujo-Jnr EV, Ahmed MZ, Welch JJ (2015) The incidence of bacterial endosymbionts in terrestrial arthropods. Proceedings of the Royal Society B: Biological Sciences 282(1807): e20150249. https://doi.org/10.1098/rspb.2015.0249

Weld LH (1952) Cynipoidea (Hym.) 1905–1950. Privately published, Ann Arbor, 351 pp.

Werren JH (1998) *Wolbachia* and speciation. In: Howard DJ, Berlocher SH (Eds) Endless Forms: Species and Speciation. Oxford University Press, Oxford, 245–260.

Werren JH, Baldo L, Clark ME (2008) *Wolbachia*: Master manipulators of invertebrate biology. Nature Reviews. Microbiology 6(10): 741–751. https://doi.org/10.1038/nrmicro1969

Yang XH, Zhu DH, Liu Z, Zhao L (2012) Sequencing and phylogenetic analysis of the *wsp* gene of *Wolbachia* in three geographic populations of an oak gall wasp, *Andricus mairei* (Hymenoptera: Cynipidae), fron Hunan, South China. Acta Entomologica Sinica 55: 247–254.

Yang XH, Zhu DH, Liu Z, Zhao L, Su CY (2013) High levels of multiple infections, recombination and horizontal transmission of *Wolbachia* in the *Andricus mukaigawae* (Hymenoptera; Cynipidae) communities. PLoS ONE 8(11): e78970. https://doi.org/10.1371/journal.pone.0078970

Zhou W, Rousset F, O'Neil SL (1998) Phylogeny and PCR-based classification of *Wolbachia* strains using *wsp* gene sequences. Proceedings of the Royal Society B: Biological Sciences 265(1395): 509–515. https://doi.org/10.1098/rspb.1998.0324

Zhu DH, He YY, Fan YS, Ma MY, Peng DL (2007) Negative evidence of parthenogenesis induction by *Wolbachia* in a gallwasp species, *Dryocosmus kuriphilus*. Entomologia Experimentalis et Applicata 124(3): 279–284. https://doi.org/10.1111/j.1570-7458.2007.00578.x

ZooKeys 1134: 73–100 (2022)
doi: 10.3897/zookeys.1134.91348
https://zookeys.pensoft.net

RESEARCH ARTICLE

A peer-reviewed open-access journal
ZooKeys
Launched to accelerate biodiversity research

Beyond the species name: an analysis of publication trends and biases in taxonomic descriptions of rainfrogs (Amphibia, Strabomantidae, *Pristimantis*)

Carolina Reyes-Puig[1,2,3], Emilio Mancero[4]

1 *Universidad San Francisco de Quito USFQ, Instituto iBIOTROP, Museo de Zoología & Laboratorio de Zoología Terrestre, Quito, 170901, Ecuador* **2** *Universidad San Francisco de Quito USFQ, Colegio de Ciencias Biológicas y Ambientales COCIBA, Quito, 170901, Ecuador* **3** *Instituto Nacional de Biodiversidad, Unidad de Investigación, Quito, 170506, Ecuador* **4** *Biology Department, Grand Valley State University, Allendale, MI 49401, USA*

Corresponding author: Carolina Reyes-Puig (creyesp@usfq.edu.ec)

Academic editor: Uri García-Vázquez | Received 8 August 2022 | Accepted 11 November 2022 | Published 7 December 2022

https://zoobank.org/7AE44A74-4770-47DB-9E45-43FCB2648EE4

Citation: Reyes-Puig C, Mancero E (2022) Beyond the species name: an analysis of publication trends and biases in taxonomic descriptions of rainfrogs (Amphibia, Strabomantidae, *Pristimantis*). ZooKeys 1134: 73–100. https://doi.org/10.3897/zookeys.1134.91348

Abstract

The rainfrogs of the genus *Pristimantis* are one of the most diverse groups of vertebrates, with outstanding reproductive modes and strategies driving their success in colonizing new habitats. The rate of *Pristimantis* species discovered annually has increased continuously during the last 50 years, establishing the remarkable diversity found in this genus. In this paper the specifics of publications describing new species in the group are examined, including authorship, author gender, year, language, journal, scientific collections, and other details. Detailed information on the descriptions of 591 species of *Pristimantis* published to date (June 2022) were analyzed and extracted. John D. Lynch and William E. Duellman are the most prolific authors, yet Latin American researchers have scaled up and continued the description processes since the 1990s. The most common language used for descriptions is English, followed by Spanish. The great majority of authors have described only one species. The largest proportion of authors who have participated in the descriptions is of Ecuadorian nationality. Ecuador is the country with the highest description rate per year (3.9% growth rate). Only 20% of the contributions have included women and only 2% have featured women as principal authors. 36.8% of the species described are in the Not Evaluated or Data Deficient categories under the IUCN global red list. The importance of enhancing the descriptions in Spanish is emphasized and the inclusion based on equal access to opportunities for female researchers in *Pristimantis* taxonomy is encouraged. In general, if the current trends in *Pristimantis* descriptions continue, in ten years, a total of 770 or more species described could be expected.

Resumen

Las ranas de la lluvia del género *Pristimantis* es uno de los grupos de vertebrados más diversos, con una variedad de modos reproductivos y estrategias que impulsan su éxito en la colonización de nuevos hábitats. La tasa de especies de *Pristimantis* descubiertas anualmente ha aumentado continuamente durante los últimos 50 años, estableciendo la notable diversidad encontrada en este género. En este artículo, examinamos los detalles de las publicaciones que describen nuevas especies en el grupo, incluida la autoría, el año, el idioma, la revista, el género, las colecciones científicas y otros detalles. Analizamos y extrajimos información detallada sobre las descripciones de 591 especies de *Pristimantis* publicadas hasta la fecha (junio 2022). John D. Lynch y William E. Duellman son los autores más prolíficos, pero los investigadores latinoamericanos han ampliado y continuado los procesos de descripción desde la década de 1990. El idioma más común utilizado para las descripciones es el inglés, seguido del español. La gran mayoría de los autores han descrito una sola especie. La mayor proporción de autores que han participado en las descripciones es de nacionalidad ecuatoriana. Ecuador es el país con la tasa de descripción más alta por año (tasa de crecimiento del 3,9%). Solo el 20% de las contribuciones han incluido a mujeres y solo el 2% las ha presentado como autoras principales. El 36,8% de las especies descritas se encuentran en las categorías No evaluadas o Datos insuficientes de la lista roja mundial de la UICN. Destacamos la importancia de potenciar las descripciones en español y fomentar la inclusión de mujeres investigadoras en la taxonomía de *Pristimantis*. En general, si continúan las tendencias actuales en las descripciones de *Pristimantis*, en 10 años se podría esperar un total de 770 o más especies descritas.

Keywords

Author gender, herpetology, inclusion, language bias, new species, taxonomy

Introduction

Pristimantis Jiménez de la Espada, 1870 is a clade of New-World direct-developing frogs belonging to the family Strabomantidae, order Anura, class Amphibia, phylum Chordata. It is the most speciose genus of terrestrial vertebrates with 591 described species to date (Hedges et al. 2008; Frost 2022). A greater focus on molecular, acoustic, and osteological techniques combined with a significant increase in sampling efforts has led to a rise in the number of newly described species in recent years, allowing further research in understanding their taxonomy and systematics (Padial et al. 2010; Hutter and Guayasamin 2015; Kaiser et al. 2015; González-Durán et al. 2017; Reyes-Puig et al. 2020).

The earliest description of this genus was the description of the genus type *Pristimantis galdi* (Jiménez de la Espada, 1870). The genus was later placed under the synonymy of *Hylodes* sensu lato by Boulenger (1882), then synonymized as *Eleutherodactylus* by Peters (1955). *Cyclocephalus*, *Pseudohyla*, and *Trachyphrynus* were also synonymized with *Eleutherodactylus* by Lynch (1968, 1971). Heinicke et al. (2007) removed *Pristimantis* from the synonymy under *Eleutherodactylus*, with support from molecular evidence. This large and phenotypically diverse genus has faced subsequent molecular analyses confirming its monophyly and status as a closely related taxa to *Lynchius*, *Oreobates*, and *Phyrnopus*, with *Yunganastes* being suggested as well (Pyron and Wiens 2011;

Canedo and Haddad 2012; Pinto-Sánchez et al. 2012). Several discernible groups can be found within the genus, originally described based on extensive morphological data and revised on subsequent molecular analyses (Lynch and Duellman 1997; Hedges et al. 2008; Pinto-Sánchez et al. 2012; Padial et al. 2014; Mendoza et al. 2015). There are currently 13 recognized species groups, with *P. conspicillatus* as the largest with 36 species (Padial et al. 2014; González-Durán 2017; Reyes-Puig et al. 2020; Taucce et al. 2020). Several other species remain unassigned as they are demonstrably non-monophyletic. These species can maintain taxonomic value as they can be grouped among phenotypically similar species, thus revealing useful comparative information (Hedges et al. 2008; Padial et al. 2014).

Members of this genus are remarkable for laying eggs in terrestrial habitats, with the embryos developing directly into frogs, bypassing the aquatic stage of their lifecycle (Woolbright 1985; Duellman and Lehr 2009). Assemblages of *Pristimantis* species are common, as their morphology and therefore behavioral and ecological activities are remarkably similar (Arroyo et al. 2008). They are characterized as insectivorous generalists, choosing prey depending on availability and size (Lynch and Duellman 1997; Arroyo et al. 2008). Individuals are predominantly arboreal and nocturnal, commonly perching on leaves at heights below 200 cm. As their reproductive biology leads them away from congregating at ponds, a common strategy for males in this genus is to vocalize from the ground or a suitable perch in search of a mate (Lynch and Duellman 1997; Duellman and Lehr 2009).

The genus is widely distributed throughout the New World and considered the most extensive among Neotropical amphibians, with species found in tropical and subtropical forests in South America and up to lower Central America (Lynch and Duellman 1997; Pinto-Sánchez et al. 2012; Meza-Joya and Torres 2016; Armesto and Señaris 2017). The group shows particularly high levels of diversity and endemism in the Andes, predominantly at elevations above 2000 m along humid environments and surrounding lowlands and Chocoan South America (Heinicke et al. 2007; Meza-Joya and Torres 2016; Armesto and Señaris 2017; Reyes-Puig et al. 2020). The diversity of the genus is greater in Colombia, Ecuador, and Peru and the piedmont, montane, and montane cloud forests of the western and eastern slopes of the three countries concentrate the highest levels of endemism (Hedges et al. 2008; Ron et al. 2022).The continuous increase in the number of species described within this genus suggests a much greater species richness than anticipated, with subtle differences in behavior and physiology reflecting distinct evolutionary pathways (de Queiroz 2005; Hutter and Guayasamin 2015).

The conditions leading to such a high diversification rate in *Pristimantis* are not completely understood. Families of direct-developing frogs diverged quickly during the early to middle Cenozoic, favoring a wide dispersion across a range of habitats in South America, leading to a rapid accumulation of population genetic isolation (Heinicke et al. 2007; Heinicke et al. 2009; Pröhl et al. 2010). An important point of the radiation of the genus is found between 1000 and 3000 m in the northwestern Andes (Mendoza et al. 2015). The complex biogeographic dynamics in the area not only supported

allopatric speciation, but also facilitated dispersion of lowland species during the Paleocene and Pliocene, leading to a speciation pattern particularly suitable to originate cryptic and sibling lineages (Lynch and Duellman 1997; Mendoza et al. 2015).

In the last 20 years, the increase in species description rates in South America has shed light on the remarkable diversity and endemism of *Pristimantis*, while hinting at the complex patterns of speciation taking place. Given the cryptic nature found in members of this genus, the work to discover and describe new species appears far from over. Categorizing these frogs and their characteristics in a taxonomic context presents several challenges, further obscured by the high degree of plasticity evidenced across the group (Guayasamin et al. 2015).

Despite the fact that this genus is so diverse and taxonomic and systematic research continues from year to year, information on publication patterns and trends is scarce. Issues such as gender and language biases in publications have not yet been explored. Within the biological sciences, Zoology in particular, studies in this branch have been characterized as male-dominated, imposing limitations in the professional development of many women (Slobodian 2021). Similarly, it has been shown that, for example, in ecology and zoology the proportion of principal investigators publishing with women is lower compared to the proportion with men (Salerno et al. 2020). On the other hand, the language of publication continues to be dominated by the English language, although there have been approaches to improve the transmission of science so that it can be disseminated locally (Ramírez-Castañeda 2020). Latin American researchers not only tend to be under pressure to publish in English, but also to do so with colleagues from developed countries, issues that tend to be related to the number of citations an article can receive (Meneghini et al. 2008). Thus, in this article we aim to delve into the specifics of the biases and trends in publication of descriptions of new species of *Pristimantis* by carrying out a detailed review of all description parameters, emphasizing location, authorship (including author gender), scientific collection, and language.

Materials and methods

We followed the proposal of Hedges et al. (2008) and Heinicke et al. (2018) for family classification of *Pristimantis*. The updated list of species formally described to date was extracted from the Amphibian Species of the World web page from the American Museum of Natural History (Frost 2022). On 14 June 2022, the *Pristimantis* list contained 591 described species. Based on this list, we generated a detailed database for each species, extracting specific data available on the original description and the aforementioned web page. We built a database with the following fields: unique species identifier, species, journal, year of publication, first author, authors, gender of the author, nationality of authors, corresponding author, genus, country of description, type locality, holotype, synonymy, species group (if applicable), distribution, language of the description, institutional affiliations, conservation status and type of description. For more details see Suppl. material 1. We calculated the growth rate of global

descriptions and that of the seven countries with the highest number of descriptions (i.e., Ecuador, Colombia, Peru, Venezuela, Brazil, Panamá, Bolivia). In order to better represent the different historical trends seen in *Pristimantis* description, growth rates are divided into two periods: The first from 1958–1989, when descriptions begin to be more constant, and the second one from 1990–2021. Due to a significant increase in descriptions at the time, the period ranging from 2010–2021 is also considered. This is mainly because we intend to identify a realistic description rate with the latest advances in the taxonomy and systematics of the genus. In addition to the fact that the number of researchers currently working in *Pristimantis* taxonomy is greater than in previous periods (Suppl. material 1). We did not consider the periods prior to 1958, as there is no significant growth in description rates observed during them.

We carried out the search for publicly available information regarding gender and nationality of authors through individual exploration enabled by the Google search engine. This search was based on exploration of the Google search results associated with the names of authors (as self-reported in publications describing *Pristimantis* species) throughout the web. Priority was given to information associated with institutional affiliation and research endeavors, cross-referenced with professional sites such as ResearchGate, LinkedIn and Google Scholar. Information regarding the gender of authors was assessed based on a binary understanding of gender and assumed based on gender roles traditionally assigned to their names, physical appearance, and self-reported identity, when available. Information regarding conservation status was obtained from the IUCN Red List of Threatened Species (IUCN 2022). After finalizing data input, we cleaned and homogenized the database to prevent typographical errors as well as duplicate and empty cells. In order to describe the increase in women involved in *Pristimantis* descriptions over the years, we used generalized linear models (GLMs). These include a quasi-binomial error distribution, necessary given the nature of the data (i.e., dichotomous proportionality data and overdispersion). We defined years as the dependent variable and the proportion of female authors as the independent variable, in order to identify the relationship between the proportion of women featured in descriptions and time. We made a GLM of the total number of female authors and one specific to each of the five countries with the greatest diversity of *Pristimantis* (Ecuador, Colombia, Peru, Venezuela, and Brazil). The timeframe for this analysis is from 1970 onwards, corresponding to the period in which women begin to be active in describing a new species of *Pristimantis*. All management, cleaning, and analysis of the database were performed in the statistical software R (R Core Team 2022); utilizing the "tidyverse", "forcats" and "gridExtra" packages.

Results

Species descriptions of the group began in 1858 with *Pristimantis conspicillatus* (under the synonymy of *Hylodes conspicillatus*, *Lithodytes conspicillatus*, and later *Eleutherodactylus conspicillatus*). For a century the descriptions of this group remained relatively

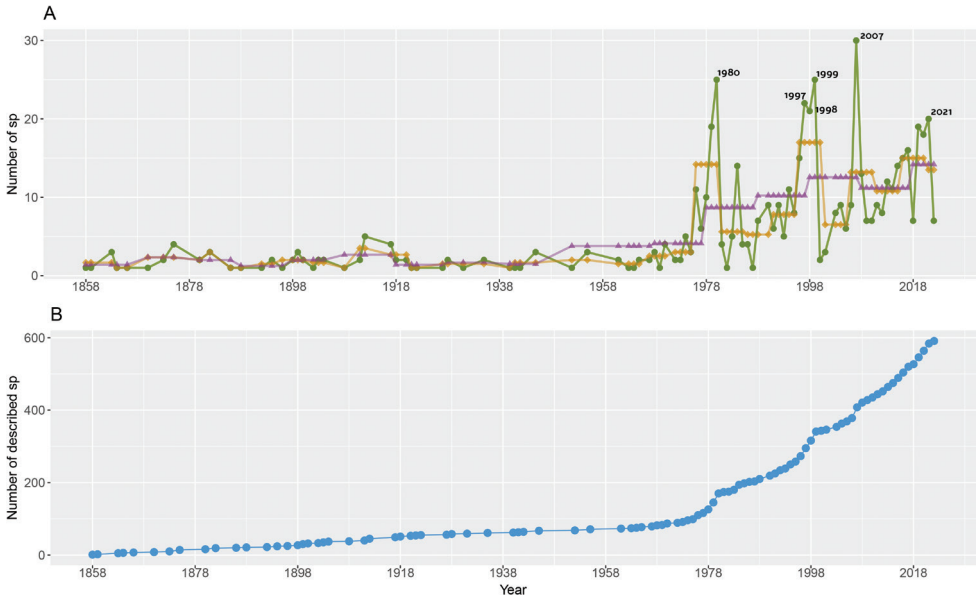

Figure 1. *Pristimantis* descriptions through time **A** species description over 164 years, dots and green lines represent new taxa per year, diamonds and brown lines five-year average, and triangles and purple lines ten-year average **B** cumulative number of species descriptions.

stable with fewer than four species described on average every ten years (Fig. 1). From the 1960s, the descriptions in the group increased significantly with several peaks towards the 70s but with a particular one towards 1980. The number of descriptions every five years increased in relation to the range between 1958–1970, with an average of 5–14 descriptions between 1978 and 1996. After this year, the most notable peaks in new descriptions were restricted to the years 1997, 1998, 1999, 2007, 2019, 2020, and 2021 (Fig. 1A). The significant increase in the descriptions of new species in this group intensified after 1978 and the accumulation curve of descriptions seems to continue increasing up to the present date, with a total of 591 formally described species (Fig. 1B). The period with the highest annual rates of *Pristimantis* description is found between 1958–1989. For Ecuador, the period with the highest description rate lies between 2010–2021, for Colombia between 1958–1989, for Peru between 1990–2021, and for both Brazil and Bolivia, a peak in the description rate is observed in the period 2010–2021 and 1990–2021, respectively. However, it is important to consider that in order to calculate the growth rate, the initial and final values of the numbers of described species are taken into account. By having such a low number of total descriptions, if the species double from one year to the next, the rate is higher; however, the total number of species is much lower compared to that of other countries (Table 1).

The distribution of *Pristimantis* extends from Honduras to Peru, specifically, Honduras east through Central America through Colombia and Ecuador to Peru, Bolivia, northern Argentina, and Amazonian and Atlantic Forest Brazil and the Guianas;

Table 1. Growth rates in *Pristimantis* descriptions.

Time series	Total	Ecuador	Colombia	Peru	Venezuela	Brazil	Panama	Bolivia
1958–1989	3.5	4.4	4.1	3.9	3.2	1.4	0	0
1990–2021	3.2	2.6	3.7	5.4	3.7	3.3	2.4	6.1
2010–2021	2.6	4.7	1.02	2.1	2.3	6.1	2.7	0
Total number of descriptions*	591	212	168	107	56	16	9	5

* Number of total descriptions in each country, growth rates instead are calculated as new descriptions - past descriptions / past descriptions.

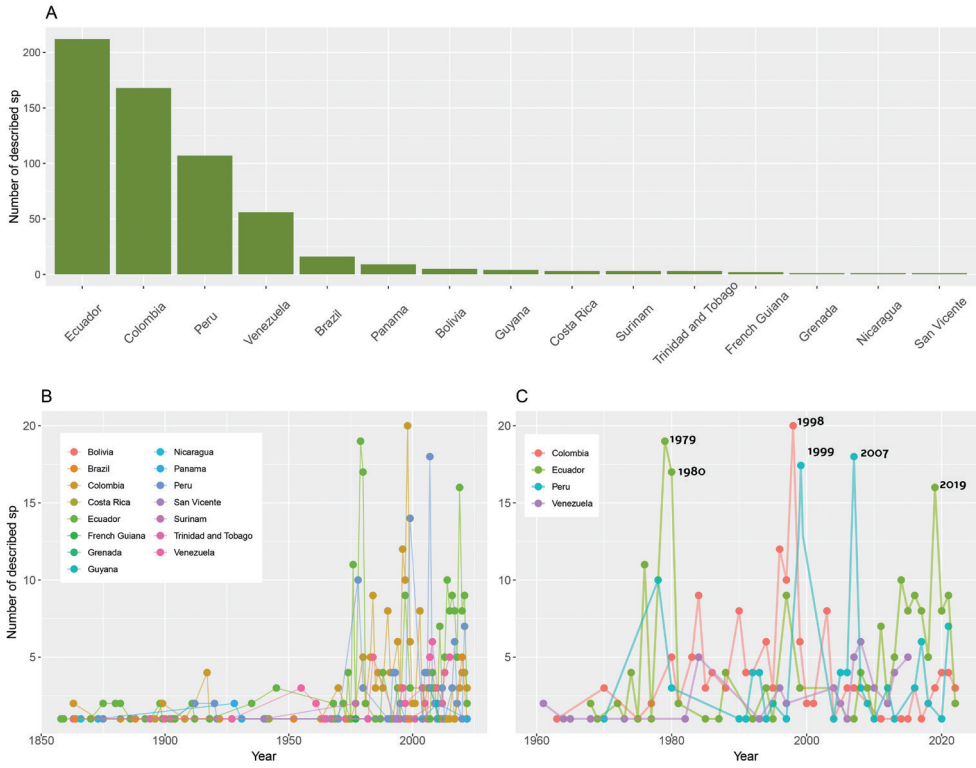

Figure 2. Descriptions of *Pristimantis* species across countries **A** number of species descriptions per country **B** number of annual species descriptions by country **C** number of annual species descriptions in the four countries with the highest species richness.

Trinidad and Tobago; and Grenada, Lesser Antilles (Frost 2022). Ecuador is the country with the highest number of described species with 212 total descriptions, followed by Colombia (168 descriptions), Peru (107 descriptions), and Venezuela (56 descriptions). Other countries within the range of this genus report fewer than ten descriptions (Fig. 2A). From the 1960s onwards, descriptions occurred predominantly in Ecuador, Colombia, and Peru, with at least two peaks of descriptions higher than the average of ten new species described per year (Fig. 2B). Ecuador exhibits three important peaks in species description (i.e., 1979, 1980, and 2019), with more than 15 new

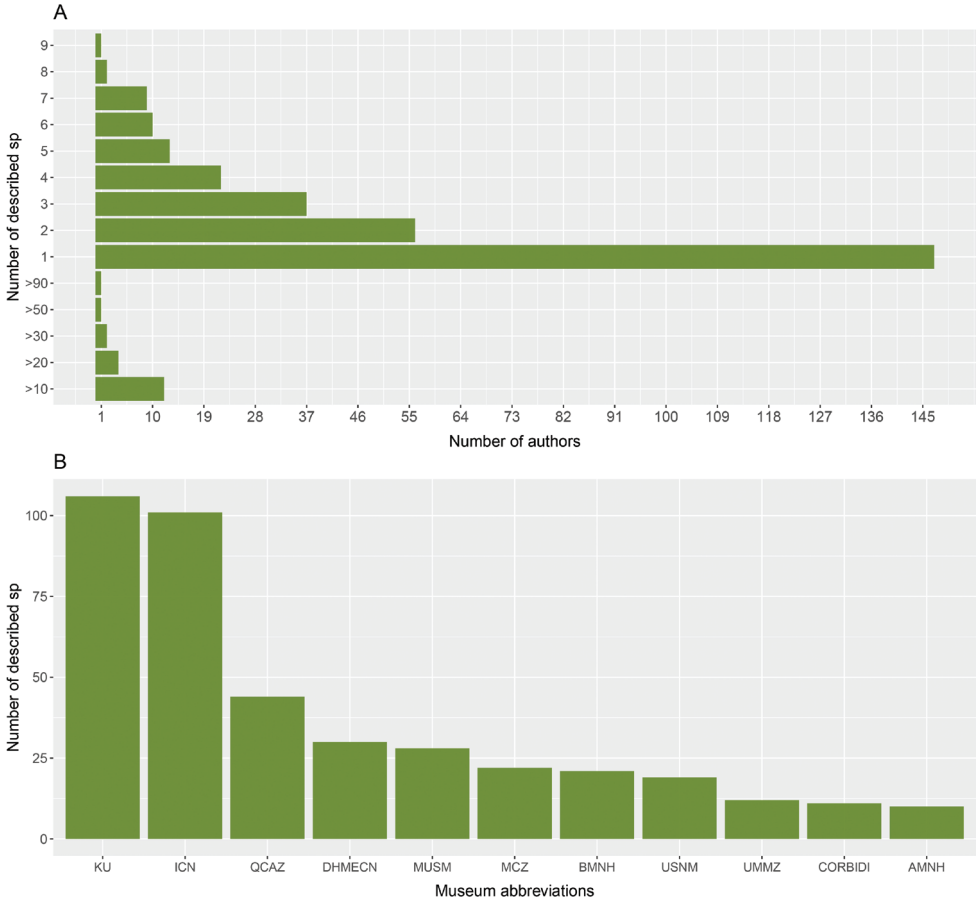

Figure 3. A Number of species described by the number of authors **B** number of holotypes of *Pristimantis* housed in the main scientific collections of natural history (an expanded list can be found in Suppl. material 1).

species described per year; Colombia peaks in 1998 reaching 20 descriptions in a single year, setting a record in descriptions for this genus; and finally, Peru peaks twice (i.e., 1999 and 2007) reaching 13 and 15 species descriptions, respectively (Fig. 2C).

In total, 320 researchers are formally recognized as authors and co-authors in publications describing new species of *Pristimantis* (Suppl. material 1). Almost half (46%) of them have described a single species, while another 46% have described between two and seven species, 6.5% of authors have described 8–30 species, and finally only 0.6% of authors have described more than 50 species (Fig. 3A). Lynch is the author with the highest count of newly described species, with 195 species descriptions to his name. He is followed by Duellman with 82, and E. Lehr and M. Yánez-Muñoz with 36 each. Details on the 20 authors with the highest count of newly described species are provided in Table 2. Across all scientific collections where the type material has been deposited, the four institutions with the highest number of holotypes are the Museum

Table 2. Top 100 authors ranked by the number of *Pristimantis* species they have described and country of origin. Authors with three or more species descriptions are included.

Author rank	Author (country)	No of described species	Author rank	Author (country)	No of described species
1	**J. D. Lynch (USA)**	**195**	51	D. Szekely (Romania)	5
2	**W. E. Duellman (USA)**	**82**	52	D. Zumel (Ecuador)	5
3	**E. Lehr (Germany)**	**36**	53	E. A. de Oliveira (Brazil)	5
4	**M. H. Yánez-Muñoz (Ecuador)**	**36**	54	E. J. Hernandez-Ruz (Brazil)	5
5	**S. R. Ron (Ecuador)**	**30**	55	G. A. Rivas-Fuenmayor (Venezuela)	5
6	**P. M. Ruiz-Carranza (Colombia)**	**25**	56	M. B. Perez (Ecuador)	5
7	**G. A. Boulenger (Belgium, Great Britain)**	**23**	57	T. Barbour (USA)	5
8	**J. M. Guayasamin (Ecuador)**	**20**	58	W. C. H. Peters (USA)	5
9	**C. Reyes-Puig (Ecuador)**	**18**	59	L. R. Rodrigues (Brazil)	4
10	**C. L. Barrio-Amoros (Spain)**	**17**	60	C. J. Goin (USA)	4
11	**J. B. Pramuk (USA)**	**17**	61	D. Armijos-Ojeda (Ecaudor)	4
12	**J. V. Rueda-Almonacid (Colombia)**	**16**	62	D. B. Means (USA)	4
13	**J. P. Reyes-Puig (Ecuador)**	**15**	63	D. Buckley (Spain)	4
14	**M. C. Ardila-Robayo (Colombia)**	**15**	64	D. M. Cochran (USA)	4
15	**J. A. Rivero (Puerto Rico)**	**13**	65	D. Rödder (Germany)	4
16	**D. Batallas (Ecuador)**	**12**	66	E. R. Wild (USA)	4
17	**A. Catenazzi (USA)**	**11**	67	E.A. Pereira (Brazil)	4
18	**E. La Marca (Venezuela)**	**11**	68	J. C. Cusi (Peru)	4
19	**J. Brito-Molina (Ecuador)**	**11**	69	J. Culebras (Spain)	4
20	**N. B. Paez (Ecuador)**	**11**	70	J. G. Martinez (Colombia)	4
21	D. F. Cisneros-Heredia (Ecuador)	10	71	J. J. Mueses-Cisneros (Colombia)	4
22	J. C. Sánchez-Nivicela (Ecuador)	10	72	J. M. Padial (Spain)	4
23	S. B. Hedges (USA)	10	73	J. M. Savage (USA)	4
24	R. von May (USA)	9	74	K. L. A. Guimarães (Brazil)	4
25	M. Rivera-Correa (Colombia)	8	75	L. Alves da Silva (Brazil)	4
26	P. A. Burrowes (USA)	8	76	M. J. Navarrete (Ecuador)	4
27	A. F. Arteaga-Navarro (Ecuador)	7	77	M. Jimenez de la Espada (Spain)	4
28	C. Aguilar (Peru)	7	78	M. Penhacek (Brazil)	4
29	F. J. M. Rojas-Runjaic (Venezuela)	7	79	P. J. R. Kok (Belgium)	4
30	G. Flores (USA)	7	80	S. Duarte-Marín (Colombia)	4
31	H. M. Ortega-Andrade (Ecuador)	7	81	A. Almendariz (Ecuador)	3
32	J. H. Valencia (Ecuador)	7	82	A. Espinosa de los Monteros (Mexico)	3
33	J. Moravec (Czech Republic)	7	83	A. J. Crawford (USA)	3
34	P. J. Venegas (Peru)	7	84	A. M. Suarez-Mayorga (Colombia)	3
35	V. L. Urgiles (Ecuador)	7	85	A. Varela-Jaramillo (Ecuador)	3
36	C. W. Myers (USA)	6	86	C. F. Walker (USA)	3
37	H. Kaiser (USA)	6	87	C. Teran (Ecuador)	3
38	J. A. Ortega (Ecuador)	6	88	E. E. Infante-Rivero ()	3
39	J. C. Chaparro (Peru)	6	89	E. R. Dunn (USA)	3
40	J. J. Ospina-Sarria (Colombia)	6	90	F. H. Test (USA)	3
41	J. M. Daza (Colombia)	6	91	F. Werner (Austria)	3
42	M. A. Donnelly (USA)	6	92	G. A. González-Durán (Colombia)	3
43	M. Schmid (Germany)	6	93	G. A. Maldonado-Castro (Ecuador)	3
44	P. Szekely (Romania)	6	94	J. C. Jordan (Peru)	3
45	S. M. Ramirez-Jaramillo (Ecuador)	6	95	J. Carrion (Ecuador)	3
46	A. G. Ruthven (USA)	5	96	J. J. Morrone (Argentina-Mexico)	3
47	C. R. Hutter (USA)	5	97	J. Köhler (Germany)	3
48	C. Steinlein (Germany)	5	98	J. Lescure (France)	3
49	D. C. Cannatella (USA)	5	99	J. S. Eguiguren (Ecuador)	3
50	D. J. Santana (Brazil)	5	100	K. Sui-Ting (Peru)	3

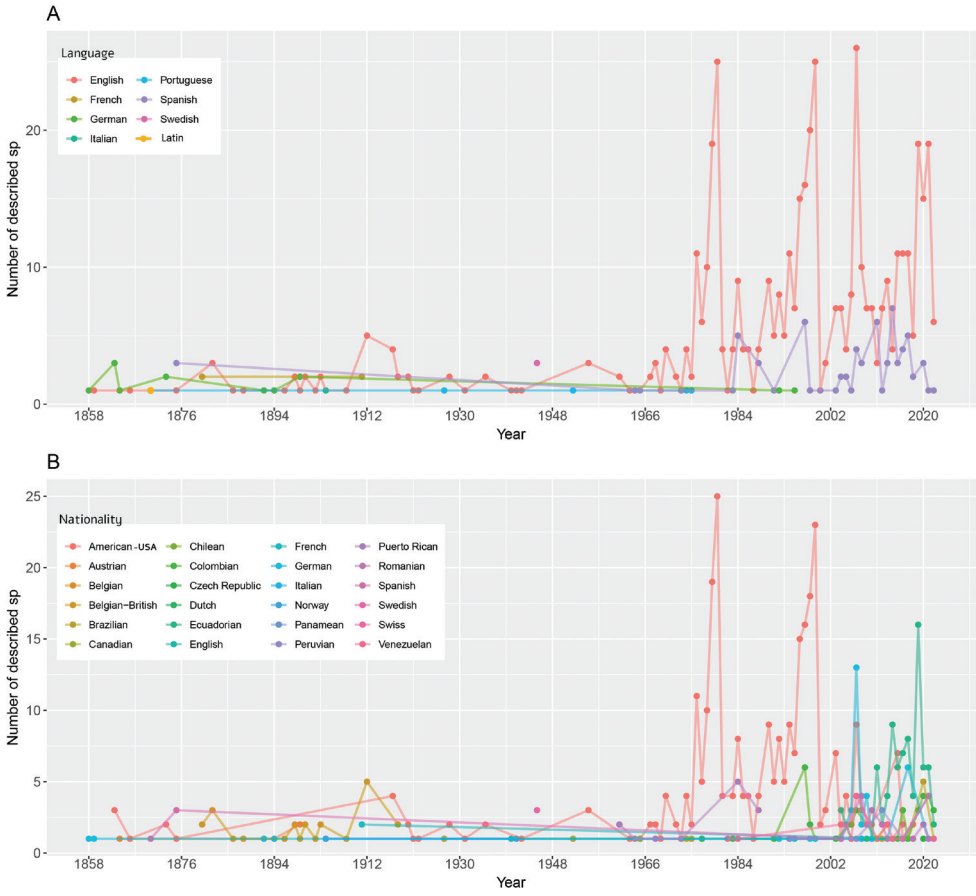

Figure 4. Languages and nationalities of authors who have participated in the descriptions of *Pristimantis* species **A** main languages used in descriptions per year **B** main nationalities of authors involved in descriptions per year.

of Natural History of University of Kansas (KU), Museo de Historia Natural del Instituto de Ciencias Naturales de Universidad Nacional de Colombia (ICN), Museo de Zoología de la Pontificia Universidad Católica del Ecuador (QCAZ), and División de Herpetología, Instituto Nacional de Biodiversidad, former Museo Ecuatoriano de Ciencias Naturales (DHMECN). KU and ICN house 35% of the typical material, and QCAZ and DHMECN have the 12.5% of type specimens of the genus (Fig. 3B). The rest of the collections hold a lower proportion of specimens than those mentioned (Fig. 3B, Suppl. material 1).

We identified a variety of eight languages used for the description of new *Pristimantis* species (Fig. 4A, Table 3), with the most common ones being English and Spanish. The English language has dominated species descriptions since the 1960s. The number of descriptions published in Spanish started to increase during the 1980s, though it remains lower than those published in English (Fig. 4A, Table 3). Conversely, there

Table 3. The most common languages in which new species of *Pristimantis* have been described.

Language	Number of descriptions	Percentage of taxa
English	492	83.2
Spanish	73	12.4
German	13	2.2
Portuguese	4	0.7
French	4	0.7
Swedish	3	0.5
Italian	1	0.2
Latin	1	0.2

Table 4. The most common author nationalities in *Pristimantis* descriptions.

Nationalities	Number of authors	Percentage of authors
Ecuadorian	67	20.9
US Americans	60	18.8
Colombian	49	15.3
Brazilian	30	9.4
Peruvian	21	6.5
German	18	5.6
Panamanian	7	2.2

are more than 20 nationalities of researchers who have participated as authors and co-authors in descriptions of new species of *Pristimantis* (Fig. 4B). Researchers from the USA have significantly dominated, not only the total number of descriptions, but also the number of annual descriptions until 2002. As of this year, the participation of Ecuadorian authors has increased in greater numbers compared to their Colombian, Peruvian, and Venezuelan peers (Fig. 4B). The greatest percentage of authors involved in descriptions of new *Pristimantis* species are of Ecuadorian nationality (20.9%), followed by US Americans (18.8%) and Colombians (15.3%) (Table 4).

From a gender perspective, 80% of the authors who have participated in the descriptions are male researchers and 20% female researchers (Figs 5, 6). In spite of an increase in the number of descriptions involving women starting in the 1950s, the participation of women in the description process continues to be considerably lower than that of their male counterparts (Fig. 5A). Ecuador is the country with the highest percentage of descriptions that incorporate female researchers with almost 18.8%, while Colombia, Peru, Venezuela, and Brazil have lower percentages (Fig. 5B). The bias towards male authors is overwhelmingly disproportionate in terms of principal authorship (i.e., first author or corresponding author). Where 50% of male authors featured as main authors, only 2% of female authors have held this role (Fig. 6, Table 5). We detected a significant slope between the proportion of female authors who participated in descriptions of all *Pristimantis* and the years (estimate = 0.03, SE = 0.01, $t = 2.2$, $p = 0.02$; Fig. 7). Of the four countries with the highest number of *Pristimantis* species descriptions, Ecuador was the only one with a significant positive slope between the proportion of female authors and time (estimate = 0.09, SE = 0.02, $t = 3.8$, $p = < 0.001$), while that on the contrary Colombia (estimate = 3.7 *10-3, SE = 0.01,

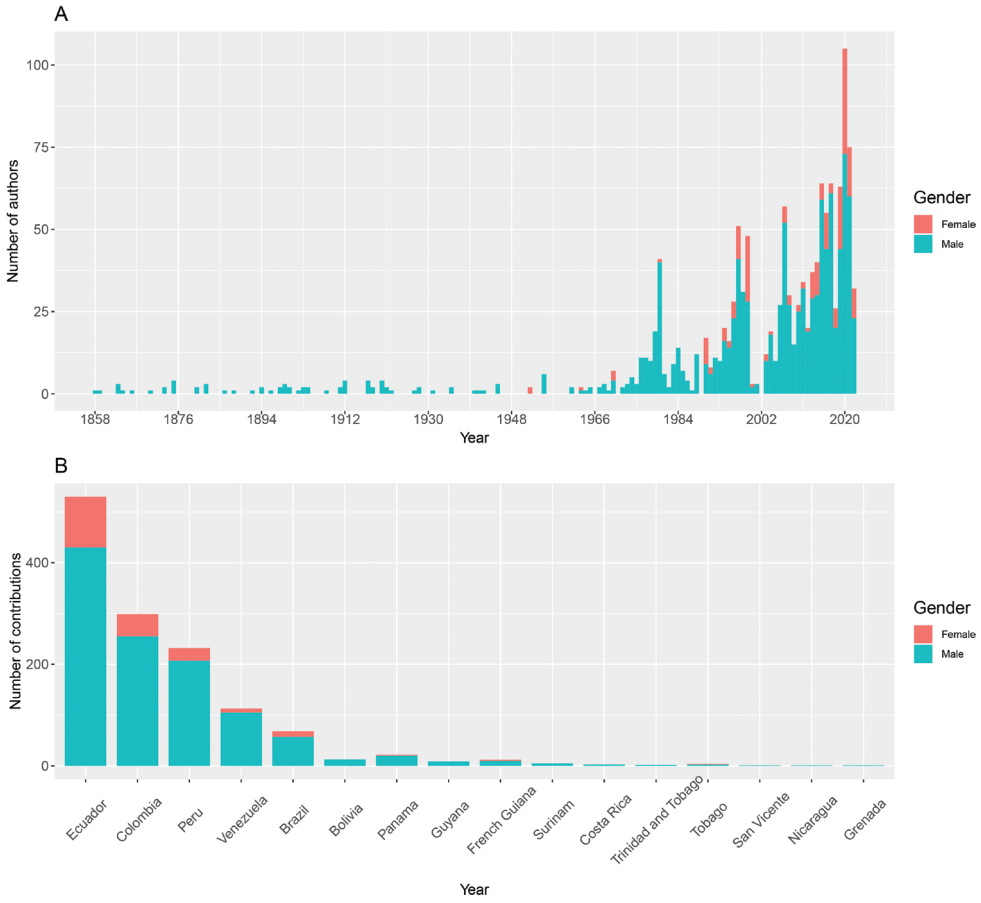

Figure 5. Male and female contributions to *Pristimantis* descriptions **A** number of female and male authors that participated in descriptions per year **B** contributions of female and male authors to descriptions per country.

t = 0.2, p = 0.8), Peru (estimate = -0.01, SE = 0.02, t = 3.8, p = 0.5),Venezuela (estimate = -0.01, SE = 0.03, t = -0.5, p = 0.7), and Brazil (estimate = -0.04, SE = 0.02, t = -2.25, p = 0.06) did not show any correlation between these variables (Fig. 7).

In relation to peer-reviewed journals in which the descriptions of new species of the genus have been published, Zootaxa and the Revista de la Academia Colombiana de Ciencias, Exactas, Físicas y Naturales have published the highest number of descriptions with 20.6% of the total described species. Other journals such as Herpetologica, ZooKeys, and Miscellaneous Publication of Museum of Natural History of University of Kansas have published 15.7% of the descriptions of *Pristimantis* (Fig. 8A). From the beginning of the descriptions of this diverse genus until the first decade of the 2000s, descriptions have been based mainly on morphology. Phylogenetic analyses were gradually incorporated into descriptions over the last 12 years, leading to a significant reduction in morphology-only descriptions of new *Pristimantis* species (Fig. 8B).

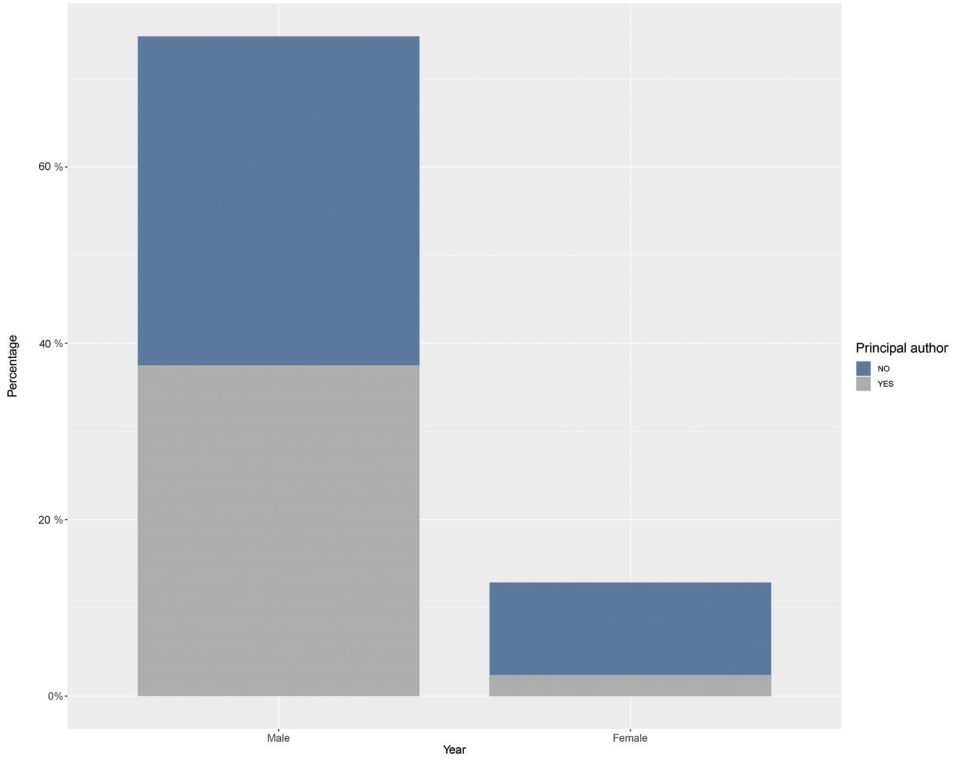

Figure 6. Contributions in which authors have been principal author and defined as either first or corresponding author.

Table 5. Top 21 female authors ranked by the number of species they have described. * Principal author is defined as being either the first or corresponding author.

#	Author	Nationality	Number of taxa	Principal author*
1	C. Reyes-Puig	Ecuadorian	18	13
2	J. B. Pramuk	US American	17	17
3	M. C. Ardila-Robayo	Colombian	15	-
4	N. B. Paez	Ecuadorian	11	11
5	P. A. Burrowes	US American	8	-
6	V. L. Urgiles	Ecuadorian	7	5
7	J. A. Ortega	Ecuadorian	6	-
8	M. A. Donnelly	US American	6	-
9	D. Szekely	Romanian	5	-
10	M. B. Perez	Ecuadorian	5	-
11	M. J. Navarrete	Ecuadorian	5	2
12	D. M. Cochran	US American	4	3
13	K. L. A. Guimarães	Brazilian	4	-
14	A. Almendariz	Ecuadorian	3	-
15	A. M. Suarez-Mayorga	Colombian	3	-
16	A. Varela-Jaramillo	Ecuadorian	3	-
17	C. Teran	Ecuadorian	3	-
18	G. A. Maldonado-Castro	Ecuadorian	3	-
19	K. Sui-Ting	Peruvian	3	-
20	P. Bejarano-Muñoz	Ecuadorian	3	-
21	Y. Sagredo	Ecuadorian	3	-

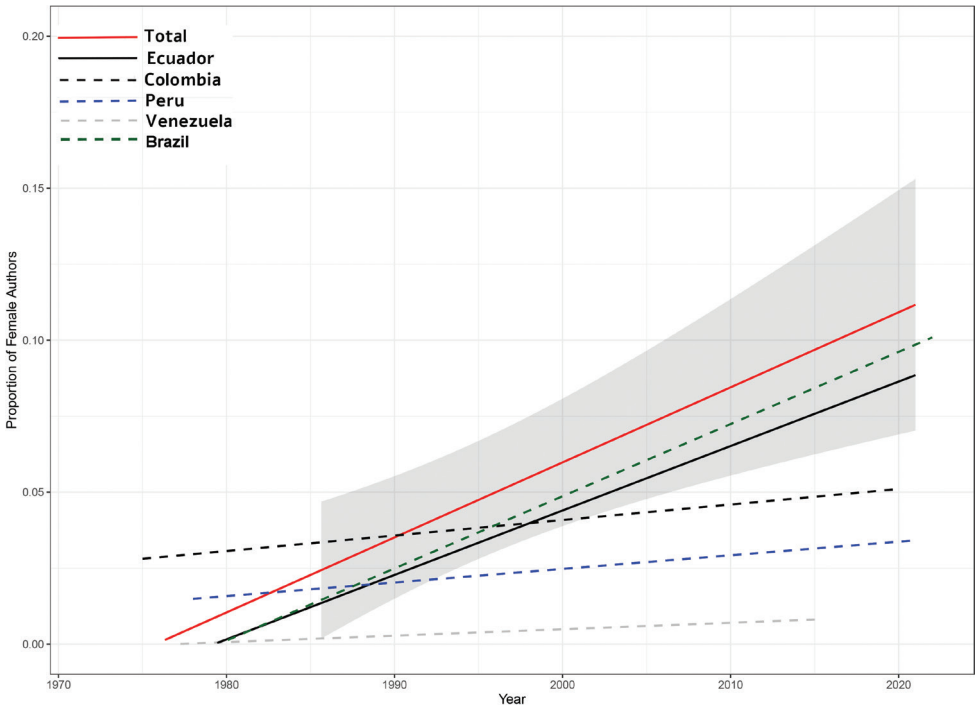

Figure 7. Change in the proportion of female authors over time. Gray shadow represents the confidence intervals of the Generalized Linear Model of the total proportion of female researchers (red solid line). Solid lines depict significant GLMs.

Regarding the conservation status of *Pristimantis* species, 24% are categorized by the IUCN Reed List as Least Concern, 31% are threatened (i.e., CR, EN, or VU), and 36.8% are Not Evaluated or Data Deficient (Fig. 9A). The country with the highest number of Not evaluated species is Ecuador (i.e., 39% of all Ecuadorian species). Peru and Venezuela host the highest percentages of species under the Data Deficient category, 31.8% and 42.8% of their total species, respectively. In Ecuador and Colombia, at least 30% of *Pristimantis* species are under some form of threat (Fig. 9B).

Discussion

Most prolific authors and countries with the highest numbers of descriptions

The contributions made by Lynch and Duellman to the advancement of *Pristimantis* taxonomy and systematics since the 70s are indisputable. Their most significant contributions focus on large compendiums that include analyses of distribution patterns and advances in systematics and descriptions of several new species (Lynch 1979; Lynch and Duellman 1980, 1997; Duellman and Pramuk 1999). Their work initially focused

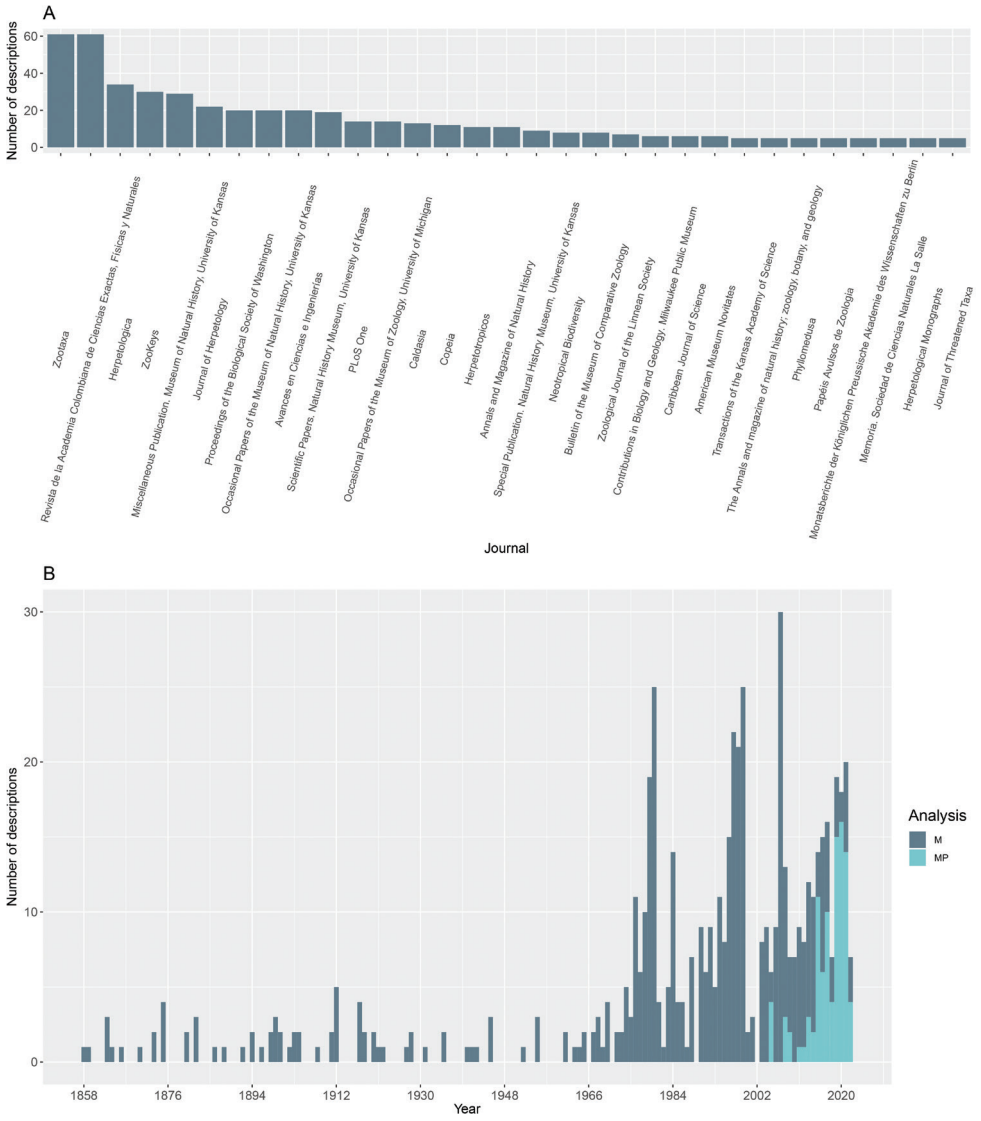

Figure 8. A Main scientific journals where descriptions of new *Pristimantis* species are published **B** type of descriptions per year, M = Morphological description, MP = morphological and phylogenetic description.

on the eastern slopes of Ecuador (Lynch 1979; Lynch and Duellman 1980) and later towards the 1990s their interests shifted over to the Colombian and Peruvian foothills (Lynch 1998; Duellman and Pramuk 1999). The most representative works and the most productive years for the descriptions of new species of this genus were:

- 1979 with "Leptodactylid frogs of the genus *Eleutherodactylus* from the Andes of southern Ecuador" by J. D. Lynch and the description of 16 new species;

- 1980 with "*Eleutherodactylus* of the Amazonian slopes of the Ecuadorian Andes (Anura: Leptodactylidae)" by Lynch and Duellman, which includes 12 new species;
- 1997 with "Frogs of the genus *Eleutherodactylus* in western Ecuador" by Lynch and Duellman;
- 1998 with "New frogs of the genus *Eleutherodactylus* from the eastern flank of the northern Cordillera Central of Colombia" by Lynch and Rueda-Almonacid and "New species of *Eleutherodactylus* from the Cordillera Occidental of western Colombia with a synopsis of the distributions of species in western Colombia" by Lynch, in which nine new species are described;
- 1999 with "Frogs of the genus *Eleutherodactylus* (Anura: Leptodactylidae) in the Andes of northern Peru" by Duellman and Pramuk, describing more than 15 species;
- 2007 with "Three new species of *Pristimantis* (Anura: Leptodactylidae) from the Cordillera de Huancabamba in northern Peru" and "New eleutherodactyline frogs (Leptodactylidae: *Pristimantis*, *Phrynopus*) from Peru" both by Lehr with three and four new species each;
- 2019 with "Systematics of *Huicundomantis*, a new subgenus of *Pristimantis* (Anura, Strabomantidae) with extraordinary cryptic diversity and eleven new species" by Páez and Ron which added 11 new species to Ecuador after almost 40 years of a contribution that includes joint descriptions of *Pristimantis*, as previously published by Lynch and Duellman (Lynch 1979; Lynch and Duellman 1980);
- 2021 with several descriptions from different authors (see Suppl. material 1). We assume that the pandemic due to COVID 19 had a negative effect on field trips in all countries actively working on *Pristimantis* taxonomy. In addition, pure research activities were probably reduced by the effect of the lockdown and COVID 19, as has been observed in other lines of research (Donthu and Gustafsson 2020).

If current trends in the growth rate of annual *Pristimantis* descriptions are maintained and taking into consideration the entire temporal history of descriptions of each country, the total number of species of is expected to increase in the next 10 years to ~777 described species, with ~299 in Ecuador, ~217 in Colombia and ~153 in Peru, ~73 in Venezuela, ~22 in Brazil, ~11 in Panama, and ~6 in Bolivia.

Why does Ecuador lead in the number of new species of *Pristimantis* described?

The contributions of Lynch and Duellman in defining the group as a diverse and highly endemic genus became extremely influential to local researchers, leading to further discoveries mainly around Ecuador, Colombia, and Peru (Lynch 1979; Lynch and Duellman 1980, 1997). Despite being the smallest by area of these three, Ecuador sports both the highest number of descriptions of new species of *Pristimantis* and the greatest richness of the genus, followed by Colombia and Peru, suggesting that the known diversity of the genus is underestimated in these countries (Frost 2022; Ron et al. 2022). Out of the six peaks Pistimantis described per year, three of them took place in Ecuador, highlighting the commitment to taxonomic efforts in the region. In addition, Ecuador has had more academic approach to amphibian taxonomy more noticeable

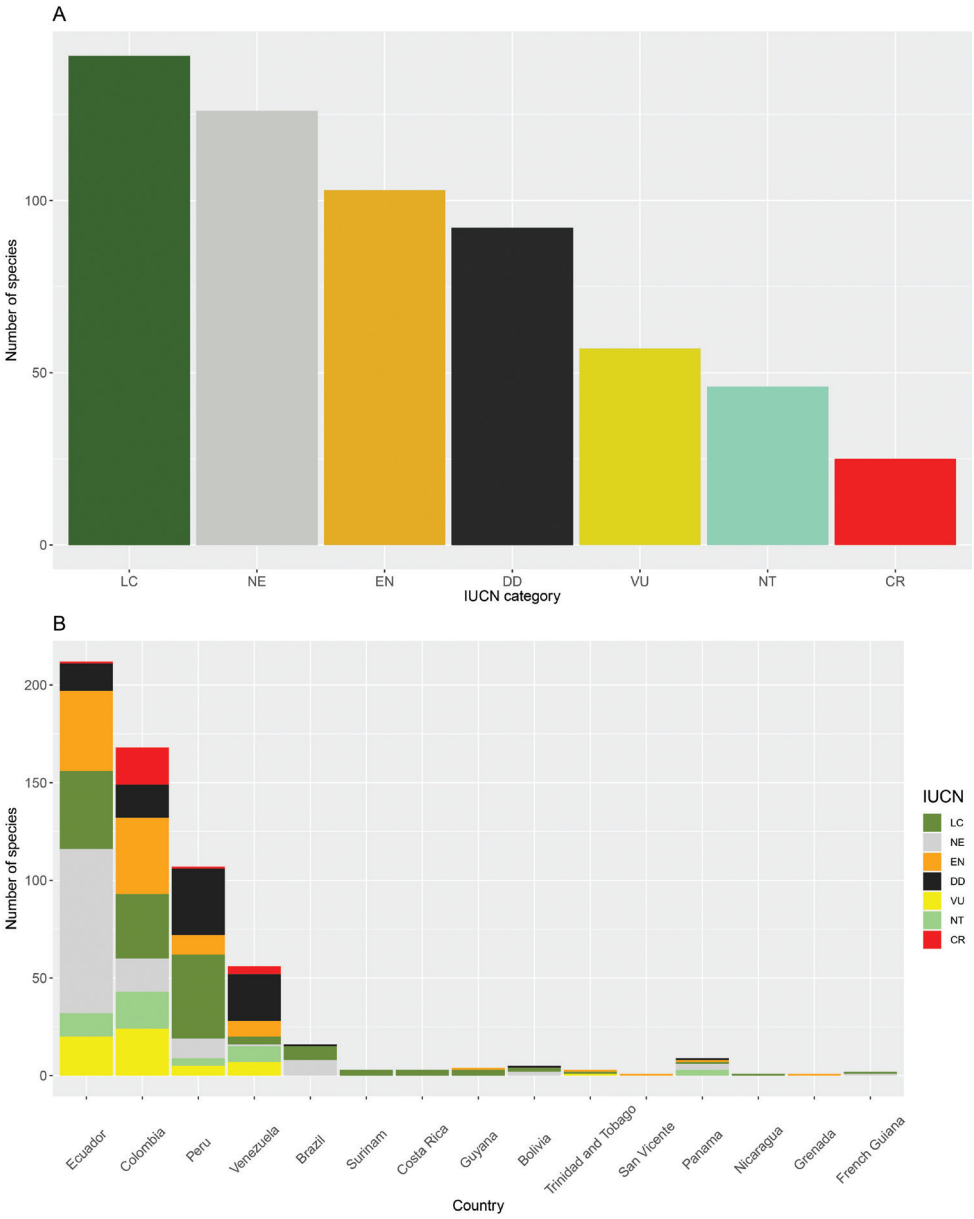

Figure 9. Conservation status categories established by the IUCN Red List for *Pristimantis* species **A** number of species per category **B** number of species in each category per country.

than it's neighboring countries: some Ecuadorian taxonomists often pursue higher education abroad in the USA and return to the country to develop their lines of research (e.g., Santiago R. Ron, Juan Manuel Guayasamin, Luis Coloma). However, younger generations of ecuadorian taxonomists have contributed significantly to the taxonomy and systematics of the group, despite not being trained abroad (e.g., Mario H. Yánez-

Muñoz, Carolina Reyes-Puig, Juan P. Reyes-Puig, Jorge Brito Molina, Diego Batallas) (Table 2). However, it is important to consider that alliances with colleagues, researchers, and institutions have been crucial for the advancement of *Pristimantis* descriptions in Ecuador. As mentioned by Costello et al. (2013) it seems that South America would have an increase in the number of taxonomists in general, but this is related to the region being much more diverse than others. The Convention on Biological Diversity has proposed some strategies to improve the productivity of taxonomy, including collaborations with both national and international researchers, the requirement to include national institutions when the research is being carried out by foreign researchers, etc. Ecuador has been successful in this context, and this is evidenced by its productivity.

John D. Lynch, an US American herpetologist and taxonomist credited with the greatest number of described species; a total of 149. After working 30 years at the University of Nebraska-Lincoln, he became associate professor and curator of herpetology at the Instituto de Ciencias Naturales de la Universidad Nacional de Colombia in 1997. William E. Duellman, a prominent US American zoologist who was Curator Emeritus of the Herpetology Division of the Natural History Museum of University of Kansas (Coloma and Guayasamin 2022), is the second most productive taxonomist with 82 formally described species. Next in the ranking are authors such as Edgar Lehr, M. H. Yánez-Muñoz, and Santiago R. Ron taking up the mantle from Lynch and Duellman, the three of them are responsible for 15% of the total number of descriptions in the genus. Edgar Lehr is a herpetologist at the University of Illinois and his work has focused on amphibian systematics, mainly from Peru (Illinois Wesleyan University 2022). Mario H. Yánez-Muñoz of Instituto Nacional de Biodiversidad and Santiago R. Ron, professor and curator of the Museum of Zoology QCAZ (Museo de Zoología de la Pontificia Universidad Católica del Ecuador), have focused on the taxonomy and systematics of the genus in the Andean slopes and lowlands of Ecuador for the last 15 years (Ron et al. 2020; INABIO 2022).

The first two positions of the most prolific taxonomists for *Pristimantis* are occupied by US American researchers, who account for 46.8% of the known diversity of the genus. However, among the 20 authors with the most descriptions, 70% are Latin American authors following in the footsteps of Lynch and Duellman. The increase of Latin American researchers interested in the genus arises from the empowerment of local science and biodiversity, driving further interest as research goals are met. Although the last few years have seen an increase in the number of researchers interested in describing new species of *Pristimantis*, most of them describe between one and four species, which reflects the number of authors participating in the publications (Suppl. material 1; e.g., Guayasamin et al. 2017).

Species description language

English and Spanish are the dominant languages for descriptions of *Pristimantis* species. From a temporal perspective, all the work developed mainly by Lynch and Duellman (Lynch and Duellman 1980, 1997; Duellman and Pramuk 1999; Duellman

and Lehr 2009) correlates with language, scientific collections, years of production, etc. Although the number of descriptions published in Spanish has steadily increased since 1980, publication trends have encouraged an increase in English descriptions as well during the last two decades. The irony of this relationship is that most of the current researchers of the genus are Spanish-speaking Latin Americans, publishing in English mainly for other Spanish speakers. Even this article is an example of this conundrum. However, our aim is to visualize the specifics of descriptions in *Pristimantis*, highlighting patterns and trends in order to visualize to a wider audience the information that lies behind a new description in such a diverse group. In addition, as suggested by Ramírez-Castañeda (2020), we included a full Spanish translation of this manuscript as Suppl. material 2.

The publication of results in English is directly related to pressures from academic institutions to publish in high-impact journals, where English is established as the official language of publication. Publishing in this language for non-English speakers can be time-consuming, demanding, and stressful, and some efforts have been made to understand this in the framework of Latin American researchers (Ramírez-Castañeda 2020). Despite English being the common language for communicating science, the incorporation of Spanish for taxonomic groups geographically distributed in Latin American countries could also be a valuable alternative for disseminating results. Therefore, mechanisms to promote the advancement of research in *Pristimantis* published in Spanish in specialized journals (taxonomy and systematics journals) (e.g., Fig. 7) are necessary.

Author nationalities

The number of Ecuadorian researchers is proportionally higher than that of other nationalities describing new *Pristimantis* species during the last few years (e.g., Yánez-Muñoz et al. 2010; Guayasamin et al. 2017; Páez and Ron 2019; Reyes-Puig et al. 2020; Ron et al. 2020). However, it is also worth mentioning that the number of authors per description is higher compared to descriptions from the 1980s (e.g., Lynch and Duellman 1980). There are currently descriptions with up to nine authors (e.g., Ron et al. 2020; see Suppl. material 1), and the average number of authors per species described in the 1980s is between 1 and 2, while during the last decade the average number of authors participating in descriptions is between 5 and 6. In many of these multi-author descriptions, most individual authors have very low description rates while the lead author is an experienced researcher in the study of taxonomy and systematics of the genus.

In this paper we also identify a gap in the presence of *Pristimantis* taxonomists in Peru, Venezuela, Brazil, Panama, and Bolivia compared to Ecuador and Colombia. The inclusion and empowerment of local scientists from these countries would seem necessary in order to increase the study of rainfrog species in their territory, which has been mainly led by foreign authors (e.g., Duellman and Pramuk 1999; Catenazzi and Lehr 2018; Lehr et al. 2021) (details on authors, years, and descriptions can be downloaded from Suppl. material 1).

Natural history museum collections

Due to the extensive work of Lynch and Duellman, the museums related to their research currently hold the largest amount of type material from *Pristimantis* (i.e., KU and ICN). The QCAZ is an institution with more than 40 years dedicated to safeguarding and researching Ecuadorian biodiversity and has positioned itself as an international benchmark regarding management and open access to scientific collections, not only for amphibians but also for other vertebrates. This institution is notable for hosting holotypes for 44 species of *Pristimantis* until June 2022 (Ron et al. 2022; Torres-Carvajal et al. 2022). Other South American institutions that preserve a large number of holotypes are the DHMECN (División de Herpetología del Instituto Nacional de Biodiversidad, Ecuador) and the MUSM (Museo de Historia Natural, Universidad Nacional Mayor de San Marcos). The DHMECN of Instituto Nacional de Biodiversidad has focused on the taxonomy and systematics of Ecuadorian herpetofauna for the last 15 years, primarily on *Pristimantis* from the Andean slopes of Ecuador (INABIO 2022). The Herpetology Division of MUSM has a long record of researching Peruvian herpetofauna since 1946. However, since 2007 its scientific production related to descriptions of new species has decreased (MUSM 2022). In addition, virtual access to its collections and databases is limited compared to that of Ecuadorian collections (Ron et al. 2022).

Author gender

Historically, zoology has been a male-dominated field. The barriers that limited the number of women in scientific fields before the 20th century has led to the study of animals being an exclusively male discipline (Slobodian 2021). Herpetology is no exception, although there are now far more women in the field than men (Rock et al. 2021). In general, the proportion of female authors is lower, at least in the actively publishing population (Salerno et al. 2019). In the case of descriptions of new species of *Pristimantis*, the number of women actively working in this group is low (20% of the authors are women). Consequently, women are poorly featured as principal authors, a position considered to be the most important indicator of the author's role in the description process. Of a total of 66 female authors, only six have been principal authors. It is necessary to reflect on this pattern, as it is consistent with other studies on the underrepresentation of women in science (West et al. 2013; Fox et al. 2018; Salerno et al. 2019). If current trends continue, female participation in *Pristimantis* descriptions would increase to 50% over the next 25 years (2047). This would mean that in this period the proportion of women in the field could potentially be the same as men, considering only authorship and not principal authorship. Ecuador, being the country with the most researchers, also has the largest number of female researchers; however, many of them are thesis students of principal investigators, so their incursion into the study of the taxonomy of the group is temporary. In this article we encourage the active inclusion of female researchers interested in the field of taxonomy, promoting the advancement of the diversity of *Pristimantis*. We also strongly encourage male researchers to open the doors of their laboratories to women, where their roles are not limited to field assistants

or specific sections of descriptions, but also as leaders taking on critical positions in particular taxonomic works. The best way to promote this in the future will be through increasing the proportion of women in senior author positions (Salerno et al. 2019).

Peer-reviewed journals

The journals with the highest number of contributions of rainfrog descriptions are Zootaxa and Revista de la Academia Colombiana de Ciencias, Exactas Físicas y Naturales. We can identify two critical issues: the first is the problem of taxonomy today (i.e., underestimation of this area of knowledge being considered a basic science), and the second is how to get other journals to climb to better academic positions if they are local, free, and open access. This question does not have a simple answer since the scaling of these journals will depend entirely on metrics such as the impact factor (IF), an index that assesses the relative importance of a scientific journal in a particular field. The effect of the IF has repercussions on the endless cycle of not citing journals that do not have a medium high IF. Publishing purely taxonomic articles is becoming increasingly complex, both because of the decrease in the number of researchers interested in the field and the number of journals interested in this topic (Wägele et al. 2011). In 2020, Zootaxa was excluded from the Journal Citation Report (JCR) for 2019 (2020 release) by Clarivate Analytics due to excessive use of self-citations. Following a petition that included more than 3900 signatures from research biologists, Clarivate Analytics reversed the decision (Parise Pinto et al. 2021). This misunderstanding and lack of knowledge on how taxonomy works raises concerns about the difficulty of publishing new species discoveries and which journals can be chosen for such a task. Zootaxa shows its importance not only because it has included descriptions of more than 25% of the world's known biodiversity (Parise Pinto et al. 2021), but in the case of *Pristimantis* it is the main journal in which descriptions have been published.

Description type

It is important to note that in the past the vast majority of new species descriptions have been based on morphologic data (83.7% of total descriptions). However, during the last 20 years the molecular revolution has transformed the description process, including DNA sequences that allow phylogenetic positioning of taxa. The continuous increase in available molecular techniques has made the costs to implement them lower and thus more accessible. Therefore, the inclusion of sequencing has become a common tool to better understand the ancestry-descent relationships of living organisms (Malakhov 2013). However, it is worth considering that in the description of new species, sequencing should not replace a detailed taxonomic assessment with morphological characters that allow observers to clearly differentiate one species from another (Guerra-García et al. 2008). Positioning taxonomy as a necessary science to discover and describe biodiversity is essential in its own right. This is evident in the case of *Pristimantis*, as supported by this review, given the trend of increasing numbers of described species and descriptions of highly cryptic species (Padial and De la Riva 2009; Hutter and Guayasamin 2015; Páez and Ron 2019; Ortega-Andrade et al. 2015).

Global threat categories

Finally, regarding the IUCN global conservation status of *Pristimantis*, we highlight that a representative proportion of the species described to date (i.e., 36.8%) are found in uncertainty categories such as Not Evaluated and Data Deficient. These categories reflect the need for a global evaluation of the species of this genus, on account of its high endemism and species richness. On the other hand, it also highlights the increasing rate of species descriptions. Conservation status assessments are generally carried out by the global IUCN every four to five years (IUCN 2022), a period in which there are likely to be 10–15 new species of *Pristimantis* per year. Therefore, global red list assessments will always be one step behind the evaluation of threat criteria. An alternative to address this matter could be through local and regional red list assessments, which would be more readily updated and may include other variables for categorization (Ortega-Andrade et al. 2021). In addition, many of the new species of *Pristimantis* have restricted distribution ranges with populations facing various threats (e.g., Brito-Zapata et al. 2021), implying a higher degree of vulnerability. Nevertheless, if global assessments are not conducted for many of these species, the conservation priorities of the genus remain underestimated. In this work we include the categories proposed by the IUCN global red list (IUCN 2022), since the local and regional evaluations of each country are not updated and standardized and therefore cannot be compared. Ecuador has made the most recent effort for a more complete and up-to-date cataloguing, establishing 50% of Ecuadorian *Pristimantis* species under some degree of threat (Ortega-Andrade et al. 2021). This estimate is considerably higher than that reported by the IUCN of 33.5%, likely due to the proportion of species not evaluated or with insufficient information. All these aspects reinforce the importance of continuing to invest not only in the advancement of taxonomic research on the genus, but also in conservation strategies articulated between countries in the region.

Acknowledgements

We are extremely grateful to Gorki Ríos-Alvear, David Brito-Zapata, and Maria Antonia Izurieta for their help in entering information in the database of *Pristimantis* descriptions. This research was supported by Universidad San Francisco de Quito USFQ through COCIBA Grants (project HUBI ID 12268, 17475) to CRP. We greatly appreciate the comments of Edgar Lehr and Juan Manuel Guayasamin, which helped improve the manuscript.

References

Armesto LO, Señaris JC (2017) Anuros del norte de los andes: Patrones de riqueza de especies y estado de conservación. Papéis Avulsos de Zoologia (São Paulo) 57(39): 491–526. https://doi.org/10.11606/0031-1049.2017.57.39

Arroyo SB, Serrano-Cardozo VH, Ramírez-Pinilla MP (2008) Diet, microhabitat and time of activity in a *Pristimantis* (Anura, Strabomantidae) assemblage. Phyllomedusa: Journal of Herpetology 7(2): 109–119. https://doi.org/10.11606/issn.2316-9079.v7i2p109-119

Boulenger GA (1882) Catalogue of the Batrachia Salientias. Taylor and Francis, London, 256 pp.

Brito-Zapata D, Reyes-Puig C, Cisneros-Heredia D, Zumel D, Ron SR (2021) Description of a new minute frog of the genus *Pristimantis* (Anura: Strabomantidae) from Cordillera del Condor, Ecuador. Zootaxa 5072(4): 351–372. https://doi.org/10.11646/zootaxa.5072.4.3

Canedo C, Haddad CFB (2012) Phylogenetic relationships within anuran clade Terrarana, with emphasis on the placement of Brazilian Atlantic rainforest frogs genus *Ischnocnema* (Anura: Brachycephalidae). Molecular Phylogenetics and Evolution 65(2): 610–620. https://doi.org/10.1016/j.ympev.2012.07.016

Catenazzi A, Lehr E (2018) *Pristimantis antisuyu* sp. n. and *Pristimantis erythroinguinis* sp. n., two new species of terrestrial-breeding frogs (Anura, Strabomantidae) from the eastern slopes of the Andes in Manu National Park, Peru. Zootaxa 4394(2): 185–206. https://doi.org/10.11646/zootaxa.4394.2.2

Coloma LA, Guayasamin JM (2022) William E. Duellman (1930–2022). Phyllomedusa: Journal of Herpetology 21: 103–111.

Costello MJ, May RM, Stork NE (2013) Can we name Earth's species before they go extinct? Science 339(6118): 413–416. https://doi.org/10.1126/science.1230318

de Queiroz K (2005) A unified concept of species and its consequences for the future of taxonomy. Proceedings of the California Academy of Sciences 56: 196–215.

Donthu N, Gustafsson A (2020) Effects of COVID-19 on business and research. Journal of Business Research 117: 284–289. https://doi.org/10.1016/j.jbusres.2020.06.008

Duellman WE, Lehr E (2009) Terrestrial-breeding frogs (Strabomantidae) in Peru. Natur und Tier Verlag, Münster, 382 pp.

Duellman WE, Pramuk JB (1999) Frogs of the genus *Eleutherodactylus* (Anura: Leptodactylidae) in the Andes of northern Peru. Scientific Papers Natural History Museum, University of Kansas 13: 1–78. https://doi.org/10.5962/bhl.title.16169

Fox CW, Ritchey JP, Paine CET (2018) Patterns of authorship in ecology and evolution: First, last, and corresponding authorship vary with gender and geography. Ecology and Evolution 8(23): 11492–11507. https://doi.org/10.1002/ece3.4584

Frost D (2022) Amphibian Species of the World: an Online Reference. Version 6.1. Electronic Database. [Accessible at:] https://amphibiansoftheworld.amnh.org/index.php [accessed 30 January 2022]

González-Durán GA, Targino M, Rada M, Grant T (2017) Phylogenetic relationships and morphology of the *Pristimantis* leptolophus species group (Amphibia: Anura: Brachycephaloidea), with the recognition of a new species group in *Pristimantis* Jiménez de la Espada, 1870. Zootaxa 4243: 042–074. https://doi.org/10.11646/zootaxa.4243.1.2

Guayasamin JM, Krynak T, Krynak K, Culebras J, Hutter CR (2015) Phenotypic plasticity raises questions for taxonomically important traits: A remarkable new Andean rainfrog (*Pristimantis*) with the ability to change skin texture. Zoological Journal of the Linnean Society 173(4): 913–928. https://doi.org/10.1111/zoj.12222

Guayasamin JM, Hutter CR, Tapia EE, Culebras J, Peñafiel N, Pyron RA, Morochz C, Funk WC, Arteaga A (2017) Diversification of the rainfrog *Pristimantis ornatissimus* in the lowlands and Andean foothills of Ecuador. PLoS ONE 12: e0172615. https://doi.org/10.1371/journal.pone.0172615

Guerra García JM, Espinosa Torre F, García Gómez JC (2008) Trends in taxonomy today: an overview about the main topics in taxonomy. Zoológica Baetica 19: 15–49.

Hedges SB, Duellman WE, Heinicke MP (2008) New World direct-developing frogs (Anura: Terrarana): molecular phylogeny, classification, biogeography, and conservation. Zootaxa 1737(1): 1–182. https://doi.org/10.11646/zootaxa.1737.1.1

Heinicke MP, Duellman WE, Hedges SB (2007) Major Caribbean and Central American frog faunas originated by ancient oceanic dispersal. Proceedings of the National Academy of Sciences of the United States of America 104(24): 10092–10097. https://doi.org/10.1073/pnas.0611051104

Heinicke MP, Duellman WE, Trueb L, Means DB, Macculloch RD, Hedges SB (2009) A new frog family (Anura: Terrarana) from South America and an expanded directdeveloping clade revealed by molecular phylogeny. Zootaxa 2211(1): 1–35. https://doi.org/10.11646/zootaxa.2211.1.1

Heinicke MP, Lemmon AR, Lemmon EM, McGrath K, Hedges SB (2018) Phylogenomic support for evolutionary relationships of New World direct-developing frogs (Anura: Terrarana-nae). Molecular Phylogenetics and Evolution 118: 145–155. https://doi.org/10.1016/j.ympev.2017.09.021

Hutter CR, Guayasamin JM (2015) Cryptic diversity concealed in the Andean cloud forests: Two new species of rainfrogs (*Pristimantis*) uncovered by molecular and bioacoustic data. Neotropical Biodiversity 1(1): 36–59. https://doi.org/10.1080/23766808.2015.1100376

Illinois Wesleyan University (2022) Edgar Lehr, Ph.D. https://www.iwu.edu/biology/faculty/lehr.html [accessed 3 June 2022]

INABIO [Instituto Nacional de Biodiversidad] (2022) Colecciones científicas: Herpetología. http://inabio.biodiversidad.gob.ec/colecciones_inabio/ [accessed 3 June 2022]

IUCN (2022) The IUCN Red List of Threatened Species. https://www.iucnredlist.org [accessed 14 June 2022]

Jiménez de la Espada M (1870) Fauna neotropicalis species quaedam nondum cognitae. Jornal de Sciências, Mathemáticas, Physicas e Naturaes 3: 57–65.

Kaiser H, Barrio-Amorós CL, Rivas GA, Steinlein C, Schmid M (2015) Five new species of *Pristimantis* (Anura: Strabomantidae) from the coastal cloud forest of the Península de Paria, Venezuela. Journal of Threatened Taxa 7(4): 7047–7088. https://doi.org/10.11609/JoTT.o4197.7047-88

Lehr E (2007) New eleutherodactyline frogs (Leptodactylidae: *Pristimantis*, *Phrynopus*) from Peru. Bulletin of the Museum of Comparative Zoology 159(2): 145–178. https://doi.org/10.3099/0027-4100(2007)159[145:NEFLPP]2.0.CO;2

Lehr E, Aguilar C, Siu-Ting K, Carlos Jordán J (2007) Three New Species of *Pristimantis* (Anura: Leptodactylidae) from the Cordillera De Huancabamba in Northern Peru. Herpetologica 63(4): 519–536. https://doi.org/10.1655/0018-0831(2007)63[519:TNSOPA]2.0.CO;2

Lehr E, Lyu S, Catenazzi A (2021) A new, critically endangered species of *Pristimantis* (Amphibia: Anura: Strabomantidae) from a mining area in the Cordillera Occidental of northern Peru (Región Cajamarca). Salamandra 57(1): 15–26.

Lynch JD (1968) Systematic status of some Andean leptodactylid frogs with a description of a new species of *Eleutherodactylus*. Herpetologica 24: 289–300.

Lynch JD (1971) Evolutionary relationships, osteology, and zoogeography of leptodactyloid frogs. University of Kansas Museum of Natural History. Miscellaneous Publications 53: 1–2.

Lynch JD (1979) Leptodactylid frogs of the genus *Eleutherodactylus* from the Andes of southern Ecuador. Miscellaneous Publication Museum of Natural History, University of Kansas 66: 1–62. https://doi.org/10.5962/bhl.title.16268

Lynch JD (1998) New species of *Eleutherodactylus* from the Cordillera Occidental of western Colombia with a synopsis of the distributions of species in western Colombia. Revista de la Academia Colombiana de Ciencias Exactas, Físicas y Naturales 22: 117–148.

Lynch JD, Duellman WE (1980) The *Eleutherodactylus* of the Amazonian slopes of the Ecuadorian Andes (Anura: Leptodactylidae). Miscellaneous Publication Museum of Natural History, University of Kansas 69: 1–86. https://doi.org/10.5962/bhl.title.16222

Lynch JD, Duellman WE (1997) Frogs of the genus *Eleutherodactylus* in western Ecuador, Systematics, ecology, and biogeography. Special Publication Natural History Museum, University of Kansas 23: 1–236. https://doi.org/10.5962/bhl.title.7951

Lynch JD, Rueda-Almonacid JV (1998) Additional new species of frogs (genus *Eleutherodactylus*) from cloud forests of eastern Departamento de Caldas, Colombia. Revista de la Academia Colombiana de Ciencias Exactas, Físicas y Naturales 22: 287–298.

Malakhov V (2013) A revolution in zoology: New concepts of the metazoan system and phylogeny. Herald of the Russian Academy of Sciences 83(2): 123–127. https://doi.org/10.1134/S1019331613020044

Mendoza ÁM, Ospina OE, Cárdenas-Henao H, García-R JC (2015) A likelihood inference of historical biogeography in the world's most diverse terrestrial vertebrate genus: Diversification of direct-developing frogs (Craugastoridae: *Pristimantis*) across the Neotropics. Molecular Phylogenetics and Evolution 85: 50–58. https://doi.org/10.1016/j.ympev.2015.02.001

Meneghini R, Packer AL, Nassi-Calo L (2008) Articles by Latin American authors in prestigious journals have fewer citations. PLoS ONE 3(11): e3804. https://doi.org/10.1371/journal.pone.0003804

Meza-Joya FL, Torres M (2016) Spatial diversity patterns of *Pristimantis* frogs in the Tropical Andes. Ecology and Evolution 6(7): 1901–1913. https://doi.org/10.1002/ece3.1968

MUSM [Museo de Historia Natural de la Universidad de San Marcos] (2022) División de Herpetología. https://museohn.unmsm.edu.pe/ [accessed 3 June 2022]

Ortega-Andrade HM, Rojas-Soto OR, Valencia JH, Espinosa de los Monteros A, Morrone JJ, Ron SR, Cannatella DC (2015) Insights from Integrative Systematics Reveal Cryptic Diversity in *Pristimantis* Frogs (Anura: Craugastoridae) from the Upper Amazon Basin. PLoS ONE 10: e0143392. https://doi.org/10.1371/journal.pone.0143392

Ortega-Andrade HM, Rodes Blanco M, Cisneros-Heredia DF, Guerra Arévalo N, López de Vargas-Machuca KG, Sánchez-Nivicela JC, Armijos-Ojeda D, Cáceres Andrade JF, Reyes-Puig C, Quezada Riera AB, Székely P, Rojas Soto OR, Székely D, Guayasamin JM, Siavichay Pesántez FR, Amador L, Betancourt R, Ramírez-Jaramillo SM, Timbe-Borja B, Gómez Laporta M, Webster Bernal JF, Oyagata Cachimuel LA, Chávez Jácome D, Posse V, Valle-Piñuela C, Padilla Jiménez D, Reyes-Puig JP, Terán-Valdez A, Coloma LA, Pérez Lara MB, Carvajal-Endara S, Urgilés M, Yánez Muñoz MH (2021) Red List assessment of amphibian species of Ecuador: A multidimensional approach for their conservation. PLoS ONE 16: 1–28. https://doi.org/10.1371/journal.pone.0251027

Padial JM, De la Riva I (2009) Integrative taxonomy reveals cryptic Amazonian species of *Pristimantis* (Anura: Strabomantidae). Zoological Journal of the Linnean Society 155(1): 97–122. https://doi.org/10.1111/j.1096-3642.2008.00424.x

Padial JM, Miralles A, De la Riva I, Vences M (2010) The integrative future of taxonomy. Frontiers in Zoology 7(1): 16. https://doi.org/10.1186/1742-9994-7-16

Padial JM, Grant T, Frost DR (2014) Molecular systematics of terraranas (Anura: Brachycephaloidea) with an assessment of the effects of alignment and optimality criteria. Zootaxa 3825: 1–132. https://doi.org/10.11646/zootaxa.3825.1.1

Páez NB, Ron SR (2019) Systematics of *Huicundomantis*, a new subgenus of *Pristimantis* (Anura, Strabomantidae) with extraordinary cryptic diversity and eleven new species. ZooKeys 868: 1–112. https://doi.org/10.3897/zookeys.868.26766

Parise Pinto ÂP, Mejdalani G, Mounce R, Silveira LF, Marinoni L, Rafael JA (2021) Are publications on zoological taxonomy under attack? Royal Society Open Science 8(2): 201617. https://doi.org/10.1098/rsos.201617

Peters JA (1955) Herpetological type localities in Ecuador. Revista Ecuatoriana de Entomología y Parasitología 2: 335–352.

Pinto-Sánchez NR, Ibáñez R, Madriñán S, Sanjur OI, Bermingham E, Crawford AJ (2012) The Great American Biotic Interchange in frogs: Multiple and early colonization of Central America by the South American genus *Pristimantis* (Anura: Craugastoridae). Molecular Phylogenetics and Evolution 62(3): 954–972. https://doi.org/10.1016/j.ympev.2011.11.022

Pröhl H, Ron SR, Ryan MJ (2010) Ecological and genetic divergence between two lineages of Middle American tungara frogs *Physalaemus* (=*Engystomops*) *pustulosus*. BMC Evolutionary Biology 10(1): 2–18. https://doi.org/10.1186/1471-2148-10-146

Pyron AR, Wiens JJ (2011) A large-scale phylogeny of Amphibia including over 2800 species, and a revised classification of extant frogs, salamanders, and caecilians. Molecular Phylogenetics and Evolution 61(2): 543–583. https://doi.org/10.1016/j.ympev.2011.06.012

R Core Team (2022) R: A language and environment for statistical computing. R Foundation for Statistical Computing, Vienna. https://www.R-project.org/

Salerno PE, Páez-Vacas M, Guayasamin JM, Stynoski JL (2019) Male principal investigators (almost) don't publish with women in ecology and zoology. PLoS ONE 14: 1–14. https://doi.org/10.1371/journal.pone.0218598

Ramírez-Castañeda V (2020) Disadvantages in preparing and publishing scientific papers caused by the dominance of the English language in science: The case of Colombian researchers in biological sciences. PLoS ONE 15(9): 1–15. https://doi.org/10.1371/journal.pone.0238372

Reyes-Puig C, Yánez-Muñoz MH, Ortega JA, Ron SR (2020) Relaciones filogenéticas del subgénero *Hypodictyon* (Anura: Strabomantidae: *Pristimantis*) con la descripción de tres especies nuevas de la región del Chocó. Revista Mexicana de Biodiversidad 91(0): 913013. https://doi.org/10.22201/ib.20078706e.2020.91.3013

Rock KN, Barnes IN, Deyski MS, Glynn KA, Milstead BN, Rottenborn ME, Andre NS, Dekhtyar A, Dekhtyar O, Taylor EN (2021) Quantifying the Gender Gap in Authorship in Herpetology. Herpetologica 77(1): 1–13. https://doi.org/10.1655/0018-0831-77.1.1

Ron SR, Carrión J, Caminer MA, Sagredo Y, Navarrete MJ, Ortega JA, Varela-Jaramillo A, Maldonado-Castro GA, Terán C (2020) Three new species of frogs of the genus *Pristimantis* (Anura, Strabomantidae) with a redefinition of the *P. lacrimosus* species group. ZooKeys 993: 121–155. https://doi.org/10.3897/zookeys.993.53559

Ron S, Merino-Viteri A, Ortiz D (2022) Anfibios del Ecuador. Version 2022.0. Museo de Zoología. https://bioweb.bio/faunaweb/amphibiaweb [accessed 3 January 2022]

Salerno PE, Páez-Vacas M, Guayasamin JM, Stynoski JL (2019) Male principal investigators (almost) don't publish with women in ecology and zoology. PLoS ONE 14(6): e0218598. https://doi.org/10.1371/journal.pone.0218598

Slobodian V, Soares KDA, Falaschi RL, Prado LR, Camelier P, Guedes TB, Leal LC, Hsiou AS, Del-Rio G, Costa ER, Pereira KRC, D'Angiolella AB, de A Sousa S, Diele-Viegas LM (2021) Why we shouldn't blame women for gender disparity in academia: Perspectives of women in zoology. Zoologia 38: 1–9. https://doi.org/10.3897/zoologia.38.e61968

Taucce PPG, Nascimento JS, Trevisan CC, Leite FSF, Santana DJ, Haddad CFB, Napoli MF (2020) A new rupicolous species of the *Pristimantis conspicillatus* group (Anura: Brachycephaloidea: Craugastoridae) from Central Bahia, Brazil. Journal of Herpetology 54(2): 24–257. https://doi.org/10.1670/19-114

Torres-Carvajal O, Pazmiño-Otamendi G, Ayala-Varela F, Salazar-Valenzuela D (2022) Reptiles del Ecuador. https://bioweb.bio/faunaweb/reptiliaweb [accessed 3 June 2022]

Wägele H, Klussmann-Kolb A, Kuhlmann M, Haszprunar G, Lindberg D, Koch A, Wägele JW (2011) The taxonomist-an endangered race. A practical proposal for its survival. Frontiers in Zoology 8(1): 1–7. https://doi.org/10.1186/1742-9994-8-25

West JD, Jacquet J, King MM, Correll SJ, Bergstrom CT (2013) The role of gender in scholarly authorship. PLoS ONE 8(7): 1–6. https://doi.org/10.1371/journal.pone.0066212

Woolbright LL (1985) Patterns of nocturnal movement and calling by the tropical frog *Eleutherodactylus* coqui. Herpetologica 41(1): 1–9.

Yánez-Muñoz MH, Meza-Ramos PA, Cisneros-Heredia DF, Reyes-Puig JP (2010) Descripción de tres nuevas especies de ranas del género *Pristimantis* (Anura: Terrarana: Strabomantidae) de los bosques nublados del Distrito Metropolitano de Quito, Ecuador. ACI Avances en Ciencias e Ingenierías 2(3): B16–B27. https://doi.org/10.18272/aci.v2i3.40

Supplementary material 1

Complete database of *Pristimantis* descriptions

Authors: Carolina Reyes-Puig, Emilio Mancero

Data type: database (excel document)

Explanation note: We present the complete database of information on *Pristimantis* descriptions, including year, authors, nationalities of authors, languages, journals, etc.

Link: https://doi.org/10.3897/zookeys.1134.91348.suppl1

Supplementary material 2

Complete translation of the manuscript

Authors: Carolina Reyes-Puig, Emilio Mancero

Data type: PDF file

Explanation note: We present the complete translation of the manuscript into Spanish, including tables and figures.

Link: https://doi.org/10.3897/zookeys.1134.91348.suppl2

ZooKeys 1134: 101–127 (2022)
doi: 10.3897/zookeys.1134.94984
https://zookeys.pensoft.net

RESEARCH ARTICLE

A peer-reviewed open-access journal
ZooKeys
Launched to accelerate biodiversity research

Revision of *Gymnoscirtetes* (Orthoptera, Acrididae, Melanoplinae): a genus endemic to the grasslands of the southeastern North American Coastal Plain

JoVonn G. Hill[1]

1 *Mississippi Entomological Museum, Department of Biochemistry, Molecular Biology, Entomology, and Plant Pathology, Mississippi State University, Mississippi, USA*

Corresponding author: JoVonn G. Hill (jgh4@msstate.edu)

Academic editor: Zhu-Qing He | Received 16 September 2022 | Accepted 15 November 2022 | Published 7 December 2022

https://zoobank.org/B94BDEAF-2B62-47B8-BDF7-D726D0A694D5

Citation: Hill JG (2022) Revision of *Gymnoscirtetes* (Orthoptera, Acrididae, Melanoplinae): a genus endemic to the grasslands of the southeastern North American Coastal Plain. ZooKeys 1134: 101–127. https://doi.org/10.3897/zookeys.1134.94984

Abstract

Gymnoscirtetes is endemic to the southeastern portion of the North American Coastal Plain and previously comprised two species: *G. pusillus* Scudder, 1897 and *G. morsei* Hebard, 1918. Here, this genus is revised based on male genital morphology and geographic data, and four new species are described: *G. georgiaensis* **sp. nov.**, *G. pageae* **sp. nov.**, *G. rex* **sp. nov.**, and *G. wadeorum* **sp. nov.** *Gymnoscirtetes* is primarily associated with mesic grasslands such as pitcher plant bogs, flatwoods, and the edges of seasonal ponds, but can be found less commonly in a variety of other grasslands.

Keywords

Alabama, biodiversity hotspot, bog, Florida, Georgia, grasshopper

Introduction

The North American Coastal Plain was recently designated as the world's 36th global biodiversity hotspot based on the high levels of biodiversity and endemism of vascular plants and habitat loss greater than 70% in the region (Noss 2016). A disproportionate amount of this biodiversity is found in the imperiled grasslands of the region, though they have historically received much less attention from conservation and natural resource agencies than forests and wetlands in the region (Noss 2013; Noss et al. 2015,

2021; Hill and Barone 2018). As functionally dominant herbivores in temperate grassland systems, it stands to reason that grasshopper diversity and endemism would also be high in the region. Indeed, Hill (2018) surveyed the grasshoppers of the southeastern United States and documented 173 species (82% of the fauna) that occur in grasslands and of these 111 species (53% of the fauna) and five genera (*Aptenopedes*, *Eotettix*, *Floridacris*, *Floritettix* and, *Gymnoscirtetes*) are endemic to the region.

Gymnoscirtetes Scudder 1897 (Orthoptera: Acrididae) (Fig. 1.) is endemic to the southeastern portion of the North American Coastal Plain (Fig. 2). Scudder (1897) established the genus by describing *G. pusillus*. Hebard (1918) described a second species, *G. morsei*. Since then, no other taxonomic work has been conducted on the genus. These tiny, slender grasshoppers are inhabitants of low, moist, open portions of flatwoods, particularly when such areas slope to and border a bayhead, bog, fen, hydric hammock, swamp, or seasonal pond. Occasionally they can be found in grassy sandhills. They can often be found among dense patches of grass or other tall slender vegetation, where their gracile form and lateral striping provide effective camouflage.

Gymnoscirtetes is ideal for revisionary research. Their small size, inability to fly due to vestigial wings, habitat specialization, and disjunct distributions, combined with the high number of other endemic arthropods in the region, make it likely that new species await discovery. Also, male genitalia are typically used to delineate species in the subfamily and species established based on genitalia have been later supported by genetic analysis (Hubbell 1932; Otte 2012, 2014; Hill 2015; Huang et al. 2020). However, male genitalia have not been examined for this genus.

Materials and methods

Most specimens examined in this study were collected by Dr. Theodore Hubble and Dr. Irving Cantrall of the University of Michigan Museum of Zoology (**UMMZ**), who made extensive collections of the genus with intentions to carry out a revision. However, no such study was ever completed. Other specimens examined in this study were borrowed from the Academy of Natural Sciences of Philadelphia (**ANSP**), Auburn University Museum of Natural History (**AUMNH**), the Florida State Collection of Arthropods (FSCA), the Mississippi Entomological Museum (**MEM**), and the United States National Museum (**USNM**). All type specimens of newly described species are deposited in the MEM, and paratypes will be deposited in ANSP, USNM, and UMMZ.

In order to conduct a thorough study of the genus, the male genitalia, which are typically concealed within the terminalia, were dissected and examined. Habitus and internal genitalia photographs were taken with a Leica Z16 stereoscope equipped with a Leica DFC420 camera at different stages during dissection. Images were automontaged with the Leica Application Suite. For scanning electron micrographs, specimens were mounted on stubs with silver paste and coated with 30 nm of platinum, then imaged with a JEOL–JSM65600F SEM. Measurements were made with a reticle mounted inside a Leica MZ12.5 stereomicroscope in the following ways:

Body Length — Dorsally from the fastigium vertices to the distal end of the genicular lobe of caudal femur in a parallel plane with the abdomen.
Pronotum length — Dorsally, along the median carina.
Cercus Length — Laterally, maximum possible measurement of the left cercus.
Cercus Basal Width — Laterally, along the point of attachment from the dorsal to ventral margin.
Mid Cercus Width — Laterally, at the mid-length of the left cercus.
Cercus Apex Width — Laterally, along the distal end.
Subgential Plate Tubercule Length — Laterally, from the base to the apex.
Subgential Plate Tubercule Width — Posteriorly, at the widest point.

Results

Based on male morphology and distribution, *Gymnoscirtetes* easily divides into two distinct species groups. The *morsei* group comprises two species that are western in distribution, from Mobile Bay, Alabama, to the Ocklochnee River, Florida (Fig. 12). The *pusillus* group comprises four species that are eastern, from the Ocklochnee River, Florida (i.e., the eastern edge of the *morsei* group) to east Georgia, and south towards Lake Okeechobee, Florida.

Checklist of groups and species

morsei *group*

1. *Gymnoscirtetes morsei* Hebard 1918 — Figs 3A, B, 4A, 5A, 6A–K, 12, 14C
2. *Gymnoscirtetes rex* sp. nov. — Figs 3C, D, 4A, 5B, 7A–K, 12, 14E

pusillus *group*

3. *Gymnoscirtetes pusillus* Scudder 1897 — Figs 3E, F, 4B, 5C, 8A–K, 12, 14H
4. *Gymnoscirtetes pageae* sp. nov. — Figs 5D, 9A–K, 12, 14D, 14G
5. *Gymnoscirtetes wadeorum* sp. nov. — Figs 5E, 10A–K, 12
6. *Gymnoscirtetes georgiaensis* sp. nov. — Figs 5F, 11A–K, 12

Comparison with related genera

Gymnoscirtetes

1. Small size (11–22 mm).
2. Body linear in shape (Fig. 1).
3. Appearing apterous with wings reduced to a minute, vestigial scale.
4. Body brownish-green or bronze with a black stripe running from behind the eye to near the end of the abdomen (Fig. 1).
5. Hind tibia and tarsi dull green.

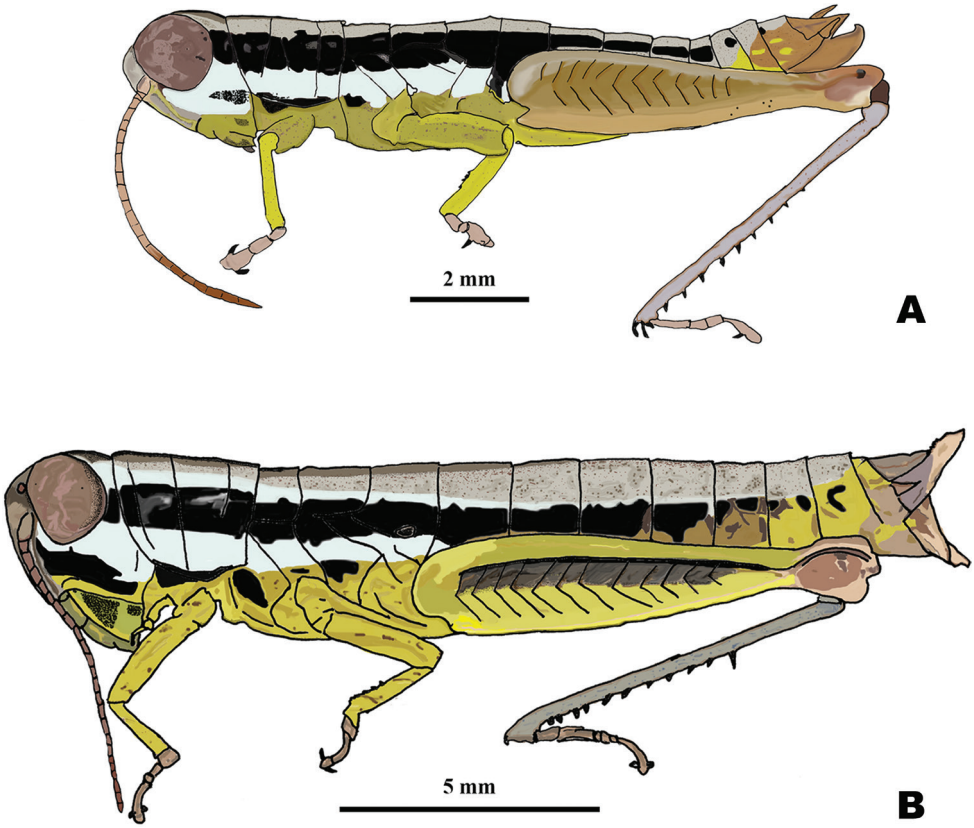

Figure 1. Habitus drawings of *Gymnoscirtetes* **A** male **B** female.

Aptenopedes

1. Large size (17–28 mm).
2. Body somewhat elongate.
3. Wings developed into small linear pads.
4. Body green or brown with white and black striping.
5. Hind tibia blue, tarsi pink.

Eotettix

1. Size variable – small (10–20 mm) to larger (18–28 mm).
2. Body more robust.
3. Brachypterous but wings obvious.
4. Body green to bronze with a metallic luster; black postocular stripe.
5. Hind tibia and tarsi black or red depending on the species.

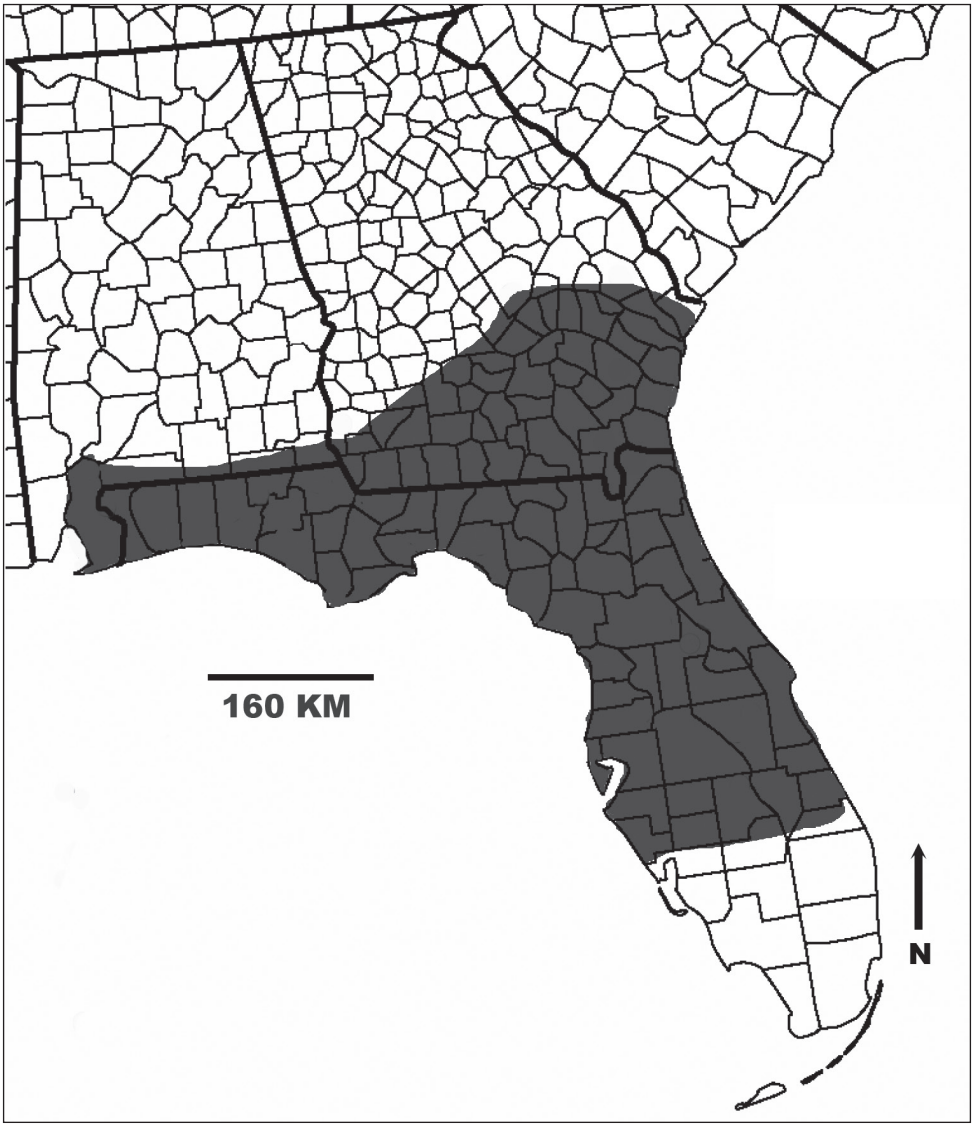

Figure 2. Geographic distribution of *Gymnoscirtetes*.

Floridacris

1. Larger (18–28 mm).
2. Body robust.
3. Wings reduced to small and slender pads.
4. Body green.
5. Hind tibia and tarsi pink.

Floritettix

1. Larger (16–29 mm).
2. Body robust.
3. Appearing apterous with wings reduced to a minute, vestigial scale.
4. Body green with black, white, or orange striping.
5. Hind tibia blue, tarsi pink.

Comparison of the species groups of *Gymnoscirtetes*

morsei group

1. Lateral lobes of subgenital plate expanded dorsally; tubercule longer than wide (Figs 3A–D, 4A).
2. Cerci generally falcate (Figs 3A–D, 4A).
3. Ventral valves of aedeagus more translucent; flattened (Figs 5A, B–7C–G).

pusillus group

1. Lateral lobes of subgenital plate not expanded; tubercule approximately as long as wide (Figs 3E, F, 4B).
2. Cerci triangular (Figs 3E, F, 4B).
3. Ventral valves of aedeagus more opaque; cylindrical (Figs 5C–F, 8–11C–G).

Key to *Gymnosciritetes*

1 Male cerci generally falcate with the apex nearly as wide as long at their bases (Figs 3A–D, 4A – *morsei* group); subgenital plate with lateral margins elevated as seen in caudal view (Fig. 4A – *morsei* group) **2**

– Male cerci generally triangular with the apex much narrower than the base (Figs 3E, F, 4B – *pusillus* group); subgenital plate without elevated lateral margins as seen in caudal view (Fig. 4B) **3**

2 Tubercule of subgenital plate broader (Figs 3A, B, 4A); apex of cerci generally more falcate (Figs 3A, B, 4A); dorsal valves of the aedeagus more rounded (Figs 5A, 6C–G); western panhandle of Florida and extreme southern Alabama (Fig. 12) ..... ***G. morsei***

– Tubercule of subgenital plate narrower (Figs 3C, D, 4A), apex of cerci less falcate and sometimes rounded (Figs, 3C, D, 4B); dorsal valves of the aedeagus more truncate (Figs 5B, 7C–G); central to eastern portion of the Florida panhandle (Fig. 12) ..... ***G. rex* sp. nov.**

3 Dorsal valves of the aedeagus shorter than the ventral valves (Figs 5C, 8C–G); north and peninsular Florida (Fig. 12) ..... ***G. pusillus***

– Dorsal valves of the aedeagus equal in length or nearly so to that of the ventral valves; not peninsular Florida **4**

4 Dorsal valves of the male aedeagus rounded apically and expanded laterally such that they appear lobate (Figs 5D, 9C–G); "Big Bend" region of Florida (Fig. 12) ..... ***G. pageae* sp. nov.**

– Dorsal valves of the aedeagus truncated or slightly angular apically and not expanded laterally, usually parallel sided (Figs 5E, F, 10C–G,11C–G); Florida and southern Georgia, but not the "Big Bend" region (Fig. 12) **5**

5 Dorsal valves of the aedeagus more truncated apically and not twisted (Figs 5E, 10C–G); southern Georgia and northern Florida (Fig. 12) ..... ***G. wadeorum* sp. nov.**

– Dorsal valves of the aedeagus more angled apically (Fig. 5F), often with slight caudally directed twist (Fig. 11C–F); eastern Georgia (Fig. 12) ..... ***G. georgiaensis* sp. nov.**

Gymnoscirtetes Scudder 1987

Gymnoscirtetes Scudder, S.H. 1897. Proc. U.S. Nation. Mus. 20 (1124): 14

External morphology. Species of small size (M: 11.8–17 mm, F: 17.5–22.2 mm). Body somewhat gracile and subcylindrical. ***Head*** slightly wider than pronotum; hypognathous with anterior margin of head steeply declivent; triangular dorsally. Fastigium broadening apically, and broadly concave. Eyes somewhat prominent, especially in males, and thinly separated by the narrow end of the fastigium. Antennae filiform, usually with 20–23 flagellomeres in males and 21–25 in females, but often 23–26; longer than the head and pronotum combined. ***Thorax*** with prosternal spine thin and subconical. Pronotum cylindrical, anterior margin sub-truncate, often somewhat emarginated, lateral margins parallel throughout, median carina either slightly indicated or obsolete, lateral carinae obsolete. Prozona 3–4 × as long as the metazona, anterior and median sulci present laterally but indistinct near the margins; prozona smooth and shiny. Metazona mostly smooth, but with occasional reticulations, posterior margin subtruncate. Lateral lobes of the pronotum declivent anteriorly and truncate posteriorly, the ventral posterior margin obtusely angulate. Wings vestigial, minute, scale-like. Metathoracic femur slender. Metathoracic tibia with 8–10 pairs of spines. Tympanal organ greatly reduced, appearing as a small depression or slit. ***Terminalia*** with furcula (males) (Fig. 1) rounded protuberances, projecting either slightly or moderately beyond the end of the segment from which they originate; bases minutely separated. Supra-anal plate (Fig. 1) triangular, slightly longer than wide, with the median groove anteriorly distinct with elevated sides, and diverging and becoming less distinct posteriorly. Cerci (Fig. 1) either short, triangular, tapering from base to apex or longer and subfalcate. Subgenital plate of male with a median tubercule (Fig. 1).

Phallic structures. The dorsal valves are translucent to semi-translucent lobes that are flat, truncate, shortened to elongate depending on the species. The ventral valves are opaque and more strongly sclerotized than the dorsal valves, caudally projecting cylindrical lobes of various shapes depending on the species (Figs 1, 3, 4). The aedeagal sheath only covers the base of the valves (Fig. 2). The epiphallus is of the typical mel-

anoploid shape, with lophi, ancorae, and an undivided bridge. But more precisely, the epiphallus of *Gymnoscirtetes* has a concave bridge, broadly rounded or arched lophi, convexly curved lateral plates that are sub-rectangular in shape with an angular anterior lobe and a short, rounded caudal tip, and ancora that are triangular, taper to a point, and are decurved ventrally.

Coloration. Overall dull greenish brown to yellow, sometimes with bronze highlights. Antenna yellowish basally, remainder ferruginous. Antennal crescent complete. Head, thorax, and abdomen pale yellow, infuscated dorsally, especially along the midline. A lateral, well-defined, piceous, post-ocular stripe extends from the caudal margin of the eye through the thorax and towards the end of the abdomen; lateral area of head and thorax below post-ocular stripe creamy-yellow. Hind femora luteous. Hind tibia, pale dull green, often dulled basally; with black or black tipped spines (Figs 1, 4–9K).

Etymology. *Gymno*, Greek, naked (in reference to the seemingly apterous condition); *skirtetes*, Greek, leaper.

Suggested common name. Naked leapers.

morsei group

Diagnosis. Typical of the genus but with male cerci generally falcate, subgenital plate with lateral lobes expanded dorsally, and central tubercle that is longer than wide (Fig. 3A–D). Ventral valves of aedeagus more translucent and not cylindrical in shape (Figs 4A, B, 6, 7C–G).

Gymnoscirtetes morsei Hebard, 1918

Figs 3A, B, 4A, 5A, 6A–J, 12, 14C

Gymnoscirtetes morsei Hebard, 1918: 142–143.

Diagnosis. Most easily differentiated from the other species in the group based on the shape of the male cerci, which in *G. morsei* are decurved apically to an acute point (Fig. 6A, B), and by the shape of the male genitalia which have the dorsal valves rounded apically (Fig. 6G). The tubercle of the subgenital plate is often broader in most individuals of *G. morsei*, especially those in the western portion of the range.

Male measurements. (mm): (n = 14) Body length 13.2–17.0 (mean = 14.6); pronotum length 1.9–2.6 (mean = 2.26); hind femur length 6.1–7.9 (mean = 6.9); cerci length 1.2–1.5 (mean = 1.3); basal width of cercus 0.4–0.7 (mean = 0.6); midcercal width 0.2–0.3 (mean = 0.2); cerci apex width 0.3–0.4 (mean = 0.4). tubercule length 0.3–0.4 (mean = 0.3); tubercule width 0.2–0.3 (mean = 0.2).

Female measurements. (mm): (n = 7) Body length 19.5–21 (mean = 20.3); pronotum length 3.0–3.2 (mean = 3.1); hind femur length 9.0–9.8 (mean = 9.3).

Type information. Florida, Walton County, Defuniak Springs, 30 August 1915, Rehn and Hebard (1♂).

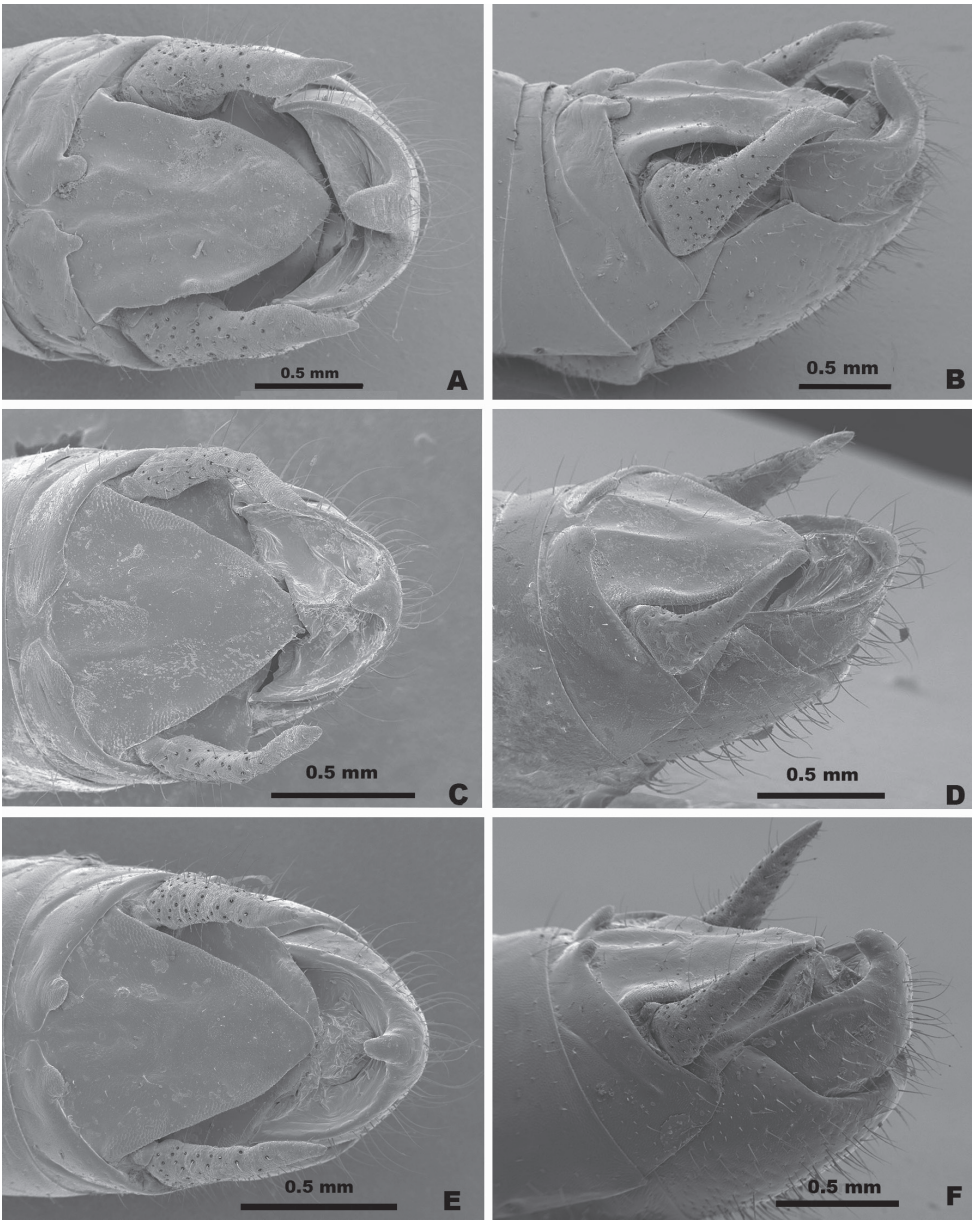

Figure 3. Dorsal and lateral SEM of *Gymnoscirtetes* male terminalia **A** *G. morsei* (dorsal) **B** *G. morsei* (lateral) **C** *G. rex* (dorsal) **D** *G. rex* (lateral) **E** *G. pusillus* (dorsal) **F** *G. pusillus* (lateral). Note: *G. pageae*, *G. wadeorum*, and *G. georgiaensis* are similar to *G. pusillus*.

Specimens examined. Alabama, Baldwin County, 5.6 mi W Ala/Fla St. line on US 90, 13 September., 1954. T.H. Hubbell an I.J. Cantrall (14♂, 3♀); 6.2 mi SW Perdido on US Hwy 31, 13 Sept. 1954, T.H. Hubbell and I.J. Cantrall (1♂); Splinter Hill Bog, 31°01'30"N, -87°41'07"W, 19 July 2012, J.G. Hill, M.J. Thorn, Pitcher

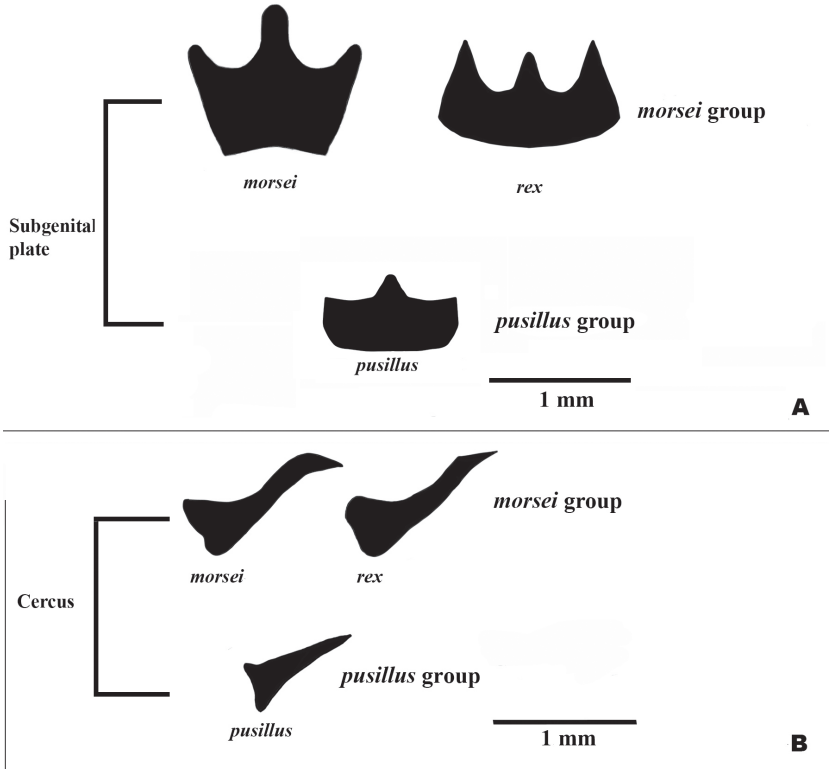

Figure 4. Partial silhouettes of *Gymnoscirtetes* male terminalia: **A** subgenital plate in caudal view **B** cerci in lateral view. Note: *G. pageae*, *G. wadeorum*, and *G. georgiaensis* are similar to *G. pusillus*. Within species groups there may be overlap in the shape of the cerci, and the shape is highly dependent on angle of view. Those pictured here are drawn from single individuals.

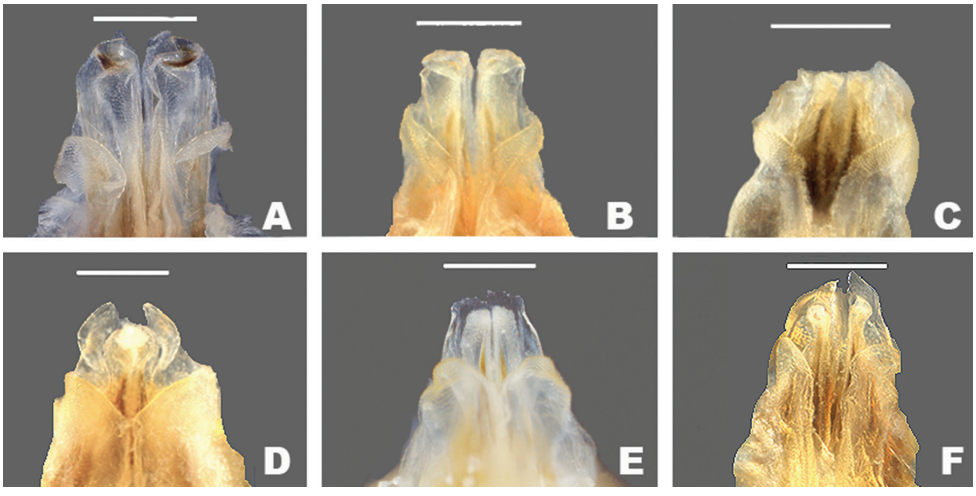

Figure 5. Caudal view of *Gymnoscirtetes* male aedeagi **A** *G. morsei* **B** *G. rex* **C** *G. pusillus* **D** *G. pageae* **E** *G. wadeorum* **F** *G. georgiaensis*. Scale bars 0.2 mm.

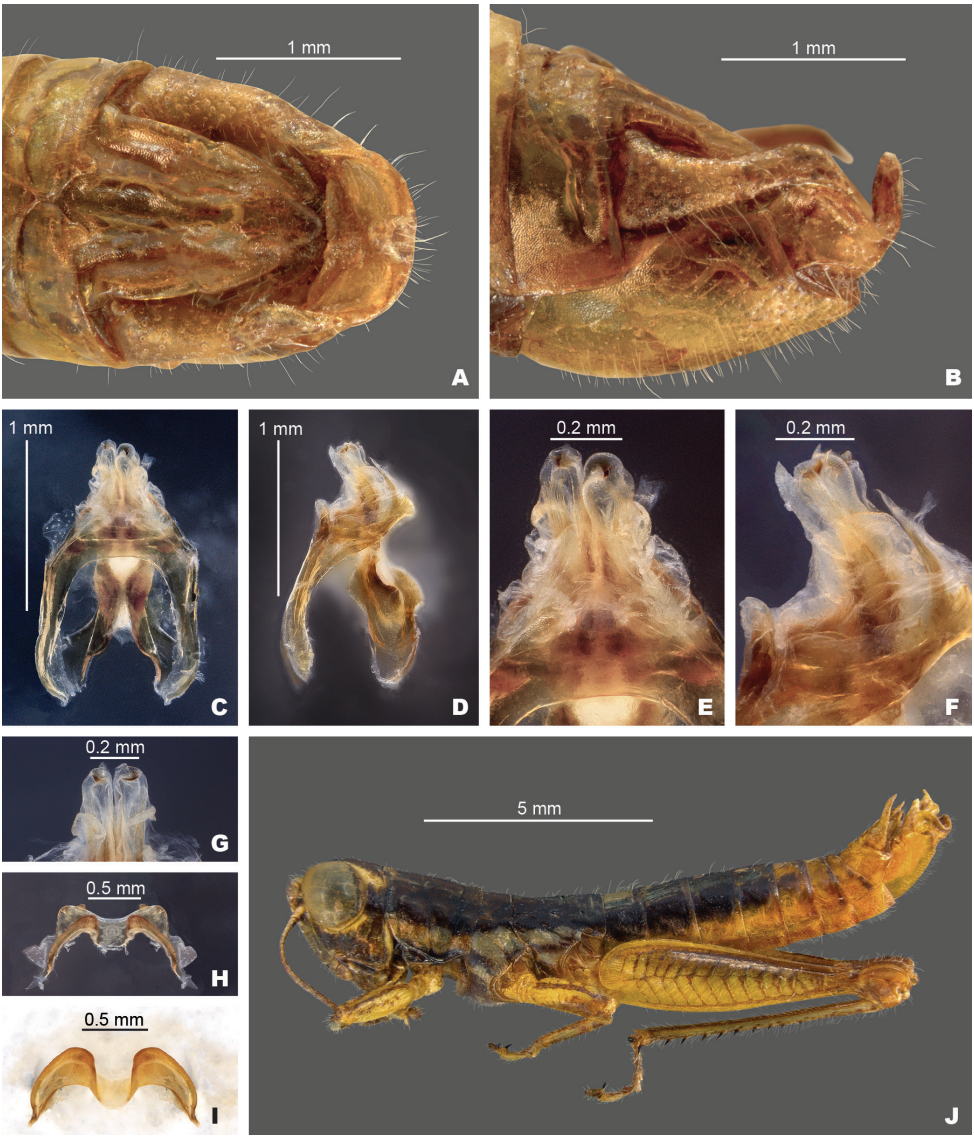

Figure 6. *Gymnoscirtetes morsei*: **A** dorsal view of male terminalia **B** lateral view of male terminalia **C** dorsal view of phallic complex **D** lateral view of phallic complex **E** dorsal view of aedeagus **F** lateral view of aedeagus **G** caudal view of the aedeagus **H** dorsal view of epiphallus **I** caudal view of epiphallus **J** habitus.

plant bog (1♂). **Florida**, Bay Co., 4.9 mi S Ebro, 16 October 1948, I.J. Cantrall (5♂), 9 mi E West Bay, 16 October 1948, I.J. Cantrall (1♂). Holmes Co., 0.4 mi E Ponce DeLeon, 14 September 1948, I.J. Cantrall (17♂); Westville, 23 August 1941 (7♂, 6♀); 0.6 mi E Bonifay, 14 October1948, I.J. Cantrall (6♂). Jackson Co., 1.4 mi W Cottondale 14 October 1948, I.J. Cantrall (1♂). Okaloosa Co., 3 mi E Crestview, 15 October 1949, I.J. Cantrall (3♂); 3.1 mi W Florosa, 15 October 1946. I.J. Can-

trall (7♂). Santa Rosa Co., 2.3 mi S Junct. U.S. Hwy 90 and Hwy 87, 15 October 1949, I.J. Cantrall (4♂); 4.4 mi S Whitfields, 21 August 1951, I.J. Cantrall (7♂, 5♀); Milton, 15 August 1955, I.J. Cantrall (1♂). Walton Co., 2.3 mi N Freeport, 15 October 1948, I.J. Cantrall (1♂). 3.8 mi N Defuniak Springs, 14 October 1948, I.J. Cantrall (14♂).

Distribution. Mobile Bay (Baldwin County, AL) east through the panhandle of Florida to Bay and Jackson counties (Fig. 12).

Habitat. Hebard (1918) describes the type locality at De Funiak Springs, Florida as being "a boggy area of wire-grass and bog plants, which was not more than fifteen yards wide by forty yards long". At Splinter Hill Bog, in Baldwin County, AL (Fig. 13A), *G. morsei* occurs in a large bog dominated by *Sarracenia leucophyllia* Raf. and other carnivorous plants.

Gymnoscirtetes rex sp. nov.

https://zoobank.org/F8AB88FD-CAFF-4317-BE60-F4E099DD46B9
Figs 3C, D, 4A, 5B, 7A–J, 12, 14H

Diagnosis. Differs from *G. morsei* in having more narrow male cerci and curving or rotating medially apically, with the apex curving back laterally. In some individuals the apex of the cerci may be less acute or sometimes rounded (Fig. 7A, B). The dorsal valves of the male genitalia are truncated and decurved distally. The ventral valves are decurved and taper to a point distally (Fig. 7G). The tubercle of the subgenital plate is often narrower in most individuals of *G. rex* than in specimens of *G. morsei*.

Male measurements. (mm): (n = 14) Body length 13.3–16.5 (mean = 14.7); pronotum length 2.3–2.5 (mean = 2.3); hind femur length 6.9–8.3 (mean = 7.5); cerci length 1.0–1.2 (mean = 1.1); basal width of cercus 0.4–0.5 (mean = 0.4); mid-cercal width 0.2 (mean = 0.2); cerci apex width 0.3 (mean = 0.3). tubercule length 0.1–0.3 (mean = 0.2); tubercule width 0.1–0.3 (mean = 0.2).

Female measurements. (mm): (n = 14) Body length 18.3–22.2 (mean = 20.7); pronotum length 2.4–3.4 (mean = 2.9); hind femur length 8.5–10.0 (mean = 9.5).

Type information. 1♂, FLA., Bay Co., Ecofina Creek WMA, 30°25'41"N, -85°35'32"W, 27 October 2015, J.G. Hill, sandhill in short grasses and *Licania michauxii* Prance (Chrysobalanaceae). Deposited in the Mississippi Entomological Museum.

Paratypes. Ecofina Creek WMA, 30°25'41"N, -85°35'32"W, 27 October 2015, J.G. Hill, sandhill (4♂, 5♀).

Other specimens examined. Florida: Bay Co. 10 mi W Youngstown, 30°25'40"N, -85°35'25"W, 13 Sept. 2013, J.G. Hill (4♂, 7♀); Calhoun, 3.5 mi N Blountstown, 22 August 1951, I.J. Cantrall (5♂, 3♀); Blountstown, 22 August 1951. I.J. Cantrall (13♂, 10♀); 3.5 mi S Altha, 22 August 1951, I.J. Cantrall (1♂). Franklin Co., 3.1 mi S Sumatra on Fla. 65, 23 August 1951, I. J. Cantrall (1♂); 8.3 mi S Sumatra on Fla 65, 23 August 1951, I.J. Cantrall (11♂, 4♀). Gulf Co., 2.2 mi S Port St. Joe, 16 October 1948, I.J. Cantrall (3♂); 6.8 mi S Wewahitchka, 16 September 1940, I.J.

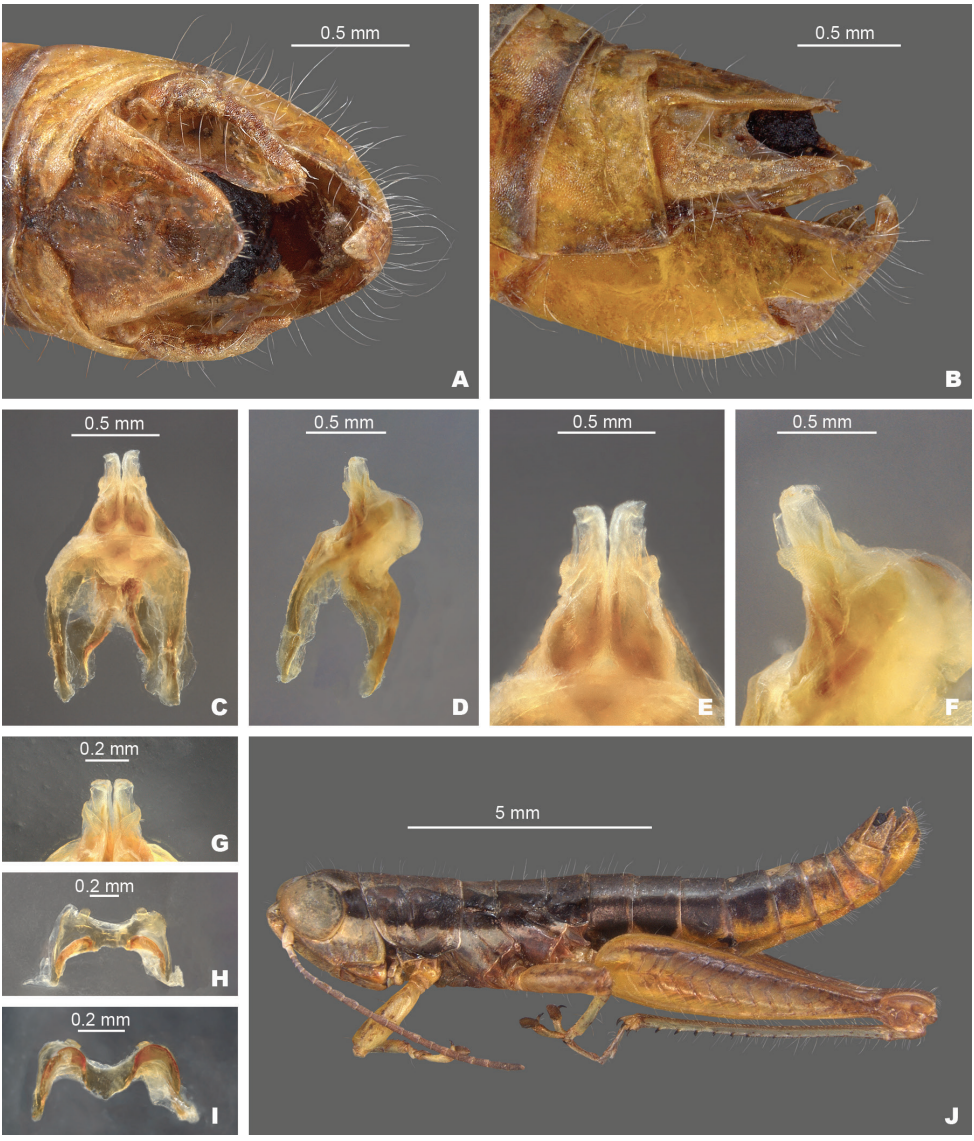

Figure 7. *Gymnoscirtetes rex*: **A** dorsal view of male terminalia **B** lateral view of male terminalia **C** dorsal view of phallic complex **D** lateral view of phallic complex **E** dorsal view of aedeagus **F** lateral view of aedeagus **G** caudal view of the aedeagus **H** dorsal view of epiphallus **I** caudal view of epiphallus **J** habitus.

Cantrall (1♂). Jackson, 0.9 mi E Grand Ridge, 14 October 1948, I.J. Cantrall (1♂). Liberty Co., 3 mi S Wilma on Fla 65, 23 August 1951, I.J. Cantrall (13♂, 5♀); 3.2 mi N Wilma on Fla 65, 23 August 1951, I.J. Cantrall (12♂, 8♀); 4.3 mi N Sumatra on Fla 12, 23 August 1951, I.J. Cantrall (8♂, 7♀) 7.9 mi N Sumatra on FLA 12, 23 August 1951, I.J. Cantrall (4♂, 3♀); 14.1 mi W Sumatra, 23 Sumatra 1941, I.J. Cantrall (9♂, 14♀).

Distribution. Occurs in a narrow portion of the eastern Florida panhandle. At present, it is known only from Bay, Calhoun, Franklin, Gulf, and Liberty counties (Fig. 12).

Etymology. From the Latin *rex* for monarch, in reference to the crown-like shape of the subgenital plate. The inspiration for this name came one day while at a local coffee shop (929) that had a crown as part of their logo. The shop was selling crown-shaped cookies by the cash register. I was working on this revision at the time and the shape of the cookies instantly remined me of the shape of the subgenital plate of this species.

Habitat. This species can be found in much drier conditions that other members of the genus. At the type locality this species inhabited fine grasses in a sandy upland with *Chrysoma pauciflosculosa* (Michx.) Greene (Fig. 13B). I have also collected this species from a large expanse of *Quercus minima* (Sarg.) Small in a sandhill. Specimen notes from other specimens indicate it inhabits bogs and savannahs as well.

pusillus group

Diagnosis. Typical of the genus, but with the male cerci triangular and subgenital plate with the lateral lobes not expanded dorsally and with the tubercule approximately as long as wide (Figs 3C, 4B). Ventral valves of the aedeagus opaque and cylindrical in shape (Figs 8–11A–G).

Gymnoscirtetes pusillus Scudder, 1897

Figs 3E, F, 4B, 5C, 8A–J, 12, 14G

Gymnoscirtetes pusillus Scudder, 1897: 15

Diagnosis. Differs from other species in the group based the shape of the internal male genitalia. In dorsal view, the dorsal valves are lightly sclerotized and semi-translucent, have apices that are rounded to sub-truncate, and shorter than the ventral valves (Fig. 8C, E). In lateral view, the dorsal valves taper to their apices and the ventral valves extend slightly past the dorsal valves with apices that are rounded to slightly angular (Fig. 8B, D, G).

Male measurements. (mm): (n = 33) Body length 11.8–15.6 (mean = 14.4); pronotum length 1.8–3.1 (mean = 2.2); hind femur length 6.3–8.3 (mean = 7.3); cerci length 0.7–1.0 (mean = 0.8); basal width of cercus 0.3–0.4 (mean = 0.3); mid-cercal width 0.2 (mean = 0.2); cerci apex width 0.1 (mean = 0.1). tubercule length 0.1–0.2 (mean = 0.2); tubercule width 0.1–0.2 (mean = 0.2).

Female measurements. (mm): (n = 28) Body length 18.5–21.2 (mean = 19.8); pronotum length 2.6–13.1 (mean = 3.1); hind femur length 8.5–10.3 (mean = 9.2).

Type information. Florida [Duval Co.,] Jacksonville. Aug. [18]85.

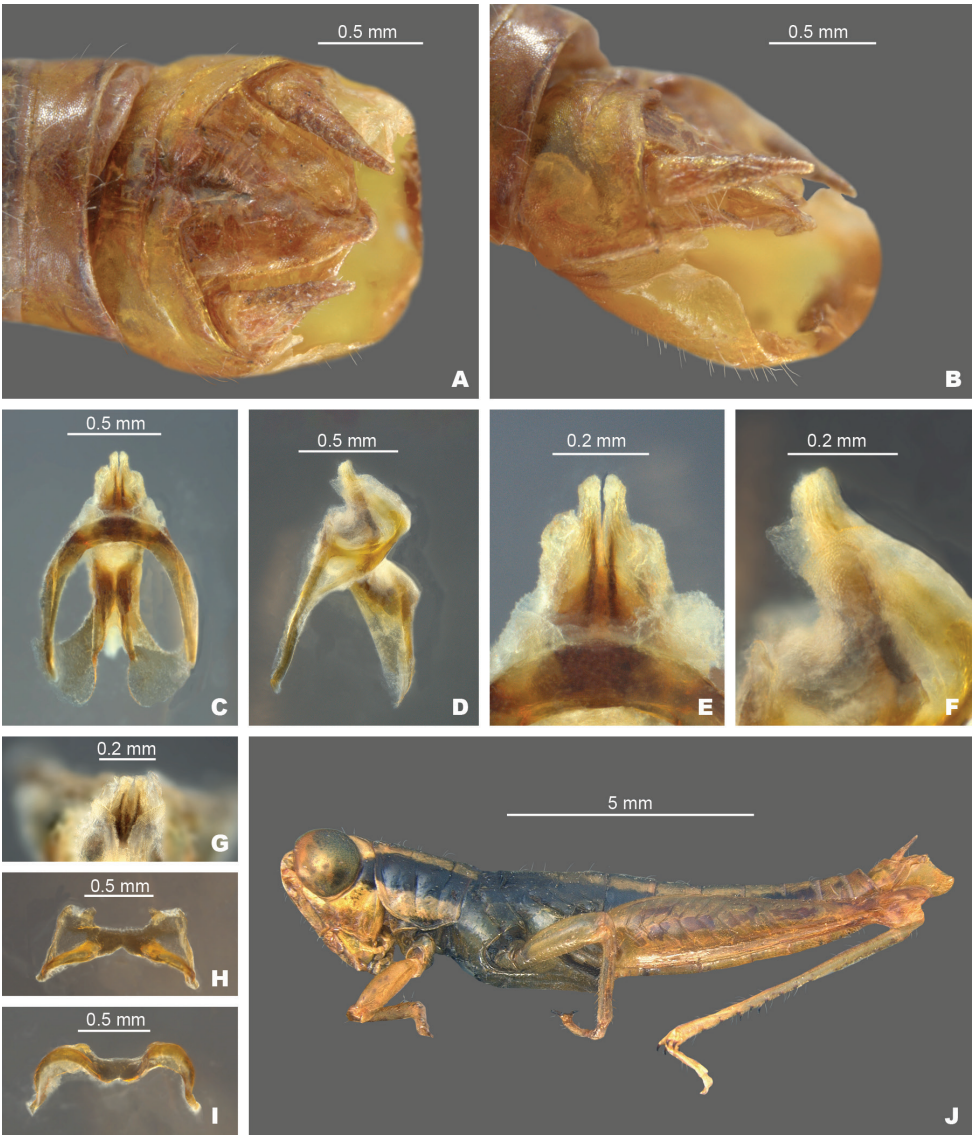

Figure 8. *Gymnoscirtetes pusillus*: (type) **A** dorsal view of male terminalia **B** lateral view of male terminalia **C** dorsal view of phallic complex **D** lateral view of phallic complex **E** dorsal view of aedeagus **F** lateral view of aedeagus **G** caudal view of the aedeagus **H** dorsal view of epiphallus **I** caudal view of epiphallus **J** habitus.

Specimens examined. Florida: Alachua Co., Fairbanks, 27 June 1924, F.W. Walker (2 ♂); Gainesville, 8 August 1925, T.H. Hubbell (4♂, 4♀); Same data as previous, except May 1926' Waldo, 13 August 1924, F.W. Walker (4♂, 6♀). Same data as previous, except M.J. Thorn (2♂, 3♀); Bradford Co., 3.5 mi NE Lawtey, 1 August 1938, Hubbell and Friauf (1♂). Clay Co., Green Cove Springs, 30 September 1925, T.H. Hubbell (1♂). Duval Co., San Pablo (1♂). Gilchrist Co., 5 mi E Trenton, 14 August

1947, T.H. Hubbell (3♂). Highlands Co., Archbold B.S., 27.1813, -81.3545, 3 October 2021, M.J. Thorn (1♂, 1♀); Avon Park AFB, 27°38'12"N, -81°18'36"W, 16 June 2015, J. Hill, J. Barone, R. Noss (2♂, 3♀); Lake Wales Ridge NWR, 27.5153, -81.4130, 18 June 2019, J.G. Hill (5♀), Lake Wales Ridge WEA, 27. 3712, -81.3412, 4 October 2021, J.G. Hill (2♂, 2♀). Hillsborough Co., 4 mi NE Thonotosassa, 18 August 1938, Hubbell and Friauf (1♂); Little Mantee River U.S. Hwy 41, Hubbell and Friauf (6♂, 3♀). Lake Co., .1 mi E Altoona, 25 July 1938, Hubbell and Friauf (6♂). Lake Co., 0.7 mi S Pitman, 27 August 1938, Hubbell and Friauf (1♂); 1.5 mi W Astor, 24 July 1938, Hubbell and Friauf (3♂); 1.5 mi E Lisbon, 24 August 1926, Hubbell and Friauf (2♂); 3.3 mi E Altoona, 28 August, Hubbell-Friauf (1♂). Levy Co., Cedar Key, 29 Sept. 1923, T.H. Hubbell (2♂); Sumner, 18 October 1924, T.H. Hubbell (3♂). Marion Co., Lake Weir, 27 August 1927 (2♂, 3♀); Ocala, 17 August 1935, (2♂, 4♀). Ocala Nat'l Forest, T17S, R26E, Sec 3, Hubbell and Friauf (6♂, 3♀), Ocala Nat'l Forest, Juniper Springs, 9 June 1938, Hubbell and Friauf (1♂), Ocala N.F., 29.2757, -81.6898, 16 June 2019, J.G. Hill (4♂, 4♀); 2.5 mi W Crow's Bluff, 29 August 1938, Hubbell and Friauf (1♂). Nassau Co., 1 mi W O'Neil, 19 August 1947, T.H. Hubble, (1♂); 1.6 mi SW Crawford, 19 October 1941, T.H. Hubbell (1♂). Okeechobee Co. 5.6 mi S. Co. line on US 441, 27 August 1951, I.J. Cantrall (3♂, 4♀); 4.3 mi N. Okeechobee, 27 August 1951, I.J. Cantrall (3♂, 3♀). Orange Co., Winter Park, 26 August 1937 (1♂, 4♀). Osceola Co., 9.2 mi S Kenansville, 27 August 1951, I.J. Cantrall (2♂, 3♀); 13.3 mi S Holopaw, 24 August 1951, I.J. Cantrall (23♂, 18♀); Disney Wilderness Pres. 28°04'06"N, -81°24'25"W, 17 June 2015, J.G. Hill, J.A. Barone (3♀); Holopaw, 27 August 1925, T.H. Hubbell (3♂). Pasco Co., Tribley (1♂). Polk Co., Haines City, 27 August 1925, T.H. Hubbell (1♂); Lake Streety, T 32S, R27S, Sec. 25, 10 August 1938, Hubbell and Friauf (1♂); Hatchineha Ranch, 28.008, -81.4839, 3 October 2022, J.G. Hill (1♂, 1♀); Lakeland, 28 June 1935, I.J. Cantrall (2♂); Lake Marion Creek WMA, 28.0992, -81.5121, 3 October 2021, J.G. Hill (1♂, 1♀); Lake Wales Ridge NWR, 28.1308, -81.5530, 3 October 2021, J.G. Hill (1♂, 1♀); Tiger Creek NA, 27°48'32"N, -81°29'24"W, 17 June 2015, J.G. Hill, J.A. Barone (2♂, 6♀). Putnam Co., Mannville, 22 Nov. 1938, T.H. Hubbell (1♂); Welaka, 21 August 1940, J.J. Friauf (1♂); same data as previous, except 8 August 1939 (1♂). St. Johns Co., 1.3 mi E jct US 1 and FLA 206, 26 August 1951, I.J. Cantrall (6♂, 8♀); Saint Augustine, 6 July 1935, I.J. Cantrall (2♂, 1♀). Suwannee Co., Houston, 23 August 1925. T.H. Hubbell (5♂). Volusia Co., 1.6 mi E Astor, 29.1667, -81.5000, 3 June 2021, J.G Hill and M.J. Thorn (3♂); 0.6 mi W Barberville, 6 Sept. 1938, Hubbell and Friauf (3♂).

Distribution. Peninsular Florida from the northeast boarder with Georgia along the Atlantic Ocean west to eastern bank of the Suwannee River and south to the southern borders of De Soto, Highlands, and Okeechobee Counties (Fig. 12).

Habitat. Found in a variety of grassland situations from seasonal ponds (Fig. 14A), cutthroat grass seeps (Fig. 13E), and flatwoods on the Lake Wales Ridge to Florida dry prairies (Fig. 13F). Irvin Cantrall reports collecting this species in saltwater flats with *Juncus* and *Batis maritima* (Cantrall 1951, field notes).

***Gymnoscirtetes pageae* sp. nov.**
https://zoobank.org/3F1242B8-CF10-4AFE-89DD-7DA9E0ECD0F2
Figs 5D, 9A–J, 12, 14D, G

Diagnosis. Differing from other species in the group based on the shape of the internal male genitalia (Fig. 9C–I). In dorsal view, the dorsal valves form two slightly translucent lobes that are equal to or are slightly longer than the ventral valves and are truncated apically. The ventral valves are opaque short cylindrical protrusions that are rounded at their apices. In lateral view, the dorsal valves are much broader than the ventral valves (~ 1.5 ×) and extend laterally up to or just short of the apex of the ventral valves. In caudal view, the dorsal valves form a girdle that almost completely encompasses the ventral valves like a hood (Fig. 9G). This species is perhaps the most distinct in the group and can readily be identified based on its unique genitalia and distinct geographic distribution (Fig. 12).

Male measurements. (mm): (*n* = 14) Body length 13.5–16.9 (mean = 14.6); pronotum length 2.1–2.5 (mean = 2.3); hind femur length 6.7–8.3 (mean = 7.4); cerci length 0.8–1.1 (mean = 1.0); basal width of cercus 0.3–0.4 (mean = 0.4); mid-cercal width 0.2 (mean = 0.2); cerci apex width 0.1 (mean = 0.1) tubercule length 0.1–0.2 (mean = 0.2); tubercule width 0.1–0.2 (mean = 0.2).

Female measurements. (mm): (*n* = 6) Body length 19.5–20.6 (mean = 20.0); pronotum length 2.5–3.0 (mean = 2.8); hind femur 8.5–9.6 (mean = 9.2).

Holotype. 6 mi S Old Town, 29.5156769, -83.0002496, 28 Sept. 2017, J.G. Hill, Collected from roadside sandhill and ditch (1♂). Deposited in the Mississippi Entomological Museum.

Paratypes. Same data as type (2♂, 2♀).

Other specimens examined. Florida: Dixie Co., 4 mi N Shamrock, 14 August 1947, T.H. Hubbell (1♂); 6 mi S. Steinhatchee R[iver], 5 August 1925, T.H. Hubbell (4♂); Cross City, 21 November 1925, T.H. Hubbell (1♂). Jefferson Co., 0.4 mi N Lamont, 16 August, 1947, T.H. Hubbell (5♂); 0.4 mi NE Fanlew, 16 August 1947, T.H. Hubbell (1♂); 0.7 mi N Jct. US 90 and Fla 257, 17 August 1947, T.H. Hubbell (1♂); 0.9 mi E Thomas City, 16 August, 1947, T.H. Hubbell (1♂); 4.4 mi NE Fanlew, 16 August 1947, T.H. Hubbell (1♂); 4.6 mi E Monticello, 17 August 1947 (1♂); near Covington, 31 Oct, 1942, T.H. Hubbell (5♂); Lloyd, 20 August 1938 (2♂, 4♀). Lafayette Co., 2 mi W Taylor County Line, 9 June 1941, Friauf and Hubbell (1♂); 12 mi W Mayo, 9 November 1941, Friauf & Hubbell (1♂). Leon Co., Chaires, 4 August1925, T.H. Hubbell (4♂). Taylor Co., 4.7 mi N Salem, 7 October 1945, T.H. Hubbell (1♂); Boyd, 15 October 1942, T.H. Hubbell (1♂); Perry, 5 August 1925, T.H. Hubbell (2♂); Hampton Springs, 31 October 1947, T.H. Hubbell (2♂). Madison Co. 2 mi E Aucilla River on US 90, 17 August 1947, T.H. Hubbell (1♂); 1.7 mi N Shady Creek, 16 Sept. 1942, T.H. Hubbell (1♂). Wakulla Co., 1.5 mi NW St. Marks, 15 August 1947, T.H. Hubbell (2♂).

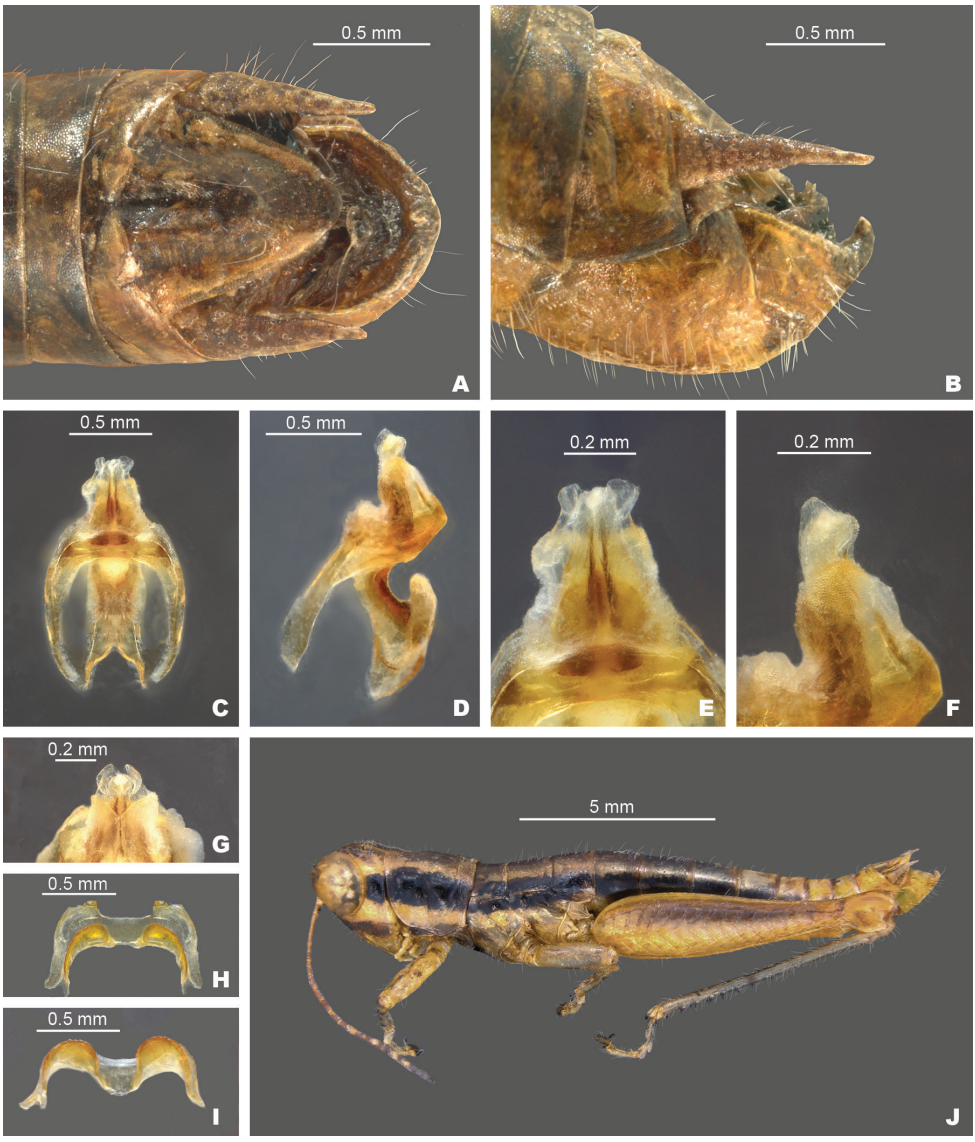

Figure 9. *Gymnoscirtetes pageae*: **A** dorsal view of male terminalia **B** lateral view of male terminalia **C** dorsal view of phallic complex **D** lateral view of phallic complex **E** dorsal view of aedeagus **F** lateral view of aedeagus **G** caudal view of the aedeagus **H** dorsal view of epiphallus **I** caudal view of epiphallus **J** habitus.

Distribution. "Big Bend" region of Florida from Leon and Wakulla counties, south through the flatwoods to the western banks of the Suwannee River in Dixie County (Fig. 12).

Habitat. Flatwoods and grassy sandhills (Fig. 13D).

Etymology. Named in honor of Bettie Mae Page, an iconic American photo model and former resident of Florida, who rose from a background of poverty and abuse to become a symbol of self-expression and body positivity.

***Gymnoscirtetes wadeorum* sp. nov.**
https://zoobank.org/E3ED601A-90E3-486B-9D8D-C74C5333D025
Figs 5E, 10A–J, 12

Diagnosis. Differing from other species in the group based on the shape of the internal male genitalia (Fig. 10C–I). In dorsal view, the dorsal valves form two translucent lobes that are equal to or slightly longer than the ventral valves and are truncated apically. The ventral valves are opaque short cylindrical protrusions that are rounded at their apices. In lateral view, the dorsal valves are broader than the ventral valves and taper to their apices. In caudal view, the dorsal valves extend above the ventral valves (Fig. 10G). This species is very similar to *G. pusillus* but is distinguished from that species by the length and angle of the dorsal valves which are longer and are angled more dorsally in *G. wadeorum*, and their separate geographic distributions (Fig. 12).

Male measurements. (mm): (*n* = 14) Body length 13.0–15.1 (mean = 14.1); pronotum length 1.8–2.3 (mean = 2.2); hind femur length 6.7–7.8 (mean = 7.0); cerci length 0.7–1.0 (mean = 0.9); basal width of cercus 0.3–0.4 (mean = 0.3); mid-cercal width 0.1–0.2 (mean = .02); cerci apex width 0.1 (mean = 0.1). tubercule length 0.1–0.2 (mean = .01); tubercule width 0.1–0.2 (mean = 0.1).

Female measurements. (mm): (*n* = 9) Body length 18.5–21.8 (mean = 20.0); pronotum length 2.5–3.0 (mean = 2.8); hind femur length 8.6–9.6 (mean = 9.1).

Holotype. GA., Thomas Co., Wade Tract, 30°45'35"N, -84°00'01"W, 4 August 2011, J.G. Hill; Old growth longleaf pine savanna (1♂). Deposited in the Mississippi Entomological Museum.

Paratypes. Same data as type (6♀).

Other specimens examined. Georgia: Berrien Co., 1.1 mi S Appling, 11 Aug 1947, T.H. Hubbell (4♂, 2♀). Colquitt Co., Doerun Nat. Area., 31°17'17"N, -83°53'03"W, 14 October 2010, J.G. Hill, longleaf pine savannah (2♂). Decatur Co., Silver Lake WMA, 30°49'44"N, -84°45'14"W, 27 August 2010, J.G. Hill (1♂). Early Co., Williams Bluff NA, 31°11'58"N, -85°04'43"W, 18 June 2011, J.G. Hill (2♂). Thomas Co., 4.3 mi N Metcalf, 30.7634, -83.9915, 8 September 2022, J.G. Hill, J.R. Fisher; Greenwood Plantation, 30°50'10"N, -84°00'40"W, 4 August 2011, J.G. Hill (1♂); Same data as above, except 26 August 2010 (2♂, 2♀); River Creek WMA, 30°51'40"N, -84°04'04"W, 27 August 2010, J.G. Hill, longleaf pine savannah (3♂, 3♀); Same data as above, except 30°51'35"N, -84°04'37"W, 4 August 2011 (1♂, 5♀); **Florida**: Baker Co., John Bethea State For. 30.4834, -82.3002, 2 June 2021, J.G. Hill (5♂, 5♀), Gasden Co., 2 mi N Ochlookonee, 14 October 1948, I.J. Cantrall (1♂). Liberty Co., 5.3 mi S Telogia on Fla 65, 23 August 1951, I.J. Cantrall (7♂, 13♀).

Distribution. Found in southern Georgia and north Florida, from Berrien County, GA west to the Chattahoochee River, and south to Liberty and Baker Counties, FL (Figs 12, 13C).

Habitat. Flatwoods and pitcher plant bogs. I observed this species feeding on *Seymeria cassioides* (J.F.Gmelin) S.F.Blake at Doerun pitcher plant bog.

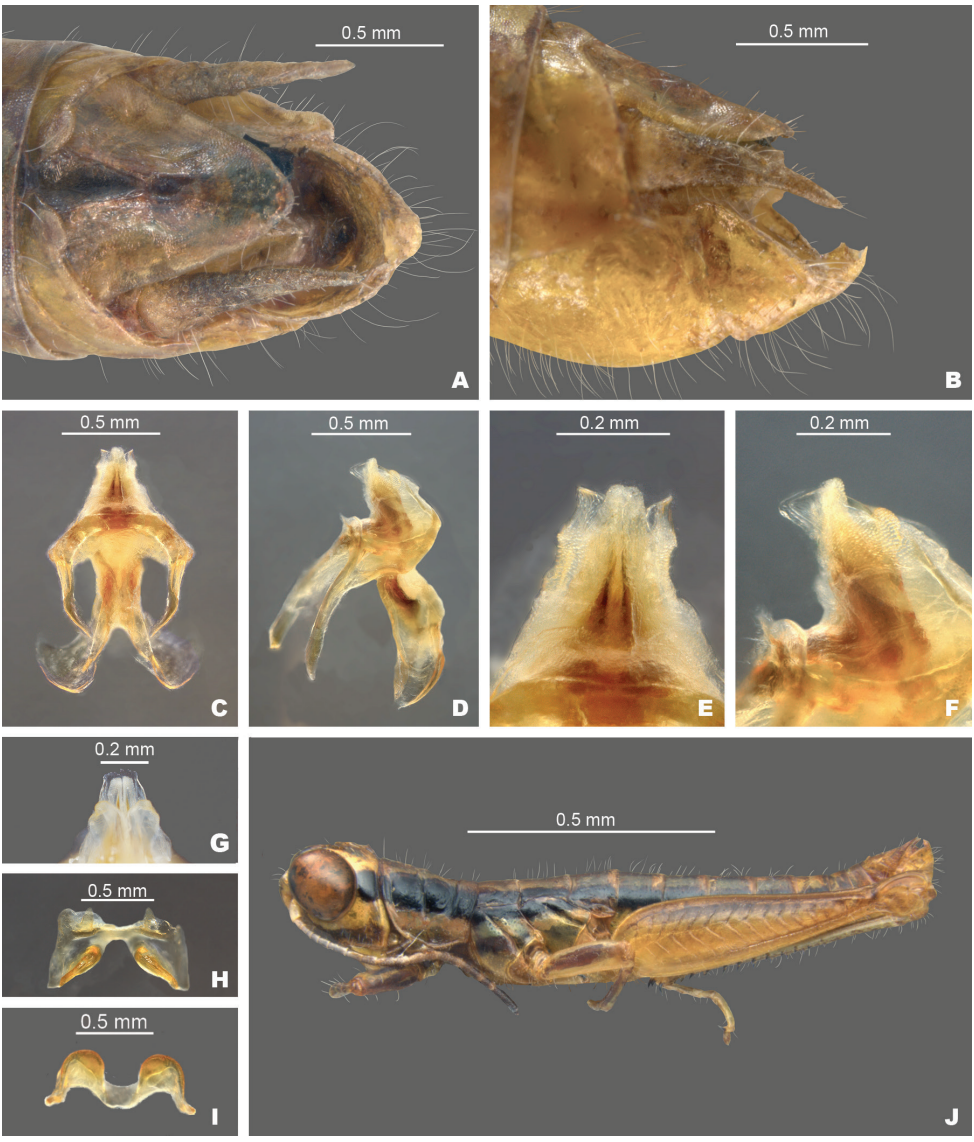

Figure 10. *Gymnoscirtetes wadeorum*: **A** dorsal view of male terminalia **B** lateral view of male terminalia **C** dorsal view of phallic complex **D** lateral view of phallic complex **E** dorsal view of aedeagus **F** lateral view of aedeagus **G** caudal view of the aedeagus **H** dorsal view of epiphallus **I** caudal view of epiphallus **J** habitus.

Etymology. Named in honor of the Wade Family who, in 1979, placed an 85-ha tract of old growth longleaf pine savanna into a perpetual conservation easement. Today, the "Wade Tract", is one of the most important remaining examples of the long leaf pine ecosystem in existence and is also the type locality of this species.

***Gymnoscirtetes georgiaensis* sp. nov.**
https://zoobank.org/58A5654C-C0D0-4DBE-8B85-9538DE377F5F
Figs 5F, 11A–J, 12

Diagnosis. Differing from other species in the group based on the shape of the internal male genitalia (Fig. 11C–I). In dorsal view, the dorsal valves form two translucent lobes

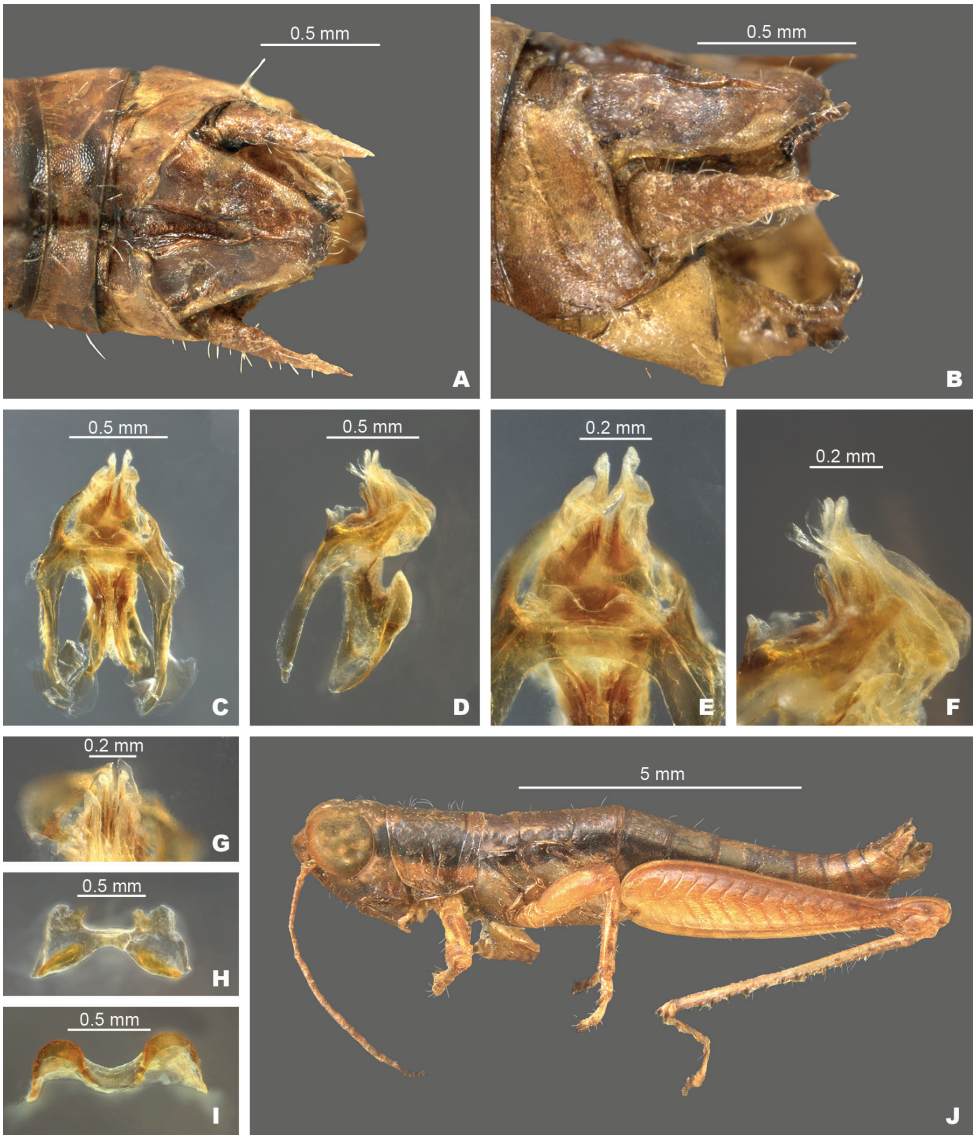

Figure 11. *Gymnoscirtetes georgiaensis*: **A** dorsal view of male terminalia **B** lateral view of male terminalia **C** dorsal view of phallic complex **D** lateral view of phallic complex **E** dorsal view of aedeagus **F** lateral view of aedeagus **G** caudal view of the aedeagus **H** dorsal view of epiphallus **I** caudal view of epiphallus **J** habitus.

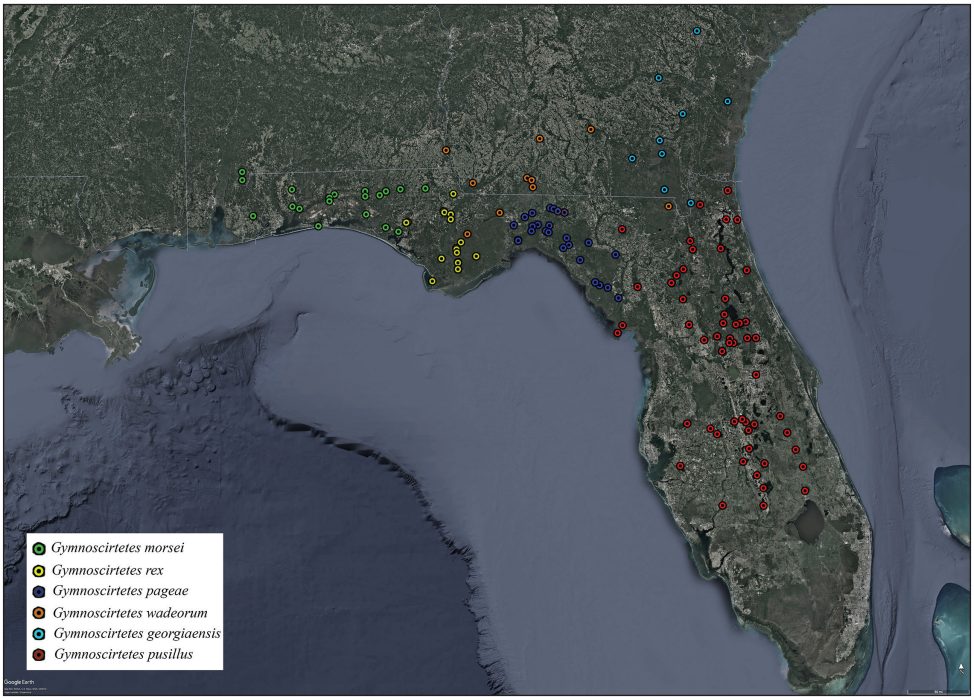

Figure 12. Distribution of *Gymnoscirtetes* species. Green dots = *G. morsei*, yellow dots = *G. rex*, dark blue dots = *G. pageae*, orange dots = *G. wadeorum*, Light blue dots = *G. georgiaensis*, red dots = *G. pusillus*.

that are nearly equal in length to the ventral valves and are pointed at their apices. The ventral valves are opaque cylindrical protrusions that are pointed at their apices. In lateral view, the dorsal valves are nearly equal in length to the ventral valves, twist caudally and taper to their apices. In caudal view, the dorsal valves extend above the ventral valves (Fig. 11G). This species can most easily be separated from *G. pusillus* by having longer dorsal and more translucent dorsal valves and from *G. wadeorum* by the more angled apices and the slight caudal twist in the dorsal valves. *G. georgiaensis* can also be distinguished from these species by their separate geographic distributions (Fig. 12).

Male measurements. (mm): (*n* = 8) Body length 11.5–14.0 (mean = 12.8); pronotum length 1.7–2.2 (mean = 1.9); hind femur length 5.8–7.2 (mean = 6.6); cerci length 0.7–0.9 (mean = 0.8); basal width of cercus 0.3–0.4 (mean = 0.3); mid-cercal width 0.1–0.2 (mean = 0.2); cerci apex width 0.1 (mean = 0.1) tubercule length 0.1–0.3 (mean = 0.2); tubercule width 0.1–0.3 (mean = 0.2).

Female measurements. (mm): (*n* = 1) Body length 13.0; pronotum length 2.0; hind femur 6.6.

Holotype. GA., Appling Co. Moody Forest N.A., 31°54'24"N, -82°18'46"W, 13 October 2010, J.G. Hill; open longleaf pine/wiregrass savannah, MEM 446532. (1♂) Deposited in the Mississippi Entomological Museum.

Paratypes. Same data as type, except BOLD DNA JGH 0066, MEM 446531 (1♀).

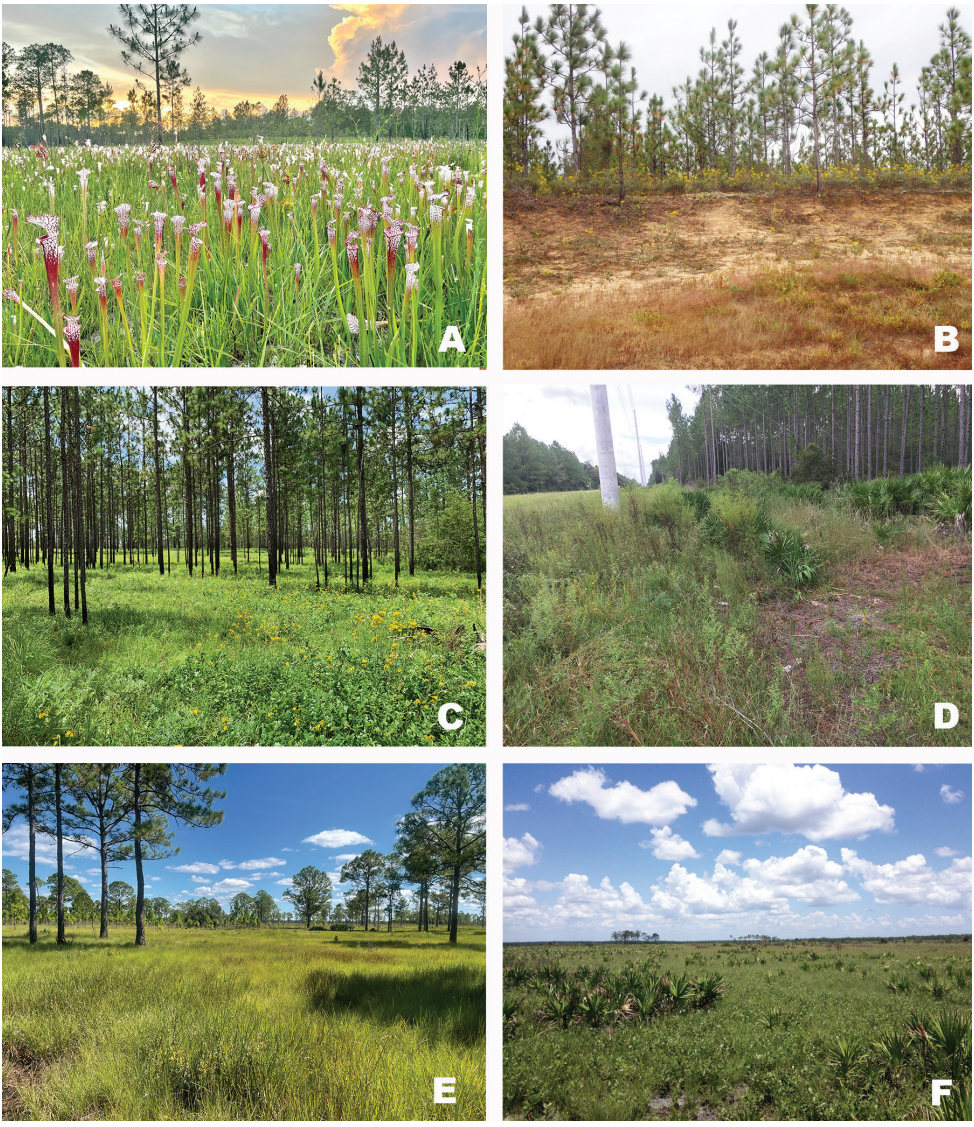

Figure 13. Plant communities at the collection localities of *Gymnoscirtetes* **A** pitcher plant bog (Splinter Hill Bog, Baldwin Co., Alabama) **B** Sandhill (Ecofina Creek Wildlife Management Area, Bay County, Florida) **C** long leaf pine savanna (Wade Tract, Thomas County, Georgia) **D** Mesic sandhill (6 mi S Old Town, Dixie County, Florida) **E** Cutthroat grass seep (Royce, Highlands County, Florida) **F** Florida dry prairie (Avon Park Air Force Range, Highlands County, Florida).

Other specimens examined. Georgia: Bullock Co. Lily Bog, 1 October 1983, D. Rymal, G. Folkerts (2♂). Charlton, St. George, 4 August 1939, Hubbell and Friauf (1♂). Clinch Co., Homerville, 27 August 1911, Rehn and Hebard (1♂). Ware Co., 10 mi S Waycross, Edge of Okefenokee Swp. 16 August 1964, Gurney (1♂); Okeefenokee

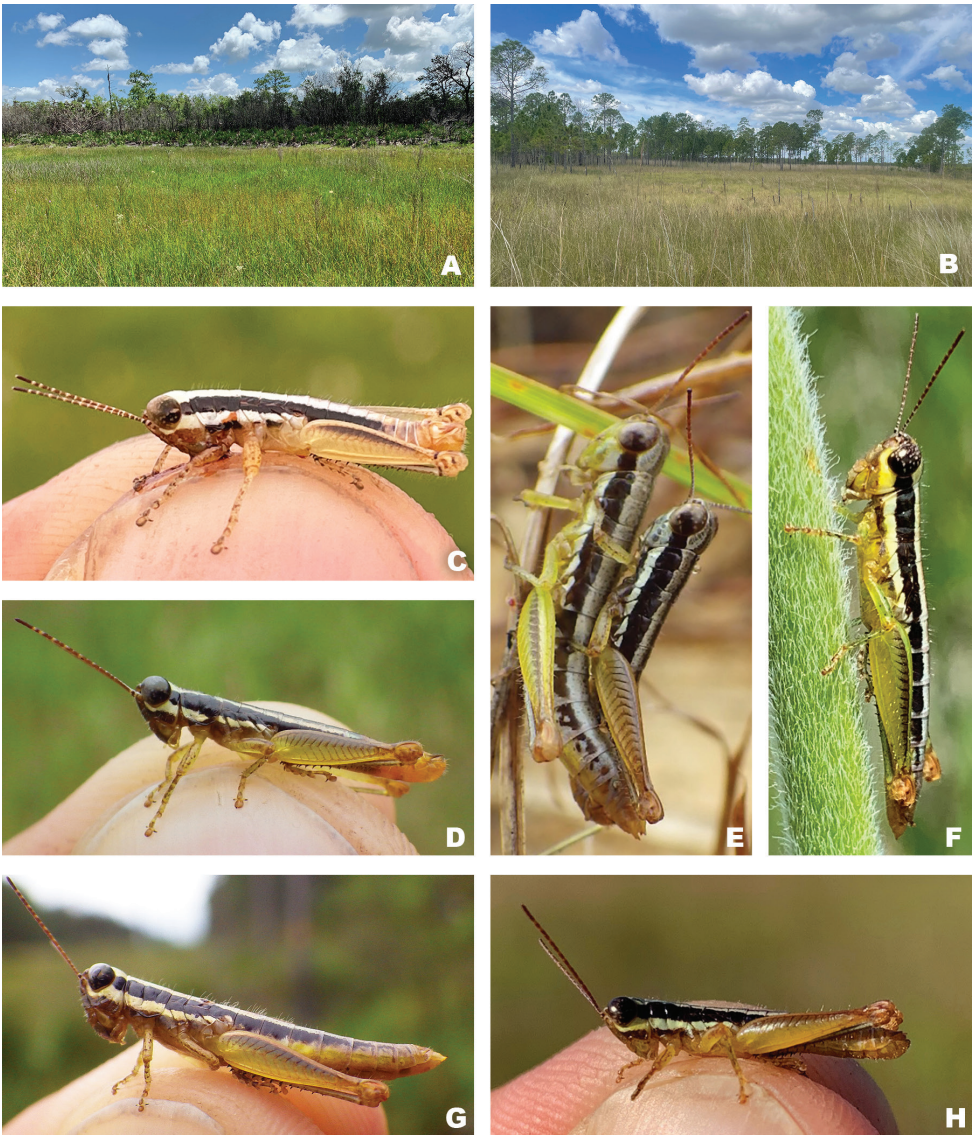

Figure 14. A Seasonal wetland (Lake Wales Ridge National Wildlife Refuge, Polk County, Florida) **B** seasonal wetland (Disney Wilderness Preserve, Osceola County, Florida) **C** *Gymnoscirtetes morsei*, male **D** *Gymnoscirtetes pageae*, male **E** *Gymnoscirtetes rex*, pair in copula **F** *Gymnoscirtetes pusillus*, female **G** *Gymnoscirtetes pageae*, male **H** *Gymnoscirtetes pusillus*, male.

Swamp, 30 July 1931, J.D Beamer (1♂). Waycross, 11 August 1903, A.P. Morse (1♂). Wayne Co., 1.8 mi N Screven, 19 October 1946. T.H. Hubbell (2♂); Jessup (1♂).

Distribution. All known locations occur on the lower Coastal Plain of Georgia Bulloch County south to Ware and Charlton Counties (Fig. 12).

Habitat. Flatwoods and pitcher plant bogs.

Etymology. Named after the state of Georgia, from which this species is apparently endemic.

Discussion

The four new species of *Gymnoscirtetes* described here further demonstrate the high levels of endemism and undiscovered biodiversity on the North American Coastal Plain. The apparent center of diversity for *Gymnoscirtetes* is the area along the northeast Gulf of Mexico where four of the six species are distributed. In this region the Apalachicola and Sewanee Rivers along with the Mobile/Tensaw River delta combined with ecological changes resulting from Pleistocene glacial cycles have produced important biogeographic barriers for isolating populations and generating new species resulting in a biodiversity hotspot with numerous terrestrial taxa that show similar patterns of divergence (Sorrie and Weakly 2001; Soltis et. al. 2006; Hill 2015; Huang et al. 2020).

A complete phylogeny of the North American Melanoplinae is under way but is still several years away from completion. As such, the origins of the five NACP endemic genera remain unknown. Until this work is completed, I hypothesize that *Gymnoscirtetes* arose from a western ancestor that spread into southeastern North America during the Miocene or Pliocene. *Gymnoscirtetes* species are inhabitants of several types of (often mesic) grasslands. Ancestral species could have spread eastward during periods of drier climatic conditions that favored the spread of grassland habitats. During the Miocene, a corridor of semiarid live oak-conifer woodlands, arid subtropic scrub, grassland, subdesert to desert vegetation existed on the Gulf Coastal Corridor (Axelrod 1958; Webb 1977; Albright 1998; Noss 2013). Arid plant conditions may not seem suitable for the spread of mesic grassland inhabiting species, but even under current conditions many of the mesic grasslands inhabited by *Gymnoscirtetes* are adjacent to or are interspersed among scrub environments. In some cases, they occur in grasslands that are only wet for a portion of the year as is the case in the hyper-seasonal Florida dry prairies. Populations of the ancestral species could have then repeatedly isolated by advancing and retreating glaciers during the Pleistocene, which would have also created larger rivers that would have acted as biogeographic barriers. The two species groups were probably isolated early on during the Pleistocene with each group radiating later during the period, as seen in the *Melanoplus scudderi* group (Huang et al. 2020).

Despite being relatively secure in terms of conservation at present, *Gymnoscirtetes* may be of conservation concern in the future. Many co-occurring plant communities (e.g., long leaf pine savannas and pitcher plant bogs) are imperiled and have undergone drastic reduction in the last 200 years. Thus, threats to *Gymnoscirtetes* are habitat loss from anthropogenic habitat alterations and potential loss of habitat from climate change which may result in the flooding of their low-lying environments near the edge of the Coastal Plain. Given the growing interest in the biodiversity of the North American Coastal Plain, and the recent classification of the region as a biodiversity hotspot, I hope that this study helps further conservation efforts in the region.

Acknowledgements

This publication is a contribution of the Mississippi Agriculture and Forestry Experiment Station and was partially supported by funding from the National Institute of Food and Agriculture, the National Science Foundation OPUS (2043909), the U.S. Fish and Wildlife Service, and Tall Timber Research Station. Some of the specimens used in this study were collected under permits from Florida State Parks, Florida Fish and Wildlife Commission, the U.S. Fish and Wildlife Service, Tall Timbers, The Georgia Department of Natural Resources, and The Nature Conservancy. I thank Irvin Cantrall, Ted Hubbell, and J.J. Friauf for collecting many of the historic specimens used in this study, and Matt Thorn for assisting with collecting some of the modern specimens. Additionally, I thank Steve Orzell for facilitating access to the wonderful natural areas on Avon Park Air Force Base and to Ashley Baker for her assistance producing the figures for this article.

References

Albright LB III (1998) The Arikareean land mammals age in Texas and Florida: Southern extension of Great Plains faunas and Gulf Coastal Plain endemism. Geological Society of America Special Papers 325: 167–183. https://doi.org/10.1130/0-8137-2325-6.167

Axelrod DL (1958) Evolution of the Madro-Tertiary geoflora. Botanical Review 24(7): 433–509. https://doi.org/10.1007/BF02872570

Cantrall IJ (1951) Field notes from Cantrall's trips to Florida, Michigan, and Alabama 1946–1951. University of Michigan Museum of Zoology Insect Field Notebooks UMMZI–FN115, 108 pp.

Hebard M (1918) New genera and species of the Melanopli found within the United States (Orthoptera: Acrididiae). Transactions of the American Entomological Society 44: 141–170. https://doi.org/10.5962/bhl.title.58215

Hill JG (2015) Revision and biogeography of the *Melanoplus scudderi* Species Group (Orthoptera: Acrididae: Melanoplinae) with a description of 21 new species and establishment of the Carnegiei and Davisi Species Groups. Transactions of the American Entomological Society 141(2): 252–350. https://doi.org/10.3157/061.141.0201

Hill JG (2018) The grasshopper fauna of southeastern grasslands: A preliminary investigation. In: Hill JG, Barone JA (Eds) Southeastern Grasslands: Biodiversity, Ecology, and Management. University of Alabama Press, 163–182.

Hill JG, Barone JA (2018) Southeastern Grasslands: Biodiversity, Ecology, and Management. University of Alabama Press, 344 pp.

Huang JP, Hill JG, Ortego J, Knowles LL (2020) Paraphyletic species no more—genomic data resolve Pleistocene radiation and validate morphological species of the *Melanoplus scudderi* species complex (Insecta: Orthoptera). Systematic Entomology 45(3): 594–605. https://doi.org/10.1111/syen.12415

Hubbell TH (1932) A revision of the *Puer* Group of the North American genus *Melanoplus*, with remarks on the taxonomic value of the concealed male genitalia in the Cyrtacanthacrinae (Orthoptera, Acrididae). University of Michigan Museum of Zoology Miscellaneous Publication 23, 64 pp.

Noss R (2013) Forgotten Grasslands of the South: Natural History and Conservation. Island Press, 336 pp. https://doi.org/10.5822/978-1-61091-225-9

Noss R (2016) Announcing the world's 36th biodiversity hotspot: The North American Coastal Plain. Critical Ecosystem Partnership Fund. http://www.cepf.net/news/top_stories/Pages/Announcing-the-Worlds-36th-Biodiversity-Hotspot.aspx#.WXIXQ9PytBw [accessed 20 July 2017]

Noss R, Platt WJ, Sorrie BA, Weakley AS, Means DB, Costanza J, Peet RK (2015) How global biodiversity hotspots go unrecognized: Lessons from the North American Coastal Plain. Diversity & Distributions 21(2): 236–244. https://doi.org/10.1111/ddi.12278

Noss RF, Cartwright JM, Estes D, Witsell T, Elliott KG, Adams DS, Albrecht MA, Boyles R, Comer PJ, Doffitt C, Faber-Langendoen D, Hill JG, Hunter WC, Knapp WM, Marshall M, Pyne M, Singhurst JR, Tracey C, Walck JL, Weakley A (2021) Science needs of southeastern grassland species of conservation concern — A framework for species status assessments: U.S. Geological Survey Open-File Report 2021–1047, 58 pp. https://doi.org/10.3133/ofr20211047

Otte D (2012) Eighty new *Melanoplus* species from the United States (Acrididae: Melanoplinae). Transactions of the American Entomological Society 138: 73–167. https://doi.org/10.3157/061.138.0103

Otte D (2014) *Aptenopedes* and two new related genera in Florida, with a description of fourteen new species (Acrididae: Melanoplinae). Transactions of the American Entomological Society 140(1): 245–292. https://doi.org/10.3157/061.140.0115

Scudder SH (1897) Revision of the orthopteran group Melanoplinae (Acrididae), with special reference to North American Forms. Proceedings of the United States National Museum 20(1124): 1–419. https://doi.org/10.5479/si.00963801.20-1124.1

Soltis DE, Morris AB, McLachlan JS, Manos PS, Soltis PS (2006) Comparative phylogeography of unglaciated eastern North America. Molecular Ecology 15(14): 4261–4293. https://doi.org/10.1111/j.1365-294X.2006.03061.x

Sorrie B, Weakly A (2001) Coastal plain vascular plant endemics: Phytogeographic patterns. Castanea 66: 50–82.

Webb DS (1977) A history of savanna vertebrates in the new world. Part I: North America. Annual Review of Ecology and Systematics 8(1): 355–380. https://doi.org/10.1146/annurev.es.08.110177.002035

ZooKeys 1134: 129–170 (2022)
doi: 10.3897/zookeys.1134.87853
https://zookeys.pensoft.net

RESEARCH ARTICLE

A peer-reviewed open-access journal
ZooKeys
Launched to accelerate biodiversity research

A world generic revision of Quediini (Coleoptera, Staphylinidae, Staphylininae), part 1. Early diverging Nearctic lineages

Adam J. Brunke[1]

1 *Agriculture and Agri-Food Canada, Canadian National Collection of Insects, Arachnids and Nematodes, 960 Carling Avenue, Ottawa, Ontario, Canada*

Corresponding author: Adam J. Brunke (adam.brunke@agr.gc.ca)

Academic editor: Jan Klimaszewski | Received 16 June 2022 | Accepted 26 September 2022 | Published 8 December 2022

https://zoobank.org/C79C5E40-D9C6-4E3B-816F-0201713DBA77

Citation: Brunke AJ (2022) A world generic revision of Quediini (Coleoptera, Staphylinidae, Staphylininae), part 1. Early diverging Nearctic lineages. ZooKeys 1134: 129–170. https://doi.org/10.3897/zookeys.1134.87853

Abstract

Several phylogenetically isolated, early diverging lineages of rove beetle tribe Quediini, all endemic to the western Nearctic, have recently been revealed by phylogenomic systematics. These three lineages, currently treated as either *Quedius* (*Raphirus*) or *Q.* (*Paraquedius*) warrant recognition at the genus level in the ongoing effort to achieve reciprocal monophyly of genera in Quediini. The three lineages were each morphologically studied in detail, with the following results: *Paraquedius* Casey, **stat. res.** is re-elevated to genus rank, *Quediellus* Casey, **stat. res.** is resurrected from synonymy and redefined, and *Iratiquedius* **gen. nov.** is described for the species of the Amabilis and Prostans groups. A morphological diagnosis is provided for each genus at both the global and regional (Nearctic) level. Species level revisions, with keys, are provided for *Iratiquedius*, *Paraquedius*, and *Quediellus* with the following results: *Iratiquedius uncifer* **sp. nov.** and *Paraquedius marginicollis* **sp. nov.** are described, *Quediellus nanulus* Casey is treated as **syn. nov.** of *Quediellus debilis* (Horn), and *I. amabilis* (Smetana), *I. mutator* (Smetana), and *P. puncticeps* (Horn) are substantially redefined. Where possible, CO1 barcode sequence data are integrated with the morphological species concepts used herein and their clusters were found to be congruent.

Keywords

Integrative taxonomy, North America, rove beetles, Staphylininae

Introduction

The rove beetle tribe Quediini is a hyperdiverse, mainly northern hemisphere group of just more than 800 species that are predators of invertebrates in a variety of ecosystems including forests, alpine zones, and wetlands (Smetana 1971; Brunke et al. 2021). After a series of phylogenetic papers, which gradually reduced and redefined the lineage (reviewed in Brunke et al. 2021), a more restricted Quediini was recently extensively sampled for phylogenomic analyses and was demonstrated to be monophyletic, with the exception of the south temperate species that still formally remain in *Quedius* Stephens but instead belong to Amblyopinini pending generic revision (Jenkins Shaw et al. 2020). The final elements of *Quedius* shown to belong to other tribes by Brunke et al. (2021) were formally transferred out of Quediini and described as genera of Cyrtoquediini and Indoquediini by Brunke (2021).

Despite delimiting a morphologically well-defined and monophyletic Quediini, analyses by Brunke et al. (2021) also revealed that, unless all 800+ species of Quediini and its corresponding broad morphological diversity were treated as *Quedius*, an extensive generic revision will be required to achieve diagnosable, monophyletic genera. Aside from the *Quedionuchus* lineage, which consisted only of *Quedionuchus* Sharp and *Queskallion* Smetana, Quediini was resolved by Brunke et al. (2021) as four diverse clades (*Distichalius* lineage, *Microsaurus* lineage, *Quedius* lineage, and *Raphirus* lineage) and four smaller lineages (Fig. 1). Of these latter four, three of them are endemic to the Nearctic region and will be the topic of this first paper: 'Clade A' (here described as *Iratiquedius* gen. nov.), *Paraquedius* Casey, and the *Quedius debilis* group (here treated as genus *Quediellus* Casey stat. res.). The final small lineage of Brunke et al. (2021), 'Clade B', includes the 'Aenescens group' of Smetana (1971), the 'Daedalus group' of Smetana (2017), and the species related to *Quedius riparius* Kellner. It is generally Holarctic in distribution and will be treated in a following contribution.

Materials and methods

Depositories

BIO Biodiversity Institute of Ontario, University of Guelph, Ontario, Canada (M. Pentinsaari);

CNC Canadian National Collection of Insects, Arachnids and Nematodes, Ottawa, Ontario, Canada;

DEBU University of Guelph Insect Collection, University of Guelph, Ontario, Canada (S. Paiero);

FMNH Integrative Research Center, The Field Museum of Natural History, Chicago, Illinois, USA (M. Thayer, M. Turcatel);

MCZ Museum of Comparative Zoology, Harvard University, Massachusetts, USA (C. Maier);

UTCI University of Tennessee at Chattanooga, Chattanooga, Tennessee, U.S.A. (S. Chatzimanolis).

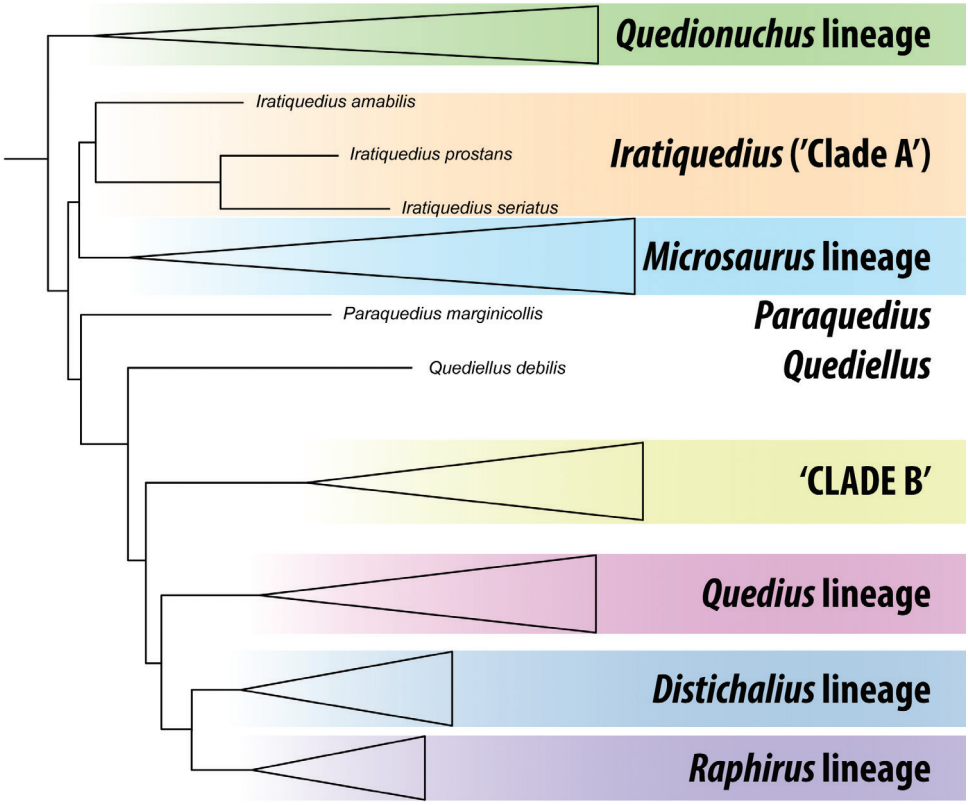

Figure 1. Schematic summary of Quediini (Staphylinidae: Staphylininae) topology recovered by Brunke et al. (2021) based on a partitioned maximum likelihood phylogenetic analysis of nearly 500 protein-encoding loci, and with taxonomy updated based on the results of the present paper.

Specimen data

Type label data are given verbatim, with labels separated by "/" and comments indicated in square brackets. Non-type label data were standardized to improve clarity. Specimens were georeferenced using Google Earth or Google Maps.

Microscopy, illustration, and photography

All specimens were examined dry using a Nikon SMZ25 stereomicroscope. Genitalia and terminal segments of the abdomen were dissected and placed in glycerin filled vials, pinned with their respective specimens. Line illustrations were made from standard images and then digitally inked in Adobe Illustrator CC-2021. All imaging, including photomontage was accomplished using a motorized Nikon SMZ25 microscope and NIS Elements BR v. 4.5. Photos were post-processed in Adobe Photoshop CC-2021.

Measurements were performed using the live measurement module in NIS Elements BR v4.5. Measurements were taken as listed below, but only proportional

(HW/HL, PW/PL, EW/ EL, ESut/PL, PW/HW) and forebody measurements are stated directly in descriptions due to variability in body size. Total body length is generally difficult to measure accurately in Staphylinidae due to the contractile nature of the abdomen.

Abbreviations for measurements are as follows:

HL Head length, at middle, from the anterior margin of frons to the nuchal ridge;
HW Head width, the greatest width, including the eyes;
PL Pronotum length, at middle;
PW Pronotum width, greatest width;
EL Elytral length, greatest length taken from level of the anteriormost large, lateral macroseta to apex of elytra. Its length approximates the length of the elytra not covered by the pronotum and therefore contributing to the forebody length;
EW Elytral width, greatest width;
ESut Sutural length, length of elytral suture;
Forebody HL + PL + EL.

Molecular data

Extraction, amplification, and sequencing of the barcoding fragment of CO1 were performed by the Canadian Centre for DNA Barcoding (CCDB), Biodiversity Institute of Ontario (BIO) (Guelph, Ontario, Canada). DNA was extracted from both dried museum specimens and 95% alcohol-preserved specimens. In some cases where Sanger-based methods failed to produce full-length sequences, re-attempts on existing DNA extracts were made with the NGS service of CCDB, which uses SMRT sequencing on a PacBio Sequel. Sequences were uploaded to BOLD and those sequences deemed to be barcode compliant by BOLD were assigned BINs (Barcode Index Numbers, Ratnasingham and Hebert 2013) and were considered as tentative species hypotheses. Using the Taxon-ID tree tool in the workbench of BOLD, barcodes and their associated BINs were visualized in a neighbour-joining tree using the BOLD aligner and Kimura-2 Parameter (K2P) distances. As the genera in question are phylogenetically isolated within Quediini and do not have clear sister groups among available barcode data, *Fluviphirus elevatus* (Hatch) (Indoquediini) was used to root the trees. The final dataset including voucher information is available on BOLD as the published dataset DS-QUEDREV1.

A sequence clustering analysis was performed on the dataset, using the workbench in BOLD to identify potential Operational Taxonomic Units (OTUs) using the refined single-linkage algorithm of Ratnasingham and Hebert (2013). This analysis is similar to that used to determine BINs but is useful to group sequences in advance of a BIN assignment or for those sequences that are too short to be BIN compliant. Results of the clustering analysis are reported with each species, under Comments.

Phylogenetic analyses of the single-locus alignment using maximum likelihood were attempted but did not provide sufficient resolution to be useful, likely due to saturation at such deep divergences between the phylogenetically isolated lineages, including within genera. Monophyly of these clades was already demonstrated by phylogenomics (Fig. 1) (Brunke et al. 2021).

Taxonomic account

Staphylininae Latreille, 1802

Quediini Kraatz, 1857

Diagnosis. Quediini (as recently redefined by Brunke et al. (2021)) can be distinguished from other Staphylininae based on the following combination of characters: disc of head and pronotum with microsculpture, at least on lateral part of either head or pronotum; head with frontoclypeal punctures, and with posterior frontal and basal macropunctures (e.g., Fig. 3C) that are distinguishable from ground punctation by their larger diameter and longer, thicker setae; pronotum shield-shaped, slightly elongate to strongly transverse; profemora without apical row of lateroventral spines; protibiae without distinct subapical notch; all pretarsi with pair of empodial setae; all abdominal segments with only anterior transverse line (no traces of posterior transverse line), this line not encompassing spiracles (e.g., Fig. 3E, F).

***Iratiquedius* gen. nov.**
https://zoobank.org/9DF5C736-97AD-48AD-9BDA-A49203711E06
Figs 2A–F, 3A, C–F, 4A–D, 6A–P, 7A–N, 9A–E

Type species. *Quedius amabilis* Smetana, 1971.

Etymology. The generic name is a combination of the Latin adjective 'iratus' and *Quedius*. It refers to the characteristic shape of the eyes, which are strongly convergent anteriad and create a comical, angry appearance.

Diagnosis. Within Quediini, *Iratiquedius* can be distinguished from all other genera of the tribe by the distinctive eyes, which occupy nearly the entire lateral head margin, and are so convergent anteriad that their inner margin forms an obtuse angle with the suprantennal ridge (Fig. 3A). The global diagnosis is the same as the regional Nearctic diagnosis.

Description. Medium to small rove beetles, with variable coloration (Fig. 2A–F). With the character states of Quediini (see Brunke et al. (2021)) and the following: antennomere 3 longer than 2, without dense setation; outer antennomeres (8–10) about as long as wide or shorter; antennae inserted close to inner margin

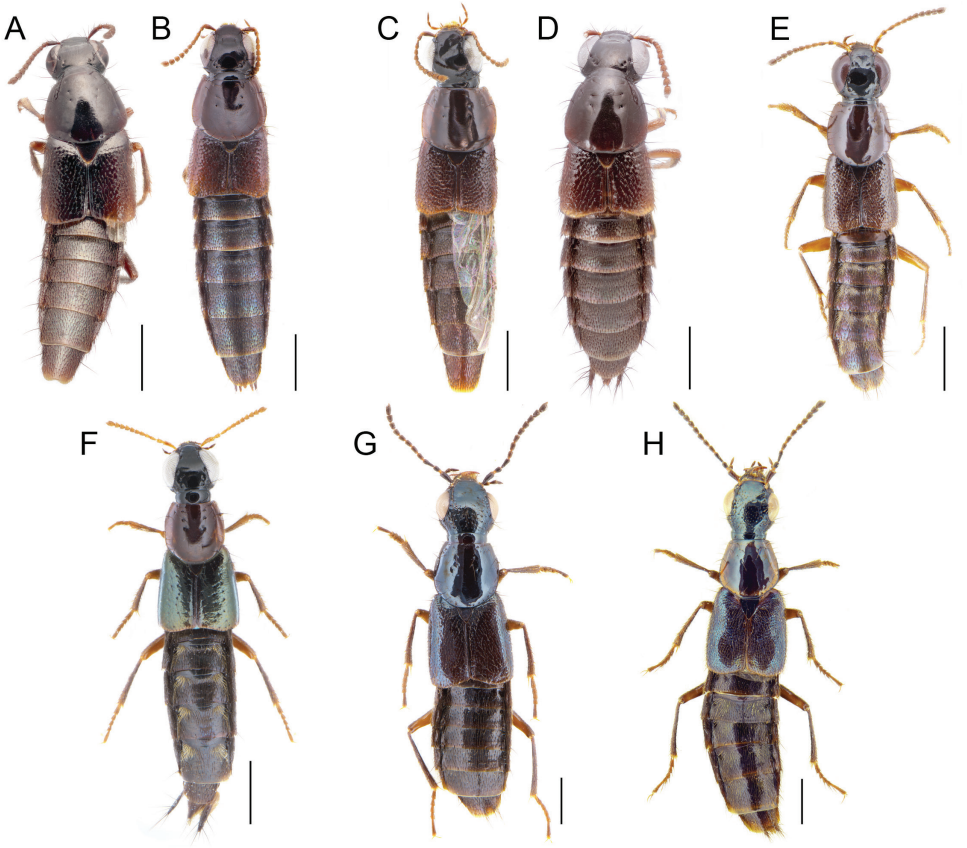

Figure 2. A–H dorsal habitus of **A, B** *Iratiquedius amabilis* (Smetana) **A** male holotype **B** female non-type **C, D** *I. mutator* (Smetana) **C** male non-type **D** female holotype **E** *I. prostans* (Horn) **F** *I. seriatus* (Horn) **G** *Paraquedius puncticeps* (Horn) **H** *P. marginicollis* sp. nov. Scale bars: 1 mm.

of eye, separated by about the width of the antennal sclerite or less; head with eyes large, strongly convex, bulging from and nearly occupying entire lateral head outline, convergent anteriad and with inner margin forming obtuse angle with suprantennal ridge (Fig. 3A); with basal puncture doubled (at least one side), interocular punctures present in some individuals of some species (*I. amabilis*, *I. mutator*) or absent, paraocular punctures absent, genal puncture absent (Fig. 3C, D); frons not well-developed anterolaterad of antennal insertions; labrum notched medially, creating two lobes; apical maxillary and labial palpi fusiform and glabrous; infraorbital ridge complete to mandibles; gular sutures converging towards neck and narrowly spaced posteriad; mandibles with dorsal lateral groove absent or rudimentary, right mandible with single proximal tooth, tooth simple (Fig. 3D) or bifid (Fig. 3C); pronotum transverse to elongate, non-explanate, with three punctures in dorsal row, sublateral row at most reaching large lateral puncture, not extended posteriad; with only single large lateral puncture (e.g., Fig. 4A–D); hypomeron strongly

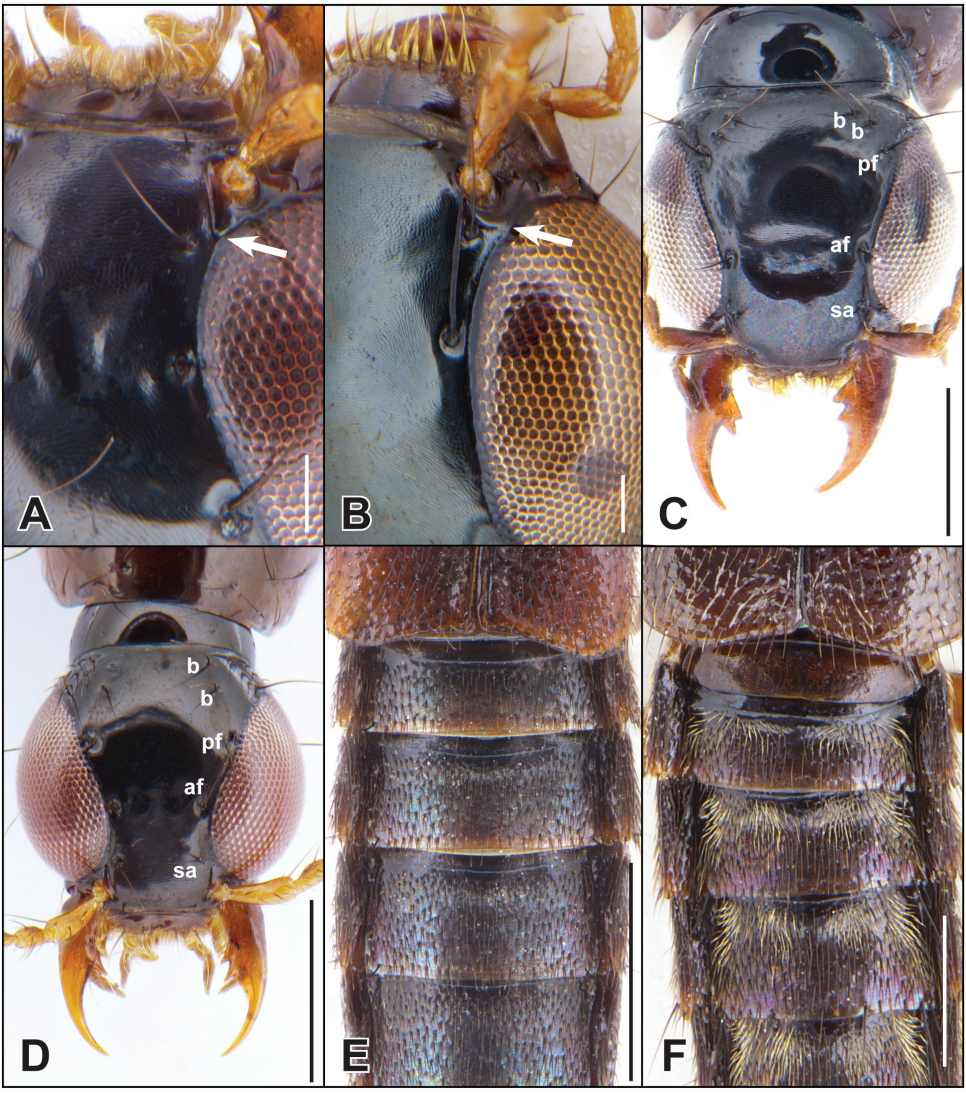

Figure 3. A–D dorsal head **A, B** showing confluence of inner eye margin and supra-antennal carina (arrow) **E, F** abdominal tergites **A, D** *Iratiquedius seriatus* (Horn) **B** *Quedius* (*Raphirus*) *probus* (Casey) **C, E** *I. amabilis* (Smetana) **F** *I. prostans* (Horn). Abbreviations: af = anterior frontal puncture; b = basal puncture; pf = posterior frontal puncture; sa = supra-antennal puncture. Scale bars: 0.1 mm (**A, B**); 0.5 mm (**C–F**).

inflexed, not visible in lateral view; basisternum with pair of macrosetae (reduced in *I. seriatus* and *I. prostans*) and well-developed longitudinal carina; scutellum impunctate; elytron with subbasal ridge complete and forming scutellar collar, disc without microsculpture between punctures; row of humeral spines present and well-developed; elytral punctation evenly distributed or in serial rows (*I. seriatus*); foretibia with lateral spines (reduced in *I. seriatus*, absent in *I. prostans*) and apical

spurs; metatarsomeres with disc setose; metatibia with at least three spines on outer face; abdominal tergite I with prototergal glands developed as moderately deep impressions, outer margin with row of setae; abdominal tergites not deeply impressed at base but some species with paired median impressions causing a 'pinched' appearance; abdominal sternite III with basal transverse line forming obtuse angle at middle, not produced posteriad; aedeagus with well developed paramere bearing peg setae; at least some species with discrete, paired internal sac sclerites that may be homologous with the ventral paired sclerites described by Brunke et al. (2016) (e.g., *I. seriatus*, *I. uncifer* (Fig. 7H–K)).

Distribution. *Iratiquedius* is endemic to western North America.

Bionomics. Species of *Iratiquedius* are most often found in wet moss, though *I. prostans* is more of a generalist and can be collected from a variety of wet debris along running water.

Comments. The three included species of *Iratiquedius* (*I. amabilis*, *I. prostans*, *I. seriatus*) were resolved together in 'Clade A' using a phylogenomic dataset (Brunke et al. 2021). Although Clade A was recovered by the concatenated but not coalescent analyses, the morphological configuration of the eyes, unique in Quediini, provides strong further evidence for its monophyly.

Key to the species of *Iratiquedius*

1 Microsculpture broken or missing on at least parts of pronotum; elytra with macropunctures arranged in rows, disc metallic blue to green but appearing brownish in greasy or teneral specimens (Fig. 2F) **2**

– Entire surface of pronotum with distinct, uninterrupted microsculpture; elytra with sparse to dense, even punctation, not arranged in rows, disc without metallic reflection (Fig. 2A–E) **3**

2 Pronotum entirely without microsculpture, at most with a few short lines touching punctures; median lobe of aedeagus weakly produced ventrad in lateral view (Fig. 7F, G); ventral paired sclerites of internal sac with sharp, hooked apex (Fig. 7J, K); disc of female tergite X with distinct oval depression (Fig. 9E) ..... ***I. uncifer* sp. nov.**

– Pronotum microsculpture variable, ranging from evenly covered with broken transverse waves to entirely without microsculpture; median lobe of aedeagus strongly curved ventrad in lateral view (Fig. 7D, E); ventral paired sclerites of internal sac with rounded apex (Fig. 7H, I); disc of female tergite X evenly convex (Fig. 9D) ..... ***I. seriatus* (Horn)**

3 Basal abdominal tergites with paired median impressions, creating a 'pinched' appearance, tergites and sternites with distinct patches of pale pubescence at base (Fig. 3F) ..... ***I. prostans* (Horn)**

– Abdominal tergites evenly convex, tergites and sternites without patches of pale pubescence at base (Fig. 3E) **4**

4 Anterior angles of pronotum with shallow but distinct micropunctation (Fig. 4A, B); apex of median lobe in lateral view relatively short and rounded (Fig. 6A, B), in ventral view, apex slightly to distinctly emarginate (Fig. 6E, F); paramere with marginal row of peg setae remaining dense throughout (Fig. 6H, I); apex of female tergite X broader, with dense marginal setae (Fig. 9A); Sierra Nevada of California ..... ***I. amabilis*** **(Smetana)**

– Anterior angles of pronotum with barely perceivable micropunctation (Fig. 4C, D); apex of median lobe in lateral view relatively elongate and sharp (Fig. 6C, D), in ventral view, apex entire and pointed (Fig. 6G); paramere with marginal row of peg setae becoming sparse distally (Fig. 6J, K); apex of female tergite X sharply projected to a point, with sparse marginal setae (Fig. 9B); Coast Range Mountains and Central Valley of California..... ***I. mutator*** **(Smetana)**

Iratiquedius amabilis **(Smetana, 1971), comb. nov.**
Figs 2A, B, 3C, E, 4A, B, 6A, B, E, F, H, I, 9A, 11A (map)

Quedius (*Raphirus*) *amabilis* Smetana, 1971: 205.
Quedius (*Raphirus*) *amabilis*: Smetana 1990 (distributional records).
Quedius amabilis: Brunke et al. 2021 (member of 'Clade A', non-*Raphirus*).

Type locality. Near Strawberry, El Dorado County, California, United States.

Type material. ***Holotype*** (male, CNC): N.r. Strawberry, Eldorado Co. Cal., 16–17.61 [handwritten label] / #67, 45 [illegible, 'mi camp'?] [handwritten label] /R. Schuster Collector [printed label] / HOLOTYPE *Quedius amabilis* Smetana 1968, CNC No. 10876 [red printed label] / CNC935809 [identifier label].

The aedeagus of the male holotype was never fully dissected by A. Smetana and was glued to the point with the specimen. For the present study, the aedeagus was relaxed, photographed and placed in glycerin within a genitalia vial.

Non-type material. United States: California: Sierra Co.: 14 mi E Sierra City, Yuba Pass, 6,700' [2,042 m], 26.VI.1976, L. & N. Herman (1 male, CNC); same except 26–28.VI.1976 (2 females, CNC).

Diagnosis. *Iratiquedius amabilis* may be recognized within the genus by a combination of the evenly punctate elytra, the lack of golden setae or impressions at the base of the abdominal tergites and the distinctly impressed micropunctures on the anterior angles of the pronotum. The species most closely resembles *I. mutator* and can be distinguished from it by the distinct micropunctures of the anterior angles of the pronotum, the shorter apex of the median lobe in lateral view in males or broader, more densely setose apex of female tergite X.

Redescription. Measurements ♂ (n = 2): HW/HL 1.21–1.22; PW/PL 1.29–1.32; EW/EL 1.28–1.31; ESut/PL 0.83; PW/HW 1.16–1.33; forebody length 3.3–3.4 mm.

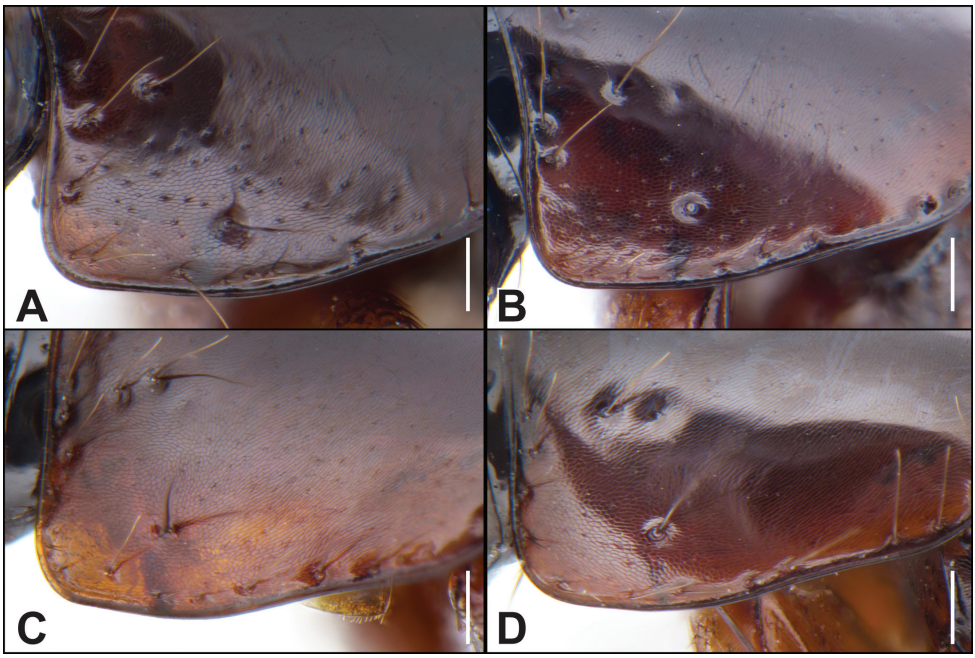

Figure 4. A–D anterior angle of the pronotum **A, B** *Iratiquedius amabilis* (Smetana) **C, D** *I. mutator* (Smetana) **A, C** macropterous morphotype **B, D** brachypterous morphotype. Scale bars: 0.1 mm.

Measurements ♀ (n = 2): HW/HL 1.18–1.21; PW/PL 1.17–1.24; EW/EL 1.45–1.59; ESut/PL 0.60–0.69; PW/HW 1.22–1.27; forebody length 2.9–3.0 mm.

Dark brown with pronotum becoming slightly to distinctly paler toward margin, elytra variably paler at base, sides and apically, in some individuals only scutellar area darkened, pale areas varying from brownish red to yellowish red or brownish yellow; antennomeres 1–3 sometimes slightly darker than remaining segments, which are brownish yellow to dark brown; pro- and mesofemora paler, yellowish brown; abdominal tergites narrowly paler apically, sternites with broader pale area at apex.

With distinct macropterous and brachypterous morphotypes (Fig. 2A, B). Head distinctly transverse, temples extremely short, immediately converging to neck posteriad of eyes; disc of head with microsculpture intermediate between transverse waves and transverse meshes, meshes becoming tighter on frons; posterior frontal puncture located at posterior fourth of eye; interocular punctures present or absent; labrum short, strongly transverse, forming two lobes; area between anterior frontal punctures with broad, transverse and shallow impression, encompassing interocular punctures, if present; antennomeres 1–5 (macropterous) or 1–4 (brachypterous) clearly elongate, segments becoming shorter toward apex, 8–10 weakly to moderately transverse; pronotum strongly (macropterous) to moderately (brachypterous) transverse; disc with microsculpture of transverse waves, often changing direction, becoming isodiametric meshes on anterior angles, anterior angles with distinct, shallow micropunctures, strongly (macropterous) (Fig. 4A)

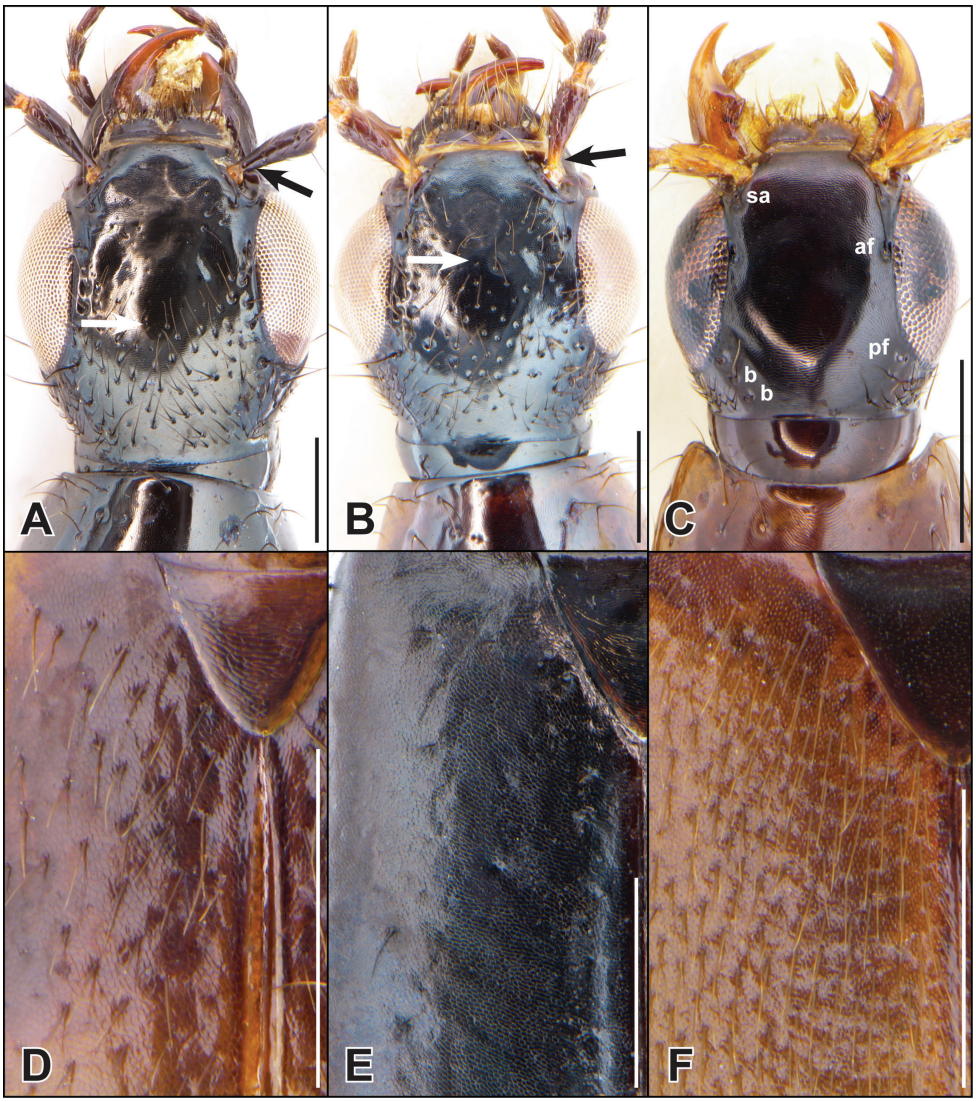

Figure 5. A–C dorsal head **A, B** showing extent of head punctation (white arrow) and color of first antennomere base (black arrow) **D–F** elytral punctation and microsculpture **A** *Paraquedius puncticeps* (Horn) **B** *P. marginicollis* sp. nov. **C, D** *Quediellus debilis* (Horn) **E** *Quedionuchus longipennis* (Mannerheim) **F** *Quedius densiventris* (Casey). Abbreviations: af = anterior frontal puncture; b = basal puncture; pf = posterior frontal puncture; sa = supra-antennal puncture. Scale bars: 0.5 mm.

to moderately (brachypterous) impressed (Fig. 4B); elytra moderately (macropterous), to strongly transverse (brachypterous), at suture moderately (macropterous) to markedly (brachypterous) shorter than pronotum at midline, disc without microsculpture, punctation sparse, most punctures separated by about one puncture width (brachypterous) to slightly denser, with several punctures touching each other laterally (macropterous); abdomen with dense microsculpture of transverse

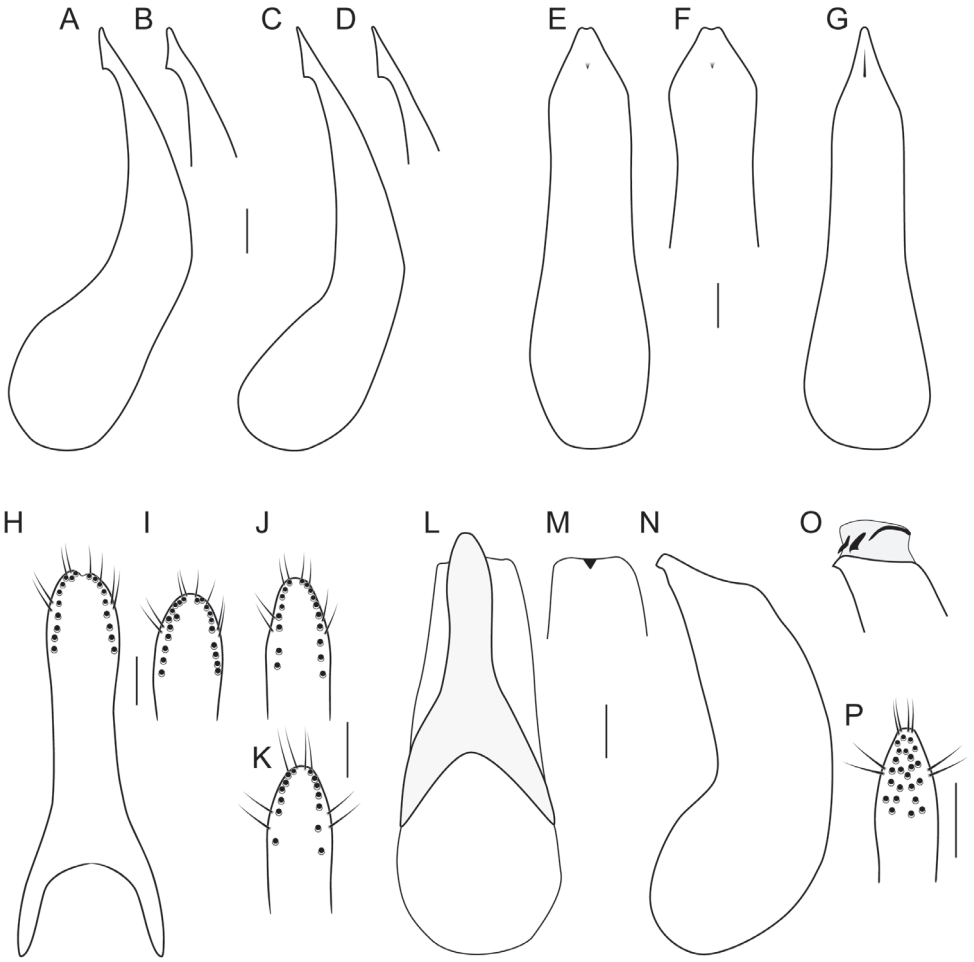

Figure 6. A–G, L–O median lobe of aedeagus **A–D, N, O** in lateral view **E–G, L, M** in ventral view **O** with internal sac everted **H–K, P** underside of paramere showing peg setae **A, B, E, F, H, I** *Iratiquedius amabilis* (Smetana) **C, D, G, J, K** *I. mutator* (Smetana) **L–P** *I. prostans* (Horn). Scale bars: 0.1 mm.

waves, punctures slightly (macropterous) to distinctly (brachypterous) denser on bases of segments.

Male. Sternite VIII with distinct, wide V-shaped emargination; tergite X triangular, with short, rounded apex; sternite IX overall narrow, with long asymmetrical basal part and narrow, minutely emarginate apex; median lobe in ventral view with short tooth, subparallel, with slight expansion subapically, before converging to narrow, truncate apex bearing slight to distinct emargination (Fig. 6E, F); median lobe in lateral view arcuate ventrad, with moderately long apical area, wide tooth and narrow, rounded apex (Fig. 6A, B); paramere subparallel, slightly expanded subapically, converging to moderately narrow, rounded apex, with or without small emargination, peg setae arranged in dense marginal row (Fig. 6H, I).

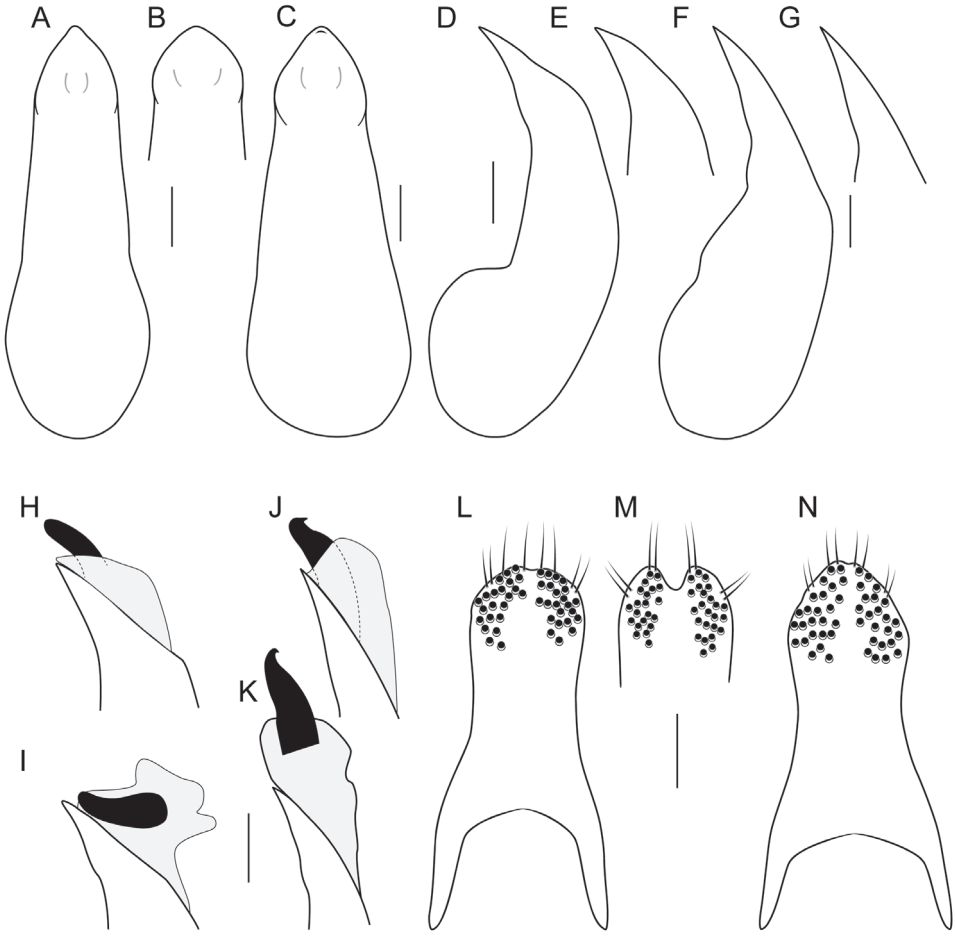

Figure 7. A–K median lobe of aedeagus **A–C** in ventral view **D–K** in lateral view **H, J** internal sac partly everted, showing paired ventral sclerites **I, K** completely everted **L–N** underside of paramere showing peg setae **A, B, D, E, H, I, L, M** *Iratiquedius seriatus* (Horn) **C, F, G, J, K, N** *I. uncifer* sp. nov. Scale bars: 0.1 mm.

Female. Tergite X narrowly triangular, with apex slightly attenuate, with dense marginal setae (Fig. 9A).

Distribution. United States: CA.

This species is known only from two rather close localities in the Sierra Nevada of California.

Bionomics. Nothing specific is known about this species' microhabitat preferences, though it probably lives in moss along the margins of springs and spring-fed creeks.

Comments. Smetana (1971) described *Quedius amabilis* and *Q. mutator* as the only members of the Amabilis group of *Quedius* (*Raphirus*). The former was known from one male and one female, both macropterous and collected from the Sierra Nevada, while the latter was only known from a single, brachypterous female collected at a different

locality in the northern Coast Range mountains to the west. In addition to elytral and wing size, Smetana (1971) cited differences in the punctation of the abdominal tergites, shape of the antennomeres, elytral punctation and pronotum shape. Nothing was reported for many years until Smetana (1990), reported two brachypterous female specimens as *Q. mutator* and four macropterous males (one studied here) as *Q. amabilis*, both collected on Yuba Pass, California (Sierra Nevada) on different dates. He considered the possibility that *Q. mutator* may simply be a brachypterous morph of *Q. amabilis*.

A macropterous male from Yuba Pass was dissected and its aedeagus closely resembles that of the holotype of *I. amabilis* (Fig. 6A, B). The apical emargination of the median lobe in ventral view is less pronounced in the holotype compared to the nontype, and the paramere is slightly emarginate in the holotype, but these differences are considered to be intraspecific variation. In lateral view, the two specimens are nearly identical. The specimens are also similar externally and I agree with Smetana (1990) that they are conspecific. The two brachypterous females differ from the macropterous male in all other characters (antennae, pronotum, elytra, punctation of abdominal tergites) previously used to differentiate *I. amabilis* and *I. mutator*. One male and one female from the Yuba Pass series were sequenced and their half-length (325 bp) barcodes were only 0.34% divergent (Fig. 10). This result suggests that the two morphotypes collected together on Yuba Pass are conspecific, correspond to *I. amabilis* and they are here treated as such. The existence of a macropterous female (the unstudied allotype), if it is indeed a female, indicates that females of *I. amabilis* are wing dimorphic.

However, the female holotype of *I. mutator* differs from the Yuba Pass females by the even shorter elytra, shorter antennomeres 4–10 and the distinctly different apex of tergite X (Fig. 2D). This suggests that *I. mutator* is a valid species and that macropterous and brachypterous morphotypes confusingly exist in both species. All characters used previously to differentiate the two species are here considered to be associated with wing-dimorphism. Two fully winged males from the Central Valley of California were recently found in the FMNH collection (see below) and differ both externally (micropunctation of pronotum) (Fig. 2C) and in male genitalia from the known males of *I. amabilis*. One specimen was sequenced and its partial barcode was found to be 11.3% different from the Yuba Pass specimens (Fig. 10). Instead, these two males more closely resemble the female holotype of *I. mutator* in external morphology, and the concept of *I. mutator* is expanded below.

Iratiquedius mutator **(Smetana, 1971), comb. nov.**

Figs 2C, D, 4C, D, 6C, D, G, J, K, 9B, 11A (map)

Quedius (*Raphirus*) *mutator* Smetana, 1971: 206.

Quedius (*Raphirus*) *mutator*: Smetana 1990 (distributional records, misidentification of *Q. amabilis*, in part).

Type locality. 8 miles north of Post Pile Camp [possibly 'Valentine Spring', ~ 1660 m], Tehama County, California, United States.

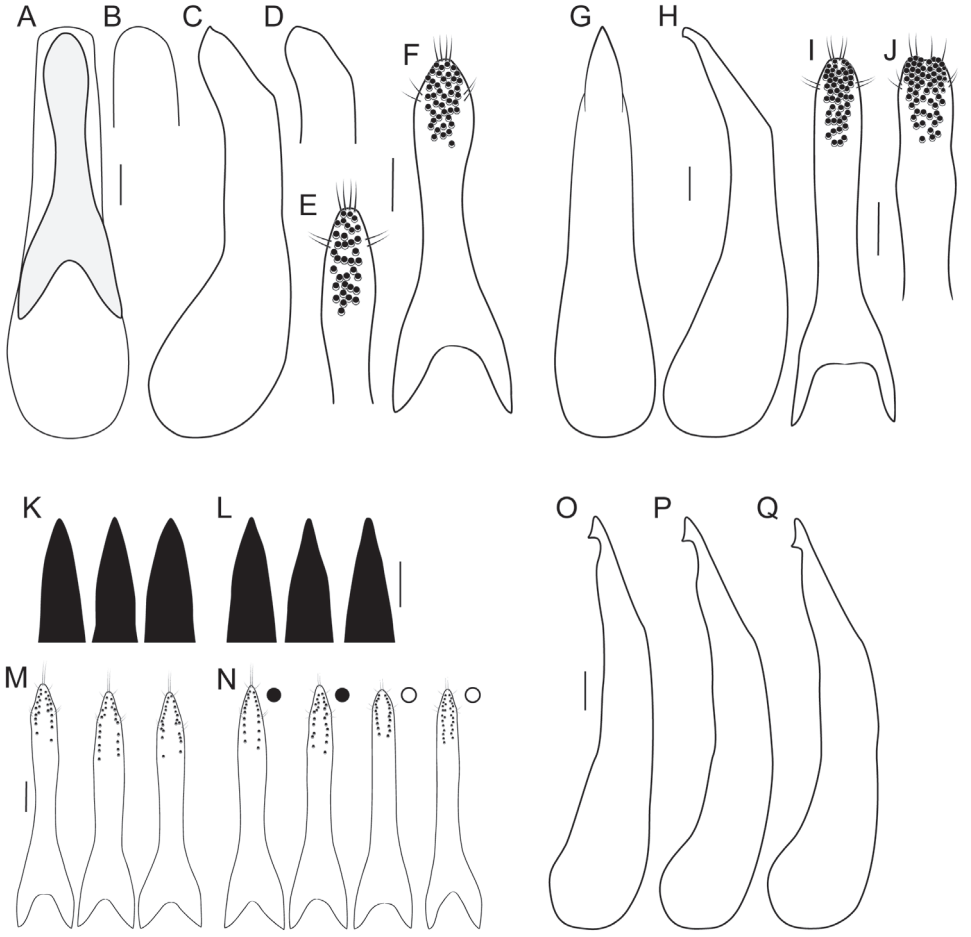

Figure 8. A aedeagus in ventral view **B, C, D, G, H, K, L** median lobe of aedeagus **B, G, K, L** in ventral view, **C, D, H, O–Q** in lateral view **E, F, I, J, M, N** underside of paramere showing peg setae **A–F** *Paraquedius marginicollis* sp. nov. **E** atypical specimen from Clallam County, Washington, United States **G–J** *Paraquedius puncticeps* (Horn) **I** lectotype, from Vancouver, British Columbia, Canada **J** non-type specimen from Vancouver Island **K–Q** *Quediellus debilis* (Horn), specimens from east (**K, M**) and west (**L, M**) sides of the continental divide. Filled circles = typical 'nanulus' morphotype; open circles = typical 'debilis' morphotype. Scale bars: 0.1 mm.

Type material. ***Holotype*** (female, CNC): 8 mi N Post Pile Camp, Tehema [Tehama] Co., Cal, VIII-30-60 [handwritten label] / R.O. Schuster Collector [printed label] / HOLOTYPE Quedius mutator Smetana 1968, CNC No. 10877 [red printed label] / CNC [handwritten label] / CNC93512 [identifier].

The female holotype has the shortest, most sparsely punctate elytra of all known individuals attributed here to either *I. mutator* or *I. amabilis*. The shape of female tergite X is unique and differs from the other examined females (here attributed to *I. amabilis*) by the projected, sharp apex (Fig. 9B).

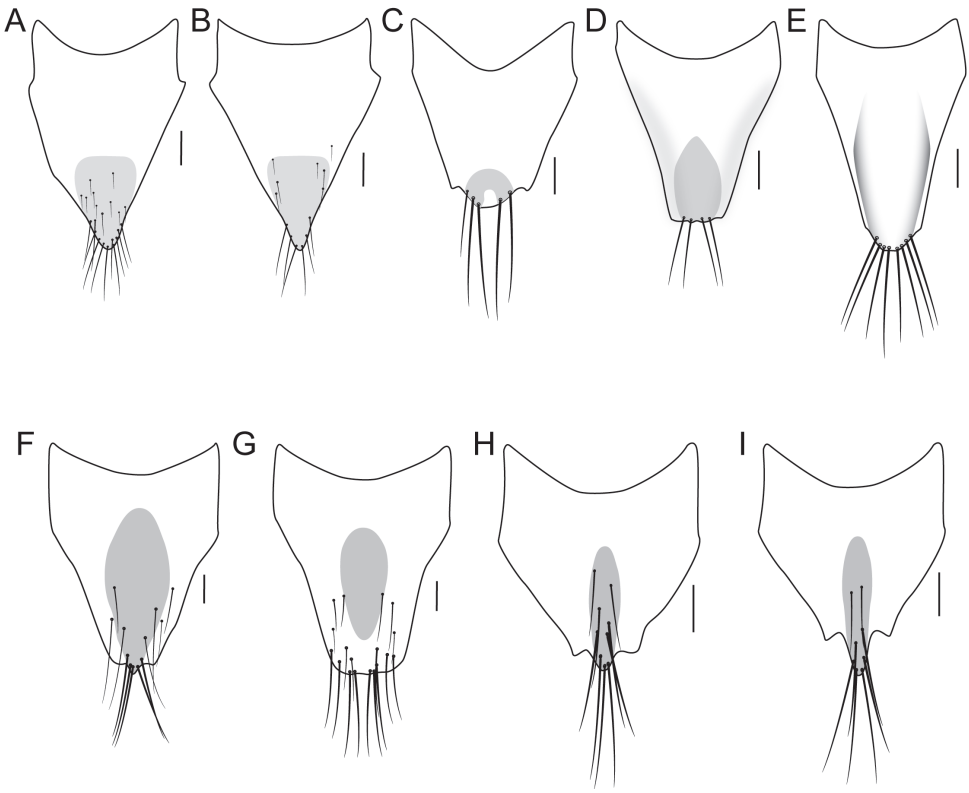

Figure 9. A–I female tergite X **A** *Iratiquedius amabilis* (Smetana) **B** *I. mutator* (Smetana) **C** *I. prostans* (Horn) **D** *I. seriatus* (Horn), evenly convex **E** *I. uncifer* sp. nov., discal impression **F** *Paraquedius puncticeps* (Horn) **G** *P. marginicollis* sp. nov. **H–I** *Quediellus debilis* (Horn). Pigmented area on tergite in **E** not shown for clarity but similar to *I. seriatus.* Scale bars: 0.1 mm.

Non-type material. United States: California: Butte Co.: 3 mi NE Loma [Loma Rica], 39.354, -121.411, 151 m, 3.V.1981, sifting litter along spring, D. Chandler (2 males, FMNH).

Diagnosis. *Iratiquedius mutator* may be recognized within the genus by a combination of the evenly punctate elytra, the lack of golden setae or impressions at the base of the abdominal tergites and the indistinct micropunctures on the anterior angles of the pronotum. The species most closely resembles *I. amabilis* and can be distinguished from it by the indistinct micropunctures of the anterior angles of the pronotum, the longer apex of the median lobe in lateral view in males or sharp, pointed apex of female tergite X.

Redescription. Measurements ♂ (*n* = 2): HW/HL 1.22–1.25; PW/PL 1.20–1.24; EW/EL 1.37–1.38; ESut/PL 0.68–0.71; PW/HW 1.21–1.23; forebody length 3.4–3.5 mm.

Measurements ♀ (*n* = 1): HW/HL 1.20; PW/PL 1.22; EW/EL 1.70; ESut/PL 0.58; PW/HW 1.16; forebody length 2.8 mm.

Extremely similar to *I. amabilis*, and differing only in the following: antennomeres 1–4 (macropterous) or 1–3 (brachypterous) clearly elongate; pronotum moderately

(macropterous) to weakly (brachypterous) transverse; pronotum with micropunctures of anterior angles indistinct (Fig. 4C, D); elytra overall shorter, and at suture relatively shorter than pronotum when comparing morphotypes; male sternite VIII with emargination vaguely more rounded at middle but varying from moderately narrow to as wide as *I. amabilis*; male tergite X more slender with narrower apex; male sternite IX broader, more strongly convergent to apex; apex of median lobe in lateral view longer, more elongate and sharp (Fig. 6C, D), median lobe in ventral view with apex entire and pointed (Fig. 6G); paramere with marginal row becoming sparser distally (Fig. 6J, K); apex of female tergite X sharply projected to a point, with sparse marginal setae (Fig. 9B).

Distribution. United States: CA.

This species is known only from two localities: one in the mountains of the northern Coast Range and one in the Central Valley region.

Bionomics. Both known localities are at least near springs, within areas of relatively dry, open woodland. Specimens of strongly hydrophilous species *I. uncifer* and *I. prostans* were co-collected at the type locality. The two non-type males were collected in litter along the margins of a spring. The holotype was collected at around 1600 m, while the non-type males were collected around 150 m.

Comments. The concept given here for *Iratiquedius mutator* is considered to be a step forward but may need to be modified in the unlikely case that the population in the Central Valley is a third, undescribed species. Males from near the type locality will be needed to determine this with certainty.

***Iratiquedius prostans* (Horn, 1878), comb. nov.**
BIN BOLD:ACA6753
Figs 2E, 3F, 6L–P, 9C, 11B (map)

Quedius prostans Horn, 1878: 165.
Quedius rupimontis Casey, 1915: 418.
Quedius (*Raphirus*) *prostans*: Smetana 1971 (redescription); Brunke et al. 2016, 2019, 2021 (phylogeny, outside of *Raphirus*).

Type locality. 'California', United States.

Type material. *Lectotype* (male, MCZ): The lectotype of this common, widespread species was not examined as its identity was not in doubt.

Non-type material. Canada: British Columbia: Central Kootenay: 8 mi W Creston, 10.VI.1968, Campbell and Smetana (8, CNC); Columbia-Shuswap: Mount Revelstoke National Park, 600 m, 17.VIII.1971, J.M. Campbell (1, CNC); Fraser Valley: 7 mi W Hope, 3.VI.1968, Campbell and Smetana (1, CNC); Squamish-Lillooet: Garibaldi Provincial Park, Diamond Head Trail, 1128 m, 1.VIII.1975, J.M. Campbell & B.A. Campbell (3, CNC); Garibaldi Provincial Park, Mimulus Creek, 1645 m, 8.VIII.1975, J.M. & B.A. Campbell (1, CNC); Mount Garibaldi, 30.V.1968, Campbell and Smetana (22, CNC); Vancouver Island: Elk Lake trail, 48.534470, -123.398647,

27.IX.2020, A. Davies, sedge litter at base of cottonwood, edge of lake (1, CNC); Goldstream Park, 27.Vl1968, A. Smetana (1, CNC); Goldstream Park, 5 mi N Victoria, 27.V.1968, Campbell and Smetana (21, CNC); same except, 6.VI.1975, JM & BA Campbell (3, CNC); Gabriola, sifting moss along pond edge, 3.V.1994, Lot 3, BF & JL Carr (1, CNC); same except Lot4, under wood on wet muck near pond (1, CNC); Nitinat Lake, at Caycuse River, 21.VI.1989, sifting wash up on beach, Lot 5, BF & JL Carr (2, CNC); Duncan, Mount Tzouhalem, 19.X.2008, A. Davies (2, CNC); Lake Cowichan, South Shore Road, 2.3 km N of town, wet moss, 16.VI.1979, I. Smith (9, CNC); Lake Cowichan, spring run beside North Shore Road, 1.7 km N town, moss and litter, 7.VI.1979, I. Smith (5, CNC); 10 mi E [Port] Alberni, MacMillan Provincial Park, 26.V.1968, Campbell and Smetana (1, CNC); near Mount Finlayson Trail, Malahat, Goldstream Provincial Park, moss on rock, 11.VII.1979, I. M. Smith (4, CNC); Port Alberni, Mount Arrowsmith, nr. road to ski area, 11.6 km off Highway 4, 28.VI.1979, I.M. Smith, moss on rocks and sticks in stream (5, CNC); Hillcrest Rd., 16 km S Mesachie Lake, along Lens Creek, 12.VII.2010, A. Davies (1, CNC).

United States: Arizona: Apache Co.: Chuska Mountains, Wagonwheel Campground, sifting leaf litter, 2250 m, 12.VII.1976, J.M. Campbell (5, CNC); same except: sifting moss along waterfall (28, CNC); **California:** Butte Co., 3 mi NE Loma, 3.V.1981, sift litter along spring, DS Chandler (1, FMNH); Mountain House [Brush Creek], 7.V.1981, sift litter along spring, DS Chandler (1, FMNH); Calaveras Co.: Big Trees State Park, 38.2775, -120.310556, 25.V-26.VI.2010, FIT, A.R. Cline & S.L. Winterton (12, UTCI); El Dorado Co.: 5 mi SW Kyburz, 1219 m, 6.V.1968, Campbell & Smetana (23, CNC); same except: 7 mi E Kyburz (6, CNC); Glenn Co.: 5 mi NE Alder Spring, 20.IX.1979, sift oak litter along spring, DS Chandler (2, FMNH); Humbolt Co.: Garberville, Garberville-Harris Road, 5–6 miles east of Garberville, 13.VII.1965, under stones and pieces of sod, Lot 2, BF & JL Carr (1, CNC); Los Angeles Co.: Mount Wilson, 600 m, 26.V.1978, J.O. Martin (1, CNC); Marin Co.: Point Reyes National Seashore, 2 mi W Inverness, 22.III.1983, A. Smetana (3, CNC); Mendocino Co.: Mendocino, 24.VI.1954, Helfer (2, CNC); Placer Co.: 4 mi S Truckee, Truckee River, 5.V.1968, Campbell and Smetana (1, CNC); Lake Tahoe, Tahoe City, 1950 m, 7.VII.1986, A. Smetana (1, CNC); San Bernardino Co.: San Bernardino Mountains, 1 mi NE Angelus Oaks, Cold Creek at Highway 38, 1828 m, 12.III.1983, A. Smetana (33, CNC); San Bernardino Mountains, Highway 38, 3 mi SW Onyx Summit, 2346 m, 14.III.1983, A. Smetana (13, CNC); San Diego Co.: Laguna Mountains, Little Laguna Lake, 5.III.1983, A. Smetana (10, CNC); Mount Laguna, Carex clumps at stream, 25.IX.1981, JM Campbell (3, CNC); Mount Palomar, 1524 m, sifting leaf litter, 27.IX.1981, J.M. Campbell (2, CNC); Mount Palomar, Fry Trail Campground [Fry Creek], 8.III.1983, A. Smetana (1, CNC); San Francisco Co.: San Francisco, 30.V.1911, Van Dyke (4, CNC); Siskiyou Co.: Calahan, Lillypad Lake, old rotten logs, 8.VII.1991, Lot 1,BF & JL Carr (1, CNC); McBride Springs, Mount Shasta, 1447 m, 20.VI.1974, A&D Smetana (1, CNC); Trinity Co.: 10 mi N Junction City, 762 m, 10.VII.1979, J.M. & B.A. Campbell (4, CNC); 12 mi N Junction City, 1030 m, 13.VII.1979, J.M. & B.A. Campbell (4, CNC); Upper Canyon Creek

Meadows, 1463 m, 13.VII.1979, J.M. & B.A. Campbell (2, CNC); 19 mi W Coffee Creek Station, Shasta National Forest, 1219 m, 14.VII.1979, J.M. & B.A. Campbell (1, CNC); 4 mi W Forest Glen, 9.VII.1979, J.M. & B.A. Campbell (2, CNC); Tulare Co.: Wishon Campground, 12 mi NE Springville, Meadow Creek, sifting washed up debris in fast flowing creek, 21.VI.1993, Lot 11 BF & JL Carr (4, CNC); 28 mi NNW Kernville, Thompson Camp Spring, 1676 m, 30.V.1981, L. Herman (1, CNC); Tuolumne Co.: Strawberry, 3.VIII.1960, DG Cavanaro (3, CNC); **Idaho:** Boise Co.: 10 mi NE Idaho City, 10 Mile Campground, sifting moss, 18.VII.1981, J.M. Campbell (23, CNC); Elmore Co.: Boise National Forest, Ice Springs, 1463 m, 21.VII.1981, J.M. Campbell (1, CNC); middle fork of Boise River and Dutch Creek, 1370 m, sifting moss, 19.VII.1981, J.M. Campbell (20, CNC); **Nevada:** Douglas Co.: Zephyr Cove, 1900 m, 9.VII.1986, A. Smetana (13, CNC); **New Mexico:** Sandoval Co.: Sandia Mountain, Cibola National Forest, Las Huertas Creek, wet-soaked moss encrusted with calcareous deposits, springy slope, 8.VII.1981, A. Smetana (11, CNC); **Oregon:** Benton Co.: Mary's Peak, 1158 m, 27.VII.1979, J.M. & B.A. Campbell (1, CNC); Mary's Peak, waterfalls, 1066 m, 5.V.1973, E.M. Benedict (1, CNC); Clackamas Co.: Camp Creek, 3.5 mi SE Rhododendron, 700–730 m, 27.VI.1974, A&D. Smetana (2, CNC); Timberline Lodge Road, Mt. Hood, 28.VI.1974, A&D Smetana (1, CNC); Coos Co.: Dune Park, 3 mi N and 2 mi W North Bend, sunny frost pockets, 15.I.1972, E. M. Benedict (1, CNC); Curry Co.: Agness Rd., [crossing at Wake Up Rilea Creek, under stones and in little pools of water along shady, cascading creek, 10.VIII.1978, B.F. & J.L. Carr] (4, CNC); Deschutes Co.: 12 mi SW Sisters, 1341 m, J.M. & B.A. Campbell, 23.VII.1979 (11, CNC); Douglas Co.: 27.3 miles NE Reedsport, at Smith River Falls, 29.VI.1978, L & N Herman (2, CNC); Grant Co.: Dixie Summit, Highway 26, 1615 m, sifting moss, 22.VII.1981, J.M. Campbell (71, CNC); Malheur National Forest, 2 km NW Highway 26, Forest Road 1218, 1670 m, sifting moss, 22.VII.1981, JM & BA Campbell (13, CNC); Malheur National Forest, 7 km NW Highway 26, 2040 m, sifting old pile of hay, 22.VII.1981, JM & BA Campbell (2, CNC); road 2610, below Dixie Butte, 2050 m, 2.VI.1989, A. Smetana (8, CNC); Strawberry Range, Strawberry Campground, 1780 m, 1.VI.1989, A. Smetana (1, CNC); Strawberry Range, road 650, Fawn Spring, 1480 m, 30.V.1989, A. Smetana (16, CNC); Jackson Co.: highway 140, Little Butte Creek, 23.VI.1974, A.&D. Smetana (17, CNC); Klamath County: 13 mi NE Bly, near Deming Creek, 1706 m, 21.VII.1979, J.M. Campbell & J. Schuh (3, CNC); 16 mi NE Bly, Deming Creek Road, 1828, 21.VII.1979, J.M. Campbell & J. Schuh (9, CNC); 6 mi S Fort Klamath, Crooked Creek, 25.VI.1974, A.&D. Smetana (2, CNC); 9 mi NE Bly, Deming Creek, 1500–1760 m, A.&D. Smetana (6, CNC); Bly Mountain, 24.VI.1974, A.&D. Smetana (1, CNC); Gearhart Mountain, 1980–2194 m, 24.VI.1974, A.&D. Smetana (1, CNC); Sevenmile Creek, 1280 m, 20.VII.1979, J. Schuh & J.M. Campbell (2, CNC); Woodriver Springs, Jackson F. Kimball State Park, 25.VI.1974, A.&D. Smetana (15, CNC); same except, 1295 m, 20.VII.1970, JM Campbell (11, CNC); Mare's Egg Spring, 1280 m, 20.VII.1979, J. Schuh & JM Campbell (1, CNC); same except, 25.VI.1975, A.&D. Smetana (7, CNC); Tecumseh Spring, 1280 m, 20.VII.1979, J. Schuh & J.M. Campbell (2, CNC); Tillamook Co.: 1 mi S

Hebo, 28.VII.1979, J.M. & B.A. Campbell (2, CNC); Umatilla Co.: Umatilla National Forest, North Side Sugarloaf Mountain via Daniel Spring, mixed conifer forest, in wet moss at edge of spring/seep, 12.V.2012, A. Newton & M. Thayer (2, FMNH); 12 km NE Tollgate, Blue Mountain Road 63, 1250 m, A. Smetana (12, CNC); Union Co.: Blue Mountains, 9 km NW Elgin, Philips [Gordon?] Creek Road, 950 m, 27.V.1989, A. Smetana (22, CNC); same except 900 m, 25.V.1989 (3, CNC); Blue Mountains, Road 62, Jarboe Creek, 1200 m, 29.V.1989, A. Smetana (1, CNC); **Utah:** Cache Co.: Logan Canyon, 2 km N Wood Camp, sifting moss, 1706 m, 14.VII.1981, J.M. Campbell (36, CNC); **Washington:** Clallam Co.: 5 mi W Forks, 14.V.1968, Campbell and Smetana (1, CNC); Okanogan Co.: 8 mi NNW Republic, Sweat Creek [picnic area], 1097 m, 20.VII.1978, L&N. Herman (1, CNC); Pierce Co.: Mount Rainier National Park, Tahoma Creek, 700 m, 12.VIII.1973, A, Z & D Smetana (14, CNC); same except, 730 m, 10.VIII.1973 (2, CNC); Spokane Co.: 2 mi E Nine Mile, 13.IX.1955, R.A. Ward (1, CNC); Mount Spokane State Park, 1 km NE park entrance, 1000 m, sifting moss, 1.VIII.1981, JM Campbell (19, CNC); Mount Spokane State Park, Bald Knob campground, sifting moss, 1524 m, 31.VII.1981, JM & BA Campbell (1, CNC).

Diagnosis. *Iratiquedius prostans* can be distinguished by a combination of elytra with even punctation, not arranged in rows, and pale pubescence at the bases of the abdominal tergites and sternites.

Redescription. Measurements ♂ (n = 5): HW/HL 1.10–1.14; PW/PL 1.03–1.13; EW/EL 1.23–1.33; ESut/PL 0.65–0.76; PW/HW 1.05–1.15; forebody length 2.5–2.9 mm.

Measurements ♀ (n = 5): HW/HL 1.11–1.16; PW/PL 1.01–1.10; EW/EL 1.23–1.31; ESut/PL 0.69–0.78; PW/HW 1.06–1.09; forebody length 2.8–3.3 mm.

Head dark brown, pronotum and often elytra paler, dark reddish brown to reddish brown, abdominal segments broadly paler apically; antennae dark brown, antennomeres 1–3 with pale base; palpi reddish brown with apical segment dark brown; legs yellowish brown, tibia and metacoxae dark brown, tarsi brownish.

Head slightly transverse, appearing orbicular, temples extremely short, following outline of eye to neck; disc of head with moderately sparse microsculpture of transverse waves, becoming vaguely meshed in places, often completely meshed on frons, where it is denser; posterior frontal puncture located at posterior third of eye; interocular punctures absent; labrum short, transverse, forming two lobes; area between anterior frontal punctures with Y-shaped impression; antennomeres 1–4 or 1–5 elongate, 6–10 subquadrate, nine or ten, sometimes weakly transverse, antennomeres generally becoming shorter toward apex of antennae; pronotum roughly shield-shaped, subquadrate to slightly transverse; disc with microsculpture similar to that of head but becoming meshed on anterior angles; elytra appearing moderately to distinctly transverse; disc without microsculpture, evenly, moderately densely punctate, punctures generally closer than one puncture diameter but only sometimes touching, setae pale yellowish, appearing dark in greasy or wet specimens; abdominal tergites III–V, sometimes weakly on VI, with paired median impressions creating a 'pinched' appearance (Fig. 3F); tergites with paired patches of golden setae, one medial and one occupying entire basolateral corner; sternites with basal areas of golden setae; tergites with micros-

culpture of very fine and dense transverse waves; tergites with punctation varying from moderately dense at base to very sparse at apex.

Male. Sternite VIII with distinct, moderately deep and rounded emargination; tergite X elongate triangular to triangular, with several long marginal setae; sternite IX distinctly dilated at midlength, with long asymmetrical basal part and moderately deep emargination; median lobe in ventral view with one small, short, median tooth, apex truncate (Fig. 6L, M); median lobe in lateral view strongly narrowing to small apical part, apex rounded and with small ventral tooth, apical part projecting ventrad (Fig. 6N); internal sac with paired sclerites including a pair of slender, curved rod-like sclerites and a pair of broader fang-shaped sclerites (Fig. 6O); paramere longer than median lobe, elongate spoon-shaped in apical half, basal half markedly broad, apex narrowly rounded, peg setae arranged in single, elongate median field (Fig. 6P).

Female. Female tergite and sternite VIII with apex truncate to vaguely emarginate. Tergite X roughly pentagonal, with basal margin deeply incised, disc with faint to distinct, narrow median sulcus, apical area with inverted U-shaped darkening, apex slightly projected (Fig. 9C).

Distribution. Canada: BC. **United States:** AZ, CA, CO, ID, MT, NM, NV, OR, UT, WA.

Iratiquedius prostans is the most widespread species of the genus. It occurs along the entire western cordillera, including both sides of the continental divide, and as far south as New Mexico in the east and near the United States border with Mexico, in the west. The species is not yet known from mountainous southern Alberta but is expected there.

Bionomics. Although this species, like other *Iratiquedius*, seems to prefer moss, it has also been collected in other types of wet litter and even in rotting hay. This broader tolerance of microhabitats has likely allowed for a much wider distribution, across the drier forested areas of the western cordilleras to reach the eastern side of the continental divide.

Comments. Specimens from across the distribution range were dissected and no consistent differences were observed in the aedeagus. This species varies enormously in size and in proportion of the body, giving the impression of multiple species. All specimens sequenced for CO1 barcodes, including those from both sides of the continental divide, were found to belong to a single cluster with 1.50% maximum pairwise distance (Fig. 10).

***Iratiquedius seriatus* (Horn, 1878), comb. nov.**
BIN BOLD:AEO6948
Figs 2F, 3A, D, 7A, B, D, E, H, I, L, M, 9D, 11C (map)

Quedius seriatus Horn, 1878: 166.
Quedius (*Raphirus*) *seriatus*: Smetana 1971 (redescription); Brunke et al. 2016, 2019, 2021 (phylogeny, non-Raphirus).

Type locality. Vancouver, British Columbia, Canada.

Type material. ***Holotype*** **(male, MCZ):** Van. [Vancouver] [printed label] / [male symbol] / Q. seriatus H. [handwritten label] / Type 7272 [red label]. Examined virtually.

The holotype male, although not dissected, was collected in Vancouver, British Columbia, Canada and far from the known distribution of *I. uncifer*. Therefore, the identity of this specimen is not in doubt.

Non-type material. Canada: British Columbia: Fraser Valley: 7 mi W Hope, 3.VI.1968, Campbell and Smetana (2, CNC); Greater Vancouver: Stanley Park, 28.V.1968, Campbell and Smetana (1, CNC); Vancouver Island: 10 mi E [Port] Alberni, MacMillan Provincial Park, 26.V.1968, Campbell and Smetana (1, CNC); Port Alberni, Mount Arrowsmith, nr. road to ski area, 11.6 km off Highway 4, wet moss on rocks, 20.VII.1979, I.M. Smith (20, CNC); same except: moss on rocks and sticks in stream, 28.VI.1979 (10, CNC); Squamish-Lillooet: Garibaldi Provincial Park, Diamond Head Trail, 1128 m, 1.VIII.1975, J.M. Campbell & B.A. Campbell (3, CNC); Garibaldi Provincial Park, Mimulus Creek, 1645 m, 8.VIII.1975, J.M. & B.A. Campbell (2, CNC).

United States: California: El Dorado Co.: 5 mi SW Kyburz, 1219 m, 6.V.1968, Campbell and Smetana (5, CNC); Sierra Co.: 10 mi W Goodyears Bar, Hwy 49, under sandy-muddy moss clumps along cliff by a waterfall, 29.VI.1991, BF & JL Carr (1, CNC); Marin Co.: Point Reyes, 4.VI.1910, A. Fenyes (1 male, CNC); Siskiyou Co.: 5.4 mi SE Seiad Valley, O'Neil Creek, 457 m, 5.VII.1976, L & N Herman (1 female, CNC); **Oregon:** Benton Co.: Mary's Peak, 1158 m, 27.VII.1979, J.M. & B.A. Campbell (8, CNC); same except 9.V.1968 (5, CNC); Mary's Peak, 1066 m, waterfalls, 5.V.1973, E.M. Benedict (3, CNC); Clackamas Co.: mile 1 Timberline Lodge Road, 1463 m, 29.VII.1979, J.M. & B.A. Campbell (8, CNC); same except 28.VI.1974, A. & D. Smetana (2, CNC); Mt. Hood National Forest, Still Creek, Tributary at Highway 173, 1280 m, conifer forest, moss at stream edge, 15.V.2012, A. Newton and M. Thayer (1, FMNH); Douglas Co.: Scottsburg Bridge on Umpqua River, Hwy 38, moss, 11.XII.1971, E.M. Benedict (3, CNC); Hood River Co.: Mount Hood National Forest, Switchback Falls, 1340 m, 30.VII.1979, J.M. & B.A. Campbell (1, CNC); Mount Hood National Forest, Umbrella Falls, 1828 m, 30.VII.1930, J.M. & B.A. Campbell (2, CNC); Mount Hood National Forest, near Barlow Pass, 1220 m, 29.VI.1974, treading wet moss intermixed with low vegetation, muddy edge of small forest marsh, A. & D. Smetana (23, CNC); Jackson Co.: Highway 140, Little Butte Creek, 23.VI.1974, A. & D. Smetana (1, CNC); Tillimook Co.: 1 mi S Hebo, 28.VII.1979, J.M. & B.A. Campbell (1, CNC); **Washington:** Clallam Co.: 10 mi S Sequim, 12.V.1968, Smetana and Campbell (3, CNC); 5 mi W Forks, 14.V.1968, Smetana and Campbell (3, CNC); 6.5 mi N Sappho, 16.VII.1978, 365 m, L&N. Herman (1, CNC); 7 mi S Port Angeles, Sphagnum moss at water's edge, 640 m, 14.VII.1975, A. Newton & M. Thayer (2, CNC); same except: 11.VIII.1979, J.M. & B.A. Campbell (4, CNC); 5 mi N Elwah Ranger Station, sifting moss and leaf litter along small stream, 12.VIII.1979, J.M. & B.A. Campbell (1, CNC); Jefferson Co.: Hoh Rainforest Ranger Station, 13.V.1968, Campbell and Smetana (4, CNC); Pierce Co.: Mount Rainier National Park, end of West Line Road, 3.VIII.1973, 1127 m, J.M. & B.A. Campbell (11, CNC); Mount Rainier National Park, Larrupin Falls, 1097 m, 3.VIII.1979, J.M. & B.A. Campbell (2, CNC); Mount Rainier National Park, Nisqually River, 1219 m, 16.V.1968, Campbell and Smetana (4, CNC); Mount Rainier National

Park, Tahoma Creek, 730 m, 10.VII.1973, beaver ponds on creek, treading moss and grassy vegetation, A. & D. Smetana (9, CNC); Mount Rainier National Park, Van Trump Park Trail, 1645 m, 4.VIII.1979, J.M. & B.A. Campbell (1, CNC); Skamania Co.: Mount St. Helens, Spirit Lake, Bear Creek, 975 m, 6.VII.1974, A. & D. Smetana (1, CNC); Whatcom Co.: Mount Baker National Forest, Bagley Creek nr. Silver Creek Campground, 10.VII.1974, 609 m, A. & D. Smetana (1, CNC).

Diagnosis. *Iratiquedius seriatus* can be distinguished from all other *Iratiquedius* except *I. uncifer* by a combination of: pronotum missing microsculpture on at least parts of the pronotum; elytra with serial punctation. From *I. uncifer*, it can be distinguished either by the rounded apices of the ventral paired sclerites of the internal sac, or the evenly convex disc of female tergite X.

Redescription. Measurements ♂ (n = 5): HW/HL 1.06–1.11; PW/PL 1.00–1.03; EW/EL 1.22–1.26; ESut/PL 0.76–0.81; PW/HW 1.03–1.06; forebody length 2.3–2.6 mm.

Measurements ♀ (n = 5): HW/HL 1.07–1.10; PW/PL 1.01–1.04; EW/EL 1.22–1.27; ESut/PL 0.82–0.86; PW/HW 1.00–1.06; forebody length 2.4–2.9 mm.

Head dark brown; pronotum dark reddish brown, with sides often paler, red to reddish orange, some individuals with pronotum entirely pale reddish orange; elytra with metallic blue to greenish blue reflection, base, sides and apices often non-metallic, pale red to reddish orange; antennae yellowish brown, segments generally becoming darker toward the apex, segments usually with apices darker, antennomeres 6–11 often entirely dark brown; maxillary and labial palpi usually dark brown, sometimes brownish yellow with apical segment darker; legs brownish yellow, all femora, tarsi and metacoxae dark brown; abdominal tergites dark brown, sternites with broadly pale apices.

Head slightly transverse, appearing orbicular, temples extremely short, following outline of eye to neck; disc of head with sparse transverse waves, becoming vague meshes in places, frons with similar microsculpture but twice as dense; posterior frontal puncture located at posterior third of eye; interocular punctures absent; labrum short, transverse, forming two lobes; right mandible with single, simple tooth (Fig. 3D); area between anterior frontal punctures with Y-shaped impression; antennomeres 1–4 or 1–5 distinctly elongate, 6 and 7 subquadrate, 8–10 subquadrate to transverse; pronotum roughly shield-shaped to subparallel-sided, about as long as wide to scarcely wider than long; disc with variable microsculpture that is always broken or missing on at least some parts, or disc entirely without microsculpture; microsculpture when present consisting of transverse waves, often becoming meshes on anterior angles; elytra moderately transverse, slightly to markedly dilated at apex, slightly longer at suture relative to pronotum in females; disc with only serial rows of macropunctures in sutural, two discal, and one lateral row, disc without microsculpture; epipleuron with fine, evenly distributed setae; abdominal tergites III–V with slight basal impression, tergites III–VII with discrete patches of sparse, golden setae in a larger basal pair and smaller pair posterolaterad of basal pair, patches often blending together, golden setae often appearing brownish if specimen is greasy or wet; punctation of tergites sparse, generally becoming less dense toward apex and middle of disc, tergite VI–VIII very sparsely punctate in apical half, punctures separated by many times their diameter; tergites with dense microsculpture of transverse waves; sternites without patches of golden setae.

Male. Sternite VIII with distinct, moderately deep and rounded emargination; tergite X triangular to elongate triangular, with apical row of setae on or slightly removed from the margin; sternite IX overall moderately narrow to strongly dilated at midlength, with short to moderately long asymmetrical basal part and wide, with moderately deep to shallow emargination; median lobe without teeth, in ventral view with expanded subapical part delineated by a pair of marginal ridges, narrowing to rounded apex that is obtuse to acute, with pair of inner ridges (Fig. 7A, B); median lobe in lateral view strongly projected ventrad, slender to broadly triangular, ventral face evenly arcuate or with distinct bulges, apex sharp and narrow (Fig. 7D, E); internal sac with paired ventral sclerites, shape most apparent when everted, in situ with only apices showing, apices narrow and rounded, narrow part variable in length and curvature, expanded to wide rounded basal part (Fig. 7H, I); paramere about as long or slightly longer than median lobe, stout, subparallel to slightly converging apicad, with slightly to markedly emarginate, rounded apex, peg setae arranged in pair of longitudinal, slightly curved fields (Fig. 7L, M).

Female. Tergite X elongate triangular, with apex nearly truncate and subrectangular to narrowly rounded, disc evenly convex, with row of marginal setae (Fig. 9D).

Distribution. Canada: BC. **United States:** CA, OR, WA.

Bionomics. This species is strongly associated with water-soaked moss, especially growing along waterfalls and small, fast flowing creeks. Other specimens were collected in moss and other debris along the margins of forested marshes. *Iratiquedius seriatus* is known from a wide range of elevations ranging from near sea level (Stanley Park, BC) to 1828 m.

Comments. Within *I. seriatus*, there is some variation in the length and curvature of the narrow, rounded end of the ventral paired sclerites within the internal sac (Fig. 7H–I), which seems to be consistent within a collecting event. The species is also unusually variable in the microsculpture of the pronotum, and shapes of male tergite X, sternite IX and the median lobe. Sequencing of additional CO1 barcodes is underway to establish whether molecular clusters correspond with this variation. With the barcode data available thus far (including two full length), a single OTU was identified by the cluster analysis, with 2.29% within-cluster variation (Fig. 10). This OTU cluster also contained a half-length sequence of *I. uncifer* and a subcluster of entirely *I. seriatus*, with little divergence between the two. The paramere may be distinctly emarginate in some individuals (Fig. 7M) but this is variable among co-collected specimens and is considered to be intraspecific variation.

***Iratiquedius uncifer* sp. nov.**

https://zoobank.org/1777598B-4305-47ED-9485-B6F273A87720

Figs 7C, F, G, J, K, N, 9E, 11C (map)

Quedius (*Raphirus*) *seriatus*: Smetana 1971 (partial misidentification).

Type locality. Bear Creek (~4.5 km north of Dedrick), ~19.3 km north of Junction City, Trinity County, California, United States.

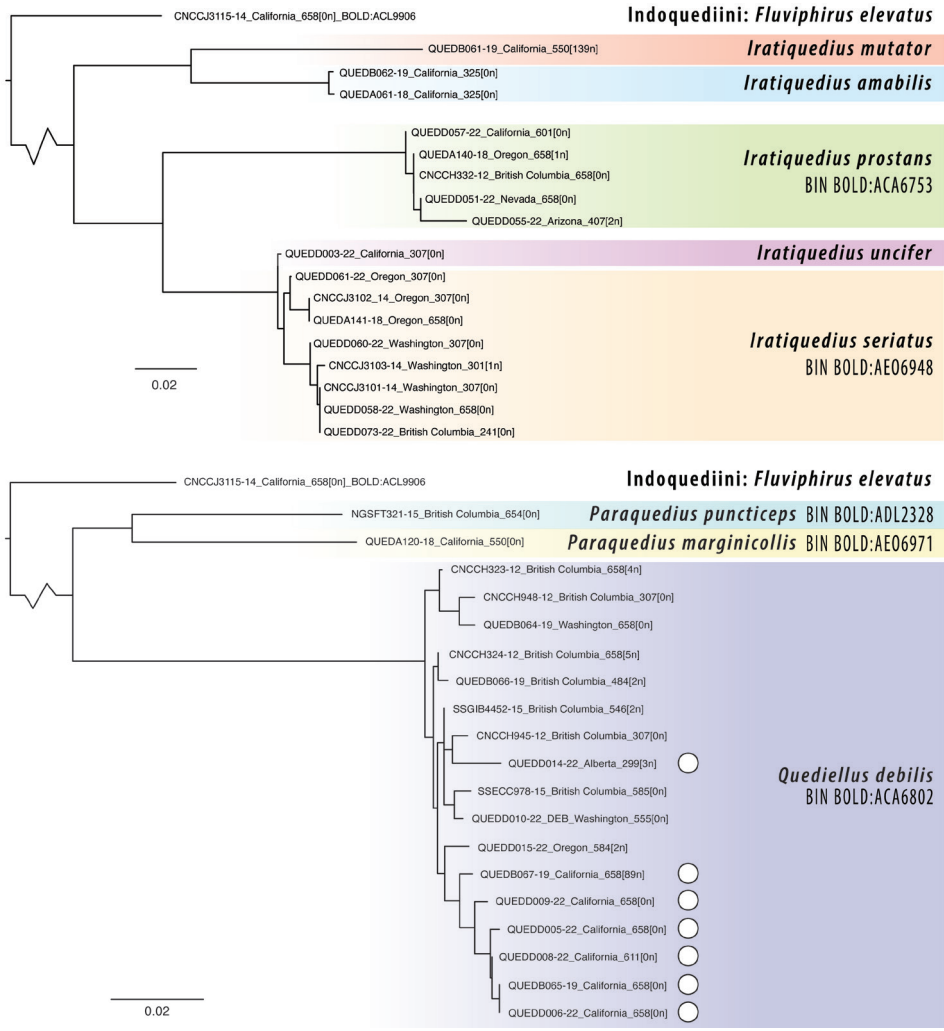

Figure 10. Neighbor-joining trees of CO1 barcode sequences for species of *Iratiquedius, Paraquedius*, and *Quediellus*, calculated under the Kimura-2 model for pairwise distance. White circles indicate macropterous 'debilis' morphotypes of *Q. debilis*, all other *Q. debilis* are of brachypterous 'nanulus' morphotypes. Scale bar equivalent to 2% divergence. Sequence length, including number of ambiguous base pairs (N's), is given at the end of each sample name.

Type material. ***Holotype*** **(male, CNC):** 12 mi N Junction City, Bear Creek, 3110', 13.VII.1979, J.M. & B.A. Campbell [printed label] / CNC1014441 [identifier] / HOLOTYPE *Iratiquedius uncifer* Brunke sp. nov., des. Brunke 2022 [red printed label] ***Paratypes*** **(69, CNC). United States: California:** Humboldt Co.: Hydesville, VI.1901, Van Dyke (1 female, CNC); Sonoma Co.: Duncans Mills, 18.VII.1908, F.E. Blaisdell (1 female, CNC); Tehama Co.: 8 mi N post pile camp, 30.VIII.1960, R.O. Schuster (2 females, CNC); Trinity Co.: 10 mi N Junction City [possibly near Ripstein

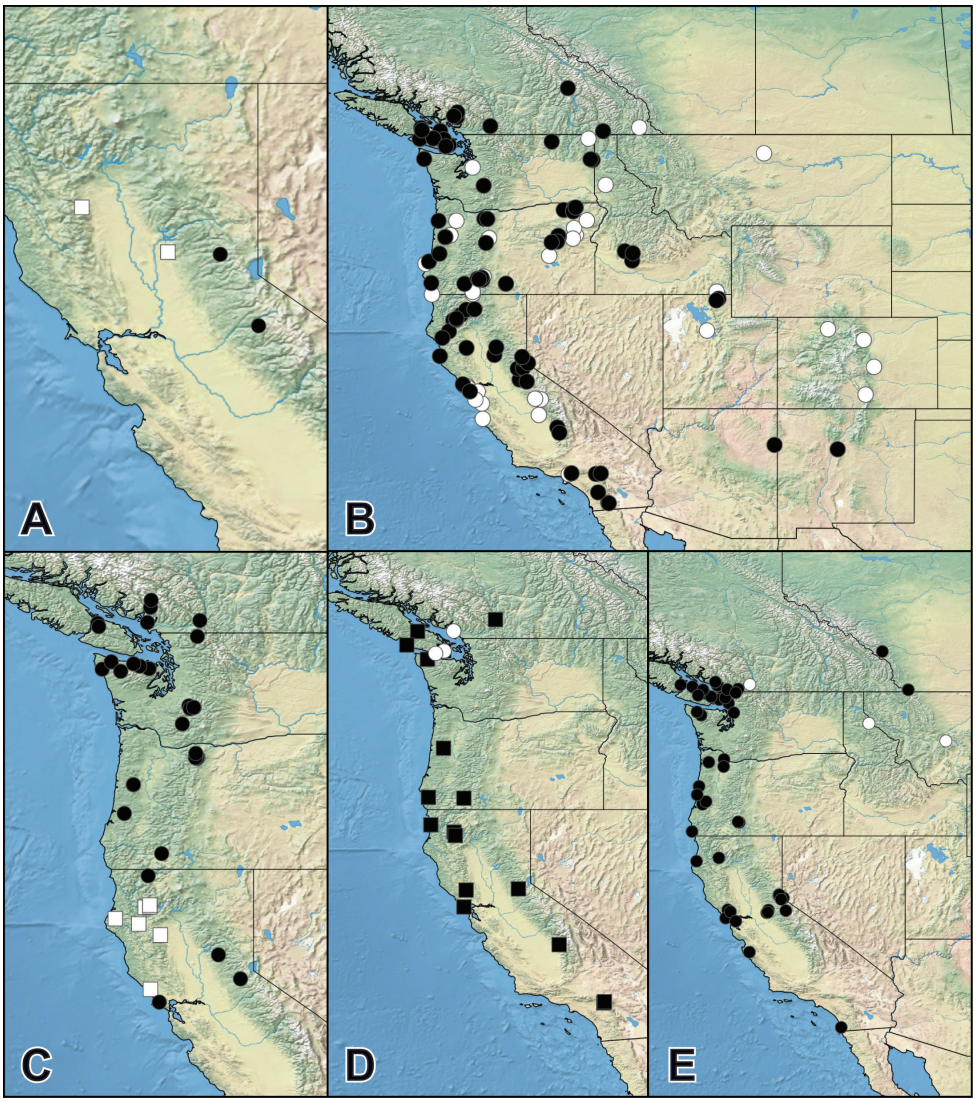

Figure 11. Distributions of **A** *Iratiquedius amabilis* (Smetana) (circles), *I. mutator* (Smetana) (squares) **B** *I. prostans* (Horn) (black – specimens examined, white – literature records) **C** *I. seriatus* (Horn) (circles), *I. uncifer* sp. nov. (squares) **D** *Paraquedius puncticeps* (Horn) (circles), *P. marginicollis* sp. nov. (squares) **E** *Quediellus debilis* (Horn) (circles) (black – specimens examined, white – literature records).

Campground], 762 m, 10.VII.1972, J.M. & B.A. Campbell (11, CNC); 12 mi N Junction City, Bear Creek, 1036 m, 13.VII.1979, J.M. & B.A. Campbell (34, CNC); 16 mi N Junctional City, Upper Canyon Creek Meadows, 1463 m, 13.VII.1979, J.M. & B.A. Campbell (2, CNC); 4 mi W Forest Glen, 9.VII.1979, J.M. & B.A. Campbell (19, CNC).

All specimens with: PARATYPE *Iratiquedius uncifer* Brunke sp. nov., des. Brunke 2022 [yellow printed label].

Etymology. The species epithet refers to the diagnostic hooked apex of the ventral paired sclerites of the internal sac.

Diagnosis. *Iratiquedius uncifer* can be distinguished from all other *Iratiquedius* except *I. seriatus* by a combination of: pronotum entirely without microsculpture; elytra with serial punctation (Fig. 2F). From *I. seriatus*, it can be distinguished either by the sharp, hooked apices of the ventral paired sclerites of the internal sac, or the distinctly impressed disc of female tergite X.

Description. Measurements ♂ (*n* = 5): HW/HL 1.07–1.11; PW/PL 1.01–1.08; EW/EL 1.17–1.32; ESut/PL 0.76–0.93; PW/HW 1.01–1.07; forebody length 2.2–2.4 mm.

Measurements ♀ (*n* = 5): HW/HL 1.06–1.10; PW/PL 1.03–1.08; EW/EL 1.19–1.29; ESut/PL 0.74–0.87; PW/HW 1.01–1.06; forebody length 2.2–2.6 mm.

Extremely similar to *I. seriatus* and overlapping in most characters except: specimens of *I. uncifer* on average smaller, more slender, most examined specimens with bright orange-red pronotum and greenish elytra; pronotum entirely without microsculpture, at most with a few fragments of lines around the punctures; median lobe in ventral view with apical ridge (Fig. 7C); median lobe in lateral view less projected ventrad (Fig. 7F, G); internal sac with ventral paired sclerites sinuate, broad at base, strongly converging toward narrow, hooked apex (Fig. 7J, K); paramere with emargination smaller or absent, peg setae fields more truncate at base (Fig. 7N); female tergite X with long oval impression on disc occupying about half of its length (Fig. 9E).

Distribution. United States: CA.

This species is currently known only from a cluster of localities in the Klamath Mountains and Coast Ranges of California.

Bionomics. Nothing specific is known about this species' preferred microhabitat but based on the locality data, it probably lives close to the edge of streams and springs. The specimens from Trinity County were co-collected with *I. prostans* and *Paraquedius marginicollis*, indicating a very wet microhabitat along the edge of running water.

Comments. Based on the material at hand, *I. uncifer* has yet to be collected together with *I. seriatus*. More collecting is needed in California to determine whether these two species are sympatric and if so, whether they occupy different microhabitats. A few females from the material originally examined by Smetana (1971) were found to belong to *I. uncifer*. This species was likely overlooked by Smetana (1971) due to the large amount of external variation in *I. seriatus* and *I. uncifer*, in addition to the fact that morphology of female tergite X was not yet routinely examined. The single half-length barcode sequence of this species was scarcely divergent from all available sequences of *I. seriatus* (Fig. 10) and it is not clear whether these two species will be reliably diagnosed using CO1 barcodes given further sampling. However, they are easily distinguished using the morphological features provided under Diagnosis.

***Paraquedius* Casey, 1915 stat. res.**
Figs 2G, H, 5A, B, 8A–J, 9F–G

Paraquedius Casey, 1915: 397, 400.
Quedius (*Paraquedius*): Leng 1920; Hatch 1957 (characters); Smetana 1971 (redescription); Solodovnikov 2006 (phylogeny); Brunke 2016 (phylogeny); Brunke et al. 2019 (phylogeny), 2021 (phylogeny, non–*Quedius*, to be re-instated as genus).

Type species. *Quedius puncticeps* Horn, 1878.

Diagnosis. *Paraquedius* is easily recognized within Quediini by a combination of the dark metallic blue/green reflections on the forebody, the punctate head and punctate scutellum. Within the Nearctic Region, *Paraquedius* is the only genus of Quediini with the disc of the head evenly punctate, at least on the posterior half. Worldwide, *Paraquedius* is superficially similar to the members of 'Clade L' of Brunke et al. (2021) (the Oriental and Palaearctic Multipunctatus and Intricatus groups of *Quedius* (*Raphirus*)), which are also metallic blue or green and have extensive head punctation. However, the latter have an impunctate scutellum, larger eyes and shorter appendages. *Paraquedius* is also superficially similar in habitus to members of the West Palaearctic clade (part of 'Clade B', Brunke et al. 2021) that consists of *Quedius riparius* and its close relatives. However, in *Paraquedius* the head is evenly punctate on the posterior half and the scutellum is punctate.

Redescription. Medium sized rove beetles, with metallic blue to greenish forebody and long appendages (Fig. 2G, H). With the character states of Quediini (see Brunke et al. 2021) and the following: antennomere 3 longer than 2, with dense but not tomentose setae; all antennomeres longer than wide; head with eyes large, slightly more than twice as long as temples, convex, bulging from lateral head outline, subparallel and with inner margin well separated from suprantennal ridge (Fig. 5A, B); antennal insertions distant from inner margin of eye, separated by about 1.5 times the width of antennal sclerite (Fig. 5A, B); frons well developed anterolaterad of antennal insertions (Fig. 5A, B); head chaetotaxy obscured by the presence of many setae, though with clearly present anterior and posterior frontal punctures and frontal area glabrous, with interocular setae absent, genal puncture absent; labrum notched medially, creating two lobes; apical maxillary and labial palpi fusiform and glabrous, penultimate maxillary palpomere setose, some setae quite long, extending to about half length of apical maxillary palpomere; infraorbital ridge complete to mandibles; gular sutures converging towards neck and narrowly spaced posteriad; mandibles with dorsal lateral groove; right mandible with single bifid proximal tooth; pronotum subquadrate; hypomeron slightly inflexed, partly visible in lateral view; with only single large lateral puncture; dorsal row of pronotum with three to five punctures; sublateral row not reaching level of large lateral puncture; basisternum with pair of macrosetae though surrounded by many shorter setae, with longitudinal ridge on apical half; elytron with subbasal ridge complete, forming scutellar collar; scutellum punctate; row of humeral spines reduced to short row of darker, shorter regular setae; disc of elytra with even punctation, without microsculpture; foretibia with lateral spines and apical spurs; metatarsomeres with disc setose; metatibia spinose with at least three spines on outer face; abdominal tergite

I with prototergal glands weakly developed as shallow impressions, impressions surrounded by some setae; abdominal tergites without impressed, glabrous basal areas; abdominal sternite III with basal transverse carina forming obtuse angle at middle, not produced; abdominal sternite VII unmodified; abdominal sternite VIII with distinct median emargination but emargination lacking membranous extension; aedeagus with well-developed paramere bearing peg setae (Fig. 8E, F, I, J).

Distribution. *Paraquedius* is endemic to western North America, from coastal British Columbia, along the Coast, Cascade and Sierra Nevada Ranges, and as far south as the San Bernardino Mountains of California (Smetana 1981).

Bionomics. Most specimens were taken in water-soaked moss or algae-covered rocks at waterfalls, fast streams or freshwater outflows to ocean beaches. A few specimens were collected near a stream under stones on muddy ground covered in algae (Smetana 1971).

Comments. The two available specimens from the San Bernardino Mountains were females and males should be sought to determine whether there are additional species present. Given that some specimens were collected at cold seeps amongst rather dry, scrubby forest, this genus may eventually be found further south in California, and potentially in the forested mountain valleys of Baja California and Baja California Sur, Mexico.

Key to the species of *Paraquedius*

1 Head with glabrous area extended posteriad to about middle of eyes (Fig. 5A); antennomere 1 entirely dark (Fig. 5A); pronotum and humeral area entirely dark (Fig. 2G); median lobe in lateral view strongly convergent to narrow apex (Fig. 8H); paramere elongate with apical part gradually narrowed (Fig. 8I, J); female tergite X with short, acute apex (Fig. 9F) .... ***P. puncticeps* (Horn)**

– Head with glabrous area not extended posteriad to middle of eyes (Fig. 5B); antennomere 1 with pale base (Fig. 5B); margins of pronotum and at least extreme base of elytra paler, orange-red (Fig. 2H); median lobe in lateral view broad, narrowed only at the very apex (Fig. 8C, D); paramere spoon-shaped (Fig. 8E, F); female tergite X with truncate apex (Fig. 9G)..... ..... ***P. marginicollis* sp. nov.**

***Paraquedius puncticeps* Horn, 1878, comb. res.**
BIN BOLD:ADL2328
Figs 2G, 5A, 8G–J, 9F, 11D (map)

Quedius puncticeps Horn, 1878: 156, 166.
Paraquedius puncticeps; Casey 1915 (redescription).
Quedius (*Paraquedius*) *puncticeps*; Smetana 1971 (redescription, partial misidentification of *P. marginicollis*).

Type locality. Vancouver, British Columbia, Canada.

Type material. ***Lectotype*** **(male, MCZ – Horn coll.):** ‘Vanc.’ [= Vancouver] [printed label] / LectoTYPE 3048 [red printed label] / Q. puncticeps H. [handwritten label] / MCZ00732196 [identifier] / LECTOTYPE *Quedius puncticeps* det. A. Brunke 2022 [red printed label]

Paralectotype **(male, MCZ – LeConte coll.):** ‘Van.’ [printed label] / [male symbol, printed] / Type 7273 [red printed label] / Q. puncticeps H. [handwritten label] / PARALECTOTYPE *Quedius puncticeps* det. A. Brunke 2022 [yellow printed label].

Paralectotype **(female, MCZ – LeConte coll.):** ‘Van.’ [= Vancouver] [printed label] / MCZ00732195 [identifier] / PARALECTOTYPE *Quedius puncticeps* det. A. Brunke 2022 [yellow printed label].

Non-type material. Canada: British Columbia: Vancouver Island: Goldstream Park, 5 mi N Victoria, 27.V.1968, Campbell and Smetana (2 females, CNC); Goldstream Park, 27.V.1968, A. Smetana (1 female, CNC); near Mount Finlayson Trail, Malahat, Goldstream Provincial Park, moss on rock, 11.VII.1979, I.M. Smith (1 male, 2 females, CNC); ~2.2 km W Shirley, on beach, algae-covered sandstone in freshwater outflow, 18.X.2018, iNaturalist observation 18374642 by user thomasbarbin. **United States: Washington:** ‘W.T.’ [= Washington Territory], 1 male (MCZ).

Diagnosis. *Paraquedius puncticeps* is most easily distinguished from the only other species of the genus by the entirely dark first antennomere and pronotum. For other differences see the key above.

Redescription. Measurements ♂ (*n* = 4): HW/HL 1.06–1.07; PW/PL 1.01–1.04; EW/EL 1.09–1.18; ESut/PL 0.88–0.91; PW/HW 1.03–1.07; forebody length 4.2–4.5 mm.

Measurements ♀ (*n* = 5): HW/HL 1.05–1.13; PW/PL 1.05–1.08; EW/EL 1.12–1.21; ESut/PL 0.88–0.94; PW/HW 1.00–1.06; forebody length 4.3–4.9 mm.

Head, pronotum and elytra dark brown, slight metallic bronze-green reflection (Fig. 2G); antennae dark brown, antennomere 1 entirely dark, base of antennomere 2 paler, red to dark red (Fig. 5A); palpi dark brown; legs dark brown with paler, brownish yellow femora, tarsi often paler than tibiae; abdomen dark brown with narrowly to broadly paler apices.

Head slightly transverse, temples short and rather strongly rounded to neck, eyes bulging and distinctly protruding from lateral head margin; frons with central glabrous area extended posteriad to at least middle of eyes (Fig. 5A); disc of head with microsculpture of sparse, superficial transverse waves, often changing direction and forming irregular meshes especially on frons; head with moderately deep, circular impressions mediad of anterior frontal punctures (Fig. 5A); labrum short, transverse, forming two lobes; antennomeres 1–9 elongate, becoming shorter toward apex of antennae, antennomere 10 subquadrate; pronotum slightly transverse, roughly shield-shaped, varying from flattened with apex broader than neck, to distinctly convex with apex about as wide as neck; pronotum with microsculpture as on head, becoming meshed in places, especially on anterior angles; elytra moderately to distinctly transverse, appearing elongate, distinctly dilated at apex; disc without microsculpture, with sparse, moderately fine and even punctation, most punctures separated by 1.5–2.0 times the width of a puncture, disc weakly convex and uneven, most specimens with only weak discal

impressions; with fully developed hind wings; abdominal tergites III–V with basal impression, tergites III–VI with paired, sparse lateral whorls of pale setae (visibility depends on lighting or condition of specimen); tergites with moderately sparse microsculpture of transverse waves, lines separated by at least their widths, tergites with very sparse punctation, punctures separated by many times their diameter.

Male with sternite VIII with moderately deep emargination, slightly less than twice as wide as deep; tergite X triangular, with narrow but broadly rounded apex; sternite IX rather stout, with asymmetrical base, rounded sides and narrow, non-emarginate apex; median lobe of aedeagus in ventral view strongly converging to acute apex, with slightly delimited subapical part (Fig. 8G); median lobe in lateral view strongly converging to elongate and curved apical part, apex narrow and slightly bent ventrad (Fig. 8H); paramere slightly longer than median lobe, elongate and sub-parallel, with slight middle and subapical expansions or evenly, gradually expanded to subapex, apex slightly emarginate and broad to entire and rounded, with numerous peg setae arranged into long median field that is narrowed basad (Fig. 8I, J). Female with tergite X elongate triangular, with short acute apex (Fig. 9F).

Distribution. Canada: BC. **United States:** WA.

Thus far, *P. puncticeps* is known only from the Vancouver area and Vancouver Island, British Columbia, Canada, and from one male collected somewhere in Washington. More collecting in its preferred microhabitats is needed to determine the full distribution of *P. puncticeps*.

Bionomics. Specimens have been collected in moss on rocks near a stream, under stones on muddy ground covered in algae (Smetana 1971) and on algae-covered sandstone in a freshwater outflow to the ocean (iNaturalist observation: https://www.inaturalist.org/observations/18374642).

Comments. It is unusual in Staphylinidae for sister species to be sympatric but the morphological differences between the two known species of *Paraquedius* are so great that they may have diverged allopatrically long ago, with populations coming into secondary contact since then. Indeed, their CO1 barcodes are 8.79% different (Fig. 10).

Paraquedius marginicollis sp. nov.

https://zoobank.org/75E79E2A-CDE5-4FA2-A6F6-9BD36A2CAE1B
BIN BOLD:AEO6971
Figs 2H, 5B, 8A–F, 9G, 11D (map)

Quedius (*Paraquedius*) *puncticeps* Horn (misidentification): Smetana 1981 (distribution records); Brunke et al. 2016, 2019, 2021 (phylogeny).

Type locality. 5.4 miles southeast of Seiad Valley [probably at O'Neil Creek], Siskiyou County, California, United States.

Type material. ***Holotype*** **(male, CNC):** Siskiyou County, 5.4 mi SE Seiad Valley, 457 m, 4.VII.1976, #1272, L. & N. Herman [printed label] / CNC977001 [identifier] /

HOLOTYPE *Paraquedius marginicollis* Brunke, des A. Brunke 2022 [red printed label]. ***Paratypes* (19, CNC, FMNH, UTCI, MCZ).** Same data as holotype (2 females, CNC).

Canada: British Columbia: Vancouver Island: 'V.I' [no data] (1 female, CNC); Darling River, Pacific Rim National Park, 13.VII.1975, J.M. Campbell & B.A. Campbell (1 male, CNC); 10 mi E [Port] Alberni, MacMillan Provincial Park, 26.V.1968, Campbell and Smetana (1 female, CNC); Lower Mainland: Hells Gate, rest stop approx. 2 km S on Hwy 1, mountain stream, under weeds, 17.IX.1982, B & J. Carr (1 male, CNC).

United States: California: 'Cal.' (1 female, MCZ); El Dorado Co.: 0.7 mi E Pacific House, 38.758, -120.493, 1190 m, ex. screening flume, 18.VI.1989, A.R. Hardy & D. Carlson (1 male, UTCI); Humboldt Co.: Prairie Creek Redwoods State Park, ca. 2 mi S Fern Canyon, base of Gold Bluffs, 41.3748, -124.07, 10 m, scrubby coastal forest, on algae and vertical rock face at seep, 18.VI.2006, A. Newton & M. Thayer (1 female, FMNH); Marin Co.: Samuel P. Taylor State Park, 4.V.1968, Campbell and Smetana (1, CNC); Napa Co.: 10.1 mi N Calistoga, 579 m, flood debris, forest stream, 21.V.1976, A. Newton & M. Thayer (1 male, CNC); San Bernardino Co.: 1 mi SW [W] Mountain Home Village, 15.III.1983, A. Smetana (1 female, CNC); Camp Angelus [= Angelus Oaks], 1.VII.1970, K. Stephan (1 female, CNC); Trinity Co.: Upper Canyon Creek Meadows, 16 mi N Junction City, 1463 m, 13–19.VII.1979, J.M. & B.A. Campbell (1 female, CNC); Tulare Co.: Ash Mountain Power Station [Sequoia National Park], 23.XI.1982, J.A. Halstead (1, CNC); **Oregon:** Benton Co.: Mary's Peak, 1158 m, 27.VII.1979, J.M. & B.A. Campbell (1 female, CNC); Curry Co.: Agness Rd., crossing at Wake Up Rilea Creek, under stones and in little pools of water along shady, cascading creek, 10.VIII.1978, B.F. & J.L. Carr (1 male, CNC); Jackson Co.: Highway 140, Little Butte Creek, 23.VI.1974, A. & D. Smetana (1 male, CNC); **Washington:** Clallam Co.: 6.5 miles N Sappho, 366 m, 16.VII.1978, #1669, L. & N. Herman (1 male, CNC.

All paratypes with: PARATYPE *Paraquedius marginicollis* Brunke, des A. Brunke 2022 [yellow printed label]

Etymology. The species epithet refers to the diagnostic pale margin of the pronotum.

Diagnosis. *Paraquedius marginicollis* is most easily distinguished from the only other species of the genus by the pale base of antennomere 1 and margins of the pronotum. For other differences see the key above.

Description. Measurements ♂ (*n* = 5): HW/HL 1.04–1.09; PW/PL 1.01–1.08; EW/EL 1.13–1.17; ESut/PL 0.83–0.88; PW/HW 0.99–1.07; forebody length 4.0–4.3 mm.

Measurements ♀ (*n* = 5): HW/HL 1.06–1.10; PW/PL 1.01–1.08; EW/EL 1.11–1.17; ESut/PL 0.86–0.89; PW/HW 1.01–1.08; forebody length 4.3–4.5 mm.

Similar to *P. puncticeps* and differing only in the following: antennomeres 1 and 2 with pale base (Fig. 5B); marginal area of pronotum and at least extreme base of elytra, suture and sometimes scutellar area, paler (Fig. 2H); maxillary palpi usually slightly paler; head and pronotum with microsculpture more distinct; frons with central glabrous area not reaching posteriad to middle of eyes (Fig. 5B); frons with pair of impressions shallower and usually more linear, forming a border around raised central area (Fig. 5B); elytra with punctures slightly finer, disc always strongly uneven, with

metallic greenish blue reflection; abdominal tergites with central, sparsely punctate to impunctate, raised areas, in addition to usual basal impressions; whorls of pale setae on tergites appearing more distinct from surrounding setae; male with emargination of sternite VIII slightly shallower, about twice as wide as deep; tergite X more slender, with narrower apex and setae more restricted to apical area; sternite IX with apex broadly, shallowly emarginate; median lobe of aedeagus in ventral view subparallel-sided, with truncate or broadly rounded apex (Fig. 8A, B); median lobe in lateral view with short apical area that is acute to obtusely pointed (Fig. 8C, D); paramere varying from slightly longer to slightly shorter than median lobe, spoon-shaped to lancet-shaped (Fig. 8E, F), peg setae forming long, oval-shaped median field (Fig. 8E, F). Female with tergite X shorter, with apex broader and truncate (Fig. 9G).

Distribution. Canada: BC. **United States:** CA, OR, WA.

Bionomics. Specimens with microhabitat data were collected at a variety of elevations (near sea-level to 1463 m), on or under surfaces (under rocks, on vertical rock-face), in association with running water, including mountain streams, vertical seeps and waterfalls. The specimen from flood debris was likely washed out of its normal microhabitat by heavy rains.

Comments. Initially, it was thought that the specimen from Clallam County, Washington represented yet another species, as the paramere is remarkably lancet-like (Fig. 8E) and longer than the median lobe, while most specimens have a spoon-shaped paramere that is shorter than the median lobe. With further dissections, a few intermediate forms were found, though this specimen still represents the extreme of variation.

Quediellus Casey, 1915, stat. res.

Figs 5C, D, 8K–Q, 9H, I

Quediellus Casey, 1915: 398, 402; Smetana 1971 (as synonym of *Quedius* (*Raphirus*)), Brunke et al. 2021 (phylogeny, isolated position, non-*Raphirus*, to be reinstated as genus).

Type species. *Quedius debilis* Horn, 1878.

Diagnosis. *Quediellus*, in the restricted sense used here, can be recognized within Quediini by a combination of: head with genal and interocular punctures absent; pronotum without extra punctures between dorsal and sublateral rows, sublateral rows not extended posteriad of single large lateral puncture (but sometimes at same level); prosternum without trace of longitudinal carina; scutellum impunctate; elytra with punctures not arranged in distinct rows, spaces between with distinct meshed microsculpture (Fig. 5D). *Quediellus* and *Quedionuchus* are the only genera of Quediini with meshed (scale-like) microsculpture on the elytra (Fig. 5D, E), while other lineages may have granulose microsculpture composed of micropunctures or microsetae (Fig. 5F), superficially giving a similar dull appearance at low magnification. *Quediellus* differs from *Quedionuchus* by the irregularly scattered (not rows) or evenly distributed elytral

punctures (Fig. 5D versus Fig. 5E) and complete infraorbital ridge, running from the neck to the base of the mandibles under the eye.

Quediellus shares plesiomorphic, simple head chaetotaxy (though the basal puncture is often doubled, e.g., Fig. 5C) with members of the mostly Palaearctic subgenus *Quedius* (*Raphirus*) (sensu Brunke et al. 2021), with which it was long considered to be synonymous. However, all *Quedius* (*Raphirus*) differ by the lack of meshed microsculpture on the elytra and those with a dull reflection between the punctures (e.g., *Q. cincticollis* Kraatz, *Q. fumatus* (Stephens), the members of clade 'X2' of Brunke et al. 2021 (*Q. lateralis* (Gravenhorst) and its relatives)) have micropunctures rather than meshes, much denser elytral punctation and most have an, at least partly, carinate prosternum.

Redescription. Small and slender, to medium-sized and fusiform rove beetles, often with pale yellow markings on apex, humerus and sides of elytra (Fig. 12). With the character states of Quediini (see Brunke et al. 2021) and the following: antennomere 3 longer than 2, without dense setae; head with eyes large, much more than twice as long as temples, convex, bulging from lateral head outline, weakly convergent anteriad and with inner margin well separated from suprantennal ridge (Fig. 5C); antennal insertions close to inner margin of eye, separated by about the width of antennal sclerite (Fig. 5C); frons weakly developed anterolaterad of antennal insertions; with single or doubled basal puncture; interocular, parocular and genal punctures absent; labrum notched medially, creating two short lobes; apical maxillary and labial palpi fusiform and glabrous; infraorbital ridge complete to mandibles; gular sutures converging towards neck and narrowly spaced posteriad; mandibles with dorsal lateral groove; right mandible with single, simple tooth (Fig. 5C); pronotum subquadrate; hypomeron strongly inflexed, not visible in lateral view; with single large lateral puncture; dorsal row of pronotum with three punctures; sublateral row not reaching level of large lateral puncture; basisternum with pair of distinct macrosetae, without trace of longitudinal carina; elytron with subbasal ridge complete, forming scutellar collar; scutellum impunctate; with row of three or four humeral spines; disc of elytra with even punctation, with distinct meshed microsculpture; foretibia with lateral spines and apical spurs; metatarsomeres with disc setose; metatibia spinose with at least three spines on outer face; abdominal tergite I with prototergal glands well developed, with one side surrounded by row of well-developed setae; abdominal tergites without impressed, glabrous basal areas; abdominal sternite III with basal transverse carina forming obtuse angle at middle, not produced; abdominal sternite VII unmodified; abdominal sternite VIII with distinct median emargination; aedeagus with well-developed paramere bearing peg setae (Fig. 8M, N).

Distribution. *Quediellus* is endemic to the western Nearctic, occurring along the western cordilleras from southern British Columbia to southern California on the western side of the continental divide, and known from the Rocky Mountains of Alberta, Idaho and Montana on the eastern side.

Bionomics. Specimens have been collected mainly from sifting leaf litter, rotting wood and moss along streams, in forests and in montane meadow.

Comments. Casey (1915) erected the genus *Quediellus* to unite species belonging to the Debilis and Brunnipennis groups of Smetana (1971), based on an entire labrum. This concept was correctly recognized by Smetana (1971) as erroneous as not only did

he consider these two groups to be distantly related but only *Quedius densiventris* exhibited an entire labrum and only in some individuals. The always bilobed labrum of *Quediellus* is quite transverse in some specimens and sometimes at lower magnification it can be difficult to observe its shape. The type species of *Quediellus*, *Q. debilis*, was assigned to the Debilis group of *Quedius* (*Raphirus*) by Smetana (1971) and has been treated as such ever since. Quite recently (Brunke et al. 2021), the Debilis group (as *Quedius nanulus* (Casey)) was shown to be one of the smaller, phylogenetically isolated lineages of Quediini and quite distantly related to true *Quedius* (*Raphirus*), despite sharing several morphological, though plesiomorphic, character states including the simple head chaetotaxy. In order to achieve monophyly of both *Quedius* and subgenus *Raphirus*, *Quediellus* is here resurrected as a valid genus under a morphological concept that is similar to that given by Smetana (1971) for the Debilis group.

***Quediellus debilis* (Horn, 1878), comb. res.**
BIN BOLD:ACA6802
Figs 5C, D, 8K–Q, 9H, I, 11E (map), 12

Quedius debilis Horn, 1878: 156, 165.
Quediellus debilis; Casey 1915 (redescription).
Quediellus helenae Casey, 1915: 403 syn. nov.
Quediellus humilis Casey, 1915: 403 syn. nov.
Quediellus nanulus Casey, 1915: 402 syn. nov.
Quedius (*Raphirus*) *debilis*; Smetana 1971 (redescription); Brunke et al. 2021 (phylogeny, as *Q. nanulus*).

Type locality. California (unknown locality), United States.

Type material. *Lectotype* (female, MCZ, examined digitally): 'Cala' [white typed label] / Q. debilis H. [handwritten label] / Type 7270 [red label].

The female lectotype of this species is a classic example of the 'debilis' morphotype (see below): a larger specimen with elytra at sides much longer than pronotum at midline, elytra at apex wider than pronotum.

***Quediellus nanulus* Casey**

Type material. *Lectotype* (male, United States National Museum of Natural History, not examined): Lane Co. Or / Casey bequest 1925 / Type USNM 48307 / nanulus Csy.

Smetana (1971) stated that the male lectotype was a typical member of *Q. nanulus* (e.g., short, narrow elytra, small-bodied). Several non-type male specimens from the type locality matching this description and consistent with the 'nanulus' morphotype, were available for study. The aedeagi of these specimens fell within the range of morphological variation considered to belong to a single, variable *Q. debilis*.

***Quediellus helenae* Casey**

Type material. *Holotype* (female, United States National Museum of Natural History, not examined): "Helena Mont." / Casey bequest 1925 / Type USNM 48305 / helenae Csy.

Smetana (1971) stated that the male lectotype was also a typical member of *Q. nanulus*. All available specimens from the Rockies were small-bodied, winged, with palisade fringe and narrow elytra. Subtle differences in the aedeagus were observed between individuals on either side of the continental divide (see Redescription below) but the single available barcode sequence from the east clustered deep within the western sequences of *Q. debilis*.

***Quediellus humilis* Casey**

Type material. *Holotype* (male, United States National Museum of Natural History, not examined): "Cal". / Casey bequest 1925 / Type USNM 48306 / humilis Csy. Smetana (1971) mentioned that this specimen was a small male of *Q. nanulus*. While it was not studied, several small non-type males were examined from northern California that perfectly fit the 'nanulus' morphotype, including some examined by Smetana (1971) himself and identified as *Q. nanulus*.

Non-type material. Canada: Alberta: Marmot Creek, 10 mi SW Kananaskis F.E.S., 15.VIII.1971, 5000', sifting deciduous litter along large stream, J.M. Campbell (1 male, 1 female, CNC); Waterton Lakes N.P., mi 2 of Red Rock Canyon Road, 16.VI.1980, 4400', J.M. Campbell (1 male, 1 female CNC); Waterton Lakes N.P., 1 mi N Pass Creek Bridge, 4500', sifting *Populus* litter in moist deciduous forest, 5.VIII.1976, J.M. Campbell (1 male, 1 female, CNC). **British Columbia:** Greater Vancouver: Stanley Park, 20.V.1989, A. Smetana (2, CNC); same except 28.V.1968, Campbell and Smetana (1, CNC); same except 21.V.1968, Campbell and Smetana (1, CNC); Brunswick, 20.V.1968, Campbell and Smetana (1, CNC); Langley, open oak forest, 10.XII.1979, S. Rahe (2, CNC); Fraser Valley: Mission, berlese sample, 25.VII.1953, W.R.M. Mason (2, CNC); Vancouver Island: Chemainus Lake, mushrooms and rotten fir wood, edge of path, 25.IX.2020, A. Davies (1, CNC); Mesachie Lake, Forest Experiment Station, 1950 m, woody debris from log, 23.VII.1979, I. Smith (2, CNC); Salt Spring Island, Fulford Harbour, Petroglyph, 25.IX.1974, BD Ainscough (2, CNC); Gabriola Island, Gabriola, marsh with sedges, pitfall traps, 30.IX.1994, BF & JL Carr (1, CNC); same except sifting maple litter beside firewood and compost bin, 30.IV.1993 (3, CNC); same except sifting moss in forest near Hoggan Lake, 14.VI.1989 (1, CNC); Englishman River Provincial Park, cedar litter, 10.III.1997, B.D. Ainscough (1, CNC); Yellow Point, Cedar, under rotten log, 18.V.1978, B.D. Ainscough (1, CNC); Lake Cowichan, spring run beside North Shore Road, 1.7 km N town, moss and litter, 7.VI.1979, I. Smith (1, CNC); Stamp Falls [Stamp River] Provincial Park, 8 mi NW Alberni, 26.V.1968,

Campbell and Smetana (2, CNC); Victoria, sifting litter and grass, 28.X.1985, BF & JL Carr (1, CNC).

United States: California: Alpine Co.: 22 mi NE Strawberry, Clark Fork River near Cottonwood Creek, 1767 m, 14.VII.1976, L. & N. Herman (1, CNC); Amador Co.: 4 mi S Jackson, sift oak, maple and alder litter, 3.II.1979, D.S. Chandler (1, FMNH); 1 mi W Pine Grove, 24.VI.1975, A. Newton and M. Thayer (1, CNC); 'Mokel Hill' [= Mokelumne Hill], VII.1925, VanDyke (4, CNC); Alameda Co.: Berkeley, under Umbellifera duff, 23.II.1962, J.F. Lawrence (1, CNC); El Dorado Co.: Lake Tahoe, Taylor Creek at Camp Richardson, 1900 m, 9.VII.1986, A. Smetana (2, CNC); Humboldt Co.: 5 mi N Trinidad, Patricks Point State Park, hemlock/pine/alder litter, 14.VIII.1966, J+S Cornell (1, FMNH); Eureka, VI.1902, H.S. Barber (2, CNC); Marin Co.: Lagunitas Creek, near Tocaloma, 18.III.1983, A. Smetana (5, CNC); Monterey Co.: Jamesburg, Ian Moore (1, CNC); Placer Co.: Meeks Bay, West Lake Blvd, 1917 m, ex. riparian litter, 15.XI.2008, A. Brunke (1, DEBU); Lake Tahoe, Tahoe City, 1950 m, 7.VII.1986, A. Smetana (2, CNC); Tahoe Pines, 3.V.1968, Campbell and Smetana (1, CNC); Tahoe Pines, 1889 m, 10.VIII.1969, A. Smetana (2, CNC); San Diego Co.: San Diego, F.E. Blaisdell (1, CNC); Sonoma Co.: Annadel State Park, Hunter Spring nr. Canyon Trail, 220 m, 26.IV.–17.V.2007, P. Kerr and S. Blank (1, UTCI); Sobre Vista, 24.IV.1910, Van Dyke (1, CNC); Trinity Co.: Upper Canyon Creek Lake, 17mi N Junction City, 1737 m, 12.VII.1979, JM & BA Campbell (6, CNC); Upper Canyon Creek Meadows, 16mi N Junction City, 1463 m, 13–19.VII.1979 (1, CNC); **Nevada:** Douglas Co.: Zephyr Cove, 1900 m, 9.VII.1986, A. Smetana (3, CNC); **Oregon:** Columbia Co.: Oak Island, Sauvies Lake, Columbia River, 5mi N 2mi E Burlington, 30 m, Oregon oak and snowberry duff, 7.X.1972, E.M. Benedict (2, CNC); Curry Co.: 4mi S Pistol River, on US 101 (Mark 342), 60 m, Sitka spruce duff and soil, 12.II.1972, E.M. Benedict (1, CNC); Douglas Co.: 1mi S & 2mi W Ash, 152 m, deciduous Myrtle litter and duff, 11.XII.1971, E.M. Benedict (1, CNC); ~4.5mi E Wells Creek, Ranger Station, Umpqua River, 91 m, oak duff and soil, 11.XII.1971, E.M. Benedict (1, CNC); Klamath Co.: Mares Egg Springs, 1280 m, 20.VII.1979, JM Campbell & J Schuh (4, CNC); same except 25.VI.1974, A. & D. Smetana (1, CNC); 7 mile Creek, west of Forth Klamath, 20.VII.1979, JM Campbell & J Schuh (1, CNC); Lane Co.: Coast Guard Road, Approximately 1mi N Florence, 152 m, moss festoons, 6.V.1972, E.M. Benedict (2, CNC); Lincoln Co.: Eakman [= Ekman] Lake, 5mi E Waldport, 0 m, beach grass, 5.V.1973, E.M. Benedict (2, CNC); Tillamook Co.: Rest area, Wilson River Highway, 0.5mi S & 1mi W Lee's Camp, western red cedar and red alder, 4.XI.1972, E.M. Benedict (2, CNC); Washington Co.: 0.25mi E Sherwood Highway & US-99W, 60 m, rotten hay, barley and dung, 1.I.1972, E.M. Benedict (2, CNC); **Washington:** Jefferson Co.: Olympic National Park, Hoh Ranger Station, 182 m, 13.V.1968, Campbell and Smetana (1, CNC); same except 19.VIII.1979, JM & BA Campbell (4, CNC); San Juan: San Juan Islands, Jones Island, 2.V.1988, J. Bergdahl (2, CNC); San Juan Islands, Matia Island, 28.VIII.1988, J. Bergdahl (2, CNC); San Juan Islands, Flattop Island, 22.I.1988, J. Bergdahl (1, CNC); San Juan Islands, Stewart Island, 18.X.1987, J. Bergdahl (1, CNC); same except 6.VIII.1988 (1, CNC);

Sucia Island, 28.VIII.1988, J. Bergdahl (4, CNC); same except 30.VIII.1988; San Juan Islands, Jones Island, 2.V.1988, J. Bergdahl (3, CNC); San Juan Islands, Clark Island, 27.VIII.1988, J. Bergdahl (1, CNC); Skagit Co.: San Juan Islands, Fidalgo Island, 5.IV.1986, J. Bergdahl (4, CNC); Snohomish Co.: Chase Lake, 15.VIII.1961, W. Suter (2, CNC); Siskiyou Co.: VII, C.V. Riley (2, CNC); Whatcom Co.: Deming, S end Sumas Mt., Reardon property, ANMT site 1275, 95 m, berl., leaf & log litter incl. under *Phlebia* polypores on log, 2nd growth *Pseudotsuga-Thuja-Alnus-Acer macrophyllum* & *circinatum*, 13.XI.2014, A. Newton & M. Thayer (1, FMNH).

Diagnosis. As in generic diagnosis.

Redescription. Measurements ♂ (*n* = 10 (5 macropterous; 5 brachypterous)): HW/HL 1.07–1.17; PW/PL 1.02–1.19; EW/EL 1.08–1.29; ESut/PL 0.54–0.79; PW/HW 1.14–1.27; forebody length 2.3–3.1 mm.

Measurements ♀ (*n* = 10 (5 macropterous; 5 brachypterous)): HW/HL 1.10–1.15; PW/PL 1.04–1.14; EW/EL 1.15–1.36; ESut/PL 0.56–0.82; PW/HW 1.14–1.30; forebody length 2.5–3.2 mm.

Head dark brown, darker than pronotum, which is paler, entirely brown to pale reddish with yellow borders; elytra brownish, often with epipleural area, and lateral and apicolateral parts of disc paler, frequently contrasting yellow; abdomen dark brown, tergites at most narrowly paler at apex; antennae brown, with antennomeres 1–3 paler, yellow-brown or at least bases paler; legs pale, yellow to yellowish brown, tibiae dark brown; palpi yellowish brown to dark brown (Fig. 12).

Head slightly transverse, eyes large, moderately convex and protruding from lateral outline, temples small, about 1/4 to 1/3 of eye length (Fig. 5C); disc of head with sparse microsculpture of transverse waves, spaces between lines greater than width of lines; antennomeres of varying shape depending on morphotype, with 'nanulus' type having 1–3 elongate, 4 quadrate to elongate, 5 or 6–10 transverse and macropterous individuals of the 'debilis' morphotype having 1–5 or 1–6 elongate and 7–10 or 8–10 distinctly transverse; pronotum about as wide as long to moderately transverse, moderately wider than head; disc with microsculpture as on head; elytra moderately to distinctly transverse, markedly variable from scarcely longer at sides than pronotum at middle to moderately longer (1.06–1.21, 'nanulus' morphotype), or distinctly longer than pronotum at middle (1.26–1.41, 'debilis' morphotype) (Fig. 12); disc of elytra with punctures varying from superficial, sparse and widely scattered (nanulus type) to slightly denser and coarser in individuals with the longest elytra (Fig. 12); wings as non-functional stubs or fully developed; abdomen generally sparsely punctate, denser at bases of tergites but variable, with punctation overall denser in 'debilis' morphotype; abdomen with dense, very fine microsculpture of transverse waves; abdominal tergite VII without or with palisade fringe.

Male. Sternite VIII with distinct emargination of variable depth and width; tergite X triangular, with moderately long, narrowly rounded apex; sternite IX varying from slightly expanded to broad at middle, with long, slender asymmetrical basal part and narrow, rounded apex; median lobe in ventral view with acute apex, sides of apex

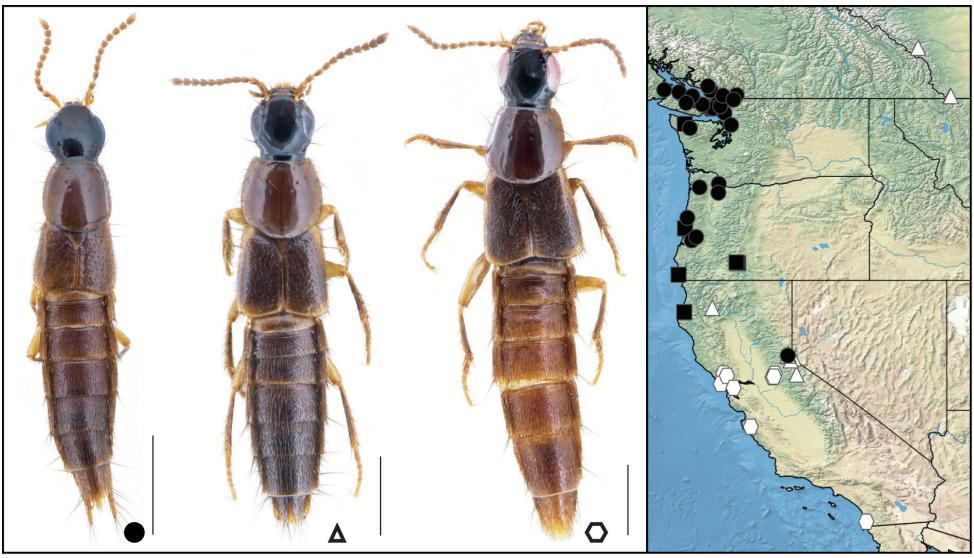

Figure 12. Habitus and distribution of *Quediellus debilis* (Horn) morphotypes: brachypterous, palisade fringe absent (circle), brachypterous, palisade fringe present (square – habitus as in previous), winged, shorter and narrower elytra (triangle), winged, longer and broader elytra (hexagon). Scale bar = 1 mm.

straight to acuminate resulting in a pinched appearance (Fig. 8L), individuals from the Rockies with sides broadly arcuate (Fig. 8K); median lobe in lateral view bearing a distinct tooth of variable distance from apex and with variably-sized emargination ventrad of tooth, apex narrow and rounded (Fig. 8O–Q); paramere slender and varying from fusiform (basal constriction, widest subapically) to subparallel-sided or weakly narrowing apicad (Fig. 8M, N); paramere with peg setae arranged in two rows, varying from well-organized to slightly disorganized and doubled in places, rows divergent from sides of paramere and weakly to strongly convergent basad in western individuals (Fig. 8N); in eastern individuals, rows generally following the margins of paramere and not convergent basad (Fig. 8M).

Female. Tergite X overall pentagonal, with emargination on each side of protruding, pointed apex, with longitudinal, median pigmented area, setae generally limited to midline (Fig. 9H–I).

Distribution. Canada: AB, BC. **United States:** CA, ID, MT, NV, OR, WA.

Broadly distributed along the western cordilleras on both the eastern and western sides of the continental divide (Fig. 11E). At the northern edge of its western distribution, *Q. debilis* is entirely flightless and appears to extend eastward along the Fraser River in British Columbia to at least the Hope area but it is not clear how distantly east and west populations are separated by the drier, central interior, if at all.

Bionomics. In the northern part of its range on the western side of the continental divide (British Columbia to Oregon, Fig. 12), *Q. debilis* is entirely flightless (wings as

small stubs) and lives more or less in moist, forest litter-based microhabitats, including leaf litter, moss on rocks, treehole litter, and decaying wood and fungi, though it is sometimes collected in litter or moss along the water's edge. Further south, south of northernmost California (Fig. 12), the species is more typically found in wet litter along creeks and most commonly fully winged with longer elytra. On the eastern side of the continental divide, examined specimens (all from Alberta) were fully winged with palisade fringe but with narrow elytra. In Alberta, specimens were collected in deciduous litter (*Populus* sp.) in a forest and along a stream.

Comments. Smetana (1971) treated *Quediellus nanulus* (as *Quedius*) as a separate though variable species that could be confidently diagnosed from *Q. debilis* solely by the 'smaller aedeagus' and in the key by the shorter and less narrow paramere with peg setae rows shorter. A more northern population of generally narrower, smaller-bodied individuals with shorter elytra was considered to correspond to *Q. nanulus*, while a more southern population of generally larger, more fusiform specimens with longer and broader elytra was considered to correspond to *Q. debilis*. Based on the material Smetana (1971) had available, there was some degree of geographic overlap in California, especially the northern Sierra Nevada (Lake Tahoe area).

An examination of dissected males from across this range on the western side of the continental divide, including many of the original specimens examined by Smetana (1971), revealed no reliable differences in the highly variable aedeagus in ventral or lateral view (but see below), despite remarkably disparate morphological forms at either end of the range of variability (Fig. 12). On average, individuals in the north of the distribution tend to have a paramere with a distinct basal constriction and long apical part, while individuals in the far south of the distribution have a more parallel-sided paramere with a shorter apical part (Fig. 8N). However, there are exceptions, even within the same series. These trends do not correspond with the drawings presented in Smetana (1971) for *Q. nanulus* (northern) and *Q. debilis* (southern) and it is possible that they were reversed. The length of the rows of peg setae, number of peg setae and their distribution were all found to be highly variable and did not correspond to external morphotype. Often this variation was marked, even among individuals from the same locality, despite rather uniform external morphology. Congruently, sequenced individuals of the 'debilis' and 'nanulus' morphotypes (Fig. 10, white circles) did not form separate clusters.

Individuals on the eastern side of the continental divide (Rocky Mountains) were considered by Smetana (1971) to belong to *Q. nanulus*. The three specimens examined (all Alberta) exhibited very subtle differences on the median lobe and paramere compared to all other western specimens (Fig. 8), though these differences may not hold when more males are dissected. Cluster analysis treated all specimens of *Quediellus* as a single OTU and BIN, with relatively high (3.27%) intraspecific divergence, likely due to the fact that this species is flightless and a poor disperser over much of its range (British Columbia to northern California). The single half-length sequence from the Rockies did not cluster separately from the western samples (Fig. 10). Therefore, *Q. nanulus* is here treated as a synonym of *Q. debilis* and both populations on either side of the continental divide are considered to be conspecific, leaving only one highly variable species of *Quediellus*.

Acknowledgements

I would like to thank the curators listed in Materials and methods for making specimens under the care available for study. A. Zmudzinska and undergraduate students Anika Cyr, H. Bungay, and T. Coyle (all CNC) are thanked for barcoding voucher preparation and photography. This study received financial support from A-base funding from the Government of Canada (Agriculture and Agri-food Canada: Systematics of Beneficial Arthropods – J-002276). Two reviewers are thanked for their input, which improved the manuscript.

References

Brunke AJ (2021) New relictual genera in Cyrtoquediini and Indoquediini (Coleoptera: Staphylinidae: Staphylininae). ZooKeys 1076: 109–124. https://doi.org/10.3897/zookeys.1076.73103

Brunke AJ, Chatzimanolis S, Schillhammer H, Solodovnikov A (2016) Early evolution of the hyperdiverse rove beetle tribe Staphylinini (Coleoptera: Staphylinidae: Staphylininae) and a revision of its higher classification. Cladistics 32(4): 427–451. https://doi.org/10.1111/cla.12139

Brunke AJ, Żyła D, Yamamoto S, Solodovnikov A (2019) Baltic amber Staphylinini (Coleoptera: Staphylinidae: Staphylininae): a rove beetle fauna on the eve of our modern climate. Zoological Journal of the Linnean Society 187(1): 166–197. https://doi.org/10.1093/zoolinnean/zlz021

Brunke AJ, Hansen AK, Salnitska M, Kypke JL, Predeus AV, Escalona HE, Chapados JT, Eyres J, Richter R, Smetana A, Ślipiński SA, Zwick A, Hajek J, Leschen RAB, Solodovnikov A, Dettman JR (2021) The limits of Quediini at last (Staphylinidae: Staphylininae): a rove beetle mega-radiation resolved by comprehensive sampling and anchored phylogenomics. Systematic Entomology 46(2): 396–421. https://doi.org/10.1111/syen.12468

Casey TL (1915) Studies in some staphylinid genera of North America. Memoirs on the Coleoptera VI. The New Era Printing Co., Lancaster, Pennsylvania, 460 pp.

Horn GH (1878) Synopsis of the Quediini of the United States. Transactions of the American Entomological Society 7: 149–167. https://doi.org/10.2307/25076370

Jenkins Shaw J, Żyła D, Solodovnikov A (2020) Molecular phylogeny illuminates Amblyopinini (Coleoptera: Staphylinidae) rove beetles as a target for systematic and evolutionary research. Systematic Entomology 45(2): 430–446. https://doi.org/10.1111/syen.12405

Leng C (1920) Catalogue of the Coleoptera of America, North of Mexico. J.D. Sherman, Mt. Vernon, New York, 470 pp. https://doi.org/10.5962/bhl.title.6543

Ratnasingham S, Hebert PDN (2013) A DNA-based registry for all animal species: The barcode index number (BIN) system. PLoS ONE 8(7): e66213. https://doi.org/10.1371/journal.pone.0066213

Smetana A (1971) Revision of the tribe Quediini of North America north of Mexico (Coleoptera: Staphylinidae). Memoirs of the Entomological Society of Canada 103(79): 1–303. https://doi.org/10.4039/entm10379fv

Smetana, A (1981) Revision of the tribe Quediini of America North of Mexico (Coleoptera: Staphylinidae). Supplementum 5. The Canadian Entomologist 113: 631–644. https://doi.org/10.4039/Ent113631-7

Smetana A (1990) Revision of the tribe Quediini of America North of Mexico (Coleoptera: Staphylinidae). Supplementum 6. Coleopterists Bulletin 44: 95–104.

Smetana A (2017) Quediine subtribes of Staphylinini (Coleoptera, Staphylinidae, Staphylininae) of mainland China. J. Farkač, Prague, 434 pp.

Solodovnikov AY (2006) Revision and phylogenetic assessment of *Afroquedius* gen. nov. from South Africa: toward new concepts of the genus *Quedius*, subtribe Quediina and reclassification of the tribe Staphylinini (Coleoptera: Staphylinidae: Staphylininae). Annals of the Entomological Society of America 99(6): 1065–1084. https://doi.org/10.1603/0013-8746(2006)99[1064:RAPAOA]2.0.CO;2

ZooKeys 1134: 171–183 (2022)
doi: 10.3897/zookeys.1134.93999
https://zookeys.pensoft.net

RESEARCH ARTICLE

A peer-reviewed open-access journal
ZooKeys
Launched to accelerate biodiversity research

The family Polycentropodidae (Insecta, Trichoptera) in mid-Cretaceous Burmese Amber

Wilfried Wichard[1], Chunpeng Xu[2,3]

1 *Universität zu Köln, Institute of Biology and its Didactics, Herbert Lewinstraße 2, 50931 Cologne, Germany*
2 *State Key Laboratory of Palaeobiology and Stratigraphy, Nanjing Institute of Geology and Palaeontology and Center for Excellence in Life and Paleoenvironment, Chinese Academy of Sciences, Nanjing 210008, China*
3 *University of Chinese Academy of Sciences, Beijing 100049, China*

Corresponding author: Chunpeng Xu (cpxu@nigpas.ac.cn)

Academic editor: Chen-Yang Cai | Received 24 August 2022 | Accepted 27 September 2022 | Published 9 December 2022

https://zoobank.org/0DCD69C8-6FF8-4661-8AB4-E31BAF26F6D7

Citation: Wichard W, Xu C (2022) The family Polycentropodidae (Insecta, Trichoptera) in mid-Cretaceous Burmese Amber. ZooKeys 1134: 171–183. https://doi.org/10.3897/zookeys.1134.93999

Abstract

Three described species, *Neureclipsis triangula* **sp. nov.**, *Neureclipsis acuta* **sp. nov.**, and *Neureclipsis obtusa* **sp. nov.**, expand the *Neureclipsis* cluster to six species dominating the Polycentropodidae in Burmese amber. The new species *Plectrocnemia ohlhoffi* **sp. nov.** and *Plectrocnemia bowangi* **sp. nov.** of the *Polycentropus* cluster add to the comparatively low occurrence of Polycentropodidae in Burmese mid-Cretaceous amber.

Keywords

Hukawng valley, Kachin amber, *Neureclipsis* cluster, *Polycentropus* cluster

Introduction

The caddisfly family Polycentropodidae is one of the most diverse in the trichopteran suborder Annulipalpia and is distributed worldwide, today with about 891 extant species (Chamorro and Holzenthal 2011; Morse 2022). The adults can be distinguished from species of all other families by the following combination of characters: ocelli absent in adult; antennae never longer than forewings; maxillary palpi each five-segmented, first two segments short, each shorter than the third or fourth, the fifth longest and annulated; mesoscutum with a pair of rounded setal warts; mesoscutellum with a rounded setal mesal wart; tibial spurs 2–3/4/4; in male genitalia inferior appendages each one-segmented.

According to Oláh and Johanson (2010), the Polycentropodidae are divided into four diagnostic clusters, based primarily on wing venation and number of spurs on the legs: *Neureclipsis* cluster, *Polycentropus* cluster, *Cyrnus* cluster, and *Cyrnodes* cluster.

In contrast to the cosmopolitan extant Polycentropodidae, the findings of extinct polycentropodid species are confined to four amber deposits:

1. In Miocene Dominican amber, the family Polycentropodidae is represented by only two species of *Cernotina* (Wichard 2007; Wichard and Neumann 2021) which belong to the *Cyrnodes* cluster.
2. In Baltic Pleistocene amber (including findings in Saxonian Bitterfeld amber and Ukrainian Rovno amber), polycentropodids represent the dominant group of fossil caddisflies, accounting for well over 80% of all caddisfly specimens found. According to Ulmer (1912), these polycentropodids belong to 67 extinct species. More recently, several more species have been described from Pleistocene amber deposits (e.g., Mey 1986; Wichard et al. 2009; Ivanov and Melnitsky 2013; Wichard 2013; Melnitsky et al. 2021a, b), increasing the number of species to 118 (Morse 2022).

Most species belong to the genera *Holocentropus*, *Plectrocnemia*, and *Polycentropus* and are assigned to the *Polycentropus* cluster; other species belong to the genus *Nyctiophylax* of the *Cyrnus* cluster. The small *Neureclipsis* cluster includes only a few species, which are four *Neureclipsis* species and two *Archaeoneureclipsis* species which were transferred to the genus *Neureclispsis* by Oláh and Johanson (2010).

3. From Late Cretaceous Taymyr amber (Siberia, Russian Federation), six polycentropodid species have been described (Botosaneanu and Wichard 1983; Melnitsky and Ivanov 2022a, b). All belong to the extinct genus *Archaeopolycentra*, which cannot be assigned to any of the extant four diagnostic clusters, sensu Oláh and Johanson (2010).
4. In mid-Cretaceous Burmese amber, eight polycentropodid species have been found belonging to the *Neureclipsis* and *Polycentropus* clusters. Of these, five species are described in this paper.

Materials and methods

The amber material was collected by local people in the Hukawng Valley of northern Myanmar, (Myitkyina District, Kachin State) and dates from the middle Cretaceous (Cenomanian) period about 98.8 ± 0.6 Ma ago (Shi et al. 2012), but the geological age of Burmese amber can be expected to be slightly older.

The Burmese amber with the embedded trichopteran inclusions was cut, face-grinded, and polished using a cutting machine and a polishing machine, a RotoPol-25 (Struers), with grinding paper for metallography: 800, 1200, 2500, and 4000 grit. Colour photographs were produced for the documentation of specimens. A Leica M420 macroscope with Apozoom 1:6 was used in combination with a Canon EOS 80D, EOS 3.0 utility software, and Zerene Stacker software. Measurements were made with a Leica SApo ocular micrometer.

Adult caddisflies embedded in amber are slightly flattened and visible in ventral and/or dorsal views. Very rarely forewings and hind wings are separately visible in amber inclusions. The wings are often saddle-roofed and cover the abdomen and genitalia in dorsal and lateral views. The genitalia are visible only in ventral or ventral-lateral views. Therefore, diagnoses and descriptions of male genitalia are usually limited to the ventrally located pair of inferior appendages alone.

Type-specimens in this study are deposited in the following repositories:

NIGP Nanjing Institute of Geology and Palaeontology, Nanjing, China
ZFMK Zoological Research Museum Alexander Koenig, Bonn, Germany

Systematic palaeontology

Order Trichoptera Kirby, 1813
Suborder Annulipalpia Martynov, 1924
Superfamily Psychomyioidea Walker, 1852
Family Polycentropodidae Ulmer, 1903

Genus *Neureclipsis* McLachlan, 1864

Type species. *Phryganea bimaculata* Linnaeus, 1758.

Description and diagnosis. Ocelli absent. Filiform antennae no longer than forewings. Maxillary palps each five-segmented with 1st and 2nd segments much shorter than 3rd segment, terminal segment longest, annulated, and flexible. *Neureclipsis* species have complete wing venations with apical forks I, II, III, (IV), V on forewings and apical forks I, II, III, V on hind wings. In fore- and hind wings, fork I petiolate, fork II sessile, discoidal cell subtriangular, closed, crossvein *m* sloping. In forewings medial and thyridial cells usually present. Tibial spur formula 3/4/4.

Neureclipsis is distinguished from all other polycentropodid genera, except *Neucentropus*, by the presence of folk III in the hind wings. The following three new *Neureclipsis* species differ in their forewing lengths and in the number of their flagellomeres but are characterized especially by the male genitalia, clearly in the inferior appendages, which are one-segmented, long, and monolobed.

Neureclipsis triangula sp. nov.

https://zoobank.org/8F917EDA-F2C2-4193-9AA2-C185281408EE
Fig. 1

Diagnosis. The extinct species *Neureclipsis triangula* sp. nov. is characterized by a pair of slightly cupped inferior appendages running parallel in ventral view. Each appendage is tapered at the base, wider near the middle and apically forming a sub-triangular shape. Its sloping apical edge is clearly subapically toothed and highlighted in black.

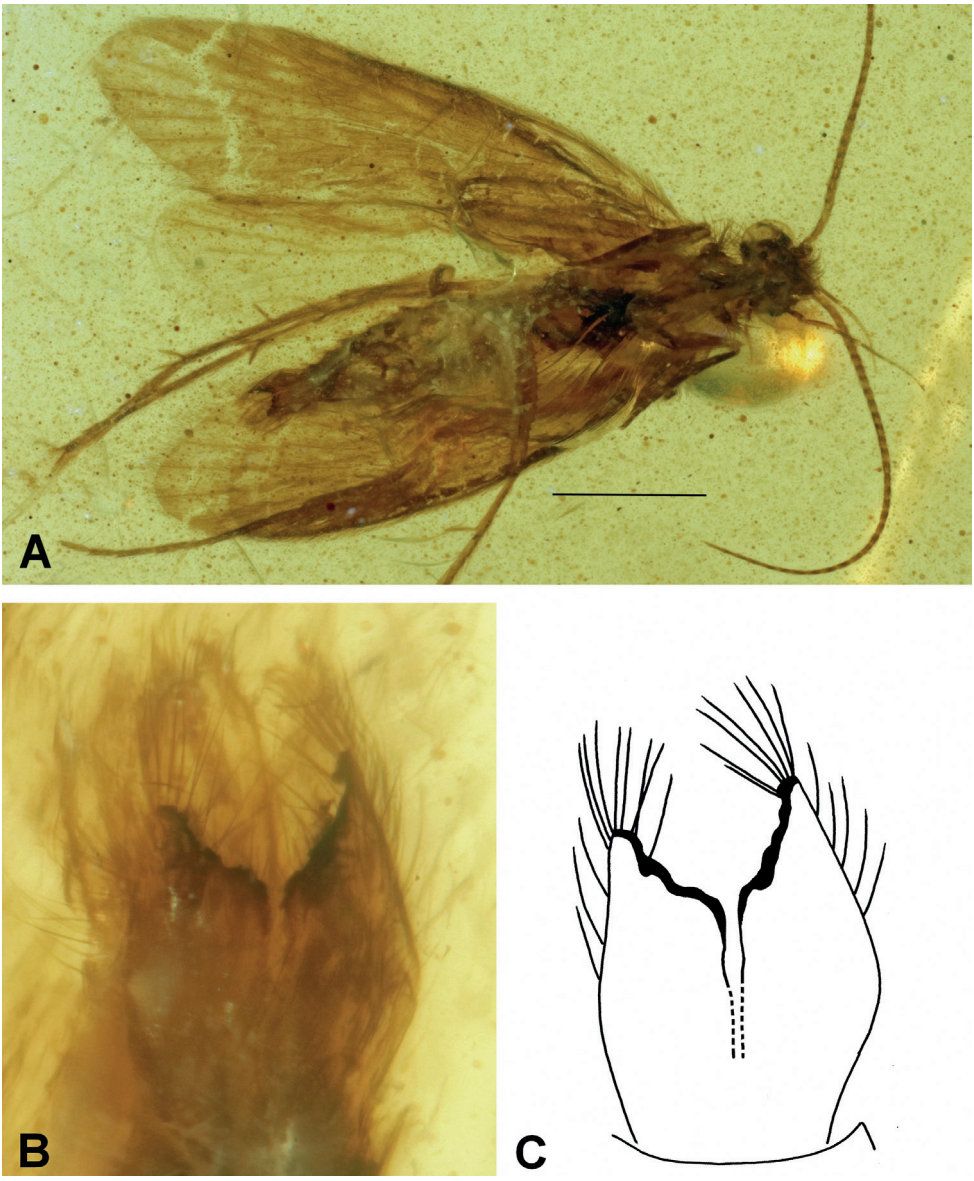

Figure 1. *Neureclipsis triangula* sp. nov. **A** male holotype (NIGP200021) habitus, ventral view **B** inferior appendages, ventral view **C** drawing of inferior appendages, ventral view. Scale bar: 1 mm.

Etymology. Species named after the inferior appendages, subtriangular (Latin adjective = triangulus, -a, -um).

Holotype. ♂; Myanmar, Kachin State, Hukawng Valley; exact locality unknown; Mid-Cretaceous Burmese amber inclusion; deposited in the amber collection of the NIGP; NIGP200021.

Description. Genus as described above. Body well preserved and visible in ventral and dorsal views. Forewing length about 4.2 mm, oblong, rounded, light brown. Antennae about two-thirds as long as forewings, with about 36 flagellomeres plus scapus and short pedicellus. Inferior appendages having subtriangular shape, with oblique, subapically toothed, and black terminal margin.

***Neureclipsis acuta* sp. nov.**
https://zoobank.org/4C948C37-9772-4D7F-B9FB-15289400065F
Fig. 2

Diagnosis. The extinct species *Neureclipsis acuta* sp. nov. is characterized by a pair of long inferior appendages tapering in the apical region and ending with a black, beak-shaped cap.

Etymology. Species named after the inferior appendages, apically sharpened (Latin adjective = acutus, -a, -um).

Holotype. ♂; Myanmar, Kachin State, Hukawng Valley; exact locality unknown; Mid-Cretaceous Burmese amber inclusion; deposited in the amber collection of the NIGP; NIGP200022.

Description. Genus as described above. Body well preserved and visible in ventral and dorsal view, dorsum partially covered by dark artefacts. Forewing length about 3.0 mm, rounded, light brown. Antennae two-thirds as long as forewings with about 24 flagellomeres plus scapus and pedicellus. Inferior appendages long, bearing black, beak-shaped cap apically.

***Neureclipsis obtusa* sp. nov.**
https://zoobank.org/10D154EC-1DD9-40B0-A88E-F2285CE3FAA5
Fig. 3

Diagnosis. The extinct species *Neureclipsis obtusa* sp. nov. has a distinctive pair of rod-shaped, long, inferior appendages. Apically, each appendage ends with an oblique oval surface, on which there a few, scattered stout bristles on the oval and a cluster of small setae on the edge of the oval.

Etymology. Species named after the inferior appendages, apically blunted (Latin adjective = obtusus, -a, -um).

Holotype. ♂; Myanmar, Kachin State, Hukawng Valley; exact locality unknown; Mid-Cretaceous Burmese amber inclusion; deposited in the amber collection of the NIGP; NIGP200023.

Description. Genus as described above. Body well preserved and visible in ventral and dorsal views, dorsum slightly decomposed. Forewing length about 3.5 mm, broad and rounded, light brown. Antennae as long as forewings, with about 42 flagellomeres plus scapus and pedicellus. Inferior appendages long, parallel-sided, apically with oblique oval surface.

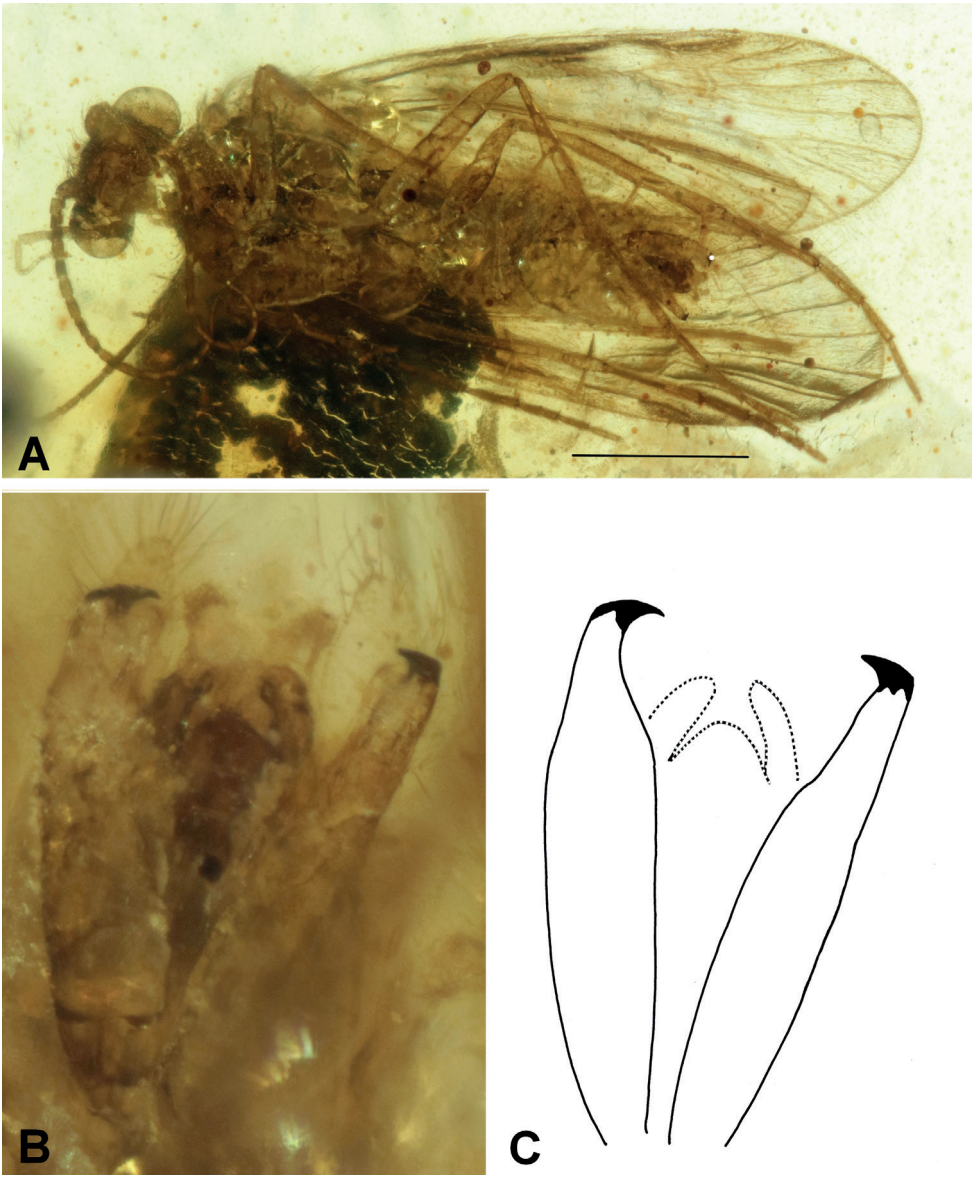

Figure 2. *Neureclipsis acuta* sp. nov. **A** male holotype (NIGP200022) habitus, ventral view **B** inferior appendages, ventral view **C** drawing of inferior appendages, ventral view. Scale bar: 1 mm.

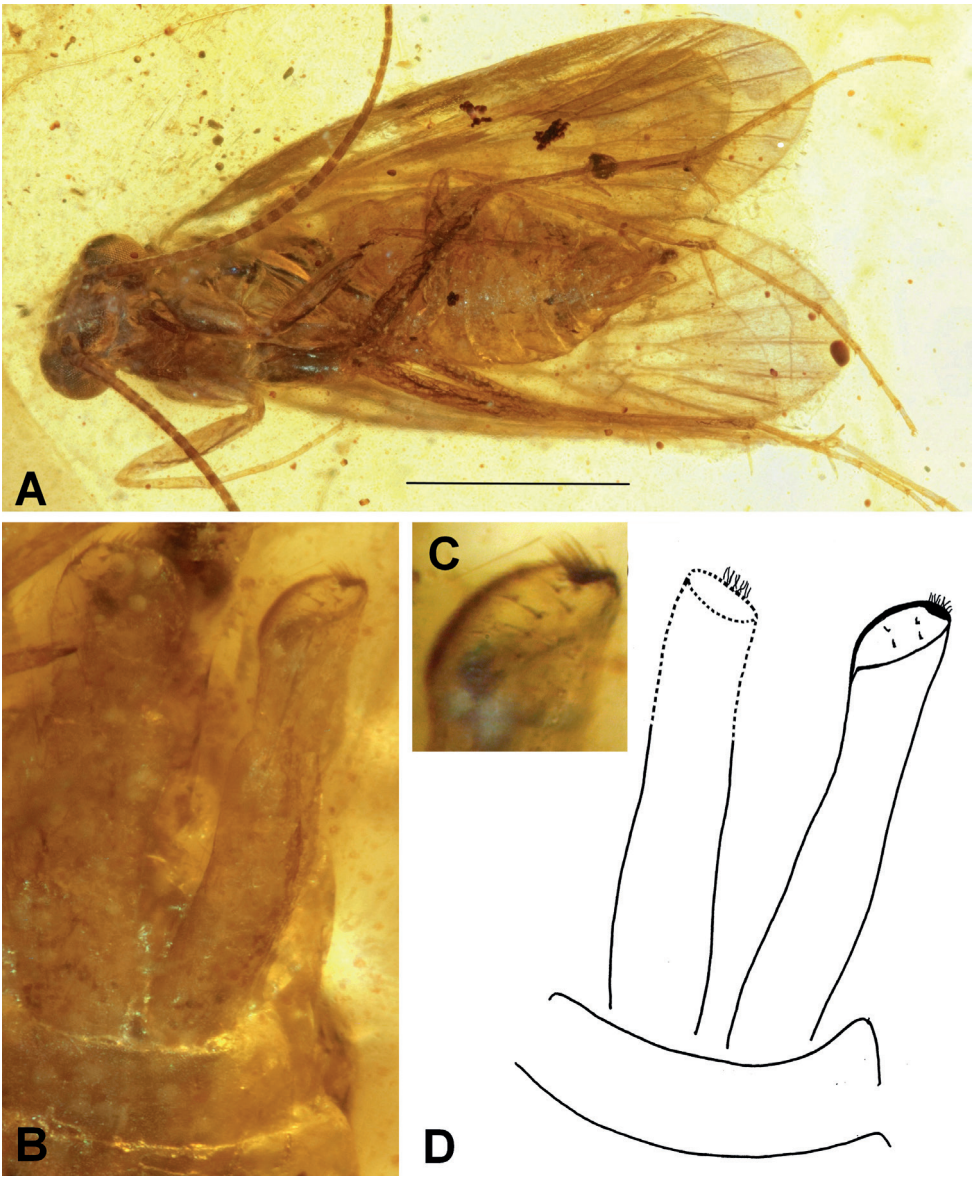

Figure 3. *Neureclipsis obtusa* sp. nov. **A** male holotype (NIGP200023) habitus, ventral view **B** inferior appendages, ventral view **C** apical oval surface of right inferior appendage, with small spines and cluster of setae, ventral view **D** drawing of inferior appendages, ventral view. Scale bar: 1 mm.

Genus *Plectrocnemia* Stephens, 1836

Type species. *Plectrocnemia senex* Stephens, 1836.

Description and diagnosis. Ocelli absent. Filiform antennae about as long as forewings or shorter. Maxillary palps each five-segmented with the 1st and 2nd segments much shorter than the 3rd segment, terminal segment longest and annulated. *Plectrocnemia* adults with complete forewing venation, apical forks I, II, III, IV, V present; fork I petiolate and fork II sessile; discoidal and median cells closed; crossveins *r*, *s*, *r-m*, and *m* usually present. In hind wings apical forks I, II, V present, fork I petiolate and fork II sessile; discoidal cell closed. Tibial spur formula 3/4/4.

The two new *Plectrocnemia* species are very similar and differ clearly in the one-segmented inferior appendages which are robust and short or long.

Plectrocnemia ohlhoffi sp. nov.

https://zoobank.org/6FE60CF6-492D-4E0D-A7E8-EB1535E863E6
Fig. 4

Diagnosis. The extinct species *Plectrocnemia ohlhoffi* sp. nov. is characterized by a pair of elongate inferior appendages, slightly diverging distally and slightly curved apically toward each other. The appendages are weakly concave mesally along their length. In ventral view, each appendage is rounded at the apex and slightly concave in shape apicolaterally, each with a subapical tooth and a weakly projecting apicomesal corner.

Etymology. The fossil species is dedicated to Rainer Ohlhoff, who donated the type specimen to the Zoological Research Museum Alexander Koenig, Bonn, Germany (ZFMK) for permanent preservation.

Holotype. ♂; Myanmar, Kachin State, Hukawng Valley; exact locality unknown; Mid-Cretaceous Burmese amber inclusion; deposited in the amber collection of the ZFMK; former Rainer Ohlhoff collection; ZFMK-TRI000834.

Description. Genus as described above. Body well preserved, visible in left ventrolateral view. Forewing length about 4.2 mm. Forewings hyaline, light brown. Antennae about two-thirds as long as forewings with about 30 flagellomeres plus scapus and pedicellus; left antenna incomplete. Inferior appendages elongate, each forming an elongate shell and both inclining towards the genital midline.

Plectrocnemia bowangi sp. nov.

https://zoobank.org/0A4CBE34-C7B9-425E-8C91-994D9B01AAB6
Fig. 5

Diagnosis. The extinct species *Plectrocnemia bowangi* sp. nov. is characterized by a pair of spoon-like inferior appendages. On the inner side of each of the two spoon-shaped appendages there is a long needle, the tips of which touch each other in about the middle of the genital space.

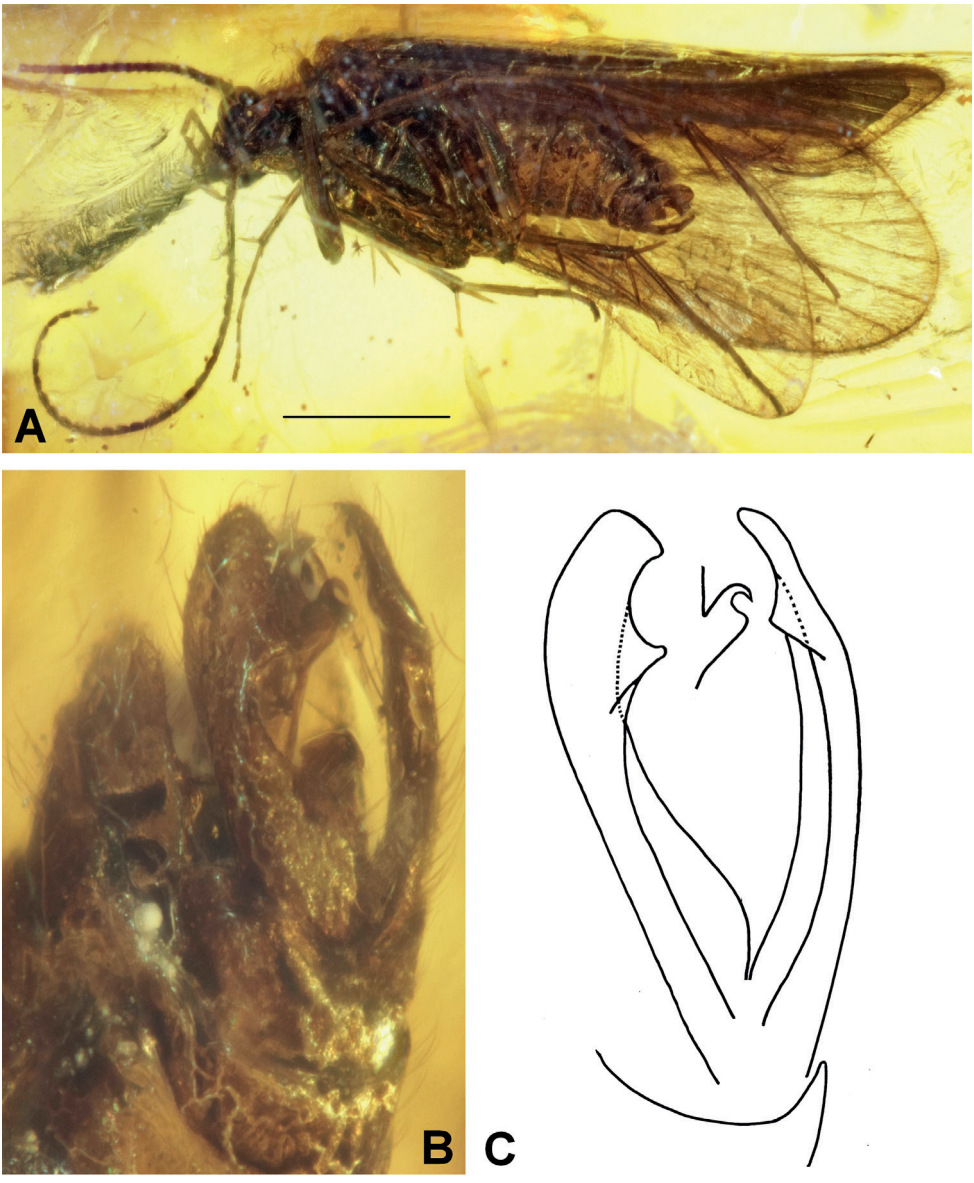

Figure 4. *Plectrocnemia ohlhoffi* sp. nov. **A** male holotype (ZFMK-TRI000834) habitus, ventral view **B** inferior appendages, left ventrolateral view **C** drawing of inferior appendages, left ventrolateral view. Scale bar: 1 mm.

Etymology. The fossil species is dedicated to Prof. Dr Bo Wang, Nanjing Institute of Geology and Palaeontology, China, who provided numerous Burmese ambers for taxonomic studies of embedded caddisflies.

Holotype. ♂; Myanmar, Kachin State, Hukawng Valley; exact locality unknown; Mid-Cretaceous Burmese amber inclusion; deposited in the amber collection of the NIGP; NIGP200024.

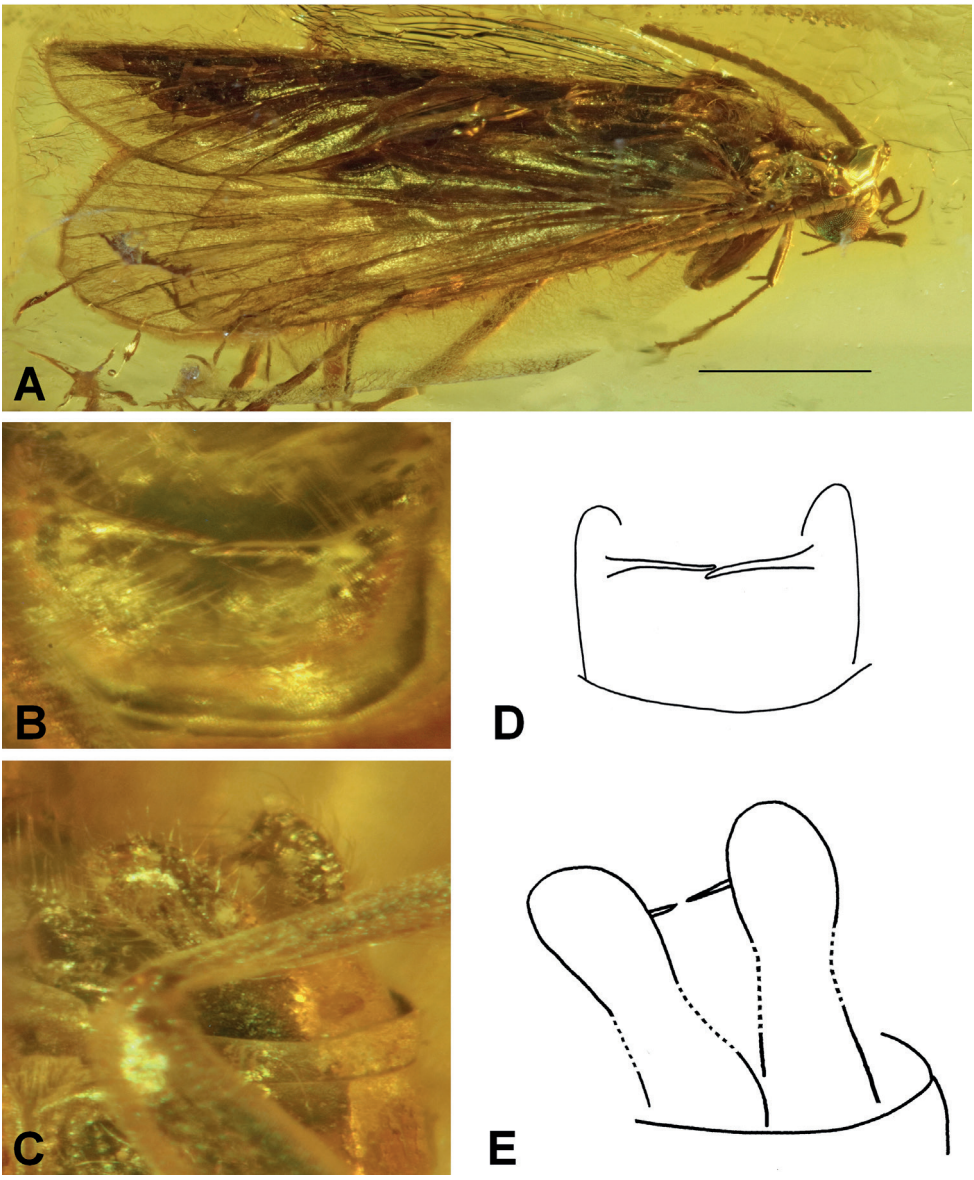

Figure 5. *Plectrocnemia bowangi* sp. nov. **A** male holotype (NIGP200024) habitus, dorsal view **B** inferior appendages, each with a long transverse needle on mesal surface, dorsal view **C** inferior appendages, in ventral view, covered by left hind leg **D** drawing of the long needles arising on the mesal surfaces of the inferior appendages, dorsal view **E** drawing of the pair of spoon-shaped inferior appendages, ventral view. Scale bar: 1 mm.

Description. Genus as described above. Body well preserved, visible in ventrolateral view; right forewing visible in lateral view. Antennae incomplete, probably antennae about two-thirds as long as forewings. Forewing length about 4 mm. Forewings hyaline, light brown. Hind wing smaller than forewings, hyaline, light brown. Inferior appendages only partially visible in lateral view because covering by basal tarsus of left hind leg.

Key of polycentropodid species in mid-Cretaceous Burmese amber

Family characters: ocelli absent. Five-segmented maxillary palps each with short 1st and 2nd segments and terminal segment longest and annulated. Forewing apical fork 1 petiolate; discoidal cell closed. Tibial spurs 3/4/4. Genital inferior appendages each one-segmented.

1 Forewing forks I, II, III, (IV), V, hindwings with fork III (*Neureclipsis* cluster)..... **2**
– Forewing forks I, II, III, IV, V, hindwings without fork III (*Polycentropus* cluster)..... **7**
2 Forewing apical forks I, II, III, V, but fork IV absent ..... ***Electrocentropus dilucidus***
– Forewing apical forks I, II, III, IV, V..... **3**
3 hind wings apical forks II, III, V ..... ***Neucentropus macularis***
– hind wings apical forks I, II, III, V..... **4**
4 Inferior appendages long and slim..... **5**
– Inferior appendages subtriangular ..... ***Neureclipsis triangula***
5 Apices of inferior appendages subapically ampullate.... ***Neurecipsis burmanica***
– Apices of inferior appendages straight **6**
6 Apices of inferior appendages beak-shaped, black..... ***Neureclipsis acuta***
– Apices of inferior appendages forming oval plate..... ***Neureclipsis obtusa***
7 Inferior appendages forming long, narrow bowl..... ***Plectrocnemia ohlhoffi***
– Inferior appendages spoon-shaped, each with thin long transverse needle arising on mesal surface..... ***Plectrocnemia bowangi***

Conclusions

Polycentropodids are found only sporadically in Burmese amber. This fact is especially true in comparison to the numerous polycentropodid specimens in Eocene Baltic amber, which belong to the *Polycentropus* cluster and its genera *Plectrocnemia*, *Polycentropus*, and *Holocentropus*, and also to the genus *Nyctiophylax* in the *Cyrnus* cluster (Ulmer 1912; Wichard et al. 2009).

Species of the *Neureclipsis* cluster predominate in the Burmese Amber. The cluster includes the genus *Neucentropus* with an extinct amber species (*N. macularis*) and an extant species that now occurs in southern Russian Far East, Mongolia, China, Vietnam, and Japan (Li et al. 1998; Morse et al. 2019), and also an extinct amber genus *Electrocentropus* (*E. dilucidus*) with the characteristically absent fork IV of the forewings (Wichard 2021), as well as the genus *Neureclipsis* of which four fossil species currently are known to occur in Burmese amber.

Additional *Neureclipsis* species are expected in the near future, as some amber inclusions indicate the *Neureclipsis* cluster, but the limited state of preservation of amber does not always allow for careful taxonomic analysis and description.

Acknowledgements

We thank Rainer Ohlhoff for the donation of a *Plectrocnemia* holotype specimen which deposited in the Zoological Research Museum Alexander Koenig, Bonn, Germany (ZFMK). Thanks to Bo Wang, Nanjing, for providing Burmese ambers with Trichoptera inclusions for our taxonomic analysis and description of four new species from the amber collection of the Nanjing Institute of Geology and Palaeontology, Nanjing (NIGP). Special thanks to Wolfram Mey and John Morse for their helpful comments to improve the manuscript.

References

Botosaneanu L, Wichard W (1983) Upper Cretaceous Siberian and Canadian amber caddisflies (Insecta: Trichoptera). Bijdragen tot de Dierkunde 53(2): 187–217. https://doi.org/10.1163/26660644-05302002

Chamorro ML, Holzenthal RW (2011) Phylogeny of Polycentropodidae Ulmer, 1903 (Trichoptera: Annulipalpia: Psychomyioidea) inferred from larval, pupal and adult characters. Invertebrate Systematics 25(3): 219–253. https://doi.org/10.1071/IS10024

Ivanov VD, Melnitsky SI (2013) Ten new species of caddisflies (Insecta: Trichoptera) from the Baltic Amber. Paleontological Journal 47(2): 166–176. https://doi.org/10.1134/S0031030113020068

Li YW, Morse JC, Wang P (1998) New taxonomic definition of the genus *Neucentropus* Martynov (Trichoptera: Polycentropodidae). Proceedings of the Entomological Society of Washington 100: 665–671.

Melnitsky SI, Ivanov VD (2022a) New species of Polycentropodidae (Insecta: Trichoptera) from the Taymyr amber locality Nizhnyaya Agapa, upper Cenomanian. Russian Entomological Journal 31: 168–171. https://doi.org/10.15298/rusentj.31.2.13

Melnitsky SI, Ivanov VD (2022b) Re-investigation of *Holocentropus spurious* Botosaneanu and Wichard, 1983 (Insecta, Trichoptera, Polycentropodidae) from the Taymyr amber and its transfer to the genus *Archaeopolycentra*. Braueria 49: 29–30. https://doi.org/10.31610/zsr/2021.30.2.298

Melnitsky SI, Ivanov VD, Perkovsky EE (2021a) A new species of *Plectrocnemia* (Trichoptera: Polycentropodidae) from Rovno amber. Zootaxa 5006(1): 106–109. https://doi.org/10.11646/zootaxa.5006.1.14

Melnitsky SI, Ivanov VD, Perkovsky EE (2021b) A new species of the genus *Holocentropus* (Trichoptera: Polycentropodidae) from Rovno amber. Zoosystematica Rossica 30(2): 298–302. https://doi.org/10.31610/zsr/2021.30.2.298

Mey W (1986) Die Köcherfliegen des Sächsischen Bernsteins (II) (Trichoptera). Deutsche Entomologische Zeitschrift [N.F.] 33: 241–248. https://doi.org/10.1002/mmnd.4800330319

Morse JC (2022) Trichoptera World Checklist. http://entweb.sites.clemson.edu/database/trichopt/ [Accessed on 2022-09-17]

Morse JC, Li J, Sun C, Zhang X, Lin L, Gao M (2019) Trichoptera of Liaoning Province, People's Republic of China. Zoosymposia 14(1): 241–249. https://doi.org/10.11646/zoosymposia.14.1.26

Oláh J, Johanson KA (2010) Generic review of Polycentropodidae with description of 32 new species and 19 new species records from the Oriental, Australian and Afrotropical Biogeographical Regions. Zootaxa 2435(1): 1–63. https://doi.org/10.11646/zootaxa.2435.1.1

Shi G, Grimaldi DA, Harlow GE, Wang J, Yang M, Lei W, Li Q, Li X (2012) Age constraint on Burmese amber based on U-Pb dating of zircons. Cretaceous Research 37: 155–163. https://doi.org/10.1016/j.cretres.2012.03.014

Ulmer G (1912) Trichopteren des Baltischen Bernsteins. Beiträge zur Naturkunde Preußens 10: 1–380.

Wichard W (2007) Overview and descriptions of caddisflies (Insecta, Trichoptera) in Dominican amber (Miocene). Stuttgarter Beiträge zur Naturkunde Serie B 366: 1–51.

Wichard W (2013) Overview and Descriptions of Trichoptera in Baltic Amber: Spicipalpia and Integripalpia. Naturkunde Museum Berlin–Verlag Dr. Kessel, Remagen, 230 pp.

Wichard W (2021) Overview of the caddisflies (Insecta, Trichoptera) in mid-Cretaceous Burmese amber. Cretaceous Research 119: 104707. https://doi.org/10.1016/j.cretres.2020.104707

Wichard W, Neumann C (2021) The polycentropodid genus *Cernotina* (Insecta, Trichoptera) in Miocene Dominican amber. Fossil Record 24: 129–133. https://doi.org/10.5194/fr-24-129-2021

Wichard W, Gröhn C, Seredszus F (2009) Aquatic Insects in Baltic Amber. Verlag Dr. Kessel, Remagen, 336 pp.

ZooKeys 1134: 185–210 (2022)
doi: 10.3897/zookeys.1134.96103
https://zookeys.pensoft.net

RESEARCH ARTICLE

A peer-reviewed open-access journal
ZooKeys
Launched to accelerate biodiversity research

Phototank setup and focus stack imaging method for reptile and amphibian specimens (Amphibia, Reptilia)

Emily M. Braker[1]

1 *Vertebrate Zoology, University of Colorado Museum of Natural History, UCB 265, Boulder CO 80309, USA*

Corresponding author: Emily M. Braker (emily.braker@colorado.edu)

Academic editor: Massimo Delfino | Received 8 October 2022 | Accepted 17 November 2022 | Published 9 December 2022

https://zoobank.org/DB37B8D3-3BBA-4EB8-AEF0-8436694B4C77

Citation: Braker EM (2022) Phototank setup and focus stack imaging method for reptile and amphibian specimens (Amphibia, Reptilia). ZooKeys 1134: 185–210. https://doi.org/10.3897/zookeys.1134.96103

Abstract

Fluid-preserved reptile and amphibian specimens are challenging to photograph with traditional methods due to their complex three-dimensional forms and reflective surfaces when removed from solution. An effective approach to counteract these issues involves combining focus stack photography with the use of a photo immersion tank. Imaging specimens beneath a layer of preservative fluid eliminates glare and risk of specimen desiccation, while focus stacking produces sharp detail through merging multiple photographs taken at successive focal steps to create a composite image with an extended depth of field. This paper describes the wet imaging components and focus stack photography workflow developed while conducting a large-scale digitization project for targeted reptile and amphibian specimens housed in the University of Colorado Museum of Natural History Herpetology Collection. This methodology can be implemented in other collections settings and adapted for use with fluid-preserved specimen types across the Tree of Life to generate high-quality, taxonomically informative images for use in documenting biodiversity, remote examination of fine traits, inclusion in publications, and educational applications.

Keywords

digitization, focus stack photography, Helicon Focus, herpetology collections, imaging, phototank

Introduction

Biological collections contribute deep reservoirs of anatomical and morphological information for extinct and extant biodiversity and are essential for our understanding of life on Earth. While molecular approaches are now a central means for delimit-

ing species and understanding phylogenetic relationships, characterization of the phenotype remains fundamental to analyzing patterns of diversity across space and time (Wiens 2008; Wake 2012; Lee and Palci 2015). Newly developed technologies and cyberinfrastructure improvements to capture, store, and disseminate phenotypic data have the potential to accelerate morphological research across wide-ranging disciplines such as evolutionary biology, ecology, and conservation science. Central to facilitating increased access to morphological information is the translation of physical specimen resources into digital datasets and products, which has increasingly become a core role of natural history collections in the 21st century.

Paralleling the global sea change from analog to digital technologies, the past two decades have witnessed a major shift in the availability of natural history data through the mass digitization of collections and associated archives. Initiatives and funding efforts, such as the US National Science Foundation's (NSF: http://nsf.org) Advancing Digitization of Biological Collections and Infrastructure Capacity for Biology programs (both replaced with the Infrastructure Capacity for Biological Research program in 2020), have mobilized collections to publish taxonomic, geographic, temporal, and morphological data at unprecedented scales, expanding the traditional reach of museums, and inviting participation of new research communities and downstream users through enabling widespread data sharing and opportunities for collaboration (Blagoderov et al. 2012; Nelson and Ellis 2019; Hedrick et al. 2020; Hilton et al. 2021). While voucher specimens remain the gold standard format for archiving biodiversity and conferring repeatability in scientific studies, digital products such as two-dimensional images and computed tomography (CT) media serve as extensions of physical collections and add value and utility to preserved specimens (Beaman and Cellinese 2012; Webster 2017; Hedrick et al. 2020; Lendemer et al. 2020; Hilton et al. 2021). Such digital proxies also play a vital role in the long-term preservation of primary resources, at times circumventing the need to loan, handle, or dissect specimens, thereby reducing risks to physical collections (Blagoderov et al. 2012; Brecko et al. 2014; Page et al. 2015; Lendemer et al. 2020).

Furthermore, building online digital media repositories is a democratizing force in promoting collections access (Boyer et al. 2016; Hedrick et al. 2020; National Academies of Sciences, Engineering, and Medicine 2020). Conducting research visits to museums, field stations, or other biological archives to examine specimens often requires significant budgetary and time investments (Page et al. 2015; Kaiser et al. 2018), limiting widespread participation and presenting major impediments to international collaborations. While specimen loans are typically less resource-intensive than coordinating collections visits, accessibility issues are still present. Specimen loan volumes are generally limited to what is deemed a reasonable quantity for collections staff to prepare and ship, with in-house examination highly encouraged for large sample sizes. Concurrent borrowing of the same physical specimen by more than one researcher is not possible, and often investigators must wait the full duration of a loan period (typically 6–24 months) for return of a needed individual(s) before it is eligible for use in their own project. Wait times are also extended by the common museum practice of loaning out no more than one half of a given taxonomic series as a safeguard against loss, whereby

investigators borrow requested material in multiple loan installments, returning each batch before the next is processed. Protective museum loan policies may necessarily circumscribe collections accessibility, often prohibiting shipments of type specimens, endangered species, fragile material, and rare series, or restricting loans to countries where wildlife shipments are viewed as overly risky or administratively burdensome. Conversely, online digital formats are free of such constraints and may expedite research timelines when specimen surrogates are suitable for use. Similarly, specimen media offer an alternative research modality when collections or loan access is disrupted by events such as natural disasters or infectious disease outbreaks, as experienced during widespread and enduring operational shutdowns amidst the COVID-19 pandemic.

Specimen images are a particularly effective tool in that they facilitate curatorial, research, and educational enterprises. For instance, photographs provide a timestamped snapshot that conveys both specimen disposition status and condition, aiding in collections security, inventory control, and assessment (Blagoderov et al. 2012). Risk of catastrophic damage and loss from natural disasters, failing infrastructure, and housing highly flammable collections is an unfortunate reality for natural history institutions (e.g., Butantan Institute and National Museum of Brazil fires in 1978 and 2018, respectively), and digitization provides an alternative preservation mechanism to virtually document and depict collections materials and ultimately sustain their utility in the case of destruction. Photographs can also be used to initially evaluate the suitability of physical specimens for research or loan (Kaiser et al. 2018), economizing resources and reducing unnecessary borrowing.

In a research context, photographs play an essential role in documenting biodiversity (Mertens et al. 2017; Lunghi et al. 2020), and baseline imagery is especially essential for conservation managers and wildlife biologists working with rare or cryptic species known to science by only a few individuals or accounts. High-quality images can enable verification of taxonomic identifications (Ariño and Galicia 2005; Wheeler et al. 2012) and support sex determinations in dimorphic species, and images are increasingly requested by researchers in lieu of physical specimen loans when diagnostic traits can be observed in a two-dimensional format. Specimens figured in publications enhance textual descriptions and are key elements for communicating morphologically representative traits or novel research concepts. Critically, high-resolution photographs provide raw trait data to be extracted and analyzed for any number of phenomic applications, such as investigations in comparative morphology, hybridism, and pattern morphs (Dittmer et al. 2015), landmark-based geometric morphometrics (Muir et al. 2012), and training convolutional neural networks in image recognition and classification (Nelson and Ellis 2019; Hedrick et al. 2020; Soltis et al. 2020; Durso et al. 2021). As new analytical tools are developed, the greater the potential for automation of rote tasks and meristic data mining from images such as scale counts and character scoring (Ziegler et al. 2010), high-throughput phenotyping, and greater yields in morphological data to advance biodiversity research, engage citizen scientists, and guide agency-based wildlife management practices (Chang and Alfaro 2016; Hedrick et al. 2020; Medina et al. 2020).

Finally, specimen images are broadly useful for public audiences, from incorporation in museum exhibitions to subject reference for field guide illustrations and artwork.

Increasingly, mobilized biodiversity data, including images, are used to enrich STEM curricula in primary, secondary, and university education, including online learning environments. Integration of digitized collections in education promotes active, inquiry-based learning in core biological concepts, bolstering scientific literacy and providing engaging and transformative experiences to inspire the next generation of biodiversity scientists (Cook et al. 2014; Powers et al. 2014; Monfils et al. 2017; Ellwood et al. 2020).

Imaging challenges

It is estimated that only 10% of biological collections data are available online of the estimated one billion specimens housed in US institutions (Page et al. 2015). More limited still is the availability of trait and morphological data, which are essential to the interpretation of the fossil record and investigations into biological and ecological processes such as adaptation, community assemblage, evolutionary convergence and divergence, and speciation (Mayr 1956; Winker 2009; Mahler et al. 2013). Challenges and bottlenecks related to specimen imaging methods likely foster the gap in phenomic data, particularly for groups with complex three-dimensional forms. This is evidenced by the overwhelming dominance of plant specimen imagery in the biodiversity media landscape, with the relatively flat herbarium sheet format more compatible with high-throughput capture methods and mass-digitization than other specimen preparation types common within zoological and paleontological collections (Baker 2011; Ball-Damerow et al. 2019). Vertebrate groups are especially poorly represented, comprising just 3.3% of all image media linked to preserved specimens on the Global Biodiversity Information Facility (GBIF: http://www.gbif.org; GBIF 2022a). In particular, species-diverse clades such as fishes, amphibians, and reptiles that collectively comprise more than 80% of vertebrate diversity make up the smallest proportion of vertebrate specimen images on GBIF (1.1%). This is almost certainly due to the standard preparation convention of fluid-preservation in these groups, which brings its own suite of imaging challenges, including glare and reflectance when removing specimens from storage solution (Sabaj 2008; Kaiser et al. 2018), and the risk of dehydration and damage to specimens when photographed outside of a wet environment.

Reptile and amphibian specimens present specific imaging challenges. Unlike the majority of fishes which share a relatively flat, compressed body plan that is conventionally photographed from a lateral aspect, reptiles and amphibians minimally necessitate dorsal and ventral views to comprehensively observe morphology. Diagnostic features such as scale shape, arrangement, texture, and patterning typically require high-resolution images and zoom magnification in order to adequately examine and quantify traits. Spiny projections and textured skin topography, significant size variation, and specimens with tall profiles such as turtles and coiled snakes can add considerable depth to images, creating out-of-focus regions within the composition. Poorly prepared specimens in nonstandard positions are also commonplace in natural history collections containing historic material. For instance, specimens fixed without use of a hardening

tray and directly immersed in formalin as a method of euthanasia (a now outmoded practice) tend to be contorted instead of neatly coiled or with limbs or tails squarely posed in a flat plane, making them difficult to position and sharply render each body element in photographs. These collective issues very likely contribute to the paucity of reptile and amphibian specimen images available online and the overall lack of concerted digitization programs that emphasize fluid-prepared herpetofauna (Longson et al. 2018; Brecko and Mathys 2020). The vast majority of the 273,657 herpetology specimen images available on GBIF are comprised of specimens photographed while being processed during fieldwork (GBIF 2022b, c). While preserving color immediately following death, these images vary greatly in terms of standardization and quality.

Two approaches that counteract these imaging complexities include focus stack photography and the use of a photo immersion tank (phototank) to image specimens. Focus stack photography (also known as Z-stacking) involves taking several images of a subject at successive focal distances that are then merged to create an image with an extended depth of field (Fig. 1). This method requires mathematical processing to combine the source images into a single composite photo that is entirely in focus. Focus stack photography has been extensively used by the entomology and macroscopy communities (Mertens et al. 2017; Longson et al. 2018) and to a lesser extent for imaging dry vertebrate material such as skulls and study skins (Nelson et al. 2012). This method produces exceptional quality research-grade images that enable close examination of fine traits.

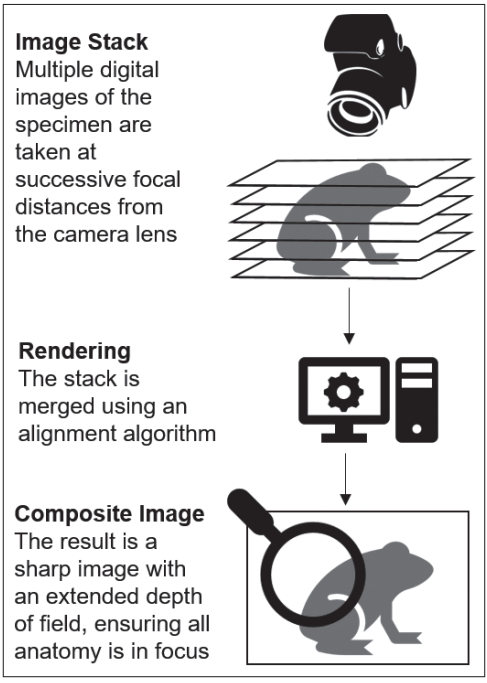

Figure 1. Focus stacking process overview.

Employing a phototank to immerse specimens in preservative during imaging eliminates reflection interference associated with dry imaging methods (Randall 1961; Emery and Winterbottom 1980; Sabaj 2008; Kaiser et al. 2018). A preservative bath also provides physical support and maintains specimen hydration, and better reproduces patterning in images, which tends to be darker and more difficult to see outside of fluid (Fig. 2). Imaging "squeeze tanks," initially developed for photographing live fish and later adopted in the digitization era for imaging preserved specimens, have been in use by the ichthyology collections community for decades (Randall 1961; Emery and Winterbottom 1980; Holm 1989; Sabaj 2008). Though photographing anesthetized salamanders under water has been documented at least once (Lanza et al. 1995), given the limited application of squeeze tanks with live herpetofauna, particularly with fully terrestrial species, a parallel technology transfer to specimen-based photography has not occurred within herpetology. Time and staffing constraints may further contribute to the relative lack of wet photography of fluid-preserved reptile and amphibian specimens.

A combined method for imaging reptile and amphibian specimens

The following methods detail a procedure for combining focus stacking and wet photography techniques used by the University of Colorado Museum of Natural History (**UCM**) as part of an NSF-funded digitization project to create high quality squamate

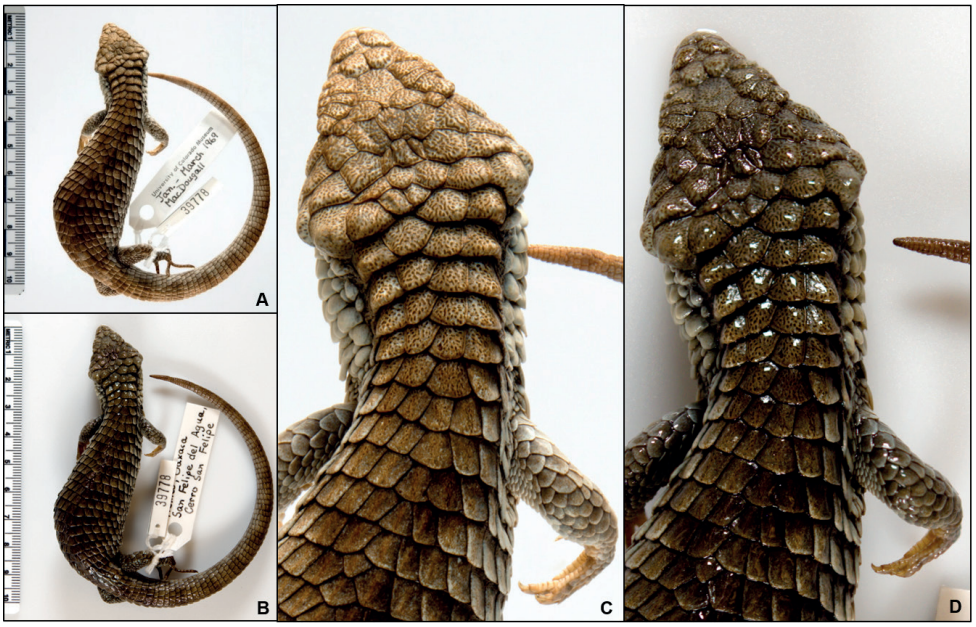

Figure 2. UCM 39778 *Abronia oaxacae*, focus stacked images under the same lighting conditions using **A** immersion in a phototank versus **B** dry photography methods. Enlarging these photographs illustrates **C** the greater legibility in scale patterning with the wet setup, while **D** glare, shadow, and a darker cast are produced when the specimen is removed from preservative for imaging.

and amphibian specimen images (NSF #2001474 oMeso: Opening Mesoamerican Herpetofaunal Diversity to Whole Phenome Imaging [oMeso]; Fig. 3). Equipment, workflow, and recommendations are provided as a roadmap for implementing this approach in other collections settings, with the opportunity to modify the system to accommodate fluid-preserved specimen types across the Tree of Life.

Equipment

This methodology requires three basic components: (i) photography equipment, (ii) photo immersion tank setup and supplies, and (iii) focus stack imaging software and accessories (Fig. 4, Table 1). While specific brands used by the UCM Herpetology Collection are noted in this section, much is possible in the way of substitution and improvisation.

Photography equipment and supplies

Camera

A digital single-lens reflex (DSLR) camera body provides dynamic range, high fidelity image detail and ISO performance, as well as versatility in exchangeable lens options. A Nikon D810 camera was used for capturing project specimens (now succeeded by the Nikon D850 model), though any modern DSLR system sourced from a major camera brand such as Canon, Fuji, Nikon, or Sony will reliably produce high-quality images.

Figure 3. Image gallery of selected specimens from the University of Colorado Museum of Natural History (UCM) Herpetology Collection produced using a combined focus stack photography and phototank methodology. The bottom row reveals the morphological detail captured with this modality using zoom magnification. Left to right: UCM 48846 *Terrapene coahuila*, UCM 21061 *Lampropeltis mexicana greeri*, UCM 35425 *Aspidoscelis stictogrammus*, UCM 25520 *Bolitoglossa lincolni*, UCM 41256 *Incilius cycladen*.

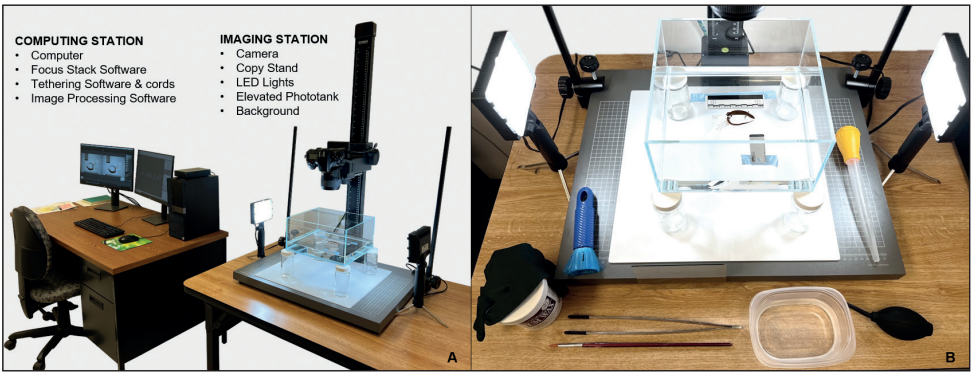

Figure 4. UCM equipment components and configuration. **A** the computing and imaging stations are physically separated to avoid liquid damage **B** detail of phototank setup and accessories with specimen positioned for imaging (shallow aquarium filled with ethanol, scale bar, white balance card, masking tape, jars, acrylic background, flocked nitrile gloves, wax, duster, coated forceps, paintbrush, rinse container, air dust blower, bulb syringe).

Table 1. Recommended equipment list summary.

Phototank and focus stack photography equipment list	
Camera equipment	**Remarks**
Camera body	Professional grade DSLR
Lens	Recommended 50–100 mm
Copy stand	High stability with arm length dependent on maximum specimen size
Studio lights with diffusers	LEDs preferred if using tabletop or copy stand attachments near tank
Backdrop	Neutral, non-reflective acrylic, blotting paper, etc.
Scalebar	
White balance card	
Air dust blower	Camera lens maintenance
Phototank and accessories	**Remarks**
Phototank	Glass adhered with silicone or prefabricated rimless, shallow aquarium
Supports/base	Custom-built frame or improvised supports, e.g., glass jars
Forceps	Silicon-coated for cushion/scratch prevention
Static duster	
Bulb syringe	
Paintbrush	Useful for positioning specimen, tags, and popping bubbles
Lab tape/masking tape	Used for affixing calibration tools to bottom of tank
Preservative	
Small Container	Pre-imaging bath - size dependent on maximum specimen size
Gloves	Recommend flocked nitrile for ease of reuse
Wax/mount	Wax/custom mount for supporting specimens (as needed)
Glass plate	Multiple sizes for flattening tags/specimens (as needed)
Software and cords	**Remarks**
Focus Stacking Software	Recommended Helicon Focus or Zerene Stacker
Tethering Software	Compatible with camera model
Power adapter	Supply kit compatible with camera model
Tethering cords	USB compatible with camera model, at least 1.5 m

Lens

A Nikon AF-S Micro-NIKKOR 60 mm f/2.8G ED lens was used to capture project specimens and can approach or achieve a 1:1 magnification ratio or greater for small-

bodied specimens. Because reptile and amphibian subjects have wide-ranging body sizes, a 50–100 mm lens is recommended for capturing herpetological specimens with a wet imaging station setup.

Copy stand

A copy stand is necessary to securely suspend the camera over the photo tank. A mid-range or high-end option is ideal for mitigating vibrations in the immediate studio facility as well as camera movement when focusing or making fine adjustments to the camera height along the rail. A Kaiser RS10 copy stand with 40" arm was selected for its flexibility in accommodating both extremes of the size spectrum for the oMeso project, from miniaturized salamanders (e.g., *Thorius*, total length ca. 2 cm) to large iguanids (e.g., *Ctenosaura*, ca. 33 cm when prepared in a curled format).

Lighting

Many lighting and diffusing options are commercially available that provide flat, even specimen illumination. Low-budget tabletop flat panel LEDs with a diffuser filter (EMART 60 LED Continuous Portable Photography Lighting Kit) were selected for the UCM phototank setup to minimize the potential for fire danger with ethanol. If necessary, a velvet drape or piece of black cardstock with a hole cut in the middle to fit over the camera lens can be used to block reflections from overhead lighting in the tank preservative.

Backdrop

A matte white acrylic board (AbleDIY Non-Reflective Acrylic Display Board) placed on the copy stand base was used as an image background. A neutral (white, grey, black), non-reflective backdrop is recommended for overall image legibility and contrast with specimens, and simple solutions such as a sheet of blotting paper or velvet cloth are also appropriate.

Calibration tools

A scale bar and white balance card (WhiBal G7) were included as standards for all project images. A physical reference ruler is necessary for calibration purposes even if a digital scale bar is to be inserted into final images. A white balance card is used as a standard to neutralize color casts when processing images. While indoor lighting conditions are far less variable than natural lighting, the color temperature of artificial lights as well as any position adjustments to studio lights between specimens necessitate calibration of each image or photo batch. The scale bar and white balance card were positioned at the periphery of the compositional frame so that they could be easily cropped from final images if desired (e.g., for use in publication figures or online exhibits). For the oMeso project, calibration tools were affixed to the outer surface of the bottom of the phototank with masking tape for ease of repositioning according to

individual specimen size. It is worth nothing that a color calibration standard was not included in this project given the known effects of formalin-fixation on specimen pigmentation, which causes significant alteration in hues such as reds, yellows, and greens (Simmons 2014). However, use of a color balance chart is highly encouraged when imaging recently deceased animals or shortly following specimen processing when coloration is still true-to-life.

Photo immersion tank and accessories

Photo immersion tank and base

Two shallow, rimless aquaria were purchased to carry out digitization (Ultum Nature Systems model 25S, 25.0 × 25.0 × 12.5 cm; model 45S, 45.0 × 28.0 × 18.0 cm). In-house construction of a phototank system is also possible using five panes of glass adhered with silicone. Tank dimensions fit within the footprint of the copy stand baseboard, with relatively short wall height specifications to prevent interference from reflections or shadows on the surface of the bath while still accommodating sufficient preservative volume to fully immerse target specimens during imaging. Whenever possible, the smaller tank size was used in order to minimize ethanol replacement costs throughout the duration of the project. This tank fits the vast majority of squamate and amphibian specimens submerged in approximately 5–10 cm of ethanol, while the larger tank was used to image oversized taxa such as iguanids and varanids, or those with tall profiles, such as turtles and coiled snakes up to 15 cm in height. Jar supports were used to elevate the tank from the copy stand baseboard in order to achieve *bokeh*, a slightly blurred, soft backdrop. Tanks placed directly in contact with a background surface produce a small zone of mirroring around specimens and tend to trap dust and microfibers that require processing out of final images. An elevated tank also allows for backlighting to reduce specimen shadows in images. A custom base frame or supports may be constructed from any number of materials, with clear acrylic recommended as an inconspicuous option. Jars offer a simple solution (Fig. 3), though a frame or supports with a sleeker profile will minimize encroachment into the useable field of view. It is worth noting that it is entirely possible to photograph reptile and amphibian specimens with a traditional squeeze tank setup as is frequently employed in ichthyology collections. This method utilizes a narrow, vertically oriented aquarium paired with a tripod-mounted camera and an angled pane of glass to suspend the specimen in the middle of the tank during imaging. This approach has the advantage of allowing fine particles and debris to fall out of the field of view to the bottom of the tank, reducing spot-cleaning during the specimen staging and image retouching phases. However, friction-pinning specimens in this position can be challenging and time-consuming and is not always possible across different taxa, body plans, and preparations. Additionally, tripods are less stable than a copy stand configuration and may be more prone to introducing vibration artifacts into Z-stacked media.

Preservative

Fresh ethanol (70% concentration) was used to shallowly immerse project specimens during imaging, minimally creating a 5–10 mm layer above each individual's tallest anatomical feature. While it may be tempting to use water to avoid mounting preservative replacement costs throughout a large imaging project, this practice must be avoided. Water-immersion causes osmotic shock in ethanol- or isopropyl-preserved specimens, warping specimens through shrinking or swelling, and diluting the preservative concentration in tissues (Simmons 2014). Loss in preservative strength may result in reduced antiseptic properties and specimen degradation, and the highly permeable skin of amphibians may be especially prone to the damaging forces associated with even brief exposures to a water bath.

Gloves

During the project, reusable flocked nitrile gloves were selected for their convenience as technicians moved between wet and dry station elements. The ability to easily don and doff wet gloves and keep hands dry to interact with the camera and computer components was essential for protecting electronics from the damaging effects of alcohol.

Coated forceps

Silicon-tipped forceps were used to prevent scratches in the bottom of the tank glass while positioning specimens and tags. Unprotected metal tools were avoided due to their incompatibility with the phototank.

Positioning and supports

Specimens prepared in non-standard poses or those not square to the camera lens when placed in the tank were gently overlain with a piece of glass to correct the plane of the body, tail, or limbs. Glass plates in standard picture glazing dimensions were stocked to provide multiple fit options to fully cover variably sized specimens. Specimens or specimens with appendages at oblique angles to the camera were propped up or stabilized with a small amount of Museum Wax (manufactured by Quakehold!).

Cleaning tools

A paintbrush was used for popping bubbles after specimen placement in the tank as well as for removing small fibers or scales from the bath and gently positioning tags. Surface film or cloudy blooms were siphoned out of the aquarium with a bulb syringe. Spot-removing dirt and debris with these tools extended the interval between full tank cleanings and preservative replacement.

Computer software and technical accessories

Tethering cords and software

Tethering cords and software link the camera to a computer and enable remote operation. While focus stack photography is possible without tethering, this process is more time-efficient for mass digitization projects. Additionally, tethering supports better-quality images through minimizing vibrations from touching the camera, automated rotation of the focus ring and precise focal steps between shots, and large-format visualization of the stage and image details on a computer monitor so that adjustments and corrections can be made in real time. Remote operation also protects the camera from needless repeat handling and enables direct image file transfers to the desired computer or hard drive storage system, eliminating manual downloads from a memory card. Helicon Remote software was selected (https://www.heliconsoft.com/heliconsoft-products/helicon-remote/) for tethering, however, other software products such as Canon EOS Utility (Canon), Nikon Camera Control Pro (Nikon), or other brand-specific applications are all capable of remote functionality, live shooting from a computer, and digital file transfers.

Image stacking software

There are many commercial focus stacking software tools in use by the museum community, including Helicon Focus (https://www.heliconsoft.com/heliconsoft-products/helicon-focus/) and Zerene Stacker (http://www.zerenesystems.com/cms/stacker), which have been found to perform equally well (Brecko et al. 2014). These programs offer various methods for combining image stacks, built-in retouching tools, batch workflows, image naming and export options, and plugin integrations with Adobe Lightroom. Helicon Focus was used to carry out oMeso project digitization.

Image processing software

Adobe Lightroom (https://www.adobe.com/products/photoshop-lightroom.html) was used for cropping, calibrating, retouching, adding image metadata, and exporting different file formats, and was selected for the project due to its integration with Helicon Focus.

Power adapter

A power adapter was used as a practical accessory and is recommended for iterative imaging projects to enable the camera to run off electricity, eliminating the need to replace batteries while continuously shooting or conducting full-day imaging sessions. Power supply kit options are specific to camera system and should be vetted for safety features that ensure proper camera performance such as power surge and short circuit protection.

Workflow

Setup

Cleaning

Minimizing dirt, dust, and lint on photo station components is vital for an efficient digitization pipeline and results in less post-processing time spent on image editing (Brecko and Mathys 2020). The acrylic backdrop and camera optics were dusted immediately prior to imaging sessions, and when not in use, the photo immersion tank remained covered, and the lens cap affixed to the camera. A small container filled with 70% ethanol was used to gently dip each specimen in a pre-imaging bath before placement into the photo immersion tank. This action rinsed loose debris and molting scales present that could contaminate the phototank, ultimately extending the longevity of the imaging bath before cleaning and replacement were required.

Positioning

Each specimen was first placed dorsal side up in the tank in a left-facing orientation with nose pointed towards the zero-end of the ruler, which is consistent with widely practiced museum imaging conventions. For limbed taxa, the main axis of the body was aligned parallel to the scale bar located along the bottom edge of the tank (Fig. 5B). Snakes or other coiled taxa in non-linear formats were imaged with the head anchored at one of the major clock-bearing positions (e.g., 12 o'clock, 9 o'clock). Poorly prepared specimens or those with contorted anatomy were overlaid with a glass plate to arrange the body or tags to lie flat in one plane (Fig. 5A). This plate was large enough to fully span the field of view so that its edges were undetectable in images. If necessary, Museum Wax was occasionally applied to prop up specimens or appendages in square alignment with the camera. Tags were arranged with coated forceps or a paintbrush to extend away from the specimen and avoid overlap or obscuring of any body elements, and when possible, straightened from oblique angles so that label text remained legible in images. The exposed label surface was noted so that when the specimen was subsequently imaged from the ventral aspect, the tag was likewise rotated to capture both recto and verso label text.

Framing and final staging

The composition was then previewed on a computer monitor using the Live View function in Helicon Remote to fine-tune specimen position. The calibration tools affixed to the underside of the tank were adjusted to the body size of the subject, closely bordering the specimen but allowing adequate distance so that they could be cropped out of final images if desired (Fig. 5). During this step, the scale bar was placed along the base of the field of view, with the white balance card either positioned in line with the ruler or in the right or left upper corners of the frame. The camera height was then

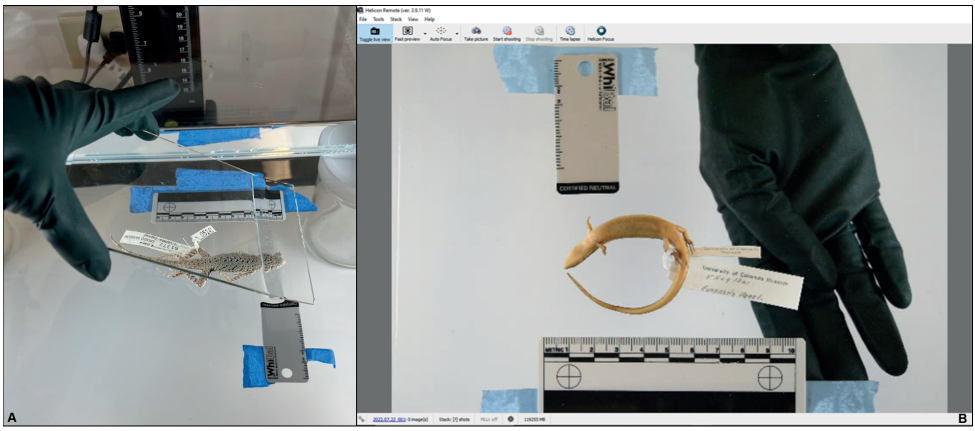

Figure 5. Positioning techniques. **A** a glass plate is used to gently flatten a twisted tag prior to imaging (specimen UCM 61372 *Uma paraphygas*). Glass is undetectable in final images **B** the specimen (UCM 24543 *Scincella assata assata*) is positioned in the frame using the Helicon Remote 'Live View' function, and the scale bar and white balance card taped to the bottom of the tank are adjusted to closely border its body shape. These standards may be cropped out of final images if desired.

adjusted on the rail until the subject filled roughly 80% of the frame, leaving sufficient negative space surrounding the specimen to prevent body elements from approaching the edges of the composition. Finally, the field of view was spot cleaned as needed using a paintbrush and/or bulb syringe. This step was especially important for removing bubbles and debris touching or floating directly above the specimen. While unwanted noise in the image background may be later remedied using digital touchup tools, impurities physically overlapping with the specimen and obscuring anatomy cannot be removed without disrupting image authenticity.

Imaging

Camera settings

Camera settings vary depending on lighting conditions and specific photo station configuration. The following parameters were used for the oMeso project and provide a good starting point when working with fluid-preserved specimens. The camera was set to manual exposure mode in order to maintain control of shutter speed, aperture, and ISO setting. A low ISO of 100 was used to prevent grainy images, as increasing this value introduces unnecessary noise that may compromise image quality. With a static subject and continuous lighting, shutter speed need not be particularly fast (e.g., 1/5–1/200 s) and should be adjusted in tandem with the aperture to achieve a balanced exposure. Because Z-stacking methods generate depth in images, it is not necessary to use a small aperture to capture a large depth of field as with single shot subject photography (generally f-stop values ≥ f/11). Rather, sharpness of the region of

interest within each focal plane was prioritized over deep focus. The Helicon Remote manual suggests using the sharpest aperture supported by the lens model, which is generally two stops above its widest aperture (e.g., a lens with a maximum aperture of f/2.8 would be set to f/5.6), and this guideline was successfully applied to project specimens. Some experimentation with changing the aperture to f/11 for specimens with relatively flat profiles, such as fence lizards (*Sceloporus*) yielded satisfactory results, ultimately necessitating capture of fewer source images given the greater depth of field afforded by the setting. However, the risk of diffraction and blurred areas within images increases when narrowing the aperture, and therefore, a conservative protocol of consistently using a wider aperture (e.g., f/5.6) and more photographs in the stack to reliably produce high-fidelity images was implemented. This saved project technicians from the burden of constantly adjusting camera settings between specimens. Finally, a "fast preview" trial shot in Helicon Remote was taken prior to photo capture of each specimen in order to interpret the exposure histogram displayed by the software, as the Live View interface may not accurately reflect the exposure settings. A peak in the middle of the exposure histogram (Fig. 6) or even slightly left of center (underexposed) is ideal, ultimately granting more flexibility during image processing than an overexposed image. If the histogram showed either exposure extreme, the shutter speed and aperture parameters were adjusted until the histogram was centered, or the intensity of the light source changed by altering the directionality or distance of the lighting units from the tank. Lighting remained consistent throughout image capture to produce the best results during the stacking process.

Focus bracketing

Focus bracketing refers to setting focal distance steps within a scene, such as one shot focused on the foreground and others on the midground and background. When pho-

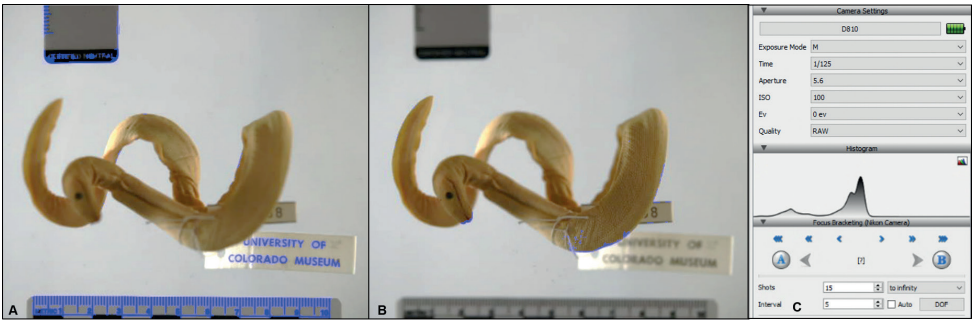

Figure 6. Setting focus bracket parameters in Helicon Focus. Blue highlights convey **A** the furthest distance points from the camera lens and **B** the nearest values, which are used to program the number of shots and step interval necessary to image the specimen when calculated with the specified aperture and focal length of the lens **C** the display panel shows the camera settings used to capture this Yellow-bellied sea snake (UCM 58908 *Hydrophis platurus*) and the centered exposure histogram.

tographing natural history subjects, each source image will contain at least one part of specimen anatomy sharply in focus, ultimately creating a seamless mosaic of crisply rendered structures in the merged extended focus photo. Programming focus brackets involved indicating the nearest focusing point from the camera lens in the frame (e.g., the apex of a specimen's back or carapace, or the caudal end of a twisting tail extending upwards towards the camera), and the furthest focusing point (generally the plane of contact between the specimen and bottom of the tank, or the calibration tools affixed underneath the tank; Fig. 6). In Helicon Focus, the distance interval between shots is automatically generated based on a combination of the specified nearest and furthest endpoints, the aperture, and focal length of the lens. A depth of field calculator is also available to ensure that the step interval provides a zone of overlap between images so that no focus band gaps (blurred areas) occur in the rendered composition. The majority of amphibians and squamate project specimens were adequately captured with 15–25 source images.

Rendering

Following capture, the image stack was aligned using an algorithm to combine the source images (Fig. 7). The three rendering methods available in Helicon Focus include a weighted average (Method A), depth mapping (Method B), and a pyramid formula (Method C), with the first two methods working best with herpetology specimens (pers. obs.), and Method B the preferred option for rendering oMeso project specimens. While scheduling batch process jobs to run overnight in Helicon Focus is an

Figure 7. Helicon Focus interface. The left pane displays a selected source image (UCM 58908 *Hydrophis platurus*) in the stack with only the upper midbody in focus. The right view shows the fully focused output image that was rendered using Method B (depth map) to combine all 20 source images.

option, it was found to be most efficient to proceed with the rendering step in real time while each specimen was still positioned in the tank. This way, a specimen could be easily reimaged should any areas in the output photo exhibit blurriness or an obscured feature from tank micro-debris without going through another **Setup** step. For this reason, imaging technicians performed a critical quality check using the magnifying glass tool immediately following rendering to ensure that all regions of the composition were in focus and satisfactory. Changes in surface depth around the margins of the specimen are especially prone to diffraction, particularly when limb elements are in relaxed positions hanging below the body plane, or with highly dimensional structures, such as the horns and modified scales in horned lizards (*Phrynosoma*), ridged tail annuli in spiny-tailed lizards (*Saara* and *Uromastyx*), and the stacked coils of preserved snakes. Blurred regions were most often remedied by adding more images to the stack to reduce the step interval, but if problem-areas persisted, the nearest and furthest focus bracketing parameters were adjusted.

Retouching

If necessary, the output image background was retouched prior to export from Helicon Focus (alternately, edits were applied at a later point in the workflow using image processing software). The Blurring Brush was used to clean up dirt flecks, bubbles or other alignment artifacts that trail through the background of the composite image due to the stacking procedure. Brush Hardiness and Color Tolerance settings were adjusted to seamlessly blend the background and remove particle interlopers (typically 40% and 75%, respectively), while carefully avoiding inadvertent editing of specimen anatomy. Though not employed for the oMeso project, the Dust Mapping feature is another option to remove known scratches or blemishes on the bottom of the tank or dust on the lens optics.

Export format

Composite images were exported as digital negative files (DNG). Like tagged image file format files (TIFF), DNG is a lossless, standardized, backward-compatible universal file format that meets best practice recommendations for archiving digital images (ADRI 2020; Corrado and Sandy 2017). Raw image formats (RAW) outputted from the camera are a proprietary lossless format that vary by manufacturer and cannot be edited by third-party software. From a digital asset management perspective, RAW is considered a less sustainable format than DNG or TIFF as there exists a greater risk of access failure and information loss over time as files become unreadable or software unsupported. Therefore, RAW formats were not maintained. During export, project images were renamed by concatenating institutional catalog number with scientific name and aspect (e.g., UCM_HERP_31447_Crotalus_lorenzoensis_dorsal.dng). Application of a standard file naming convention is highly recommended for large digitization projects for easy and intuitive file retrieval.

Rotate and repeat

Following dorsal image capture, each specimen was rotated to a ventral view (or opposite aspect for non-standard preparations) and the **Setup** and **Imaging** phases repeated. During rotation, the nose remained pointed towards the zero-end of the scale bar rather than flipped along the horizontal axis to ultimately generate paired images that portray both specimen aspects in the same orientation. At this point in the workflow, technicians opted to either proceed to the next step (**Image Processing**), or continue to batch capture specimens, consolidating imaging tasks and amassing several output media before shifting to photo editing work.

Image processing

Photo editing

Composite output images were processed using Adobe Lightroom. In Lightroom, edits are saved as a set of instructions to a catalog file (.lrcat) instead of written directly to images, thereby preserving archival DNG/TIFF formats. While image processing is a necessary workflow step, many journals will not accept images that have been modified in ways other than whole-image manipulations (Cromey 2010). Some authors also stress that original RAW or DNG files should be made available to taxonomists for comparison to avoid doubts regarding authenticity (Aguiar et al. 2017; García-Melo et al. 2019). As such, processing steps for the oMeso project were limited to basic edits such as cropping and white balance adjustments. Photographs were first cropped to frame the specimen and calibration tools. Specimens imaged on the same day under the same lighting conditions with no modifications to studio light position were white balanced in batch. If necessary, the Lightroom Spot Removal tool was used to clean up any background blemishes not already retouched in Helicon Focus. Because focus stacking can result in darker images (Geiger 2013; Brecko and Mathys 2020), the exposure level was occasionally brightened, especially for specimens with dark coloration. This step was limited to Joint Photographic Experts Group (JPEG) image versions to ensure that online media are legible to web users, while all other imager versions are maintained without this adjustment (the processed large format TIFF and the original archival DNG, see section below), which is ultimately left to the discretion of researchers or other end users.

Metadata, file format specifications, and data management

Basic Exchangeable Image File Format (EXIF) metadata were packaged and added to processed images using a preset in Lightroom to inform end users of image properties. These included: institution, image technician and date, copyright, image licensing, and Creative Commons attribution requirements (https://creativecommons.org/licenses/by-nc-sa/4.0/). UCM ultimately maintains three versions of each image: the original

composite DNG without edits, a processed TIFF file that meets publication criteria, and a processed JPEG. High-resolution TIFFs (300 ppi, no compression) are intended for inclusion in publications, exhibits, or digital loans, and serve as a processed large format archival version of each image. Web-accessible JPEGs (long edge set to 3500 pixels, resolution 72 ppi) have a compressed file size and are therefore more easily distributed and accessed online. Despite down-sampling, JPEGs produced using the combined focus stack and phototank setup are incredibly detailed and likely meet the needs of most stakeholders and applications. As a best practice against catastrophic data loss, three copies of each image file are maintained in different storage locations (an external hard drive, a local peta-storage architecture at the University of Colorado, and dedicated Arctos database servers at the Texas Advanced Computing System), and regularly backed up.

Discussion

Challenges

The time-intensive nature of this methodology may be perceived as a major limitation. Tank preparation, specimen setup, and paired dorsal and ventral image capture and processing ranges from 18–45 min per specimen. This range does not include other associated digitalization tasks such as specimen selection, project tracking, or linking images with database records and/or publishing media to biodiversity data portals. While many specimens require only minor adjustments and cleaning of the stage when placed in the tank, those in non-standard positions may extend setup times as technicians must carefully manipulate and prop anatomy to achieve the most standard view. Similarly, an ethanol bath that is approaching its expiration will extend workflow timelines given the need to edit out accumulated tank debris from images. After setting focus brackets, image capture for a stack of 20 source images runs for ca. 1.75 min. Rendering time depends both on the number of images captured in the stack as well as the processing power of the computer used, with project specimens averaging less than a minute on a Dell Intel Core i7-10700 computer. Quality checking, and image retouching and processing generally ranges from 4–10 min per photo, with overall daily project outputs averaging nine specimens, or a total of 18 processed images (including accompanying file format versions).

While a high-throughput solution does not currently exist, there are some points of efficiency in carrying out a large-scale digitization project using a wet setup. Batching specimens together of the same type and size, such as ‘small frogs less than 6 cm’ or ‘coiled snakes stored in gallon jars’, has the effect of minimizing adjustments in camera height and calibration tool placement between specimens. Avoiding the use of a larger aquarium than is necessary to accommodate target specimen body size also optimizes the pipeline, as changing out used ethanol is costly and time-consuming, and maintaining additional preservative volume only compounds these issues. However, it

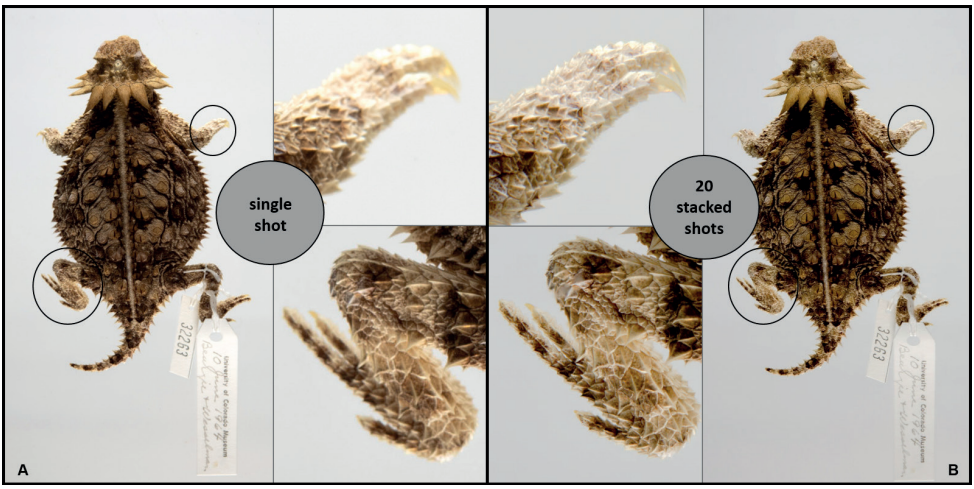

Figure 8. UCM 32263 *Phrynosoma solare* imaged with one shot and 20 stacked images. **A** the single shot was photographed using a narrow aperture (f/13) to maximize depth of field, however, extremities and other regions with changes in depth (such as nose and tail) are out of focus under 100% magnification. Z-stacking resolves these issues. Both images are high quality and suitable for a wide range of applications, however **B** the photo generated by focus stacking is more technically sound for research applications that require fine morphological detail.

is important to avoid delayed replacement of dirty solution, as there are diminishing returns if technicians are investing significant time in spot-cleaning the tank during the specimen **Setup** phase or intensively editing out numerous particles and loose scales appearing in output images. This issue also underscores the post-processing time savings of maintaining the lens optics, tank, and background environments clean through covering and/or dusting equipment before each work session.

Some institutions with limited time or budget may find that using the phototank setup alone is satisfactory for digitizing specimens. A DSLR camera produces a high-quality image with a single shot, however, morphometric, meristic, and some taxonomic applications may require images with greater depth of field to adequately extract or interpret phenotypic information (see Fig. 8). For these cases, a demand-based model may be an appropriate workaround when a larger suite of images beyond the standard dorsal and ventral body aspects are needed by end users. Without performing the Z-stacking step, institutions can slightly streamline workflows, though may need to occasionally rephotograph requested specimens to provide closeup imagery of key traits when they are obscured or out of focus with a single shot capture method. Despite these bottlenecks, the utility of wet studio focus stack photography and the potential long-term positive impacts on specimen documentation, preservation, and staff resource gains through offsetting handling and loans likely outweigh the aforementioned costs and inefficiencies. Even so, there is a clear need for scalable approaches to the mass digitization of herpetology collections - and more broadly, any

fluid-preserved specimen type with highly dimensional morphology - in order to enable synoptic imaging of collections.

While not explored in this project, adding lateral aspects to the imaging workflow would increase the amount of taxonomically informative media generated for each specimen, especially for species where ocular and labial scales or lateral patterning are diagnostic and not as readily observed from a dorsal or ventral vantage. Lateral views can be accomplished with the described setup using a mounting device in the tank to support and secure specimens while positioned on their sides. Ideally, this rig would be undetectable or minimally infringe on the overall aesthetics and composition of resulting images, making lateral views more broadly appealing and usable by diverse end users. It is worth noting that a tripod-mounted camera is a viable option for capturing lateral specimen aspects through the wall of the phototank when the specimen is already positioned in the aquarium for dorsal imaging. However, this method either involves transferring the camera from the copy stand to the tripod, which is inefficient and increases the possibility of mechanical damage from mishandling or dropping photography equipment; or requires procuring a secondary camera body and lens in order to efficiently operate two points of capture, which is beyond the budget of many collections. As already mentioned, a tripod system may also introduce vibration artifacts into images due to its lesser stability.

Other challenges relate to media storage costs and sustainability. Uncompressed Z-stacked output images are relatively large (averaging 2.2MB and 87MB for JPEG and TIFF formats respectively) and are more costly to store and maintain than single shot SLR photographs, or non-SLR images from phones or point-and-shoot cameras. The storage footprint for the oMeso project currently occupies approximately 2TB for dorsal and ventral images from nearly 500 specimens (three copies of each image version [DNG/TIFF/JPEG] and one copy of the raw image stacks). However, digital storage costs trend down over time, and Z-stacking consumes far less space when compared with increasingly popular 3D image modalities such as CT scans or photogrammetry models. Another suite of issues stem from managing digital images in a long-term preservation context, and tracking image usage through time. Before embarking on a large-scale digitization project, it is essential for media generators to create long-term strategies to protect against data loss and maintain data accessibility. These include planning for multiple image backups stored in geographically distinct locations, periodic testing for file corruption and vulnerabilities, and migrating to new formats as technologies become unsupported or obsolete. Best practice recommendations for maintaining media-object associations and enabling tracking through time include minting persistent resolvable identifiers for images (e.g., DOIs, ARKs, EZIDs, UUIDs, GUIDs) and requiring citation of institutional voucher catalog numbers when using images in projects, presentations, articles, or other forms of publication (iDigBio 2013; Guralnick et al. 2015; Nelson and Ellis 2019). As more herpetology collections engage in mass-imaging, another concern is the establishment of community-wide standards (García-Melo et al. 2019; Lunghi et al. 2020). Standardization in imaging methods and tools such as backgrounds, lighting, calibration measures, equipment,

and protocols will produce images that are more readily compared and evaluated. This has been an ongoing topic at many Integrated Digitized Biocollections conferences and workshops (www.idigbio.org) across natural history collection types, and more work in this realm is needed.

Summary

The relative lack of existing herpetology specimen images published to data aggregators is a glaring gap in the biodiversity media space and likely results from the inherent challenges of blurring and glare associated with photographing fluid-preserved reptiles and amphibians. Focus stack photography paired with a phototank setup mitigates these known issues, and the resulting exceptional specimen image quality enables precise identifications, phenomic analyses, and numerous other applications for downstream end users. Already, recently generated UCM specimen images serve as some of the singular depictions available on the web for certain rare taxa (e.g., *Lepidophyma lipetzi*, *Pseudoeurycea anitae*, *Xenosaurus rackhami*), and these taxonomic-grade images have been used to remotely verify and update identifications for dozens of specimens, and train deep learning algorithms to automate scale counts in lizards (see Cheung et al. 2021). The methods presented herein are easily transferrable to any fluid-preserved vertebrate group and can be adapted for most fluid-preserved specimens using alternative mounting strategies (e.g., crustaceans, aquatic insects, fossil amber). Development of accessible specimen image archives offers a viable pathway for researchers, students, conservation managers, and the general public to further explore collections, while preserving and enhancing primary physical voucher resources. Given the limitations to loaning and accessing physical collections, leveraging digital collections when possible is critical to making biodiversity data more rapidly available at a global scale in order to open and advance manifold avenues of research, education, and unanticipated collections uses.

Acknowledgements

I would like to thank Talia Karim for her early review of this manuscript, and Zachary Randall and Andrew Williston for their consultation on wet imaging setups in ichthyology collections. I would also like to acknowledge the reviewers, whose valuable comments and suggestions improved the quality of the manuscript. This work would not be possible without the dedicated imaging efforts of oMeso Project technicians: Genevieve Anderegg, Dahlia Ortiz, Lily Qiao Li Prestien, Allison Sewart, and Grace Yurkunas. This manuscript is based upon work supported by the National Science Foundation (NSF #2001474). Any opinions, findings, and conclusions or recommendations expressed in this material are those of the author and do not necessarily reflect the views of the National Science Foundation. Publication of this article was funded by the University of Colorado Boulder Libraries Open Access Fund.

References

Aguiar JJM, Santos JC, Urso-Guimaraes MV (2017) On the use of photography in science and taxonomy: How images can provide a basis for their own authentication. Bionomina 12(1): 44–47. https://doi.org/10.11646/bionomina.12.1.4

Ariño AH, Galicia D (2005) Taxonomic-Grade Images. In: Häuser CL, Steiner A, Holstein J, Scoble M (Eds) Digital Imaging of Biological Type Specimens. A Manual of Best Practice. ENBI, Stuttgart, 188–122. https://www.gbif.org/document/80576/digital-imaging-of-biological-type-specimens-a-manual-of-best-practice

ADRI [Australasian Digital Recordkeeping Initiative] (2020) Sustainable Digital File Formats for Creating and Using Records. Version 1.0. https://www.caara.org.au/

Baker B (2011) New Push to Bring US Biological Collections to the World's Online Community: Advances in technology put massive undertaking within reach. Bioscience 61(9): 657–662. https://doi.org/10.1525/bio.2011.61.9.4

Ball-Damerow JE, Brenskelle L, Barve N, Soltis PS, Sierwald P, Bieler R, LaFrance R, Ariño AH, Guralnick R (2019) Research applications of primary biodiversity databases in the digital age. PLoS ONE 14(9): e0215794. https://doi.org/10.1371/journal.pone.0215794

Beaman RS, Cellinese N (2012) Mass digitization of scientific collections: New opportunities to transform the use of biological specimens and underwrite biodiversity science. ZooKeys 209: 7–17. https://doi.org/10.3897/zookeys.209.3313

Blagoderov V, Kitching I, Livermore L, Simonsen T, Smith V (2012) No specimen left behind: Industrial scale digitisation of natural history collections. ZooKeys 209: 133–146. https://doi.org/10.3897/zookeys.209.3178

Boyer D, Gunnell G, Kaufman S, McGeary T (2016) MorphoSource: Archiving and sharing 3-D digital specimen data. The Paleontological Society Papers 22: 157–181. https://doi.org/10.1017/scs.2017.13

Brecko J, Mathys A (2020) Handbook of best practice and standards for 2D+ and 3D imaging of natural history collections. European Journal of Taxonomy 623: 1–115. https://doi.org/10.5852/ejt.2020.623

Brecko J, Mathys A, Dekoninck W, Leponce M, VandenSpiegel D, Semal P (2014) Focus stacking: Comparing commercial top-end set-ups with a semi-automatic low budget approach. A possible solution for mass digitization of type specimens. ZooKeys 464: 1–23. https://doi.org/10.3897/zookeys.464.8615

Chang J, Alfaro ME (2016) Crowdsourced geometric morphometrics enable rapid large-scale collection and analysis of phenotypic data. Methods in Ecology and Evolution 7(4): 472–482. https://doi.org/10.1111/2041-210X.12508

Cheung M, Jain T, Rettig S (2021) ScaleCounter (Version 0.0.5) [Source Code]. https://pypi.org/project/ScaleCounter/

Cook JA, Edwards SV, Lacey E, Guralnick RP, Soltis PS, Soltis DE, Welch C, Bell KC, Galbreath KE, Himes C, Allen JM, Heath TA, Carnaval AC, Cooper KL, Liu M, Hanken J, Ickert-Bond S (2014) Aiming up: Natural history collections as emerging resources for innovative undergraduate education in biology. Bioscience 64(8): 725–734. https://doi.org/10.1093/biosci/biu096

Corrado EM, Sandy HM (2017) Digital preservation for libraries, archives, and museums. Rowman & Littlefield, Washington DC, 373 pp.

Cromey DW (2010) Avoiding twisted pixels: Ethical guidelines for the appropriate use and manipulation of scientific digital images. Science and Engineering Ethics 16(4): 639–667. https://doi.org/10.1007/s11948-010-9201-y

Dittmer DE, Johnson JB, Hibbitts TJ (2015) Sexual dimorphism and patch size variation in three lizard species suggests potential for sexual confusion. Copeia 103(2): 310–321. https://doi.org/10.1643/CH-14-108

Durso AM, Moorthy GK, Mohanty SP, Bolon I, Salathé M, Ruiz de Castañeda R (2021) Supervised Learning Computer Vision Benchmark for Snake Species Identification from Photographs: Implications for Herpetology and Global Health. Frontiers in Artificial Intelligence 4: 1–15. https://doi.org/10.3389/frai.2021.582110

Ellwood ER, Sessa JA, Abraham JK, Budden AE, Douglas N, Guralnick R, Krimmel E, Langen T, Linton D, Phillips M, Soltis PS, Studer M, White LD, Williams J, Monfils AK (2020) Biodiversity Science and the Twenty-First Century Workforce. Bioscience 70(2): 119–121. https://doi.org/10.1093/biosci/biz147

Emery AR, Winterbottom R (1980) A technique for fish specimen photography in the field. Canadian Journal of Zoology 58(11): 2158–2162. https://doi.org/10.1139/z80-297

García-Melo JE, García-Melo LJ, García-Melo JD, Rojas-Briñez DK, Guevara G, Maldonado-Ocampo JA (2019) Photafish system: An affordable device for fish photography in the wild. Zootaxa 4554(1): 141–172. https://doi.org/10.11646/zootaxa.4554.1.4

GBIF ([29 September]2022a) GBIF Occurrence Download [Chordata preserved specimen images]. https://doi.org/10.15468/dl.9e4qpq

GBIF ([26 April]2022b) GBIF Occurrence Download [Amphibia preserved specimen images]. https://doi.org/10.15468/dl.waac75

GBIF ([26 April]2022c) GBIF Occurrence Download [Reptilia preserved specimen images]. https://doi.org/10.15468/dl.k7edvs

Geiger DL (2013) Considerations and limits of z-stacking in macrophotography. PhotoTechnique S/O: 34–36.

Guralnick RP, Cellinese N, Deck J, Pyle RL, Kunze J, Penev L, Wals L, Hagedorn G, Agosti D, Wieczorek J, Catapano T, Page RDM (2015) Community next steps for making globally unique identifiers work for biocollections data. ZooKeys 494: 133–154. https://doi.org/10.3897/zookeys.494.9352

Hedrick BP, Heberling JM, Meineke EK, Turner KG, Grassa CJ, Park DS, Kennedy J, Clarke JA, Cook JA, Blackburn DC, Edwards SV, Davis CC (2020) Digitization and the Future of Natural History Collections. Bioscience 70(3): 243–251. https://doi.org/10.1093/biosci/biz163

Hilton EJ, Watkins-Colwell GJ, Huber SK (2021) The Expanding Role of Natural History Collections. Ichthyology & Herpetology 109(2): 379–391. https://doi.org/10.1643/t2020018

Holm E (1989) Improved technique for fish specimen photography in the field. Canadian Journal of Zoology 67(9): 2329–2332. https://doi.org/10.1139/z89-327

iDigBio (2013) GUID guide for data providers [online]. https://www.idigbio.org/sites/default/files/internal-docs/idigbio-standards/iDigBioGuidGuide-2013-06-26.pdf [accessed 24 July 2022]

Kaiser C, Kaiser H, Rickerl K, O'Shea M (2018) A Portable, Low-cost approach for photographing fluid-preserved snake specimens: Recommendations with comments on optimizing specimen photography in natural history collections. Herpetological Review 49(4): 666–677.

Lanza B, Caputo V, Nascetti G, Bullini L (1995) Morphologic and genetic studies of the European plethodontid salamanders: taxonomic inferences (genus: *Hydromantes*). Monografie XVI. Museo Regionale di Scienze Naturali, Torino, 366 pp.

Lee MSY, Palci A (2015) Morphological Phylogenetics in the Genomic Age. Current Biology 25(19): R922–R929. https://doi.org/10.1016/j.cub.2015.07.009

Lendemer J, Thiers B, Monfils AK, Zaspel J, Ellwood ER, Bentley A, LeVan K, Bates J, Jennings D, Contreras D, Lagomarsino L, Mabee P, Ford LS, Guralnick R, Gropp RE, Revelez M, Cobb N, Seltmann K, Aime MC (2020[January 01]) The Extended Specimen Network: A Strategy to Enhance US Biodiversity Collections, Promote Research and Education. Bioscience 70(1): 23–30. https://doi.org/10.1093/biosci/biz140

Longson J, Cooper G, Gibson R, Gibson M, Rawlins J, Sargent R (2018) Adapting Traditional Macro and Micro Photography for Scientific Gigapixel Imaging. Carnegie Mellon University, Journal contribution, 1–12. https://doi.org/10.1184/R1/6709385.v1

Lunghi E, Giachello S, Zhao Y, Corti C, Ficetola GF, Manenti R (2020) Photographic database of the European cave salamanders, genus *Hydromantes*. Scientific Data 7(1): 171. https://doi.org/10.1038/s41597-020-0513-8

Mahler DL, Ingram T, Revell LJ, Losos JB (2013) Exceptional convergence on the macroevolutionary landscape in island lizard radiations. Science 341(6143): 292–295. https://doi.org/10.1126/science.1232392

Mayr E (1956) Geographical character gradients and climactic adaptation. Evolution 10(1): 105–108. https://doi.org/10.1111/j.1558-5646.1956.tb02836.x

Medina JJ, Maley JM, Sannapareddy S, Medina NN, Gilman CM, McCormack JE (2020) A rapid and cost-effective pipeline for digitization of museum specimens with 3D photogrammetry. PLoS ONE 15(8): e0236417. https://doi.org/10.1371/journal.pone.0236417

Mertens JEJ, Van Roie M, Merckx J, Dekoninck W (2017) The use of low cost compact cameras with focus stacking functionality in entomological digitization projects. ZooKeys 712: 141–154. https://doi.org/10.3897/zookeys.712.20505

Monfils A, Powers K, Marshall C, Martine C, Smith J, Prather L (2017) Natural history collections: Teaching about biodiversity across time, space, and digital platforms. Southeastern Naturalist 16(10): 47–57. https://doi.org/10.1656/058.016.0sp1008

Muir AM, Vecsei P, Krueger CC (2012) A perspective on perspectives: Methods to reduce variation in shape analysis of digital images. Transactions of the American Fisheries Society 141(4): 1161–1170. https://doi.org/10.1080/00028487.2012.685823

National Academies of Sciences, Engineering, and Medicine (2020) Biological Collections: Ensuring Critical Research and Education for the 21st Century. The National Academies Press, Washington DC, 244 pp. https://doi.org/10.17226/25592

Nelson G, Ellis S (2019) The history and impact of digitization and digital data mobilization on biodiversity research. Philosophical Transactions of the Royal Society B 374(1763): 20170391. https://doi.org/10.1098/rstb.2017.0391

Nelson G, Paul D, Riccardi G, Mast AR (2012) Five task clusters that enable efficient and effective digitization of biological collections. In: Blagoderov V, Smith VS (Eds) No specimen left behind: mass digitization of natural history collections. ZooKeys 209: 19–45. https://doi.org/10.3897/zookeys.209.3135

Page LM, MacFadden BJ, Fortes JA, Soltis PS, Riccardi G (2015) Digitization of Biodiversity Collections Reveals Biggest Data on Biodiversity. Bioscience 65(9): 841–842. https://doi.org/10.1093/biosci/biv104

Powers KE, Prather LA, Cook J, Woolley J, Monfils AK, Sierwald P (2014) Revolutionizing the Use of Natural History Collections in Education. Science Education Review 13(2): 24–33.

Randall JE (1961) A Technique for Fish Photography. Copeia 2(2): 241–242. https://doi.org/10.2307/1440017

Sabaj MH (2008) All Catfish Species Inventory: Tips on Digitally Imaging Fishes. [ASCI website] http://silurus.ansp.org/ACSI/corresp/digital_imaging_tips.html [NSF DEB-0315963] [accessed 28 June 2022]

Simmons J (2014) Fluid Preservation: A Comprehensive Reference. Rowman & Littlefield Publishers, Boulder, Colorado, 364 pp.

Soltis PS, Nelson G, Zare A, Meineke EK (2020) Plants meet machines: Prospects in machine learning for plant biology. Applications in Plant Sciences 8(6): e11371. https://doi.org/10.1002/aps3.11371

Wake MH (2012) Morphology and herpetology: How and why they interact. Journal of Herpetology 46(3): 279–296. https://doi.org/10.1670/11-221

Webster MS [Ed.] (2017) The Extended Specimen: Emerging Frontiers in Collections-Based Ornithological Research. CRC Press, Boca Raton, Florida, 252 pp.

Wheeler QD, Knapp S, Stevenson DW, Stevenson J, Blum SD, Boom BM, Borisy GG, Buizer JL, De Carvalho MR, Cibrian A, Donoghue MJ, Doyle V, Gerson EM, Graham CH, Graves P, Graves SJ, Guralnick RP, Hamilton AL, Hanken J, Law W, Lipscomb DL, Lovejoy TE, Miller H, Miller JS, Naeem S, Novacek MJ, Page LM, Platnick NI, Porter-Morgan H, Raven PH, Solis MA, Valdecasas AG, Van Der Leeuw S, Vasco A, Vermeulen N, Vogel J, Walls RL, Wilson EO, Woolley JB (2012) Mapping the biosphere: Exploring species to understand the origin, organization and sustainability of biodiversity. Systematics and Biodiversity 10(1): 1–20. https://doi.org/10.1080/14772000.2012.665095

Wiens JJ (2008) Systematics and herpetology in the age of genomics. Bioscience 58(4): 297–307. https://doi.org/10.1641/B580405

Winker K (2009) Reuniting phenotype and genotype in biodiversity research. Bioscience 59(8): 657–665. https://doi.org/10.1525/bio.2009.59.8.7

Ziegler A, Ogurreck M, Steinke T, Beckmann F, Prohaska S, Ziegler A (2010) Opportunities and challenges for digital morphology. Biology Direct 5(1): 45. https://doi.org/10.1186/1745-6150-5-45

ZooKeys 1134: 211–214 (2022)
doi: 10.3897/zookeys.1134.97678
https://zookeys.pensoft.net

CORRIGENDA

A peer-reviewed open-access journal
ZooKeys
Launched to accelerate biodiversity research

Corrigendum: Three new species of the genus *Biasticus* Stål, 1867 (Insecta, Heteroptera, Reduviidae, Harpactorinae) from Central Highlands, Vietnam. ZooKeys 1118: 133–180. https://doi.org/10.3897/zookeys.1118.83156

Ngoc Linh Ha[1,2], Xuan Lam Truong[2,3], Tadashi Ishikawa[4], Weeyawat Jaitrong[5], Chi Feng Lee[6], Bounsanong Chouangthavy[7], Katsuyuki Eguchi[1]

1 *Department of Biological Sciences, Graduate School of Science, Tokyo Metropolitan University, Minami-osawa 1-1, Hachioji, Tokyo 192-0397, Japan* **2** *Institute of Ecology and Biological Resources, Vietnam Academy of Science and Technology, 18 Hoang Quoc Viet Road, Nghia Do, Cau Giay, Hanoi, Vietnam* **3** *Graduate University of Science and Technology, Vietnam Academy of Science and Technology, 18 Hoang Quoc Viet Road, Nghia Do, Cau Giay, Hanoi, Vietnam* **4** *Faculty of Agriculture, Tokyo University of Agriculture, Atsugi, Kanagawa, Japan* **5** *Office of Natural Science Research, National Science Museum, 39 Moo 3, Khlong 5, Khlong Luang, Pathum Thani, 12120 Thailand* **6** *Applied Zoology Division, Taiwan Agricultural Research Institute, Taichung 413, Taiwan* **7** *Plant Protection Unit, Department of Plant Science, Faculty of Agriculture, National University of Laos, P.O. Box 7322, Vientiane, Lao People's Democratic Republic*

Corresponding author: Ngoc Linh Ha (linh.hangoc02@gmail.com)

Academic editor: Jader Oliveira | Received 18 November 2022 | Accepted 25 November 2022 | Published 9 December 2022

https://zoobank.org/C05839C0-1F1D-480B-B55F-6E54DAE93359

Citation: Ha NL, Truong XL, Ishikawa T, Jaitrong W, Lee CF, Chouangthavy B, Eguchi K (2022) Corrigendum: Three new species of the genus *Biasticus* Stål, 1867 (Insecta, Heteroptera, Reduviidae, Harpactorinae) from Central Highlands, Vietnam. ZooKeys 1118: 133–180. https://doi.org/10.3897/zookeys.1118.83156. ZooKeys 1134: 211–214. https://doi.org/10.3897/zookeys.1134.97678

We recently published the description of three new species of the genus *Biasticus* Stål, 1867 (Insecta, Heteroptera, Reduviidae, Harpactorinae) from Central Highlands, Vietnam (Ha NL, Truong XL, Ishikawa T, Jaitrong W, Lee CF, Chouangthavy B, Eguchi K 2022). However, the first author made mistakes when indicating the deposition of the holotype and paratype of the three new species regardless of some regulations and agreements about those specimens. In this corrigendum, we made a revision of the status of the holotype and paratype deposition.

Table 1. The data of specimens used in this study. Abbreviations and symbols: n/a: no data; HU, Matsumura Collection at the Laboratory of Systematic Entomology, Department of Agriculture, Hokkaido University, Sapporo, Japan; IEBR, Institute of Ecology and Biological Resources, Vietnam Academy of Science and Technology, Vietnam; NSMT, National Museum of Nature and Science, Tokyo, Japan; NSM, Department of Entomology, Zoological Research Division, Office of Natural Science Research, National Science Museum, Thailand; NUOL-FA, Faculty of Agriculture, National University of Laos, Laos P.D.R; TARI-AZ, Applied Zoology Division, Taiwan Agricultural Research Institute Insect Collection, Taiwan Agricultural Research Institute, Taiwan; VNMN, Vietnam National Museum of Nature, Vietnam Academy of Science and Technology, Vietnam; *, tentatively held by HNL (first author); bA–bF, morphospecies code (see in the text).

Morphospecies	Specimen code	Collecting date	Locality	Sex	Accession numbers			Depository
					16S	Uni-Minibar (COI)	COI	
Biasticus (ingroups)								
B. taynguyenensis Ha, Truong & Ishikawa, sp. nov. [bA] [Paratype]	HNL2018-036	09.v.2018	Vietnam, Dak Lak	♀	OM908207	ON542864	OM868188	IEBR*
B. taynguyenensis Ha, Truong & Ishikawa, sp. nov. [bA]	HNL2018-072	08.v.2018	Vietnam, Gia Lai	♀	OM908210	ON542867	OM868178	NSMT
B. taynguyenensis Ha, Truong & Ishikawa, sp. nov. [bA] [Holotype]	HNL2018-073	08.v.2018	Vietnam, Gia Lai	♀	OM908211	ON542868	OM868192	IEBR*
B. taynguyenensis Ha, Truong & Ishikawa, sp. nov. [bA] [Paratype]	HNL2018-074	08.v.2018	Vietnam, Gia Lai	♀	OM908212	ON542869	OM868193	VNMN
B. taynguyenensis Ha, Truong & Ishikawa, sp. nov. [bA] [Paratype]	HNL2018-075	08.v.2018	Vietnam, Gia Lai	♀	OM908213	ON542870	OM868194	VNMN
B. taynguyenensis Ha, Truong & Ishikawa, sp. nov. [bA]	HNL2018-076	08.v.2018	Vietnam, Gia Lai	♀	ON554765	ON542871	n/a	NSMT
B. taynguyenensis Ha, Truong & Ishikawa, sp. nov. [bA] [Paratype]	TXL2016-545	28.iv.2016	Vietnam, Gia Lai	♂	OM908227	ON542894	OM868177	IEBR*
B. griseocapillus Ha, Truong & Ishikawa, sp. nov. [bB]	HNL2018-007	05.v.2018	Vietnam, Gia Lai	♀	OM908197	ON542854	OM868176	NSMT
B. griseocapillus Ha, Truong & Ishikawa, sp. nov. [bB] [Paratype]	HNL2018-037	09.v.2018	Vietnam, Dak Lak	♀	OM908208	ON542865	OM868189	IEBR*
B. griseocapillus Ha, Truong & Ishikawa, sp. nov. [bB] [Holotype]	HNL2018-038	09.v.2018	Vietnam, Dak Lak	♀	OM908209	ON542866	OM868191	IEBR*
B. griseocapillus Ha, Truong & Ishikawa, sp. nov. [bB] [Paratype]	TXL2016-546	28.iv.2016	Vietnam, Gia Lai	♂	OM908228	ON542895	OM868190	IEBR*
B. luteicollis Ha, Truong & Ishikawa, sp. nov. [bC] [Paratype]	HNL2018-017	09.v.2018	Vietnam, Dak Lak	♀	OM908198	ON542855	OM868179	VNMN
B. luteicollis Ha, Truong & Ishikawa, sp. nov. [bC]	HNL2018-018	09.v.2018	Vietnam, Dak Lak	♀	OM908199	ON542856	OM868180	IEBR*
B. luteicollis Ha, Truong & Ishikawa, sp. nov. [bC]	HNL2018-019	09.v.2018	Vietnam, Dak Lak	♀	OM908200	ON542857	OM868181	IEBR*
B. luteicollis Ha, Truong & Ishikawa, sp. nov. [bC] [Paratype]	HNL2018-020	09.v.2018	Vietnam, Dak Lak	♀	OM908201	ON542858	OM868182	IEBR*
B. luteicollis Ha, Truong & Ishikawa, sp. nov. [bC]	HNL2018-021	09.v.2018	Vietnam, Dak Lak	♀	OM908202	ON542859	OM868183	NSMT
B. luteicollis Ha, Truong & Ishikawa, sp. nov. [bC]	HNL2018-022	09.v.2018	Vietnam, Dak Lak	♂	OM908203	ON542860	OM868184	NSMT
B. luteicollis Ha, Truong & Ishikawa, sp. nov. [bC]	HNL2018-023	09.v.2018	Vietnam, Dak Lak	♀	OM908204	ON542861	OM868185	NSMT
B. luteicollis Ha, Truong & Ishikawa, sp. nov. [bC] [Paratype]	HNL2018-024	09.v.2018	Vietnam, Dak Lak	♀	OM908205	ON542862	OM868186	IEBR*
B. luteicollis Ha, Truong & Ishikawa, sp. nov. [bC] [Holotype]	HNL2018-025	09.v.2018	Vietnam, Dak Lak	♂	OM908206	ON542863	OM868187	IEBR*
B. luteicollis Ha, Truong & Ishikawa, sp. nov. [bC]	HNL2018-078	08.v.2018	Vietnam, Gia Lai	♀	OM908214	ON542872	OM868195	NSMT

Morphospecies	Specimen code	Collecting date	Locality	Sex	Accession numbers			Depository
					16S	Uni-Minibar (COI)	COI	
B. luteicollis Ha, Truong & Ishikawa, sp. nov. [bC]	HNL2018-079	08.v.2018	Vietnam, Gia Lai	♂	OM908215	ON542873	OM868196	NSMT
B. luteicollis Ha, Truong & Ishikawa, sp. nov. [bC]	HNL2018-080	08.v.2018	Vietnam, Gia Lai	♀	OM908216	ON542874	OM868197	IEBR*
B. luteicollis Ha, Truong & Ishikawa, sp. nov. [bC]	HNL2018-081	08.v.2018	Vietnam, Gia Lai	♀	OM908217	ON542875	OM868198	IEBR*
B. luteicollis Ha, Truong & Ishikawa, sp. nov. [bC] [Paratype]	HNL2018-082	08.v.2018	Vietnam, Gia Lai	♀	OM908218	ON542876	OM868199	VNMN
B. luteicollis Ha, Truong & Ishikawa, sp. nov. [bC] [Paratype]	HNL2018-083	08.v.2018	Vietnam, Gia Lai	♂	OM908219	ON542877	OM868200	VNMN
B. luteicollis Ha, Truong & Ishikawa, sp. nov. [bC]	HNL2018-084	08.v.2018	Vietnam, Gia Lai	♂	OM908220	ON542878	OM868201	NSMT
B. luteicollis Ha, Truong & Ishikawa, sp. nov. [bC] [Paratype]	HNL2018-085	08.v.2018	Vietnam, Gia Lai	♂	OM908221	ON542879	OM868202	IEBR*
B. luteicollis Ha, Truong & Ishikawa, sp. nov. [bC] [Paratype]	HNL2018-086	08.v.2018	Vietnam, Gia Lai	♂	OM908222	ON542880	OM868203	IEBR*
B. luteicollis Ha, Truong & Ishikawa, sp. nov. [bC]	TXL2016-616	05.v.2018	Vietnam, Dak Lak	♀	OM908229	ON542896	OM868208	NSMT
B. luteicollis Ha, Truong & Ishikawa, sp. nov. [bC]	TXL2016-617	05.v.2018	Vietnam, Dak Lak	♂	OM908230	ON542897	OM868209	NSMT

***Biasticus taynguyenensis* Ha, Truong & Ishikawa, sp. nov.**
https://zoobank.org/290765E6-63AE-49F4-B835-B22A034E4DE7
Figs 5A, 6A–D, 13, 14, 15

Type material. ***Holotype.*** ♀; HNL2018-073; Vietnam, Gia Lai Province, Kon Chu Rang Nature Reserve; 08.v.2018; X. L. Truong leg.; **IEBR.** ***Paratypes.*** 1♂; TXL2016-545; Vietnam, Gia Lai Province, Kon Chu Rang Nature Reserve; 28.iv.2016; X. L. Truong leg.; **IEBR**. 1♀; HNL2018-036; Vietnam, Dak Lak Province, Chu Yang Sin National Park; 09.v.2018; X. L. Truong leg.; **IEBR**. 2♀; HNL2018-074; HNL2018-075; Vietnam, Gia Lai Province, Kon Chu Rang Nature Reserve; 08.v.2018; X. L. Truong leg.; **VNMN**.

Non-type material. 2♀; HNL2018-072; HNL2018-076; Vietnam, Gia Lai Province, Kon Chu Rang Nature Reserve; 08.v.2018; X. L. Truong leg.; NSMT.

***Biasticus griseocapillus* Ha, Truong & Ishikawa, sp. nov.**
https://zoobank.org/BDAB0B60-64D5-4529-8715-2E1B010AD57B
Figs 5B, 6E–I, 16, 17, 18

Type material. ***Holotype.*** 1♀; HNL2018-038; Vietnam, Dak Lak Province, Chu Yang Sin National Park; 09.v.2018; X. L. Truong leg.; **IEBR.** ***Paratypes.*** 1♀; HNL2018-037; Vietnam, Dak Lak Province, Chu Yang Sin National Park; 09.v.2018; X. L. Truong leg.; **IEBR**. 1♂; TXL2016-546; Vietnam, Gia Lai Province, Kon Chu Rang Nature Reserve; 28.iv.2016; X. L. Truong leg.; **IEBR**.

Non-type material. 1♀; HNL2018-007; Vietnam, Gia Lai Province, Kon Chu Rang Nature Reserve; 05.v.2018; X. L. Truong leg.; NSMT.

Biasticus luteicollis **Ha, Truong & Ishikawa, sp. nov.**
https://zoobank.org/752E02B7-586A-4A9C-8D70-09DE6199F2EE
Figs 5C, 6J–N, 19, 20, 21

Type material. ***Holotype.*** ♂; HNL2018-025; Vietnam, Dak Lak Province, Chu Yang Sin National Park; 09.v.2018; X. L. Truong leg.; **IEBR.** ***Paratypes.*** 2♀; HNL2018-020; HNL2018-024; Vietnam, Dak Lak Province, Chu Yang Sin National Park; 09.v.2018; X. L. Truong leg.; **IEBR**. 2♂; HNL2018-085; HNL2018-086; Vietnam, Gia Lai Province, Kon Chu Rang Nature Reserve; 08.v.2018; X. L. Truong leg.; **IEBR**. 1♀; HNL2018-017; Vietnam, Dak Lak Province, Chu Yang Sin National Park; 09.v.2018; X. L. Truong leg.; **VNMN**. 1♀; HNL2018-082; Vietnam, Gia Lai Province, Kon Chu Rang Nature Reserve; 08.v.2018; X. L. Truong leg.; **VNMN**. 1♂; HNL2018-083; Vietnam, Gia Lai Province, Kon Chu Rang Nature Reserve; 08.v.2018; X. L. Truong leg.; **VNMN**.

Non-type material. 1♀; TXL2016-616; Vietnam, Dak Lak Province, Chu Yang Sin National Park; 05.v.2016; X. L. Truong leg.; NSMT. 1♂; TXL2016-617; Vietnam, Dak Lak Province, Chu Yang Sin National Park; 05.v.2016; X. L. Truong leg. NSMT; 2♀; HNL2018-018; HNL2018-019; Vietnam, Dak Lak Province, Chu Yang Sin National Park; 09.v.2018; X. L. Truong leg.; IEBR. 2♀; HNL2018-021; HNL2018-023; Vietnam, Dak Lak Province, Chu Yang Sin National Park; 09.v.2018; X. L. Truong leg.; NSMT. 1♂; HNL2018-022; Vietnam, Dak Lak Province, Chu Yang Sin National Park; 09.v.2018; X. L. Truong leg.; NSMT. 1♀; HNL2018-078; Vietnam, Gia Lai Province, Kon Chu Rang Nature Reserve; 08.v.2018; X. L. Truong leg.; NSMT. 2♂; HNL2018-079; HNL2018-084; Vietnam, Gia Lai Province, Kon Chu Rang Nature Reserve; 08.v.2018; X. L. Truong leg.; NSMT. 2♀; HNL2018-080; HNL2018-081; Vietnam, Gia Lai Province, Kon Chu Rang Nature Reserve; 08.v.2018; X. L. Truong leg.; IEBR.

Reference

Ha NL, Truong XL, Ishikawa T, Jaitrong W, Lee CF, Chouangthavy B, Eguchi K (2022) Three new species of the genus *Biasticus* Stål, 1867 (Insecta, Heteroptera, Reduviidae, Harpactorinae) from Central Highlands, Vietnam. ZooKeys 1118: 133–180. https://doi.org/10.3897/zookeys.1118.83156